FLY-ASH PARTICLES IN LAKE SEDIMENTS:

EXTRACTION, CHARACTERISATION & DISTRIBUTION.

Thesis submitted for the degree of
Doctor of Philosophy
in the University of London
by
Neil Leslie Rose

University College London
May 1991

ProQuest LLC.
789 East Eisenhower Parkway
P.O. Box 1346
Ann Arbor, MI 48106 – 1346

ABSTRACT

Fly-ash particles produced from the high temperature combustion of fossil-fuels are found in high concentrations in the lake sediments of regions of high acid deposition. The sediment record of these particles showing the onset of industrialisation correlates well with the record of acidification as indicated by diatom analysis. There are two types of fly-ash particle; spheroidal carbonaceous particles produced from the incomplete combustion of the fossil-fuel and inorganic ash spheres formed by the fusing of mineral inclusions present within the fuel.

Procedures were developed to extract both types of particle from lake sediments. These involved selective chemical attack to remove unwanted sediment fractions thus enabling quick and accurate particle enumeration. A reference data-set of carbonaceous particle surface chemistries was produced using EDS measurements and a fuel-type characterisation developed using multivariate statistics. This characterisation allocated over 97% of the particles to the correct fuel-type. These methods were then applied to a series of sediment cores to study temporal changes in particle deposition and spatial trends over Scotland.

The concentrations of both particle types in sediment cores correlate well to fossil-fuel combustion histories, and the characterisation of the carbonaceous particles from a ^{210}Pb-dated core from a north London lake showed good agreement with the change in coal and oil use through time in the area.

Spatial trends were studied using surface sediments from 94 lakes in Scotland and the north of England. These showed higher concentrations near industrial areas and generally good agreement with sulphur deposition data. Characterisation revealed two areas where above average concentrations of oil particles occurred, indicating source areas outside the country to the east and the south-west.

There is potential to extend this characterisation to other fossil-fuel types such as peat, lignite and brown coal and to apply the techniques to a range of environmental questions in Britain, Europe and on a global scale.

ACKNOWLEDGEMENTS.

Many people have aided and abetted this project and I would especially like to thank all the members of the Palaeoecology Research Unit for their friendship and buying me drinks when necessary. In particular I would like to thank my supervisor Rick Battarbee for his encouragement and guidance throughout. I am also grateful to the following people:

Don Monteith, Simon Patrick, Julie Simpson, Helen Bennion, Tim Allott, Viv Jones and Roger Flower for their help with the fieldwork;

Steve Juggins for all his help and advice with the computing and statistics and for reading various versions of Chapter 3 and to Martin Munro and Tony Stevenson for their comments on computing matters;

Peter Street (formerly of CERL at Leatherhead) for his useful advice in the very early stages;

John Watt of Imperial College, London for all his time with the EDS analyses and for reading a few sections of this work;

Annette Kreiser, Nigel Cameron, Paul Schooling and Bill Campbell for 'top tips' in the use of MAPICS;

Ingemar Renberg, Maria Wik and Judi Natkanski for discussing ideas;

Cath Fletcher for, amongst other things, proof-reading the chapters;

Tim Aspden, Robert Bradbrook and Louise Saunders of the Geography Department Cartographic Unit for drawing most of the diagrams;

Messrs' Page, Plant, Bonham and Jones for many hours company during particle counting.

This project was partially funded by the Central Electricity Generating Board, and the Department of the Environment.

Last but certainly not least, I would like to thank my parents for their continuing support and encouragement.

LIST OF FIGURES

LIST OF PLATES

LIST OF TABLES

CHAPTER 1. INTRODUCTION.

Lake sediments provide a record of atmospheric contamination and they have been important in studies of surface water acidification. These studies have shown that the primary cause of recent lake acidification is acid deposition and one of the major pieces of evidence supporting this conclusion is the close correlation between the onset of atmospheric contamination as indicated by industrially-derived pollutants and the acidification of lakes as indicated by diatom analysis. These industrial pollutants include trace metals (e.g. Pb, Zn, Cu and Cd), polycyclic aromatic hydrocarbons (PAH) and fly-ash particles derived from fossil-fuel combustion. All are found in elevated concentrations in the upper levels of sediment cores taken from areas of high acid deposition (Battarbee et al., 1988).

Fossil-fuels can be burned to produce heat and power at both low temperatures in domestic situations and at high temperatures in the power generation and other industries. When burned at industrial temperatures of up to 1,750°C (Comm. Energy & Envir., 1981) at a rate of heating approaching 10^4°C/s, (Lightman & Street, 1983) the fuel is burned more efficiently leaving only a porous spheroid of mainly elemental carbon (Goldberg, 1985) and fused inorganic spheres from any mineral inclusions present within the fuel (Raask, 1984). These carbonaceous particles and inorganic ash spheres form fly-ash, the term used to describe the particulate matter within flue gases.

1.1. Particle formation.

The particulate matter which constitutes fly-ash has three possible sources (Chigier, 1975) :

i) Matter which was not combustible.
ii) Combustible material which was not burned.
iii) Material formed during the combustion process.

The non-combustible material (up to 25% of coal is mineral matter) when rapidly heated, undergoes some volatilisation to give rise to very fine particulates called

fume. In the case of siliceous minerals, silica fume particles of 0.01μm - 0.1μm diameter are formed. The non-volatile silicate species dispersed in coal coalesce to form cenospheres (hollow ash spheres) and less frequently plerospheres (cenospheres containing encapsulated smaller spheres - see Plate 6) (Carpenter et al., 1980), up to 200μm in diameter (Raask, 1984). The formation and size of the cenospheres are controlled by the viscosity and surface tension of the fused silicate, by the rate of change in particle temperature and by the rate of diffusion of gases in the silicate. The optimum temperature for cenosphere formation is about 1,400°C. Above this, the viscosity of the fused silicate is too low and the sphere is liable to burst. Other ash cenosphere forming criteria are the need for greater than 5% iron oxide present in the ash, the nitrogen content, and contact of the ash particle with carbonaceous material in the furnace (Raask, 1968).

Non-silicate iron minerals in coal undergo extensive fragmentation on rapid heating. Fragmented pyrite (FeS_2) and iron carbonates are oxidised to magnetite (Fe_3O_4) in the flue gases. Calcium carbonate and alkali metal sulphate minerals form fume particles of 0.1μm - 0.3μm in diameter and consequently are in high concentrations in the sub-micron fraction of emitted solids (Raask, 1984). Fuel oil contains very little inorganic material, usually less than 0.1% (Goldstein & Siegmund, 1976) and so fewer inorganic ash spheres are formed and emitted, although Mamane et al., (1986) found that mineral matter accounts for 20-25% of oil fly-ash.

When pulverised coal particles are heated rapidly in a combustion chamber, they change from angular non-porous coal fragments to porous, and often partitioned spheroids (Plate 3). This occurs in several stages. At 300°C, fissures open up in the particles and as the temperature rises to about 450°C, the fissures grow and enclosed gas bubbles can occur. By 500°C, most of the particles contain closed gas spaces and also spaces which connect to the outside of the particle. Ignition occurs at 640°C and above this temperature few obvious differences occur in the particle structure, except at the highest temperatures when 'erosion' occurs around the pores and surface holes. Burning continues both internally and externally, the final residual particle often having a molten appearance (Lightman & Street, 1968). If the particle remains in the combustion chamber, fragmentation will occur.

Pulverised coal ash normally contains 2-5% unburned combustible material, chiefly in the form of highly porous carbonaceous particles 10 - 100μm in diameter (Raask, 1984). There are four main particle types :

i) Relatively solid particles often with ash filled fissures. This type of particle is related to the fusain maceral (Street et al., 1969).

ii) Lacy cenospheres, with internal cross partitions, small pores and sometimes small ash particles embedded in the walls.

iii) Very thin walled particles with few partitions, sometimes with very large external pores.

iv) Thick-walled hollow spheres, with very large surface holes and no partitions.

In oil-droplet combustion, volatiles start to be evolved at 250°C, the droplet expands, and a halo of small droplets forms around it. At about 300°C - 400°C bubbles begin to be formed and this continues up to about 800°C accompanied by distortion and swelling. Expansion and collapse alternate rapidly but there is an overall increase in diameter. Ignition initially occurs in the expelled hydrocarbon cloud and then, as heat is given back to the droplet, burning of the volatiles remaining on the drop takes place. As volatile emission decreases, the drop collapses, becomes rigid, and at 800°C - 1,000°C becomes the final carbonaceous particle. Peak temperatures of about 1,500°C are attained soon after this has formed. Combustion proceeds with a widening of the pores, until about 75% of the carbonaceous mass has been consumed when fragmentation occurs. This process lasts about 1 second (Lightman & Street, 1983). Oil carbonaceous particles are hollow and roughly spherical (Plate 1). The outer wall has a number of holes whose size and shape vary considerably and often there is a complex internal structure. On some particles, a contour effect around the pores is seen (Plate 2) which some authors have claimed to be characteristic of oil carbonaceous particles (Lightman & Street, 1983; Kothari & Wahlen, 1984; Griffin & Goldberg, 1981). However, this contouring may also be present on the surfaces of coal particles (Plate 4).

Of the fossil-fuels commonly used in Britain, only coal and oil produce spheroidal carbonaceous particles. Those produced from peat combustion have an amorphous appearance, many still retaining a cellular structure. Peat does produce inorganic ash spheres however, and the quantity varies depending on the peat type. The combustion of moss peat produces few spheres but sedge peat produces more, probably due to the accumulation of silica in the phytoliths of the original plant.

1.2. Fly-ash particles in the environment.

The quantity of both carbonaceous and inorganic ash particles produced and ultimately emitted to the atmosphere depends on the size of the individual combustion source. According to the Electricity Council Statistics for 1986/87 a power generating station with a gross capability of 2,000MW (e.g. Didcot, Ferrybridge, Ratcliffe-on-Soar) will burn approximately 1,740kg/s of pulverised fuel. If this is 17% ash coal (the average ash content of coal - Comm. Energy & Envir., 1981), the station must dispose of over one million kilograms of ash an hour. The particles which are not removed by the various ash handling systems travel up the stack with the flue gases. If 50% is removed within the furnace in ash hoppers and the electrostatic precipitators are 99% efficient, then over 5,000kg of ash an hour will still be emitted to the atmosphere from this one station, an amount equivalent to many thousands of millions of fly-ash particles. Gaseous emissions would include over 300,000kg of sulphur oxides and 180,000kg of nitrogen oxides per day.

The material emitted to the atmosphere must sooner or later be deposited, and this will be at a point dependant on the meteorological phenomena the diffusing plume encounters, and the physical characteristics of the particles themselves, such as size and density. Particles are removed from the atmosphere by two methods, dry and wet deposition. The plume of flue gases and particulates leaves the stack and disperse at a rate dependant on wind speed and air turbulence. The plume mixes vertically down to the ground and up to the top of the turbulent layer which is about 1,000m deep. Once mixed, usually between 2km and 5km downwind of the source (Dear & Laird, 1984), dry deposition occurs, although, depending on air currents, particles may travel thousands of kilometres before this happens.

Tall stacks are an effective means of reducing ground level concentrations near to the source, but they do not reduce the amount of fly-ash in the atmosphere. For wet deposition, they are less important as this must be preceded by transport up into the rain system, during which time a difference of several hundred metres between high and low sources is not significant (Fisher, 1986). 'Washout', the removal of particulates from the atmosphere by wet deposition, usually occurs between 5km and 100km from the source.

The majority of particles generated in a coal-fired power station fall within the diameter range 0.05μm to 20μm (McElroy et al., 1982), and the size distribution for oil fly-ash is much the same (Raeymaekers et al., 1988). Airborne particles with a diameter between 1μm and 20μm have finite settling velocities which are very low with respect to normal wind speeds (Wark & Warner, 1976) and consequently fly-ash particles, and especially the smaller inorganic ash spheres, are able to travel long distances in air streams. Dust particles of 10μm and less from the Sahara Desert have been recorded as travelling over 3,000 miles of open ocean (Parkin et al., 1970), and so ash particles of this size may conceivably be found in any environment.

Spherules, most probably of industrial origin, were found in all samples taken in transects across the North Atlantic (Folger, 1970), constituting 5% of the total airborne particulates in mid-ocean samples, but over 60% near land (Parkin et al., 1970). Opaque spherules, often black and magnetic, have been recorded in marine sediments of both coastal (Puffer et al., 1980) and deep-sea locations (Fredriksson & Martin, 1963; Deuser et al., 1983), with highest concentrations occurring in the mid-latitudes of the northern hemisphere, where industrial activity is highest. Spherules have also been found at high latitudes in both Greenland (Hodge et al., 1964) and Antarctic ice deposits (Fredriksson & Martin, 1963; Hodge et al., 1967). It is possible that these may have an industrial origin, although meteorological conditions which allow such particle movement are very rare. Chemical analyses show that most spherules in polar ice are very different from those of industrial origin (Hodge et al., 1964) and these particles are most likely to be volcanic or extra-terrestrial (Hodge & Wright, 1964), although meteoritic dust and industrial fly-ash spheres have been confused in the past (Handy & Davidson, 1953; Oldfield et

al., 1978).

Spherical particles composed of magnetite have been recorded in marsh sediments and beach sands in the New York City area. Spherule concentration decreased both away from the industrial area and down sediment cores and it was concluded they were of industrial origin (Puffer et al., 1980). Oldfield et al., (1978, 1981), showed that spherules known to be the product of fossil-fuel combustion, contribute significantly to the magnetic record in ombrotrophic peat bogs. These relate directly, both spatially and temporally to industrial activity, pre-industrial levels being two or three orders of magnitude lower than recent ones. Magnetic spherules identified as industrial through chemical analysis were found in the sediments of Lake Mendota, Wisconsin (Nriagu & Bowser, 1969) and opaque spheroids and white aluminosilicate particles have been found in the sediments of the Severn Estuary (Allen, 1987).

Contamination from deposited particulate matter can affect plant and animal life, human health and may also cause corrosion of metals and stone (Del Monte & Vittori, 1985). The principal factors affecting vegetation are the blocking of stomata by deposits and attack by chemicals associated with the particles either directly or via the soil. There is an indirect effect on grazing animals through plant deterioration, respiratory illnesses or in extreme cases, poisoning (National Society for Clean Air, 1971).

Generating station particle arrestors remove larger particles more efficiently, and consequently the smaller size fraction form a larger proportion of emitted material (McElroy et al., 1982). Fine particles of less than 15μm have been considered potentially hazardous because they can penetrate deeply into the lungs (Amdur & Corn, 1963). The direct effects of inhaling such particles can be increased breathlessness, acute illnesses of the respiratory tract or bronchitis (Parker, 1978). In 1979, power stations were responsible for the emission of 28,000 tonnes of particles in this size range to the atmosphere (Comm. Energy & Envir., 1981).

Gladney et al., (1976), showed that some of the more volatile toxic trace elements, such as Sb, As, Pb, Hg, Se, Br, and I, exhibit enrichment on smaller particles. This

could be due to preferential recondensation onto smaller particles due to the higher surface area per unit mass provided (Natusch & Wallace, 1974). Above 1μm, particles are generally deposited in the nasopharyngeal system, but at the sub-micron level, the majority reach the pulmonary and tracheal respiratory systems (U.S. Dept. of Health, Education & Welfare, 1969). The sub-micron particles also have the longest atmospheric residence times so the toxic trace elements enriched on the surfaces have more chance to reach the deeper respiratory tracts (Davison et al., 1974).

1.3. Fly-ash particles in lake sediments.

The first work in studying carbonaceous particles in lake sediments was done by Griffin and Goldberg (1979). Particles were extracted from sediments and compared against oil, coal and wood fly-ash particles. It was concluded that forest and grass burning could contribute a significant amount of carbonaceous material to the atmosphere, but the concentration of the 'spherical' carbon particles reflected the history of fossil fuel combustion in the area (Griffin & Goldberg, 1979, 1983). Goldberg et al., (1981) showed that the concentrations of certain trace elements such as Sn, Cr, Ni, Pb, Cu, Co, Cd, Zn and Fe showed similar profiles in the sediment to carbonaceous particles. Magnetic ash spherules, formed by the oxidation of iron minerals in the furnace to haematite (Fe_2O_3) and magnetite (Fe_3O_4), were also correlated.

In Sweden, carbonaceous particle profiles were used as an indirect dating method by matching concentration levels with that of a core previously dated by varve counting (Renberg & Wik, 1985a). The particle concentration profiles were found to reflect the increase of industrial activity and the fossil-fuel combustion history of the twentieth century (Wik et al., 1986). There was also seen to be a spatial distribution of carbonaceous particles in both lake sediments (Renberg & Wik, 1985b) and forest soils (Wik & Renberg, 1987) which reflected the industrial regions of Sweden. Work on carbonaceous particles in British lake sediments, have involved lakes principally in Scotland (Darley, 1985; Wik et al., 1986; Battarbee et al., 1988) and Wales (Battarbee et al., 1988) and as with the cores from Sweden and the USA, the carbonaceous particle record follows the history of fossil-fuel

combustion. This is discussed in more detail in Chapter 4.

Most of the work done on inorganic ash spheres has been on power station material with studies on the distribution of elements within the ashes (e.g. Coles et al., 1979; Kaakinen et al., 1975; Gladney et al., 1976; Hulett et al., 1980 etc.), and how this relates to combustion and ash removal efficiency (Paulson & Ramsden, 1970). Other work has focused on potential uses of extracted ash and so the pozzolanic properties (for use with cements in building technology) (Watt & Thorne, 1965; Raask & Street, 1978) and leachability of toxic elements where ash has been used in land-fill sites (Wadge & Hutton, 1987) have been studied. Very little work has been done on the chemical extraction of inorganic ash spheres from sediments.

1.4. Outline of the thesis.

This study was originally designed as part of the ongoing lake acidification work at the Department of Geography, University College London, and as such set out to do two things: first, to develop methods for the extraction of fly-ash particles from lake sediments, either by improving those already available in the literature or by designing new ones, and secondly, to characterise these extracted particles to their fuel types.

Consequently, this thesis describes the development of the extraction and characterisation techniques and their applications to study the distributions of fly-ash particles in lake sediments spatially and temporally.

Chapter 2 describes the sites and methods used in this study, the development of the laboratory procedures for the particle extraction techniques and their application to a sediment core from Loch Tinker.

Chapter 3 describes previous attempts to characterise carbonaceous particles, the use of energy dispersive spectroscopy (EDS) to obtain the elemental compositions of the particle surfaces, the development of a particle reference data set from power station material, and the use of this data set and multivariate statistical techniques in the formation of a discriminant function effective at separating coal and oil

carbonaceous particles. Reference data from a peat-fired station are also used to show the potential for extending this classification to include other fuel types.

Chapters 4 and 5 describe applications of these techniques. Chapter 4 discusses the temporal patterns of fly-ash particles in sediment cores taken principally from British lakes, but also from several cores taken from Norway and France. The potential for using the profiles of carbonaceous particles in British lake sediments for indirect dating is discussed and dates for the various features of the profile are suggested for different regions within Britain. The additional dating potential of characterised carbonaceous particles and the geochronological use of inorganic ash sphere profiles are also discussed.

Chapter 5 describes the spatial distribution of the two particle types in Scottish surface sediments and how, in the absence of sediment dating, particle concentrations can be used to study regional patterns of deposition. The results from carbonaceous particle characterisation and the ratios of inorganic ash spheres to carbonaceous particles in surface sediments are used to study fossil-fuel combustion influences on the region. Finally, the relationship between fly-ash particles and sulphur deposition is discussed.

The conclusions of the study are summarised in Chapter 6. The Appendices give the particle concentrations for the surface sediments and the cores analysed during the course of this work and finally the papers already published by the author from this thesis are included.

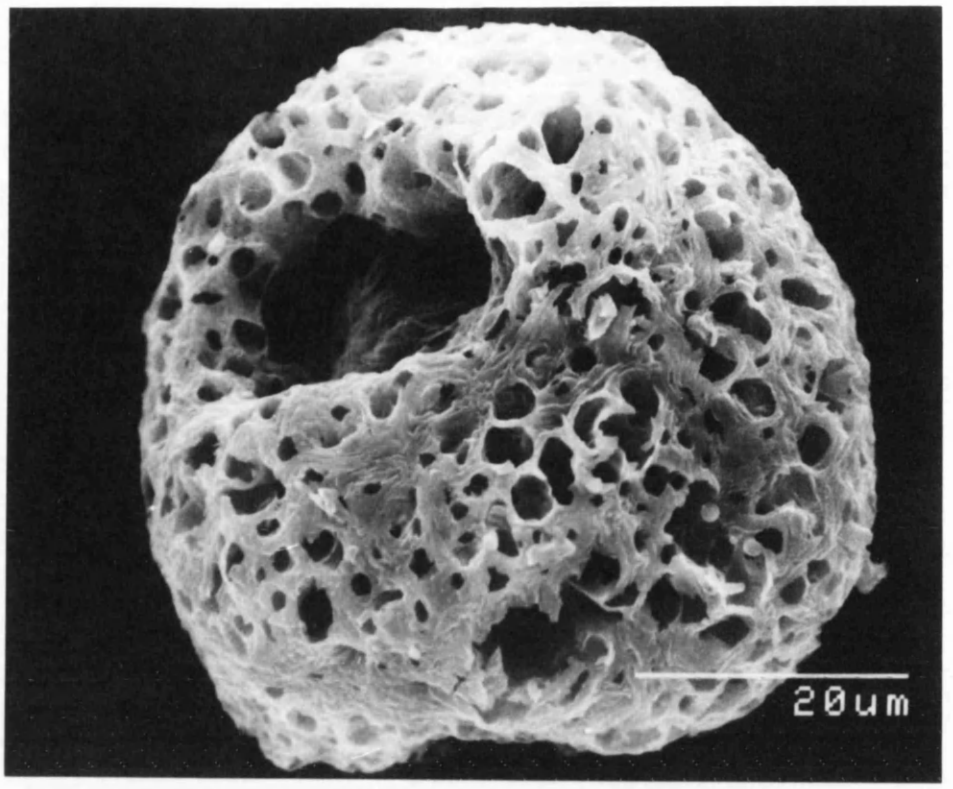

Plate 1. Carbonaceous particle derived from oil combustion (Fawley).

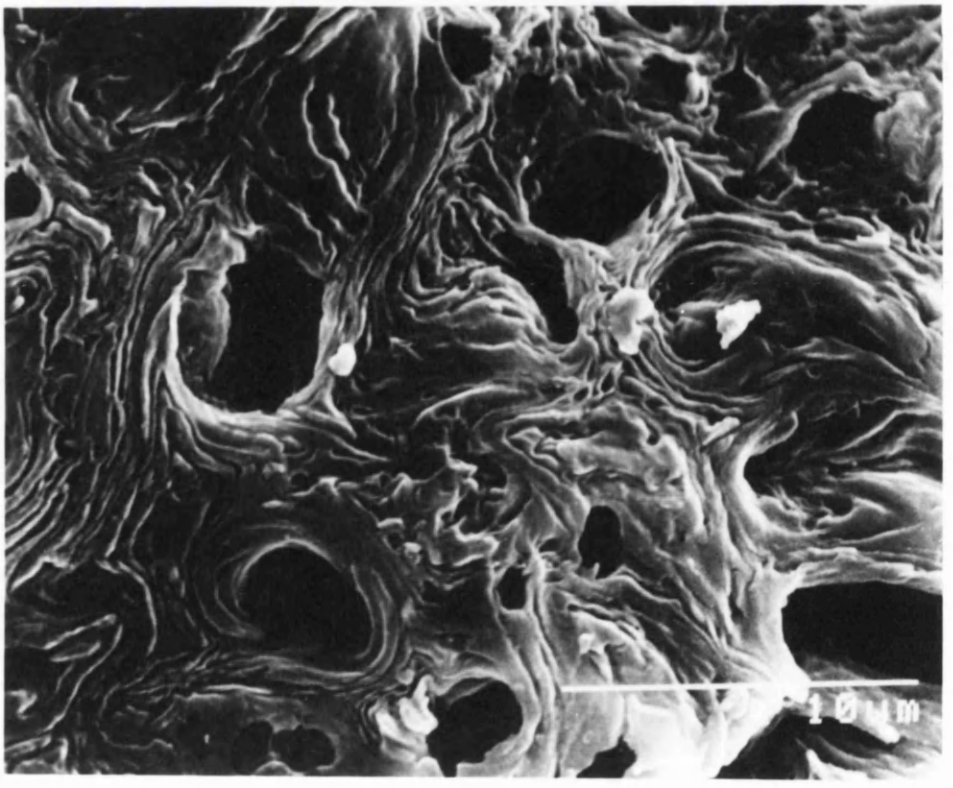

Plate 2. Typical layered surface texture of an oil carbonaceous particle.

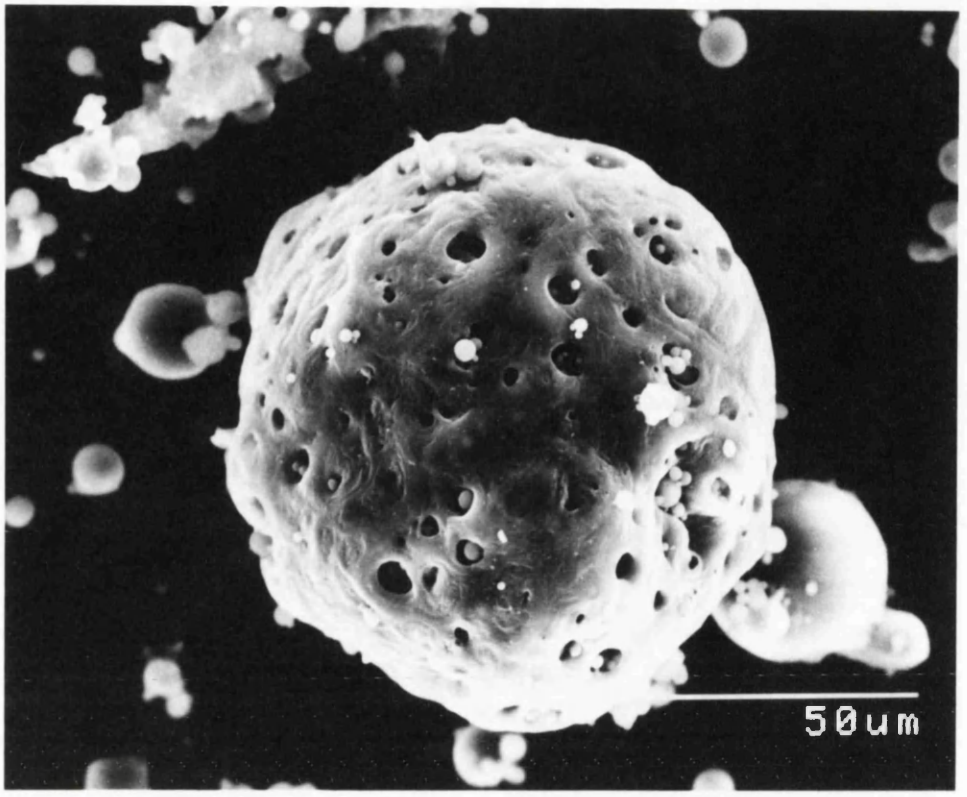

Plate 3. Carbonaceous particle derived from coal combustion (Didcot).

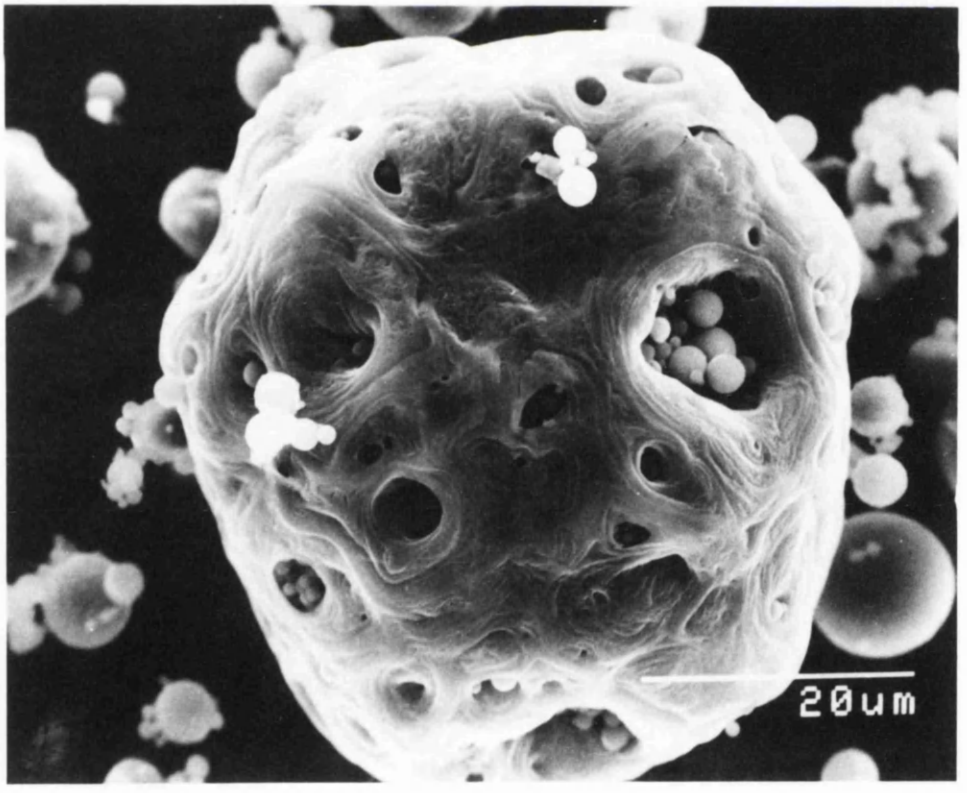

Plate 4. Carbonaceous particle derived from coal combustion (Drax), showing surface texture usually indicative of an oil origin.

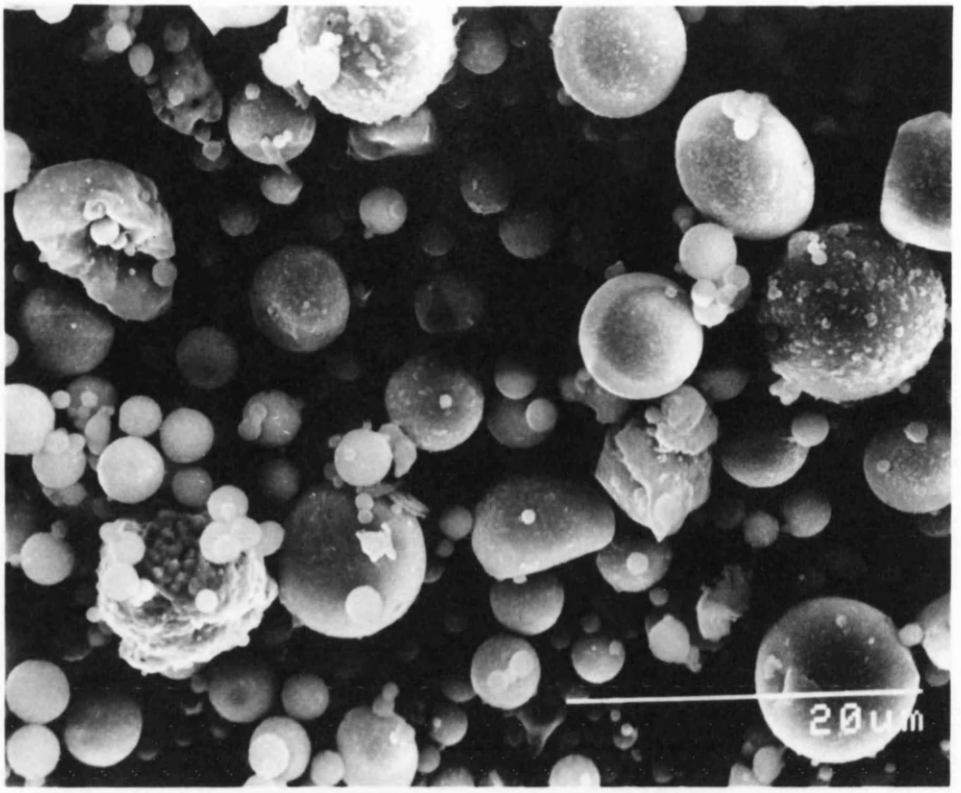

Plate 5. Inorganic ash spheres from coal combustion (Drax).

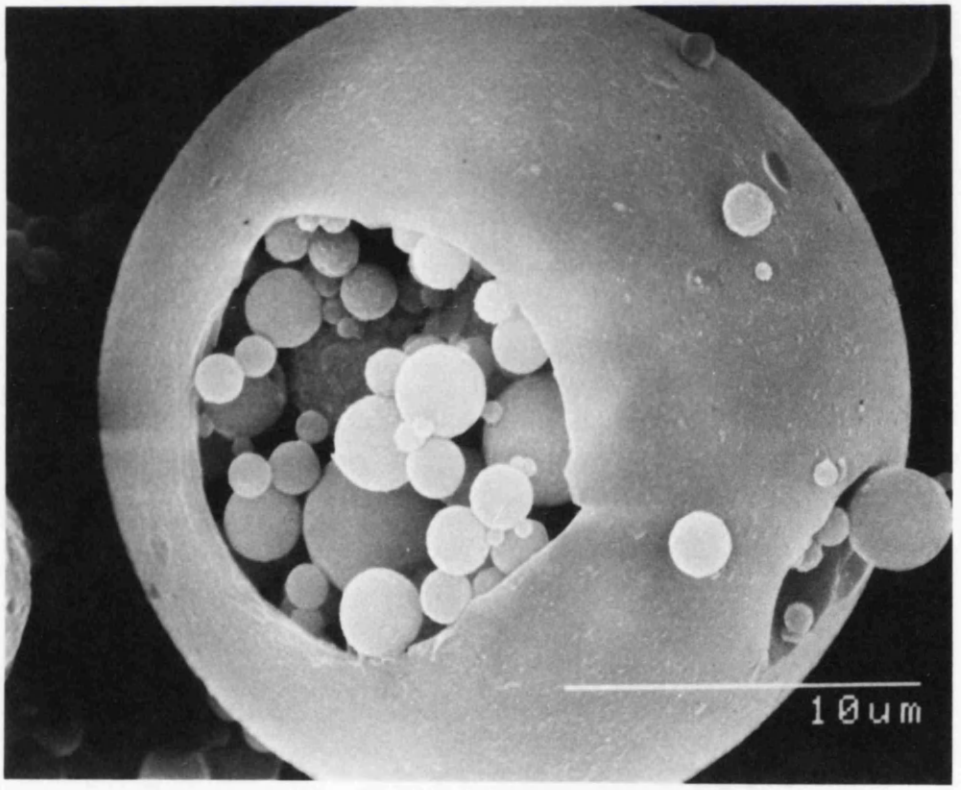

Plate 6. Ash cenosphere filled with smaller spheres formed by non-uniform heating of the original mineral particle.

CHAPTER 2. SITES AND METHODS.

2.1. Site selection.

2.1.1. Sites for spatial distribution studies.

For a study of the spatial distribution of carbonaceous particles in Scotland it was necessary to have a large number of sample sites. A total of 94 sites distributed over the country, (including two in the north Pennines), giving a roughly even coverage (see Figure 2.1), were used. These samples came from a range of sources:

i) Many sediment cores have been taken and archived from a number of lochs in Scotland by the Palaeoecology Research Unit (PRU) at U.C.L., especially in areas of high susceptibility to acid deposition. These cores were available for this work and 30 were used in the spatial distribution study.

ii) Sub-samples of surface sediments from cores taken from 16 lochs on the Outer Hebrides and the Shetland Islands were made available by Dr. Keith Bennett of Cambridge University.

iii) 48 new sites in Scotland were selected for this study.

The site selections for the PRU archived material and the samples from Cambridge were beyond the control of this project, but the criteria adopted for the 48 new sites were size (between 2ha and 60ha) and lack of catchment disturbance. After this the practical criterion of access was considered, although some of the more remote sites were visited by helicopter in the autumn of 1989. In regions such as the Grampians in the east of Scotland, the few water bodies available were mainly ornamental lakes in the grounds of large private houses. Although disturbance to these sites may have occurred at times in the past, where this was not recent they were considered suitable for the analysis of surface sediments for present day atmospheric deposition. One advantage is that the history of disturbances at such sites was well known and so they were selected where there was no suitable alternative.

Figure 2.1. Locations of sites for spatial distribution studies. (Numbers refer to Table 2.1.)

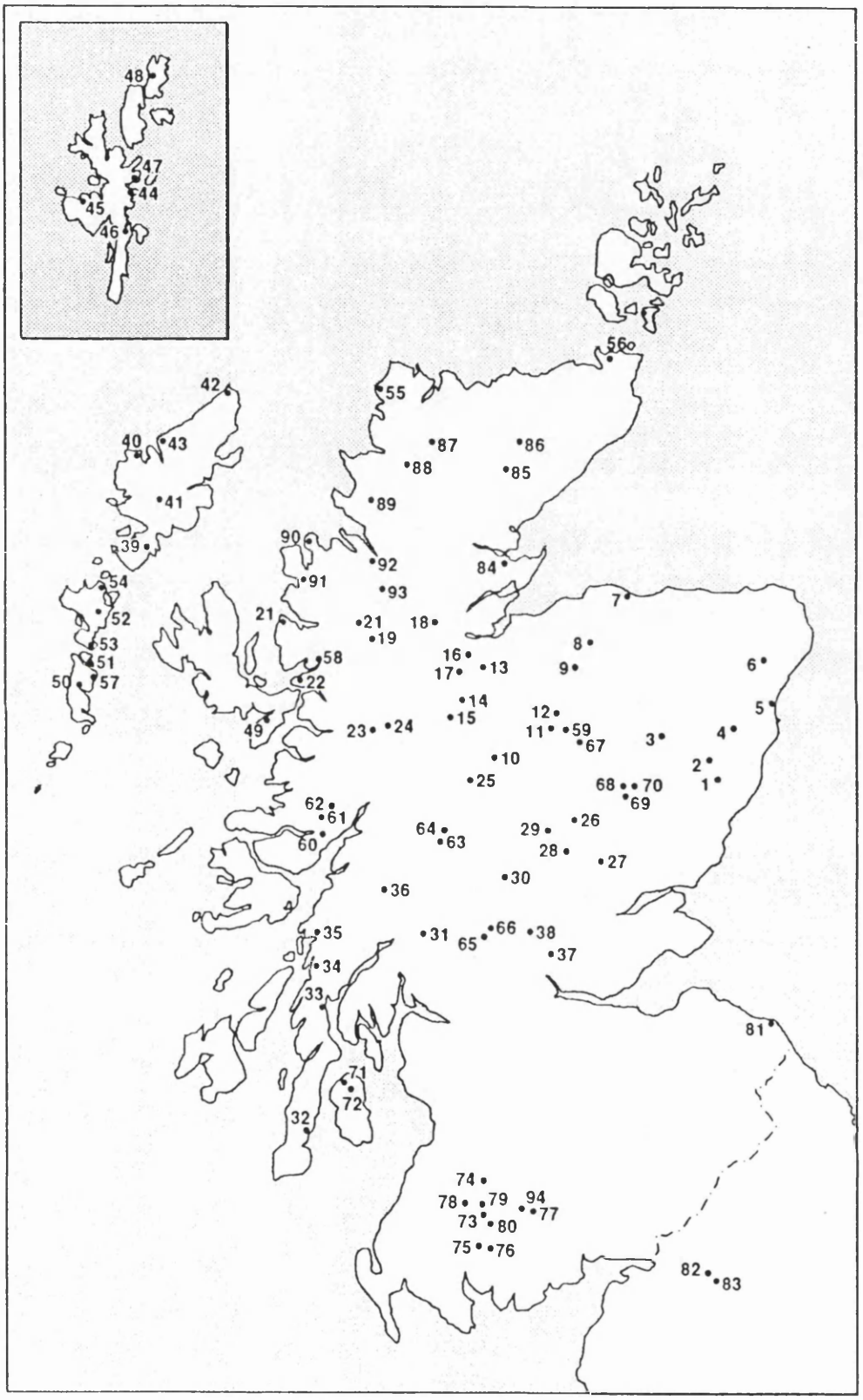

Sediment cores from other sites outside Scotland were also taken during the period of this study, especially in areas of relatively low acid deposition e.g. Western Ireland and mid-Norway. These cores were taken as part of other projects involving the PRU and samples were analysed as a continuation of the spatial distribution mapping for this study. Surface samples from cores taken from sites on the Scilly Isles by Dr. Ian Foster of Coventry Polytechnic were also used. The locations of these sites and others outside Scotland in the British Isles are shown in Figure 2.2.

2.1.2. Sites for temporal distribution studies

To test the characterisation technique using a full sediment core a site was needed in an area where there had been a significant change in the relative quantities of coal and oil burned at high temperatures. Also, to maximise energy dispersive spectroscopy (EDS) efficiency, a site with many particles at all levels would be most suitable, and this is most likely to be in a region which has been industrialised for a considerable time.

London was the area in which much of the early development of the power generation industry in Britain took place and so lake sediments in this region have a long record of atmospheric pollutants. Until the 1950's fossil-fuel combustion in London was almost exclusively coal-based, but after the Second World War an abundance of cheap fuel oil meant that increasingly more power was produced in this way. The first major oil-fired power station in Britain was commissioned in 1952 at Bankside on the River Thames and since then oil-fired generating stations have continued to supply power to London from, for example, the Isle of Grain and Belverdere plants. The ponds on Hampstead Heath in North London therefore fulfil the criteria and three sites were cored. Of these, the Men's Bathing Pond core was selected for this study.

For the other temporal studies, the cores taken at the sites described in section 2.1.1, PRU archived material, and cores taken and analysed for other projects running concurrently with this one have been used and their locations are shown in Figure 2.2.

Figure 2.2. Locations of sites for spatial distribution studies outside the area covered by Figure 2.1., and sites for temporal distribution studies. (Numbers refer to Table 2.1.)

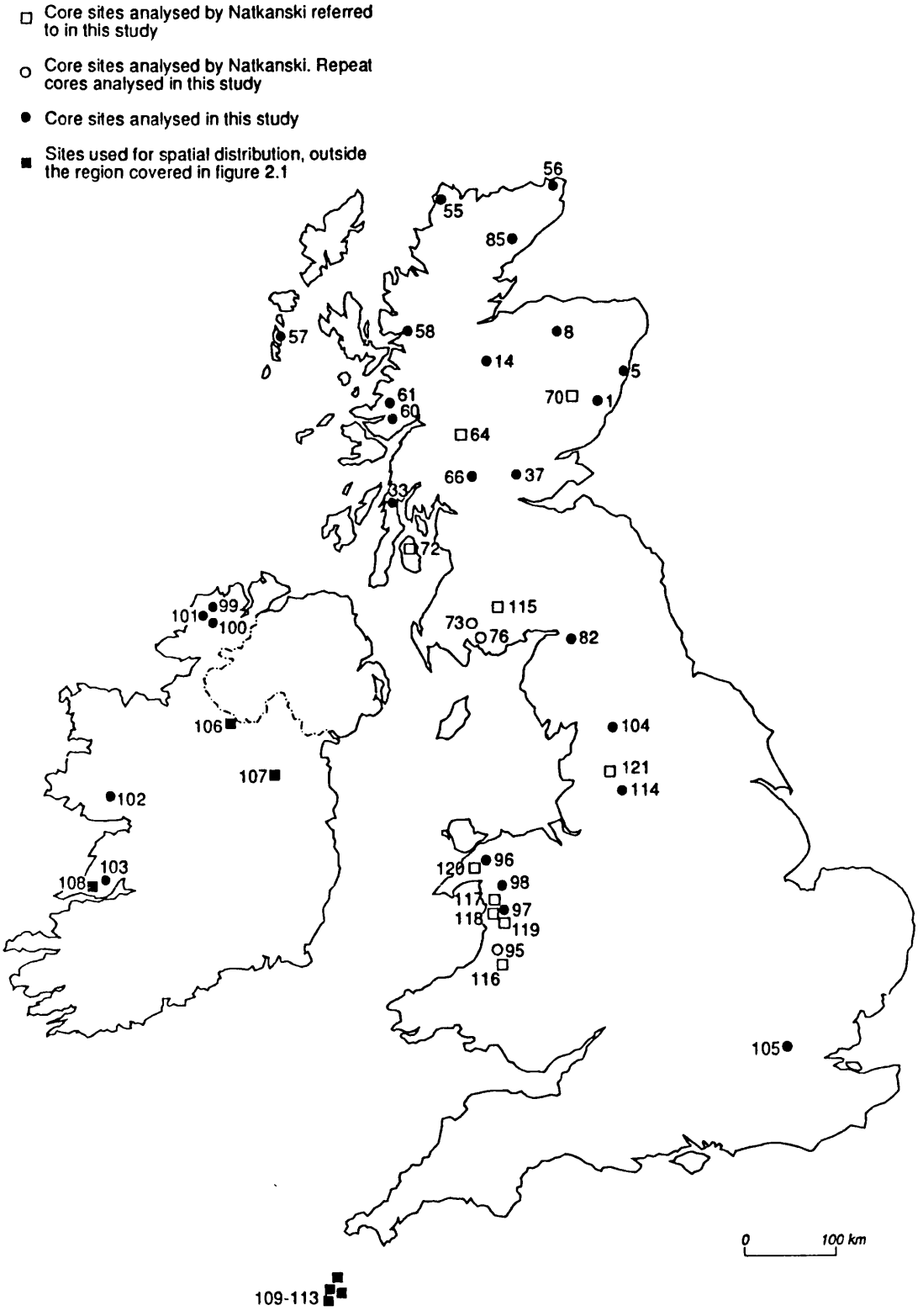

Table 2.1. Site names, grid references, dates of coring and sample sources for the sites shown in the location maps Figures 2.1 and 2.2.

Sources : PRU = PRU archived material, and cores taken for PRU work during the course of this study.
CAM = Dr. Keith Bennett, Cambridge University.
COV = Dr. Ian Foster, Coventry Polytechnic.
* = Cores taken for this study.

= Irish Grid Reference.

No.	Site.	Grid. Ref.	Date.	Source.
1.	Loch Saugh	NO 676 790	12/8/89	*
2.	Unnamed (H)	NO 653 909	"	*
3.	Braeroddach Loch	NJ 482 003	"	*
4.	Policy Loch	NJ 754 075	13/8/89	*
5.	Lily Loch	NJ 920 145	"	*
6.	Kelly Lake	NJ 880 356	"	*
7.	Loch Oire	NJ 287 608	14/8/89	*
8.	Loch Dallas	NJ 092 475	"	*
9.	Loch Mhic Leoid	NJ 008 347	"	*
10.	Loch Etteridge	NN 690 930	15/8/89	*
11.	Uath Lochan	NH 835 018	"	*
12.	Loch Beag	NH 863 093	"	*
13.	Loch a'Chlachain	NH 655 323	16/8/89	*
14.	Loch Bran	NH 506 193	"	*
15.	Loch Tarff	NH 425 100	"	*
16.	Loch Laide	NH 546 355	17/8/89	*
17.	Loch na Ba Ruaidhe	NH 498 330	"	*
18.	Loch Achilty	NH 435 565	"	*
19.	Loch Sgamhain	NH 100 530	"	*
20.	Loch Bharranch	NG 977 575	18/8/89	*
21.	Unnamed (U)	NG 714 590	"	*

Table 2.1. (cont.)

22.	Loch Iain Oig	NG 792 292	"	*
23.	Loch Coire nan Cnamh	NG 974 038	19/8/89	*
24.	Loch Bad an Losguinn	NH 158 038	"	*
25.	Loch Doire nan Sgiath	NN 515 863	"	*
26.	Loch Curran	NO 048 604	20/8/89	*
27.	Stormont Loch	NO 193 423	"	*
28.	Loch na Craig	NN 883 455	"	*
29.	Loch Kinardochy	NN 776 552	21/8/89	*
30.	Lochan Lairig Cheile	NN 558 278	"	*
31.	Loch Restil	NN 228 080	9/9/89	*
32.	Aucha Lochy	NR 726 226	"	*
33.	Loch Arial	NR 810 795	"	*
34.	Loch Leathan	NR 875 983	10/9/89	*
35.	Loch nan Druimnean	NM 845 140	"	*
36.	Lochan na Gealich	NN 048 234	11/9/89	*
37.	Loch Walton	NS 665 867	"	*
38.	Loch Rusky	NN 615 035	12/9/89	*
39.	Loch Idrigill	NG 180 925	6/88	CAM
40.	Loch a Lhighe Bhig	NB 061 307	"	CAM
41.	Loch a Bhuna	NB 170 114	"	CAM
42.	Loch Dibadale	NB 480 613	"	CAM
43.	Loch Dubh Oitheanan	NB 211 386	"	CAM
44.	Dallican Water	HU 337 707	5/89	CAM
45.	Unnamed (7)	HU 249 563	"	CAM
46.	Loch of Roonies	HU 469 524	"	CAM
47.	Loch of the Ward	HU 516 732	"	CAM
48.	Gossa Water	HP 578 057	"	CAM
49.	Loch Gauscavaig	NG 593 107	"	CAM
50.	Loch Lang	NF 807 296	7/87	CAM
51.	Loch an Rubha Dhuibh	NF 826 484	"	CAM
52.	'Horsetail Loch'	NF 867 668	"	CAM
53.	Loch an Faoileag	NF 867 568	"	CAM
54.	Cama-lochan	NF 901 739	"	CAM

Table 2.1. (cont.)

55.	Loch na Larach	NC 217 583	16/6/86	PRU
56.	Long Loch	ND 204 759	18/6/86	PRU
57.	Loch Teanga	NF 818 383	9/87	PRU
58.	Loch Coire nan Arr	NG 808 422	15/6/86	PRU
59.	Coire an Lochan	NH 943 004	20/6/86	PRU
60.	Loch Uisge	NM 808 550	9/6/86	PRU
61.	Loch Doilet	NM 808 678	8/6/86	PRU
62.	Lochan Dubh	NM 895 710	10/6/86	PRU
63.	Loch na h'Achlaise	NN 310 480	17/6/85	PRU
64.	Loch Laidon	NN 380 542	19/6/85	PRU
65.	Loch Chon	NN 422 050	1/4/87	PRU
66.	Loch Tinker	NN 445 068	20/6/85	PRU
67.	Lochan Uaine	NO 001 981	20/6/86	PRU
68.	Loch nan Eun	NO 230 854	22/6/86	PRU
69.	Dubh Loch	NO 238 828	"	PRU
70.	Lochnagar	NO 252 859	"	PRU
71.	Coire Fhionn Lochan	NR 902 459	5/6/86	PRU
72.	Loch Tanna	NR 921 428	"	PRU
73.	Round Loch of Glenhead	NX 450 805	5/84 & 6/88	PRU
74.	Loch Doon	NX 495 985	6/89	PRU
75.	Loch Grannoch	NX 541 691	"	PRU
76.	Loch Fleet	NX 560 697	7/85 & 10/89	PRU
77.	Loch Skae	NX 710 837	6/89	PRU
78.	Loch Kirrimore	NX 373 856	"	PRU
79.	Loch Enoch	NX 445 851	26/6/86	PRU
80.	Loch Dee	NX 470 790	9/86	PRU
81.	Coldingham Loch	NT 895 685	6/86	PRU
82.	Whitfield Lough	NY 724 544	6/89	*
83.	Tindale Tarn	NY 605 588	"	*
84.	Loch Muighbhlaraidh	NH 635 830	23/10/89	*
85.	Loch Dubh Cadhafuaraich	NC 682 183	"	*
86.	Loch na Gaineimh	NC 765 304	"	*
87.	Loch Coire Saidhe Duibhe	NC 450 360	"	*

Table 2.1. (cont.)

88.	Loch Bealich na h-Uidhe	NC 264 256	"	*
89.	Lochan Nigheadh	NC 182 148	"	*
90.	Loch na Beiste	NG 885 943	24/10/89	*
91.	Lochan nam Breac	NG 814 783	24/10/89	*
92.	Loch na h-Airbhe	NH 103 924	"	*
93.	Loch na h-Oidhche	NH 154 778	"	*
94.	Loch Howie	NX 696 834	6/86	PRU
95.	Llyn Hir	SN 789 675	7/84 & 10/88	PRU
96.	Llyn Glas	SH 601 546	1987	PRU
97.	Llyn Irddyn	SH 627 220	5/87	PRU
98.	Llyn Conwy	SH 788 465	"	PRU
99.	Lough Veagh	C 018 212*	5/88	PRU
100.	Lough Muck	B 958 083*	"	PRU
101.	Lough Maam	B 927 159*	"	PRU
102.	Lough Maumwee	L 977 485*	5/88	PRU
103.	Lough Nammina	R 182 710*	"	PRU
104.	Malham Tarn	SD 895 667	10/88	PRU
105.	Men's Bathing Pond, Hampstead Heath	TO 279 865	10/87	PRU
106.	Lough Annagh	H 395 126*	9/89	*
107.	Lough Sheever	N 460 553*	"	*
108.	Lough Inchiquin	R 058 572*	9/89	*
109.	Abbey Pool, Tresco	SV 896 143	1988	COV
110.	Great Pool, Tresco	SV 895 145	"	COV
111.	Porth Hellick, St.Mary's	SV 924 108	"	COV
112.	Big Pool, Bryher	SV 874 148	"	COV
113.	Big Pool, St. Agnes	SV 878 086	"	COV
114.	Tunnel End Reservoir	SE 037 121	3/6/89	PRU
115.	Loch Urr	NX 760 845	1984	PRU
116.	Llyn Gynon	SN 800 647	5/85	PRU
117.	Llyn y Bi	SH 670 265	"	PRU
118.	Llyn Dulyn	SH 662 244	8/85	PRU
119.	Llyn Cwm Mynach	SH 678 238	5/85	PRU

Table 2.1. (cont)

120.	Llyn Llagi	SH 649 483	8/85	PRU
121.	Watersheddles Reservoir	SD 965 382	5/86	PRU

2.2. Coring techniques

Short sediment cores were taken from the 48 new sites using a Kajak gravity corer (Kajak, 1966), in the summer of 1989. These cores were extruded vertically in the field in 0.5cm slices down to 5cm, and then 1cm slices to the bottom of the core. The samples were stored in plastic Whirlpak bags until they were returned to the laboratory.

The archived cores were taken with either a Kajak corer, a Mackereth mini-corer (Mackereth, 1969), or a modified piston corer between 1986 and 1988, and the sediment cores from the Outer Hebrides and Shetland Islands were taken using a Livingstone piston corer (Livingstone, 1955), in 1988/89. The Hampstead Heath Pond core was taken in October 1987 using a modified Livingstone corer.

2.3. Laboratory methods

2.3.1. Sediment analysis

For wet density measurements, each sediment sample was homogenised and a sub-sample packed into a weighed $2cm^3$ vial. Dry weight determinations were made by placing a sub-sample in a weighed crucible and drying in an oven at 105°C until constant weight was achieved. To determine loss on ignition values, the crucible was placed in a muffle furnace at 550°C for two hours. In each case the crucible was allowed to cool in a desiccator before each reweighing. Dried sediment was used for the particle extraction methods described below.

2.3.2. Dating techniques.

Where sediment cores were dated, this was done in the Department of Applied Mathematics and Theoretical Physics at the University of Liverpool using gamma

spectrometry to analyse for ^{210}Pb, ^{226}Ra, ^{137}Cs and ^{241}Am (Appleby et al., 1986).

The ^{210}Pb and the ^{226}Ra data can be used to calculate the age of each sample given various assumptions. The total ^{210}Pb in lake sediments has two components, 'supported' ^{210}Pb derived from the decay of the parent isotope ^{226}Ra, and 'unsupported' ^{210}Pb derived from the gaseous intermediate ^{222}Rn. The CRS (constant rate of supply) model (Appleby & Oldfield, 1978) assumes that unsupported ^{210}Pb supply to the lake is dominated by atmospheric fallout, resulting in a constant rate of supply of ^{210}Pb to the sediment regardless of changes in accumulation rate. Where significant sediment focusing occurs, such as at the Hampstead Heath site (see Chapter 4), the CIC (constant initial concentration) model may be applicable. This assumes a constant initial concentration of unsupported ^{210}Pb per unit dry weight at each stage of accumulation, despite variations in accumulation rates.

Lake sediments also contain a record of radio-isotope fallout from the testing of atomic weapons. The activity of ^{137}Cs in a sediment profile reflects the fallout pattern, starting in 1954 and peaking in 1963. However, where lake waters are acid and the sediment highly organic ^{137}Cs is highly mobile within the sediment column resulting in a shift in the start and peak positions in the profile. In such cases ^{241}Am can provide an alternative, as it too is derived from nuclear fallout and is far less mobile in the sediment record than ^{137}Cs.

These methods have been applied to various sediment cores used in this study, and where necessary the details of the isotope profiles are dealt with in the relevant sections.

2.4. A method for the extraction of carbonaceous particles from lake sediment.

The first aim of this work was to develop a sensitive technique for carbonaceous particle extraction suitable for use even at low concentrations, by removing unwanted sediment fractions by selective chemical digestion. Neither of the two existing methods described in the literature met these requirements.

The method described by Renberg and Wik (1984) is insensitive at low particle

concentrations due to the amount of residue left at the end of the digestion, and counting at x50 is inadequate to identify particles in the <10μm fraction.

The method used by Griffin & Goldberg (1975) is not appropriate since it deals with all charcoal, not just spheroidal particles produced from high temperature combustion. In addition, the results are expressed in per cent carbon by weight, rather than by particle concentration, and only the >38μm fraction is considered, which excludes many smaller particles and preferentially those which are oil derived. However, this method reduces 10g of dried Lake Michigan sediment to 10-30mg of some of the more persistent minerals, primarily pyrite (FeS_2), rutile (TiO_2), zircon ($Zr(SiO_4)$), and, most importantly, elemental carbon. It involves a more complete digestion than that of Renberg and Wik and is therefore the basis of the method used here.

2.4.1. Laboratory procedure.

1) Place 0.2g of dried sediment in a covered 250ml beaker. Add 30ml 6M KOH and 4ml 30% H_2O_2. Leave overnight, centrifuge at 2,000 rpm for 5 minutes and then wash the residue with distilled water and return to the beaker.

   This stage breaks up the sediment for further reaction and removes some of the organic and humic fractions.

The use of 10g of dried sediment and large quantities of reagents is unnecessary. As replicate digestions were needed, 0.2g of dried sediment was used and the reagent quantities reduced to match. Griffin and Goldberg used ultrasonic dispersion to break up the sediment in the early stages of their digestion. However, carbonaceous particles are fragile and the use of ultrasonic dispersion can cause fragmentation. As Griffin & Goldberg eventually ground up the residue for infra-red analysis this was not important. In estimating particle concentrations, however, it is essential that particle damage is minimised during preparation.

2) Add 30ml 6M HCl to the residue. Heat on a hotplate at 80°C for 2 hours. When cool, centrifuge and wash as before.

This stage removes the HCl soluble salts, such as carbonates and bicarbonates, and removes the soluble materials which may form insoluble fluorides in the next step.

3) Transfer the residue to PTFE beakers (with PTFE lids). Add 20ml 40% HF and heat on a hotplate at 150°C for 3 hours. Wash as before.

   This stage breaks down the siliceous minerals and removes the silicon as SiF_4. The time was reduced by changing this step from 6 days at room temperature to 3 hours at 150°C, effectively halving the length of the procedure.

4) Return the residue to the 250ml beakers. Add 30ml 6M HCl and heat on a hotplate at 80°C for 2 hours. Wash the residue again.

   This step removes any fluorides formed in the last step.

5) Add 20ml 6M KOH and 25ml 30% H_2O_2 in 5ml aliquots, to the residue. Leave overnight in an oven at 55°C. Cool and wash the residue.

6) Transfer the residue to a 25ml beaker and add 4ml 6M KOH and 1ml 30% H_2O_2. Leave overnight in an oven at 55°C. When the reaction is complete, cool and wash again.

   Steps 5 & 6 remove the remaining organic and humic matter.

7) Add 10ml 6M HCl and heat on a hotplate for 2 hours at 80°C. Wash again. Transfer the residue to a storage vessel.

Preparation was carried out in a clean room and all containers were kept covered to stop possible atmospheric contamination.

2.4.2. Density separations.

Further extraction of the material by density separation was considered, but due

to the high variability of 'apparent' density of the carbonaceous particles (due to varying pore size and internal gas pockets), this idea was discarded. Also, although the minerals remaining at the end of the digestion have a higher density than that of elemental carbon, there is a sufficiently small amount of them that it is not worth the extra time and potential loss of recovery to include a density separation in the standard digestion technique.

2.4.3. Filtration.

Occasionally after completing the digestion fine, amorphous, black material is present in some layers which can cause problems in the counting stage by obscuring the shapes of the particles. This material does not always occur in proportion to carbonaceous particle concentration as there is sometimes little in the surface layers. Therefore, it seems that it does not have the same origin as the particles. It has been thought it may be a precipitation product of the digestion technique itself (Renberg pers. comm.), or a product of some other form of combustion such as domestic burning, engine exhausts etc.. As this material is fine, it may be removed by filtration. This will enable a higher fraction of the residue to be counted, increasing repeatability, as well as making counting easier. However, filtration also removes the smaller carbonaceous particles and 10μm and 5μm filters reduce the recovery rate to 40% and 65% respectively. As carbonaceous particles from oil combustion are usually smaller than those from coal, this approach may selectively remove oil particles from the residue, making filtration of limited use and consequently it is not used in this extraction method.

2.4.4. Counting.

A known fraction of the remaining residues was evaporated onto coverslips. These were then mounted using 'Naphrax' diatom mountant, and the whole of each coverslip counted at x400 using a light microscope. Random views were not used, as at the base of the particle record, where there were extremely few particles to be counted on the whole coverslip, this raised the limit of detection. The method of adding a known amount of polystyrene microspheres and calculating the number of carbonaceous particles from the ratio (Battarbee & Kneen, 1982) was found to

have high errors, especially at low concentrations.

2.4.5. Repeatability.

To see if separate digestions of a sediment sample would give the same particle concentrations, 5 replicate digestions were done from 3 different sediment levels, followed by triplicate counts from each digestion. This gave 15 concentrations for each level from which the standard deviation and 95% confidence limits on the statistical counting error were calculated. The results are shown in Table 2.2.

Table 2.2. *Means, standard deviations and 95% confidence limits for 15 carbonaceous particle counts from each of three levels. All values are numbers of particles per gram dry mass of sediment (gDM^{-1}).*

Level(cm)	Counts			Mean	S.D.	95% C.L.
0-0.5	61280	73390	69000	70070	6400	68040-
	68130	75690	74800			71660
	66070	70140	74500			
	55270	66380	66120			
	75270	76430	78660			
4.5-5	41980	40970	52240	45950	4930	43980-
	33620	45710	46430			47760
	45420	46760	48300			
	52030	42960	47820			
	44100	46000	51870			
11.5-12	8940	8350	8470	8300	1020	7460-
	6480	7610	9610			9030
	8240	8890	8500			
	7430	10440	8130			
	6820	7740	8910			

2.4.6. Recovery rate.

A suspension of known carbonaceous particle concentration was made by adding a small amount of oil-fired residue from a power station to water and homogenising. A known fraction was then removed and counted at x400 under a light microscope. The concentration of the particles in suspension could then be calculated. A known number of particles from this suspension were added to a sediment sample before digestion. This sample was from below the start of the particle record (30-31cm) in a core from Loch Tinker and it could be assumed that no carbonaceous particles were present within it. After the digestion, the number of particles was counted as before and compared with the number added to give a recovery rate. These digestions were done in triplicate and the recovery range was 93.9% -100.1%, showing that very few particles are lost during the digestion. This is confirmed by examining the supernatant fraction using SEM. The residue showed no particles of any size to be present in this fraction at any stage of the digestion.

Blank digestions involving no sediment were also performed to check on atmospheric contamination and cross contamination from other digestions. These showed that as long as the digestion vessels were kept covered and reasonable precautions taken in manipulating the digestion material, no atmospheric or cross contamination occurred.

One potential source of contamination is from the smearing of surface sediments down the inside of the core tube upon coring. This pushes sediment from layers rich in carbonaceous particles down into pre-industrial depths. Carbonaceous particles have been seen in very old sediment and as these particles are not formed by any 'natural' processes, this seems to be the only explanation. This was tested by preparing digestions from a sediment layer just below the start of the carbonaceous particle record, (e.g. 30-31cm depth in Loch Tinker). Duplicate digestions were performed on samples taken from the middle of the sediment slice and from around the edges. For the 'within-slice' digestion, only one particle was found in four separate counts (a value of about 8 particles per gram dry mass) but particles resulting in a value of about 200 particles gDM^{-1} were counted on the 'slice edge' samples. This shows smearing does take place, and could have a significant effect

on particle number calculations in the lower levels of a sediment profile, demonstrating the need for 'trimming' core slices.

2.4.7. Detection limit.

The Renberg and Wik method removes only the organic fraction from the sediment, leaving a large amount of material at the end of a digestion. Therefore, unless a very long time is spent counting each sample, only a small fraction of the residual material will be counted and the limit of detection will be quite high, i.e. if only 1 particle is counted in the residual sample fraction, the result is a value of 80-100 particles per gram dry mass.

Using the method described above, the material remaining after digestion is predominantly carbonaceous. Therefore, at the bottom of the particle record, very little material remains and so 100% of this material could be counted in a short space of time. As approximately 0.2g of dried sediment is used for the digestion, if 1 particle is counted, this gives a detection limit of approximately 5 particles per gram dry mass, at least a ten-fold improvement on the older method.

2.4.8. Application to a sediment core.

The digestion method was then applied to a sediment core taken from Loch Tinker in the Trossachs region of Western Scotland. The carbonaceous particle record had previously been counted using the Renberg and Wik method so a comparison between the two methods could be drawn. The core was also dated using ^{210}Pb and the results are shown in Figure 2.3. There are several points to note:

i) The basic trends are the same for both methods, i.e. the carbonaceous particle record begins in the early 1800's and there is a large rise in concentration after the 1940's.

ii) As the method described removes more unwanted material, a higher percentage of the original sediment is available to be counted after digestion, and this improves particle counting accuracy. Using a higher magnification, x400 as opposed to x50

Figure 2.3. Comparison of the two methods of extraction for carbonaceous particles from Loch Tinker sediments (Core TIN1).

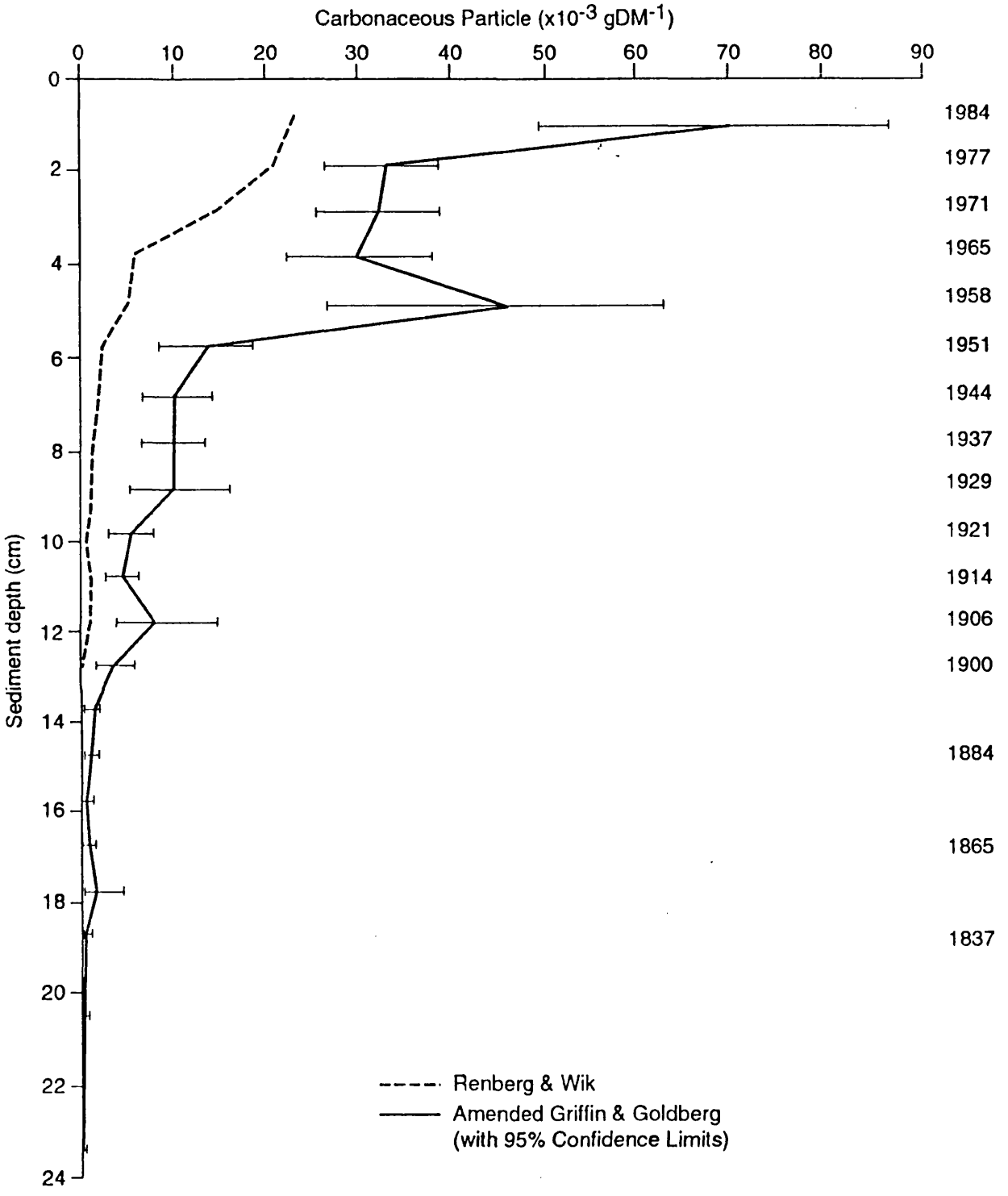

means that carbonaceous particles down to 1μm are included. Using x50 magnification, only particles down to 10μm can be counted (Renberg & Wik, 1984, 1985a, 1985b; Wik & Renberg, 1987; Darley, 1985), and because of this, at the top of the core, particle concentrations using the method described are higher than those when using the Renberg & Wik method.

Lower down, at and below the point where the limit of detection for the Renberg & Wik method is reached, the particle concentrations using the method above become lower, due to better sensitivity. This is best illustrated in an expanded bottom section of the sediment profile (Figure 2.4).

2.4.9. Discussion

The method described has a number of advantages over previous methods used to extract carbonaceous particles from sediments. It is more accurate and has a lower detection limit than the Renberg and Wik method previously used on British lakes, and it is quicker and involves less risk of fragmentation of the particles than the Griffin and Goldberg method upon which it is based.

Although the majority of the residue at the end of the digestion is carbonaceous material, some minerals do survive albeit in low concentrations. This includes some silicates, and even one or two siliceous spheres may appear in the residue, due to particles being washed in from the beaker walls after the hydrofluoric acid digestion step. This is not particularly important as the remaining non-carbonaceous material is sufficiently different both chemically and morphologically, that the counting and EDS procedures will not be confused by their presence.

This extraction method is summarised in Rose (1990a).

2.5. An extraction technique for inorganic ash spheres from lake sediments.

Little work has been done on a chemical extraction of inorganic ash spheres from either soils or sediments. Most authors rely on a magnetic extraction (Marvin & Einaudi, 1967; Nriagu & Bowser, 1969; Oldfield et al., 1978, 1981), or magnetics

Figure 2.4. Expanded bottom section of Loch Tinker carbonaceous particle profiles to show comparison of detection limits for the two methods.

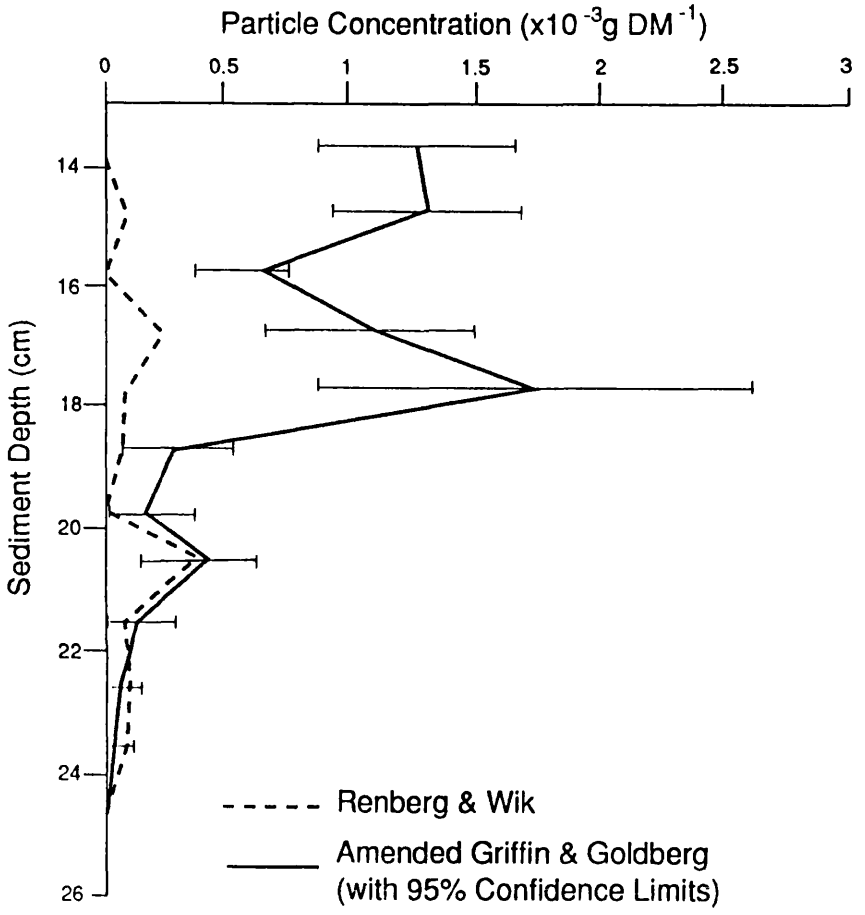

coupled with dilute hydrochloric acid to remove the calcareous fraction (Puffer et al., 1980). Not all inorganic ash spheres are magnetic and so these methods are only partial extractions. Deuser et al. (1983) used dilute hydrochloric acid to remove the calcareous fraction of sediment trap material, where this represented over 60% of the total and found that this was sufficient to enable a chemical study of the trapped spheres. In lake sediments, however, this would not be the case.

These ash spheres are formed from the inorganic material present within the fossil-fuel and so they are mostly aluminosilicate in composition with varying amounts of iron. This and other chromophore elements such as calcium and manganese (Ramsdon & Shibaoka, 1982) give the spheres colours from yellow and red to dark brown and black. Hence they have a similar chemistry to many of the lake sediment minerals from which they are to be extracted and this restricts the range of reagents that can be used. For example hydrofluoric acid (HF), used in other extractions to remove silicates as SiF_4, is very effective at dissolving the silicate ash and even at low concentrations such as a 1% solution, will etch the surface of the spheres to reveal the underlying structure (Hullett & Weinberger, 1980). However, it is possible to remove some fractions of the sediment without damaging the inorganic ash spheres.

2.5.1. Organic material.

This can be removed by using 30% hydrogen peroxide (H_2O_2), at about 50-60°C until effervescence ceases. Basic peroxide (a mixture of 6M KOH and 30% H_2O_2) and nitric acid are more effective oxidants than H_2O_2 alone, but these also damage the ash particles.

2.5.2. Biogenic silica.

Biogenic silica (that which is biologically incorporated e.g. diatom frustules and chrysophyte cysts) can be removed from other forms of silica, such as mineral silica and non-crystalline or amorphous silica (including inorganic ash) by preferential digestion. Wet alkaline extractions are best for this purpose (Krausse et al., 1983), as other methods such as fusion and mineral acid attacks are not selective for

different forms of silica.

Trials performed on lake sediment spiked with coal-fired power station ash (to ascertain the extent of etching on the spheres), compared the effectiveness of different concentrations of sodium carbonate (Na_2CO_3) and sodium hydroxide (NaOH) at dissolving biogenic silica. Silicate analyses (Goltermann et al., 1970) were performed on sub-samples removed at intervals from the digestion supernate. When the dissolved silicate concentration stopped increasing, this represented the end of biogenic silica dissolution (Figure 2.5). In most cases, interference from mineral sources is insignificant compared to the quantity of biogenic silica (Krausse et al., 1983), but were this not the case, the dissolved silicate concentration would keep increasing with time rather than levelling off. It can be seen from Figure 2.5 that for 0.3M NaOH (the most effective solution) at 100°C, this levelling off occurs after about 2 hours. No etching of the ash particles occurs until after 6 hours.

2.5.3. Carbonates.

The strongest acid attack that dissolves carbonates and bicarbonates, but leaves the ash spheres unaffected was found to be 3M HCl at 80°C for 2 hours.

2.5.4. Mineral silica.

Various techniques were tried to remove silicate mineral species from the inorganic ash. Fluorosilicic acid (H_2SiF_6), preferentially removes feldspars and certain other minerals from quartz, but this also severely etched the ash spheres. Pyrosulphate ($Na_2S_2O_7$) fusions (Chapman et al., 1969; Kiely & Jackson, 1965), digested the ash spheres as well as the minerals leaving only quartz grains, but as a 2M solution there was no effect on either ash spheres or silicate minerals. The same occurred for pyrophosphate ($Na_4P_2O_7$) digestion attempts. No satisfactory separation was achieved for mineral silicate and the ash spheres.

2.5.5. Magnetic separation.

This can be achieved either by repeatedly swirling a covered magnet in a

Figure 2.5. Dissolution profile of biogenic silica in 0.3M NaOH at 100°C.

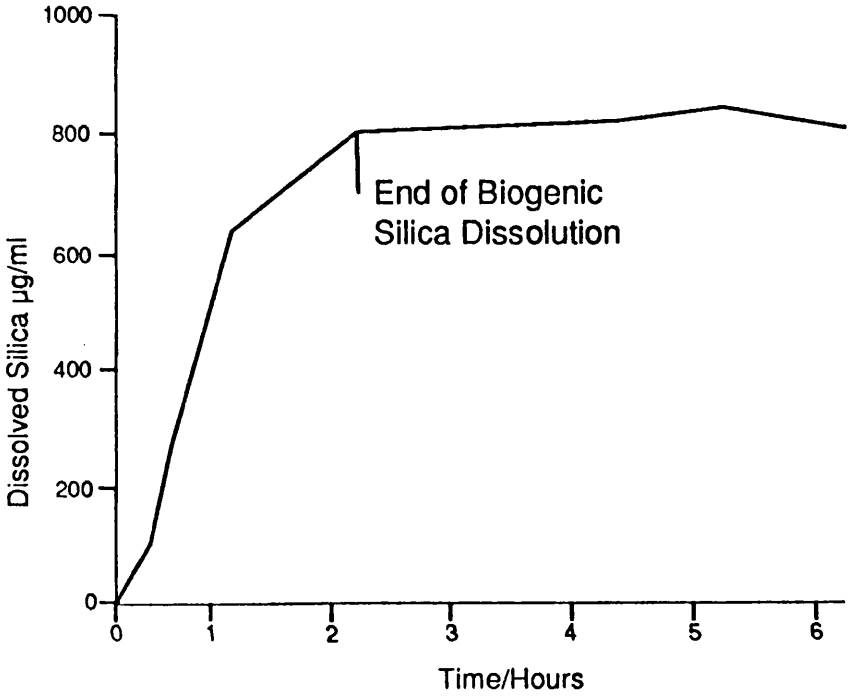

suspension of the sediment, until no more magnetic particles are removed (Nriagu & Bowser, 1969), or by using a more sophisticated technique, such as an automated self-circulating magnetic separator (Munro & Papamarinopoulos, 1978). Both methods, however, only give a partial extraction, as not all ash particles contain ferrite ($Fe_{2.3}Al_{0.7}O_4$) the magnetic component of fly-ash (Hulett et al., 1980).

2.5.6. Density separations.

Inorganic ash spheres found in lake sediments have a density of greater than 1g/cm^3. Density studies of ash from power stations (Watt & Thorne, 1965) show that virtually no particles have a density greater than 2.9g/cm^3 and so heavy minerals can be separated by using heavy liquids such as 1,1,2,2- tetrabromoethane (TBE) [$(CHBr_2)_2$] or sodium polytungstate [$3Na_2WO_4.9WO_3.H_2O$]. The greater than 2.9g/cm^3 fraction removed from lake sediment, when viewed under SEM reveals large angular mineral grains. No spheres were noted at all.

Sodium polytungstate has the advantages over TBE of being non-toxic and non-corrosive. Its density is adjustable up to 3.1g/cm^3, it is neutral in aqueous solution and stable in the pH range 2-14. It is very easy to handle, but quite viscous at higher densities and so a centrifuge is required for effective separation.

2.5.7. Laboratory procedure

The digestion is in four steps:

1) Place 0.2g of dried sediment in a 250ml beaker and add 50ml 30% H_2O_2. Once the initial reaction has died down, place in an oven at 55°C and leave overnight. If, after this, there is still effervescence, add another 10ml H_2O_2 and return to the oven. Once reaction is complete, cool, centrifuge at 2,000 r.p.m. for 5 minutes to settle the residue, and wash in distilled deionised water.

2) Return the residue to the beaker and add 50ml 0.3M NaOH. Heat at 100°C for 2½ hours (including heating up time). Cool, centrifuge and wash as before.

3) Density separation.

a) with TBE. (density = 2.96g/cm^3)

i) Wash the residue with acetone to remove the water, as water and TBE are immiscible. Remove as much of the supernatant as possible.

ii) Add 2ml TBE to a glass centrifuge tube and carefully add the sediment residue.

iii) Centrifuge at 500 r.p.m. for 2 minutes.

iv) Discard the >2.96 fraction.

v) Wash the <2.96 fraction in acetone to remove the TBE and then in water to remove the acetone.

b) with sodium polytungstate (density adjusted to 2.96g/cm^3)

i) Remove as much supernatant water from the residue as possible.

ii) Add 2ml polytungstate to a centrifuge tube and carefully add the residue.

iii) Centrifuge at 500 r.p.m. for 2 minutes.

iv) Discard the >2.96 fraction.

v) Wash the lighter fraction in distilled deionised water.

NB. Both TBE and polytungstate are recoverable from these methods.

4) Transfer the residue to a 100ml beaker, add 30ml 3M HCl and heat for 2 hours at 80°C. Wash and centrifuge.

2.5.8. Counting.

A known fraction of the final residue is evaporated onto a coverslip, mounted with Naphrax and the particles on the whole coverslip counted at x400 using a light microscope. Polystyrene microspheres (Battarbee & Kneen, 1982) were not used due to their similar appearance to the ash spheres. A known concentration of exotic spores could be added to count in this way, but due to low concentrations, large errors would be introduced lower down the core.

2.5.9. Repeatability.

The repeatability was tested in the same way as for the carbonaceous particle extraction method above. The results are shown in Table 2.3.

2.5.10. Recovery rate.

A suspension of known inorganic ash sphere concentration was made up by adding a small amount of residue from a coal-fired power station to water. After homogenisation a known fraction was then removed and counted at x400 under a light microscope, to calculate the concentration of the suspension. A known volume

Table 2.3. Means, standard deviations and 95% confidence limits of 15 inorganic ash sphere counts from each of three levels. All values in $(gDM)^{-1}$.

Level(cm)	Counts			Mean	S.D.	95% C.L.
4.5-5	267700	282000	294300	257300	21500	250497-
	219600	243800	240600			262360
	238600	248800	273100			
	272400	222100	261600			
	255200	272700	267500			
11-11.5	54240	56280	61170	56700	2760	53462-
	56900	55420	53910			59345
	60310	58510	60180			
	59350	58030	52830			
	53210	55950	54230			
22-23	12230	11670	12740	12530	1250	11322-
	11410	11920	9700			13784
	14080	12780	13450			
	12370	12210	11990			
	12570	14870	13970			

of the homogenised suspension was then added to a sediment sample before digestion. The sediment sample was from 100-101cm depth of Loch Tinker, a level which had been previously counted and had only a 'background' value of ash spheres. After the digestion, the particle concentrations were counted as before and the value compared with the number of particles added to give a percentage recovery. These digestions were done in triplicate and the recovery range was 82% - 102% .

Blank digestions show that no atmospheric or cross contamination from other digestions need occur as long as reasonable precautions are taken. Petri-dishes left in the open laboratory show that atmospheric contamination could cause false results at low concentrations. One source of contamination could again be core smearing, but as discussed in section 2.4.6 this can be avoided by core trimming.

2.5.11. Detection limit.

Due to the reagent restrictions outlined above, at the end of the digestion there is still quite a lot of material present, only a fraction of which is made up of the inorganic ash spheres. Consequently, the limit of detection for this method is quite high at about 180-200 particles gDM^{-1}, although particle numbers are rarely this low, due to non-industrial input of spheres.

2.5.12. Application to a sediment core.

The technique was then applied to a sediment core taken from Loch Tinker. The results appear in Figure 2.6.

The basic trend of the profile is similar to that of the carbonaceous particle profile produced for Loch Tinker, especially in the top 5cm. The main difference between the profiles is the continuous background value of the inorganic ash, whereas the carbonaceous particle record falls to zero at 24-25cm depth. Below this, the inorganic ash record is fairly uniform and low, between 2,000 and 3,500 gDM^{-1}. If this record is attributable to a constant background flux from non-industrial sources

Figure 2.6. Inorganic ash sphere profile for Loch Tinker (core TIN1) and comparison with carbonaceous particle profile.

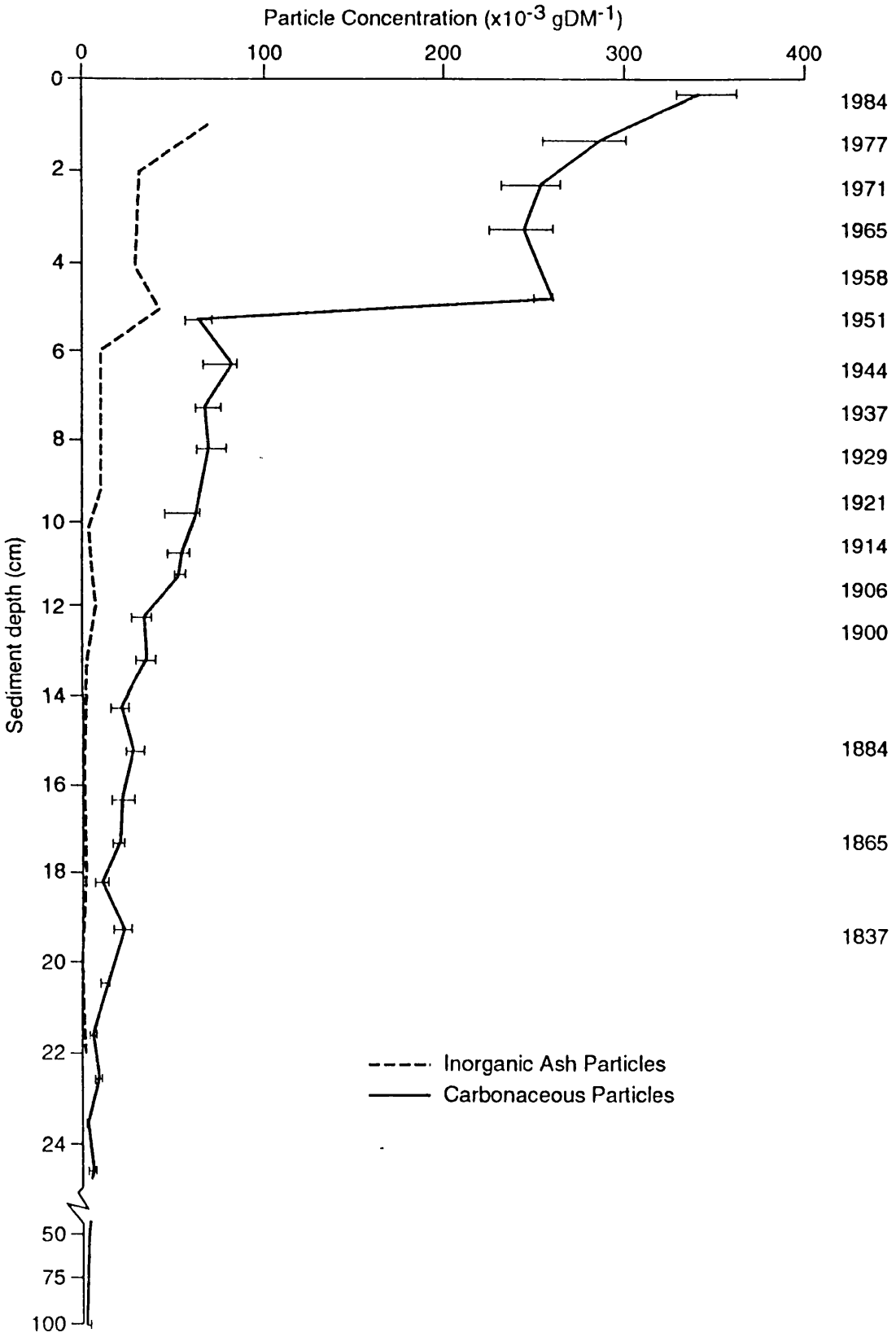

through time, the start of the 'industrial' ash sphere record can be identified and occurs at approximately the same depth/date as the carbonaceous particle record.

Marked changes in the pre-industrial background concentration of particles may be related to significant changes in sediment accumulation (causing dilution), or to changes in atmospheric flux e.g. following a volcanic eruption. The identification of such events using this technique may be of additional palaeoecological or chronological value.

This extraction method is summarised in Rose (1990b).

2.6. Reference Material.

Reference samples from sources of fly-ash particles were obtained in order to develop a reference data set upon which to base a classification scheme. The details of these reference samples are given in section 3.4.

2.7. Energy Dispersive Spectroscopy (EDS).

EDS was used to determine the surface chemistry of carbonaceous particles. Measurements on particles from known sources were used to develop a fuel-type characterisation, before similar measurements on particles of unknown origin were used in the characterisation scheme to determine potential sources. This technique and alternatives to it are described more fully in Chapter 3.

2.7.1. Sample preparation.

At the end of the carbonaceous particle extraction (section 2.4.), the particles were left as a suspension in water. A few drops of this suspension were added to the top of a column of alcohol and allowed to spread for a few seconds before being drawn through a 0.4μm Nuclepore filter. These filters provide an excellent substrate for this type of analysis because the particles are retained on the surface, rather than being absorbed into the filter. Also, the organic composition of the filter does not add any detectable X-ray peaks to the spectrum produced.

The filter samples were mounted onto glass slides using colloidal graphite paint and coated with a thin layer of carbon by evaporation in a vacuum. This forms a conducting layer over the particles and prevents the build-up of charge on the specimen in the scanning electron microscope (SEM). Carbon is used rather than a metal coating because it does not complicate the X-ray spectrum with additional peaks.

2.7.2. EDS of carbonaceous particles.

A JEOL 733 Superprobe (with Link Analytical AN10000 computer and EDS detector) at Imperial College London was used for this study as both morphology and chemistry (X-ray data) may be examined. Use is made of three detected signals: secondary electrons, backscattered electrons and X-rays. Particles can be analysed manually (i.e. one at a time) by an operator or automatically by a suitably programmed computer. The production and subsequent handling of these data is dealt with in Chapter 3.

2.8. Computer software.

2.8.1. Manipulation of EDS generated data

The initial handling of the EDS generated data was by the MIDAS interpretation program. Using this program, particle classifications were performed using obvious clusters in scatter plots and breaks in slope in quantile plots to produce groups of particles with similar chemistry (see section 3.7.1). The chemical and selected morphological data were exported from MIDAS for further analysis and a particle chemistry database was constructed using the PARADOX system. PARADOX was able to cope with the large amounts of data produced i.e. 17 chemical and 7 morphological variables for over 20,000 particles. Particles could be selected out of this database using any variable, group of variables, or ranges of values within those variables selected, with relative ease and this facilitated the identification and removal of outliers.

2.8.2. Statistical techniques.

The SAS data analysis system was used for most of the multivariate statistics on the chemical data, and other statistical packages such as SOLO, BMDP and MINITAB were used where a different approach was required or where their techniques were more applicable. Details of the various techniques used are presented in the relevant sections. Some of the maps and diagrams were produced using the MAPICS computer graphics package.

CHAPTER 3: CARBONACEOUS PARTICLE CHARACTERISATION.

3.1 Introduction

In order to determine possible emission sources for carbonaceous particles found in lake sediments, it is first necessary to characterise the particles to their fuel-type. In certain instances this information may be used to locate the specific source of the extracted particles. For example, particles of coal-fired origin found in lake sediments in western Ireland should be derived from the Moneypoint station on the River Shannon, the only coal-fired station in the country. Similarly, oil-derived particles found in recent lake sediments of the Galloway region of Scotland are most likely to have come from the stations at Ballylumford or Coolkeeragh in Northern Ireland since there are no oil-fired stations in Scotland or northern England. On an international scale, any coal-derived particles in Swedish lake sediments must have been transported from other countries as there are no coal-fired stations in Sweden.

Characterisation to individual power station level would be ideal, but over a period of months power stations use coals and oils from many different sources and it seems unlikely that each station will produce particles with an individual signature, be it morphological or chemical.

No attempt has been made here to characterise inorganic ash spheres for two reasons. Firstly, they are almost entirely of coal origin, and secondly, they are formed from the fusing of inorganic inclusions within the fuel rather than from the fuel itself and so their chemistry is not dependent upon fuel-type (Hulett et al., 1980; Ramsden & Shibaoka, 1982).

This chapter describes the steps taken to produce an effective classification of carbonaceous particles into their fuel-type, based upon surface chemistry data produced by energy dispersive spectroscopy (EDS) on reference material collected from a selection of power station sources.

3.2 Previous attempts at fuel-type separations.

3.2.1 External morphology.

The morphological characteristics of carbonaceous particles have been studied using light and electron microscopy. Fisher et al. (1978) used light microscopy to differentiate between 11 morphological types of coal fly-ash, on the basis of shape and opacity. Griffin & Goldberg (1981), used electron microscopy to separate carbonaceous particles into nine classes, the main distinction between coal and oil being the convoluted or layered patterns seen on the surface of the oil particles (Plate 2). However, not all oil-derived particles show this surface contouring, and on occasion it can also be observed on coal particle surfaces (Plate 4). Moreover, many particles of both oil and coal origin have very little surface area, being highly porous or 'lacy' (Lightman & Street, 1968), limiting the use of surface features in a classification. This group of particles are left out of the Griffin & Goldberg classification.

Size distribution studies (Shen et al., 1976) indicate that particulates emitted from coal-fired boiler stacks generally have a higher mean diameter than those from oil-fired boilers, however there is such a large overlap that little confidence could be placed in a classification based on size criteria alone.

Particles from different coal combustion techniques also appear to show morphological and size differences due to the temperatures the coal encounters in the furnace (McCrone & Delly, 1973; Falster & Jacobsen, 1982). Spreader stokers and fluidized bed plants produce the largest particles and pulverised fuel and drop tube furnaces the smallest. However, pulverised fuel is the only coal combustion technique now employed in the British power generation industry and so size differences are no longer important in the study of modern carbonaceous particles.

3.2.2 Internal structure using thin sectioning.

When embedded in resin and thin-sectioned, oil carbonaceous particles appear circular with extensive and regular cross partitioning (Raask & Street, 1978), and

in cross-polarised light they are anisotropic (i.e. they give incomplete extinction upon rotation).

There are four different types of coal-derived particle (Lightman & Street, 1968): solid, produced from the fusain maceral, 'balloons,' with thin walls and a single large cavity, 'C' shaped particles, with thick walls and a large pore opening to the surface, and 'lacy' particles, with many internal partitions similar to those from oil combustion. The relative numbers of these particles produced during coal combustion depends on the type of coal used and the burning conditions employed (size of flame, furnace type etc..), but the 'C' shaped particles are generally the most common (Lightman & Street, 1968). In cross-polarised light, low rank coals are isotropic (i.e. give complete extinction upon rotation) and mid to high rank coals are anisotropic (Griest & Harris, 1985).

This optical microscopy classification has been used with a high degree of success (80-90%) with power station ash (Street, pers. comm.). However, it is not convenient with particles extracted from lake sediments, because the number of particles available to embed in the resin is orders of magnitude lower and the 'lacy' particles would still remain unclassified.

3.2.3 Chemical parameters.

Elemental analysis has been performed on particulates from many different sources including car emissions, incinerators and cigarettes, as well as from coal and oil-fired power stations (McCrone & Delly, 1973). The results from McCrone & Delly and other studies (Shen et al., 1976; Cheng et al., 1976) show that the major elements present in power station emission particulates are, for oil: V, Fe, Si, S, and Ca, and for coal: Fe, Ti, Si, S, K, and Ca. Titanium and vanadium have, therefore been used in the past as identifiers of coal and oil particles, respectively (e.g. Ganor et al., 1988).

These elements are good indicators of origin, but both oil and coal are heterogeneous materials and vanadium is present in some coals and titanium in some oils, and so one or both of these elements may or may not be found in any

individual particle. Figures 3.1a & b show EDS spectra of typical coal and oil carbonaceous particles and here, titanium and vanadium could be used to distinguish between the two fuel-types. However, Figure 3.1c shows the EDS spectrum of another carbonaceous particle from the same coal ash sample as Figure 3.1a, and shows the presence of both elements. The use of a single chemical parameter is therefore limited as a classification tool.

The methods described above are not suitable for accurate fuel-type characterisation of unknown particle assemblages. Consequently, this study examines the potential for fuel-type separation of a multiple element technique EDS. EDS data produced from the analysis of particles can be used not only on the presence and absence basis described above, but quantitatively, so that a more statistical approach can be used for an effective separation.

3.3 Principles of Energy Dispersive Spectroscopy (EDS).

EDS permits the detection and simultaneous display of all mid-energy X-rays collected during a single analysis, and so many elements may be studied at any one time. EDS systems are also readily linked to electron microscopes enabling selection of individual particles of interest and the combination of morphological and chemical data.

When an electron beam is focused onto a specimen a number of signals result. The JEOL 733 Superprobe used in this study makes use of three of these:

- Secondary electrons are emergent electrons with an energy less than 50eV, produced by the interaction of primary and backscattered electrons with weakly bound surface electrons.

- Backscattered electrons are electrons which are elastically scattered through a large angle. The yield of these electrons increases with atomic number.

- X-rays are a form of electromagnetic radiation, and an energy dispersive X-ray

Figure 3.1. Typical EDS spectra of carbonaceous particles from (a) coal combustion, (b) oil combustion, and (c) coal, showing the presence of both vanadium and titanium.

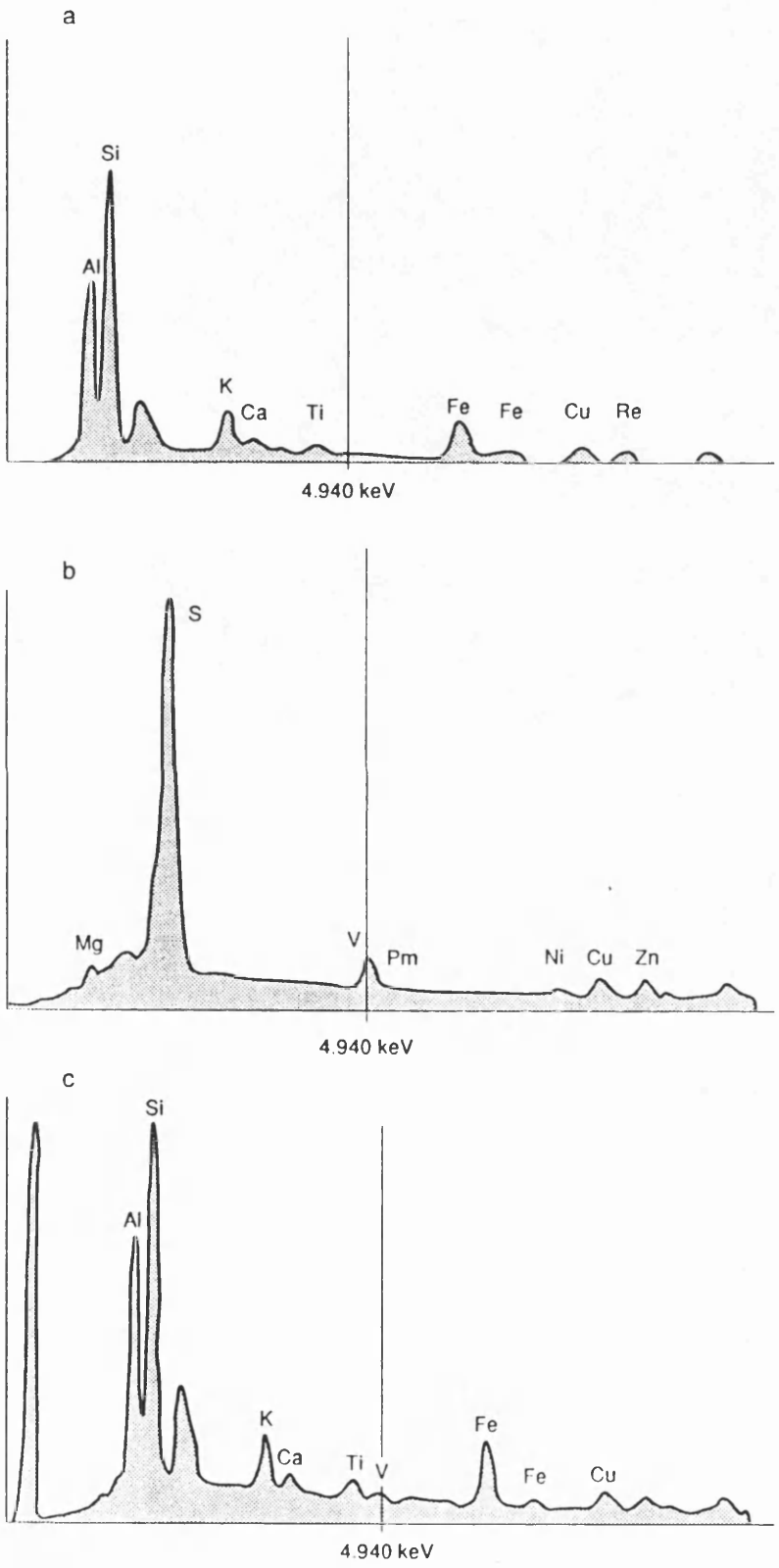

spectrum is represented as a histogram of the total X-ray photons counted by each channel of the multi-channel analyser in the detection system. This spectrum is composed of X-rays of two origins. Continuum X-rays (or bremsstrahlung radiation), which form much of the background underlying the peaks of the energy spectrum, and characteristic X-rays, produced during the interaction of incident electrons with the orbital electrons of an atom, and which form the peaks superimposed on the background (Figure 3.2).

When an incident electron interacts with an atomic orbital electron, ejection of the atomic electron may result, leaving a vacancy. The atom is now unstable and stability is restored by an electron from a higher energy level, dropping down to fill the vacancy. The excess energy is emitted as an X-ray photon. If the vacancy was created on the innermost electron or 'K' shell, these are designated K X-rays, and L and M X-rays are generated in a similar way. The vacancy can be filled by electrons from different higher energy levels, giving rise to e.g. Kα (electron from the L level) and Kβ (electron from the M level) lines in the spectrum. Hence, each element detectable by the system has one or more characteristic X-ray lines which will be produced if it is present in the sample.

3.4. Power station reference material.

In order to develop a classification system suitable for particles from lake sediments a 'transfer function' approach was used. In any palaeolimnological study where quantitative reconstruction is to take place, both 'response' variables and 'predictor' variables are needed as training data before any inferences can be made about analyses of unknown material. In pH reconstructions using diatom analysis, these variables take the form of a diatom assemblage (the response variable) and an associated pH value (the predictor variable). These can then be used to infer past pH from fossil diatom assemblages (Birks et al., 1990).

In this study, the elemental composition of the particle surfaces was taken as the predictor variable, and the fuel-type as the response variable. A training set of particles from known combustion sources was constructed representing the range of particles emitted to the atmosphere by high temperature combustion sources as a

Figure 3.2. EDS spectrum of a carbonaceous particle showing delimited regions of interest or 'windows'.

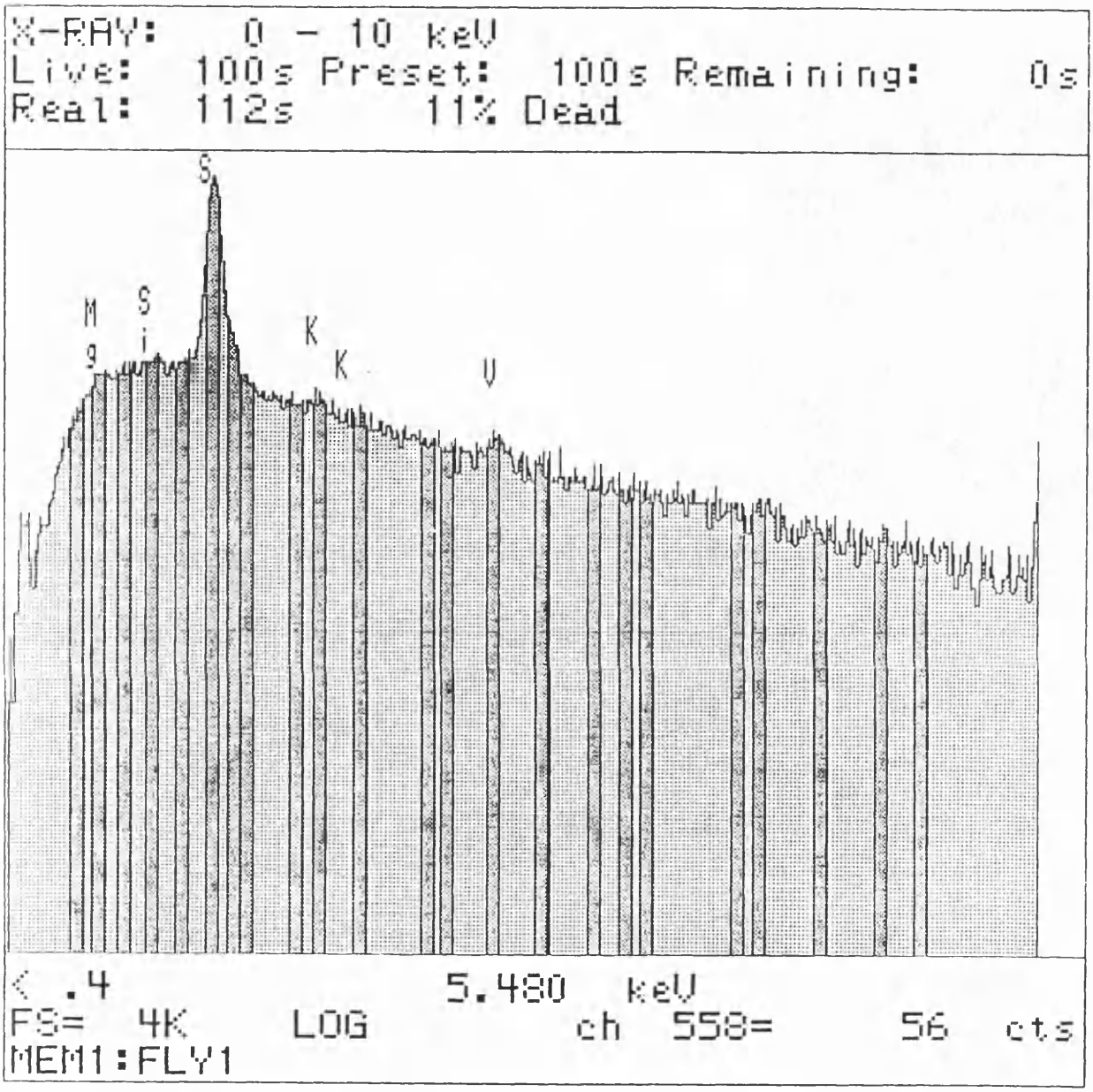

whole.

Thirty-two power station ashes were obtained, from the Central Electricity Generating Board, the South of Scotland Electricity Board, the Northern Ireland Electricity Board and the Electricity Supply Board of Ireland. Of these ashes, 23 were from coal-fired stations, 7 from oil and 2 from peat (see Table 3.1). Although peat does not produce spheroidal carbonaceous particles, its inclusion in the characterisation study was to ascertain whether the technique could be extended to include other fuel-types. It is hoped that other fuels such as lignite and brown coals will be included in the future.

The reference material supplied by the Electricity Boards was taken from the various flue-gas particle extraction systems fitted to the stations. Consequently, although the reference samples are chemically the same as the particles emitted to the atmosphere, they may be morphologically slightly different, larger particles being more easily extracted from the flue gases. This was another reason for basing a characterisation scheme on surface chemistry data only.

Preliminary MIDAS (section 3.7.1) and multivariate (section 3.7.2) approaches to assess the potential for the various separations, used material from one station of each type only. These were Ironbridge (coal), Pembroke (oil) and Gweedore (peat). For subsequent multivariate analyses, 10 power station ashes were selected from the 32 reference samples, five coal: Blyth, Drax, Eggborough, Ironbridge and Rugeley, and five oil: Ballylumford, Fawley, Isle of Grain, Pembroke and Tarbert. Only ten stations were included due to the low number of oil ashes available. There are only 14 oil-fired power stations in Britain compared to 45 coal-fired. Of these 14, ashes were obtained from 7 and EDS analysis was carried out on each. The ash from Kilroot, was most peculiar, containing only angular fragments very rich in magnesium and containing no spheroidal carbonaceous particles. This was probably due to the addition of Lycal 93HS to the oil in Kilroot. This is a high grade magnesium hydroxide and is added to the oil to improve its flow properties, but does not explain the absence of spheroidal particles in the ash. Due to this, and the fact that Kilroot closed in 1986, it was decided not to include it in the data-set. EDS analysis was also carried out on the ash from Coolkeragh but the results were

*Table 3.1. Power station ash reference collection : Fuel-type and sources (Stations selected for the reference set are shown in **bold**).*

Station	Fuel-type	Source
Isle of Grain	Oil	CEGB
Fawley	Oil	CEGB
Pembroke	Oil	CEGB
Carrington	Coal	CEGB
Padiham	Coal	CEGB
Fiddlers Ferry	Coal	CEGB
Didcot	Coal	CEGB
Aberthaw	Coal	CEGB
Ironbridge	Coal	CEGB
Kingsnorth	Coal	CEGB
Eggborough	Coal	CEGB
Thorpe Marsh	Coal	CEGB
West Thurrock	Coal	CEGB
Drax	Coal	CEGB
Agecroft	Coal	CEGB
West Burton	Coal	CEGB
Tilbury	Coal	CEGB
Uskmouth	Coal	CEGB
Blyth	Coal	CEGB
Rugeley	Coal	CEGB
Drakelow	Coal	CEGB
Methil	Coal	SSEB
Longannet	Coal	SSEB
Cockenzie	Coal	SSEB
Coolkeragh	Oil	NIEB
Kilroot	Oil (?)	NIEB
Ballylumford 'B'	Oil	NIEB
Belfast West 'B'	Coal	NIEB
Moneypoint	Coal	ESB
Tarbert	Oil	ESB
Gweedore	Peat	ESB
Bellacorrick	Peat	ESB

obtained too late to be included. This left only 5 oil-fired power station ashes and so 5 coal-fired ashes were also selected for the reference data-set. These were from the larger power stations, i.e. those using more types of coal and producing more carbonaceous particles. The Gweedore peat-fired station was also selected.

A sub-sample (approx. 0.2g) of the reference material from each of these stations was then put through the carbonaceous particle extraction technique for lake sediments (section 2.4). This was so that the reference material was subjected to the same chemical treatments as the lake sediment particles, and to remove the inorganic ash spheres from the coal ash samples. The remaining suspension of carbonaceous particles in water were prepared and mounted as described in section 2.7.1 before EDS analysis.

3.5. EDS of reference material.

3.5.1. Element selection.

Elements for the EDS analysis of carbonaceous particles were selected from elemental studies of mainly coal-fired power station ash available in the literature (e.g McCrone & Delly, 1973; Davison et al., 1974; Cheng et al., 1976; Block & Dams, 1976; Coles et al., 1979; Mamane et al., 1986.). Although very many elements exist in fly-ash (Klein et al., 1975), a short list of the 17 most abundant was finally produced to be included in subsequent analyses: Na, Mg, Al, Si, P, S, Cl, K, Ca, Ti, V, Cr, Mn, Fe, Ni, Cu & Zn. Other studies since have confirmed that most of these elements are also the common ones found in oil fly-ashes (Raeymaekers et al., 1988).

3.5.2. Automated data acquisition.

The development of image analysis software has made it possible for particle selection and analysis to be automated, allowing many particles to be analysed in a short period of time. The ability to create large data-sets means that multivariate statistical techniques can then be used to examine patterns that may not be apparent in smaller samples where operator produced bias may exist.

The controlling image analysis program, DIGISCAN (Link Analytical Ltd.), locates any features present which fall between operator selected threshold values (see section 3.5.4). This means the computer will count only those pixels (points on the image) which fall within these thresholds. The image is then scanned and the location of each of these pixels recorded. The beam is then moved under computer control to each selected feature in turn for the collection of size (all touching pixels are summed to give the two dimensional area of a feature) and X-ray information.

3.5.3. X-ray corrections.

The characteristic X-ray peaks produced span several channels in the multichannel analyser and a convenient way to summarise the data is to delimit a region of interest (or window) over the channels concerned and then to record the total counts in the whole region. This leads to a reduction in data storage since the counts for each element are now represented by a single number, rather than a number for each channel.

Using the DIGISCAN program, up to 25 windows can be defined on the spectrum and the number of X-ray counts falling in each are stored. Most of these windows are defined at the energy levels characteristic of the elements to be measured, but several other regions are also defined on parts of the spectrum where no elemental peaks are expected to occur. These are then used to subtract background counts from each of the other windows. The background channel selected and the proportion subtracted from each window form the Background Correction.

In certain cases a peak for one element will overlap a peak for another. For example, the major elemental line for Ca, ($K\alpha$), is overlapped by a minor line for K ($K\beta$). Where this occurs, one of the elements can be estimated from lines appearing elsewhere in the spectrum. The number of counts that should occur in the first region can then be calculated, and subtracted from the joint peak. The remainder can then be allocated to the overlapping element. The proportion of one peak subtracted from another in this way, is termed the Overlap Correction. A final Efficiency Correction allows a linear scaling of the elemental analysis to account for differences in detector efficiency between elements, if this is necessary.

The set of definitions of X-ray windows and the correction factors to be applied to them are stored in a separate 'window file', since it will be used repeatedly to correct the results for all measured features. For results of analyses to be fully comparable they must have been obtained using the same window file. The window file created for the analysis of carbonaceous particles is shown in Table 3.2.

Table 3.2. *Window file for carbonaceous particle analysis containing correction factors.*

Elem.	Wind.	B/ground Corr.	Wind.	Overlap Corr.	Wind.	Effic. Corr.
Na	1	0.9400	7	3.3690	22	1.0000
Mg	2	1.1000	7	0.0180	3	1.0000
Al	3	1.0000	7	0.0190	4	1.0000
Si	4	1.0000	7	0.0000	0	1.0000
P	5	1.4700	9	0.0110	0	1.0000
S	6	1.3700	9	0.0000	0	1.0000
Cl	8	0.9900	7	0.0000	0	1.0000
K	10	0.9400	9	0.0000	0	1.0000
Ca	11	0.8600	9	0.0360	10	1.0000
Ti	13	0.9200	12	0.0000	0	1.0000
V	14	0.7800	12	0.0760	13	1.0000
Cr	15	1.2800	17	0.1310	14	1.0000
Mn	16	1.0700	17	0.1110	15	1.0000
Fe	18	0.9400	17	0.0730	16	1.0000
Ni	20	0.6700	17	0.0000	0	1.0000
Cu	21	1.3300	23	0.0000	0	1.0000
Zn	22	1.1000	23	-0.0460	21	1.0000

Particles of different size and porosity with the same composition will give different totals of X-ray counts in each of the specified windows, and so the results are normalised by expressing them as a percentage of the total sum of the corrected counts from all the element windows. With the system used here, only those

elements heavier than sodium are detectable and so carbon is missing from the analyses. Consequently, in the analysis of carbonaceous particles, normalisation has the effect of making the trace elements appear as major chemical constituents. However, this lack of carbon detection may be an advantage, as it enables the trace elements to be studied in more detail, and it is these which will separate the different fuel-types and not the uniformly large carbon component.

3.5.4. Setting the wave-form thresholds.

Using the wave form of the backscattered electron image, signal thresholds are set so that carbonaceous material is included in the EDS analysis, but as many of the remaining fragments of mineral matter as possible are not. The setting of these thresholds is important, as any feature (over 600 pixels joined together) included within these limits and in the field of view will be analysed. Figure 3.3 shows the setting of such threshold values. In this example, the waveform of fragment A falls above the threshold and so will be excluded from the analysis. Fragment B, however, falls within the thresholds set and will be analysed along with the carbonaceous particles. Any extra features such as this will have to be removed at a later stage of the data manipulation.

The wave-form of a carbonaceous particle does not register greatly above that of the background and this causes problems setting the threshold levels. If the lower threshold is set high, this excludes most of the background from subsequent analysis, but also some parts of the carbonaceous particle will be excluded. If the lower threshold is set too low, all the carbonaceous particle is included, but also many extra unwanted features are included in the analysis. Consequently, the operator must balance these levels to include as much carbonaceous particle, but as little background as possible. The final threshold setting will therefore alter the number of pixels recorded for the carbonaceous particle and so alters the size of the particle as seen by the EDS. This makes size data (areas, diameters, aspect ratios etc.) generated by the EDS of doubtful quality and so parameters measured in this way should be treated with caution.

Figure 3.3. The setting of the threshold levels using the wave-form of a SEM image will determine the features that are analysed. Those particles falling within the threshold range (the carbonaceous particle and fragment B) will be included, but mineral fragment A will not as its wave-form exceeds the threshold. Unwanted analyses such as that of fragment B must be removed ata later stage of data manipulation.

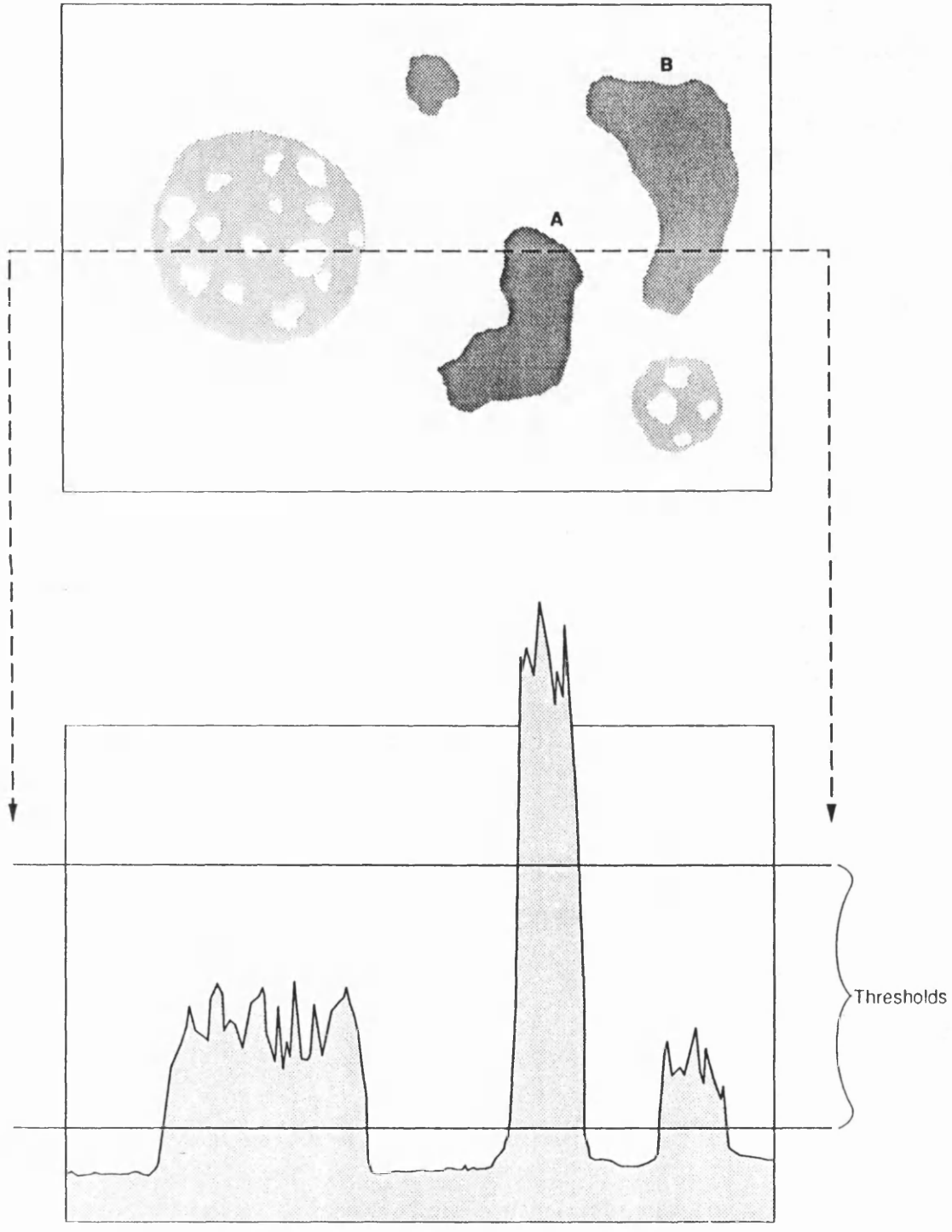

3.5.5. Data output.

Table 3.3 shows the output from MIDAS of a typical feature from a carbonaceous particle analysis. The first two columns give the raw (uncorrected) count data for each selected 'window' and the corrected percentages produced from these values for each element. The third column gives morphological data. For each feature, 60 diameters are measured by Feret projection. This is done by projecting two parallel tangents onto the particle, and calculating the distance between the two touch points. The smallest, largest and mean values are recorded as MinFer, MaxFer and MidFer respectively and the MaxFer/MinFer ratio gives the 'aspect'. CxArea or 'convex area' is calculated by measuring the area produced by joining the touch points of the 60 pairs of tangents. This does not take into account any indentations, as the tangents projected onto the particle surface will not penetrate them, and so CxArea will be too large if such irregularities exist. TrArea or 'true area' is the area measured by the number of connected pixels on the binary image falling within the thresholds. Pores will always fall below the set thresholds and so are not included in this calculation. Consequently, CxArea is always larger than TrArea for porous carbonaceous particles and a comparison of the two will give an indication of the porosity of the measured feature.

Some X-ray statistics are shown with the chemical and morphological data and these give information on the performance of the EDS analyses. Tcount is the total number of X-rays detected in all the channels after correction and where this is very low the corrected percentages will have little meaning. This is demonstrated in Table 3.4 and may be due to insufficient beam current or the counting time being too short (Watt, 1990). GCR is the gross count rate, and is defined as the number of measured counts divided by the time of acquisition in counts per second. GCR increases as the density of the material analysed increases and so features with very high GCR's are most likely to be mineral rather than carbonaceous fragments. The parameter 'Fit' is a scaled ratio between positive and negative values. A large number of negative values (see Table 3.5) in the analysis gives rise to a large value for 'Fit' and shows that either the correction factors are not working well or elements are being detected which are not included in the window file.

Table 3.3. Typical output from MIDAS of a carbonaceous feature

Feature: 1298; S/Fe

Raw Data		Elements		Shape/Size Data	
w1 :	10	Na :	-6.68	MinFer :	41.93μm
w2 :	20	Mg :	-6.18	MaxFer :	65.25μm
w3 :	30	Al :	0.51	MidFer :	53.16μm
w4 :	30	Si :	0.52	Aspect :	1.56
w5 :	17	P :	-0.33	CxArea :	1972.45μm^2
w6 :	143	S :	65.67	TrArea :	1223.56μm^2
w7 :	29	Cl :	-5.56	Xcog :	1447.00
w8 :	18	K :	0.37	Ycog :	1961.00
w9 :	12	Ca :	0.86		
w10:	12	Ti :	3.01		
w11:	12	V :	6.62		
w12:	10	Cr :	3.71		
w13:	15	Mn :	0.90		
w14:	21	Fe :	16.62		
w15:	14	Ni :	1.20		
w16:	7	Cu :	0.01		
w17:	4	Zn :	-0.67	X-Ray Statistics	
w18:	36				
w19:	7			Tcount :	192.73
w20:	5			GCR :	39.60
w21:	4			Fit :	19.43
w22:	2				
w23:	3				
w24:	0			PV file: C:\MIDAS\FLY\UCL25-28.PV	
w25:	0			Field:287	Id:754

Table 3.4. Example of an analysed feature with very low Total count.

Feature: 345; Unclassified

Raw Data		Elements		Shape/Size Data	
w1 :	0	Na :	50.00	MinFer :	73.67μm
w2 :	3	Mg :	0.00	MaxFer :	99.42μm
w3 :	0	Al :	-2.00	MidFer :	83.08μm
w4 :	0	Si :	16.67	Aspect :	1.35
w5 :	1	P :	0.00	CxArea :	4367.22μm^2
w6 :	0	S :	0.00	TrArea :	3319.70μm^2
w7 :	0	Cl :	0.00	Xcog :	1716.00
w8 :	0	K :	0.00	Ycog :	941.00
w9 :	0	Ca :	16.67		
w10:	0	Ti :	0.00		
w11:	0	V :	0.00		
w12:	1	Cr :	o·oo		
w13:	0	Mn :	0.00		
w14:	0	Fe :	16.67		
w15:	0	Ni :	0.00		
w16:	0	Cu :	0.00		
w17:	0	Zn :	0.00	X-Ray Statistics	
w18:	0				
w19:	1			Tcount :	6.00
w20:	0			GCR :	0.60
w21:	0			Fit :	79.43
w22:	0				
w23:	0				
w24:	0			PV file: C:\MIDAS\FLY\UCL25-28.PV	
w25:	0			Field:332	Id:2064

Table 3.5. *Negative values produced by an unexpected peak falling into a 'background window'.*

Feature: 123; Unclassified

Raw Data		Elements		Shape/Size Data	
w1 :	53	Na :	-53.36	MinFer :	21.29μm
w2 :	124	Mg :	-73.08	MaxFer :	35.88μm
w3 :	167	Al :	-71.87	MidFer :	27.66μm
w4 :	223	Si :	-121.98	Aspect :	1.69
w5 :	219	P :	-62.50	CxArea :	1174.31μm^2
w6 :	243	S :	-55.52	TrArea :	823.52μm^2
w7 :	275	Cl :	-40.83	Xcog :	376.00
w8 :	232	K :	-21.33	Ycog :	1042.00
w9 :	189	Ca :	-0.89		
w10:	193	Ti :	23.31		
w11:	176	V :	-11.62		
w12:	151	Cr :	13.71		
w13:	124	Mn :	8.90		
w14:	87	Fe :	6.62		
w15:	69	Ni :	-7.20		
w16:	65	Cu :	32.29		
w17:	58	Zn :	11.87	X-Ray Statistics	
w18:	35				
w19:	42			Tcount :	76.73
w20:	61			GCR :	219.60
w21:	43			Fit :	689.11
w22:	24				
w23:	19				
w24:	17			PV file: C:\MIDAS\FLY\UCL25-28.PV	
w25:	18			Field:12 Id:94	

3.5.6. Negative values in chemical data.

To produce an average background spectrum upon which to base the corrections, approximately one hundred quartz grains are analysed. These should contain only silicon peaks and are of about the correct 'weight' (as seen by EDS) for further particle analysis. The subsequent background corrections are then based upon the shape of the spectrum produced. Once the background windows have been selected, any unexpected peaks falling into those windows will result in over compensation for background and in cases where counts are reasonably low, result in negative numbers. This is shown in Table 3.5 where an unexpected peak falls in window 7, previously designated for background correction. Note that the parameter 'Fit' is also large.

Although in chemical terms these negative numbers are equivalent to zero, they are retained as they contain information apart from assessing the performance of the correction factors. If the background has been set correctly, then analyses in which there is zero of an element will produce values in a normal distribution about zero, due to the presence of random X-rays. Any values above this distribution can then be treated as 'real' values, but low positive numbers falling within the normal distribution may in reality correspond to a zero value for that element. In terms of the percentage data generated from the corrected counts, the positive values are adjusted to sum to 100%, and the negative values are treated as zeroes.

3.6. The reference data-set.

3.6.1. Removal of outliers using MIDAS.

EDS measurements were carried out as described above on carbonaceous particles from the ten power station ashes. This produced a data-set of reference material containing 5,717 particles of which 3,237 were of oil origin and 2,480 were of coal origin.

These morphological and chemical data were transferred from the EDS for analysis using the computer program MIDAS. MIDAS was designed by Particle

Characterisation Services at Imperial College, London for manipulating EDS-generated data and producing simple classification schemes on personal computers (see section 3.7.1). It is an interpretation program with the ability to handle large amounts of data and locate discrete groupings of particles with similar chemistry. It can also be used to examine the individual data of any single particle in the data-set (Watt, 1990).

Initially particles with a Tcount of greater than 5,000 were discarded. Spheroidal carbonaceous particles normally have a Tcount in the range 30 - 3,000 and particles with values much higher than this tend to be in one of two classes:

i) small, roughly spherical (aspect approximately 1.0), and almost exclusively silicon and/or aluminium. These are inorganic ash spheres from coal combustion which have survived the various chemical procedures.

ii) very high in one of the trace elements, showing them to be mineral fragments (e.g. rutile fragments high in titanium).

Removing these two groups reduces the number of particles remaining in the analysis from 5,717 to 5,565 (2,331 from coal and 3,234 from oil). The EDS analyses of the 5,565 particles from the ten selected power stations remaining after the MIDAS manipulations were brought together using the PARADOX database management program to be used as the particle reference data-set.

When studying the distribution of elements within this data-set, a small number of particles showed extreme values for several elements, well outside the distribution shown by the rest of the population. For each fuel-type (including peat), the particle data were studied an element at a time and where extreme values occurred for more than one element in an individual particle, this particle was classed an outlier. These particles tended to be extremely negative in elements such as sodium, magnesium, sulphur and silicon, and either high in copper and/or nickel and/or zinc, showing them to be mineral fragments, or very low in the Tcount variable, showing them to be highly porous carbonaceous material. These outliers may represent some of the non-particle features not excluded by the thresholds set before the EDS analysis

(see section 3.5.4). Examples of the data for three such outliers are shown in Table 3.6.

Once the particles with extreme values were classed as outliers, the remaining 'non-outlier' particles were accepted. The elemental compositions of these accepted particles form an 'allowed' composition range for each element, for each fuel-type, (i.e. this allowed range is not produced by any statistical method, only by the omission of the extreme values from the outlier particles). For both coal and oil these ranges were quite large and so only a small number of outlier particles were identified (22 out of 2,331 for coal, and 28 out of 3,234 for oil).

Table 3.6. *Examples of data for three 'outlier' particles.*

Variable			
Na	-465.38	-231.28	-242.39
Mg	-418.12	-306.42	-184.43
Al	-22.32	-47.27	-105.26
Si	-52.46	-35.96	-101.70
P	-75.49	-145.05	-171.90
S	-90.06	-117.08	-110.88
Cl	34.86	55.50	4.62
K	-5.25	-14.39	-46.95
Ca	-93.66	10.91	11.26
Ti	-40.34	-3.04	2.75
V	21.84	2.87	19.03
Cr	4.54	-23.68	-28.25
Mn	-26.72	30.72	17.73
Fe	-55.82	-15.32	-5.98
Ni	-25.94	-19.02	-32.41
Cu	29.26	-27.81	22.95
Zn	9.51	-14.07	21.67
Tcount	17.16	25.03	36.38
GCR	91.30	85.90	65.10

When combined to give a single range for all fuel-types, the largest range was kept for each element. This is a cautious approach, but is preferable to removing valid particles from subsequent analyses and altering the 'natural' element ranges for the data-set. When applied to the 5,565 particles in the data-set, only 26 particles (11 coal and 15 oil) fell outside the allowed ranges and were classed as outliers. These were removed from subsequent analyses and so reduced the number of particles in the reference data-set to 5,539. The element ranges for the peat reference data fell within those for the combined coal and oil data and so had no effect on the eventual 'allowed' levels. The final element ranges are shown in Table 3.7.

Table 3.7. *Element ranges to remove outliers from the particle reference data-set.*

Element	Range (%)	Element	Range (%)
Na	>-100	Mg	>-100
Al	>-40	Si	>-40, <90
P	>-50	S	>-35
Cl	>-35	K	>-30
Ca	>-30	Ti	>-30
V	>-20	Cr	>-20
Mn	>-25	Fe	>-20
Ni	>-20	Cu	< 20
Zn	>-15, <15		

The remaining 5,539 particles of the reference data-set were now termed 'typical' of coal and oil carbonaceous particles and all subsequent data analyses are based on this data-set or subsets of it.

3.6.2. Basic statistics of the reference data-set.

The data for the 5,539 particles comprising the reference data-set are very important as all subsequent classification schemes and analyses of extracted particles using these classifications are based upon them. Consequently, this section gives the basic statistics of these data, firstly for the coal and oil particles separately, (Tables

3.8 & 3.9), then combined as the full reference data-set (Table 3.10) and finally for the 397 peat particles from the Gweedore station (Table 3.11). The peat data were not included in the main reference data-set as they were used only to show the possibility of extending the technique to other fuel-types. The main classification developed here is for coal and oil carbonaceous particles only.

The distributions of these elements for the full reference data-set are shown in Figure 3.4 (a)-(n), except for S, V and Fe which are shown in Figures 3.5, 3.6 and 3.7 respectively. The element distributions fall into three groups.

Table 3.8. Basic statistics for the coal reference data.

Element	N	Min	Max	Mean	S.D.
Na	2320	-99.02	22.39	-16.49	12.58
Mg	2320	-97.05	14.45	-8.67	10.10
Al	2320	-34.98	99.10	26.61	18.14
Si	2320	-35.90	65.05	12.84	9.29
P	2320	-44.34	44.39	1.99	7.43
S	2320	-34.06	98.27	29.14	19.30
Cl	2320	-32.54	92.19	8.56	15.28
K	2320	-27.34	41.62	3.90	7.80
Ca	2320	-28.18	18.74	-0.66	4.61
Ti	2320	-29.11	63.89	1.20	4.87
V	2320	-17.62	15.84	0.27	3.20
Cr	2320	-19.38	17.64	0.43	3.42
Mn	2320	-21.59	14.78	0.31	2.78
Fe	2320	-14.50	20.14	0.30	2.68
Ni	2320	-15.14	10.79	0.00	2.14
Cu	2320	-11.92	14.77	0.23	2.16
Zn	2320	-12.08	10.14	0.13	1.88

Table 3.9. Basic statistics for the oil reference data.

Element	N	Min	Max	Mean	S.D.
Na	3219	-51.80	20.08	-8.26	6.28
Mg	3219	-40.98	52.75	-5.11	6.58
Al	3219	-21.18	76.39	3.80	8.53
Si	3219	-16.64	85.78	3.02	7.59
P	3219	-22.21	25.81	1.64	3.63
S	3219	-6.57	99.87	66.75	26.32
Cl	3219	-37.90	20.62	-3.83	4.18
K	3219	-16.05	29.60	0.29	2.85
Ca	3219	-15.53	46.38	-0.14	3.21
Ti	3219	-13.70	12.06	0.08	2.05
V	3219	-13.86	92.81	6.77	13.07
Cr	3219	-15.38	60.81	0.21	4.22
Mn	3219	-11.95	13.46	-0.26	1.74
Fe	3219	-8.19	89.10	7.14	11.15
Ni	3219	-8.94	31.20	0.78	2.21
Cu	3219	-11.58	9.30	0.09	1.23
Zn	3219	-11.09	7.36	0.02	1.06

Table 3.10. Basic statistics for the full reference data-set.

Element	N	Min	Max	Mean	S.D.
Na	5539	-99.20	22.39	-11.72	10.35
Mg	5539	-97.05	52.75	-6.60	8.42
Al	5539	-34.98	99.10	13.38	17.63
Si	5539	-35.90	85.78	7.24	10.03
P	5539	-44.34	44.39	1.76	5.63
S	5539	-34.06	99.87	50.81	30.18
Cl	5539	-37.90	92.19	1.34	12.05
K	5539	-27.34	41.62	1.78	5.80
Ca	5539	-28.18	46.38	-0.36	3.90
Ti	5539	-29.11	63.89	0.55	3.56

Table 3.10.(cont.)

V	5539	-17.62	92.81	4.04	10.68
Cr	5539	-19.38	60.81	0.33	4.03
Mn	5539	-21.59	14.78	-0.02	2.28
Fe	5539	-14.50	89.10	4.26	9.30
Ni	5539	-15.14	31.20	0.46	2.47
Cu	5539	-11.92	14.77	0.15	1.72
Zn	5539	-12.08	10.14	0.07	1.48

Table 3.11. *Basic statistics for the peat reference data (Gweedore).*

Element	N	Min	Max	Mean	S.D.
Na	397	-58.36	7.06	-11.87	10.90
Mg	397	-26.87	20.37	1.91	7.64
Al	397	-5.20	47.73	18.31	9.07
Si	397	-5.20	89.34	25.53	15.83
P	397	-28.57	42.71	2.94	2.90
S	397	-19.72	40.16	10.56	8.89
Cl	397	-17.29	37.30	6.39	8.44
K	397	-16.75	10.66	0.48	4.76
Ca	397	-13.15	70.26	17.01	14.60
Ti	397	-12.97	18.03	0.33	3.87
V	397	-13.23	13.81	0.04	3.29
Cr	397	-12.94	62.29	0.61	5.20
Mn	397	-10.62	9.77	0.31	2.69
Fe	397	-9.65	13.99	2.06	3.07
Ni	397	-7.74	10.82	-0.14	2.04
Cu	397	-7.79	23.00	0.38	2.63
Zn	397	-7.14	6.10	0.16	1.84

Figure 3.4. Distribution of element compostions for the full reference data-set. (a) sodium, (b) magnesium and (c) aluminium.

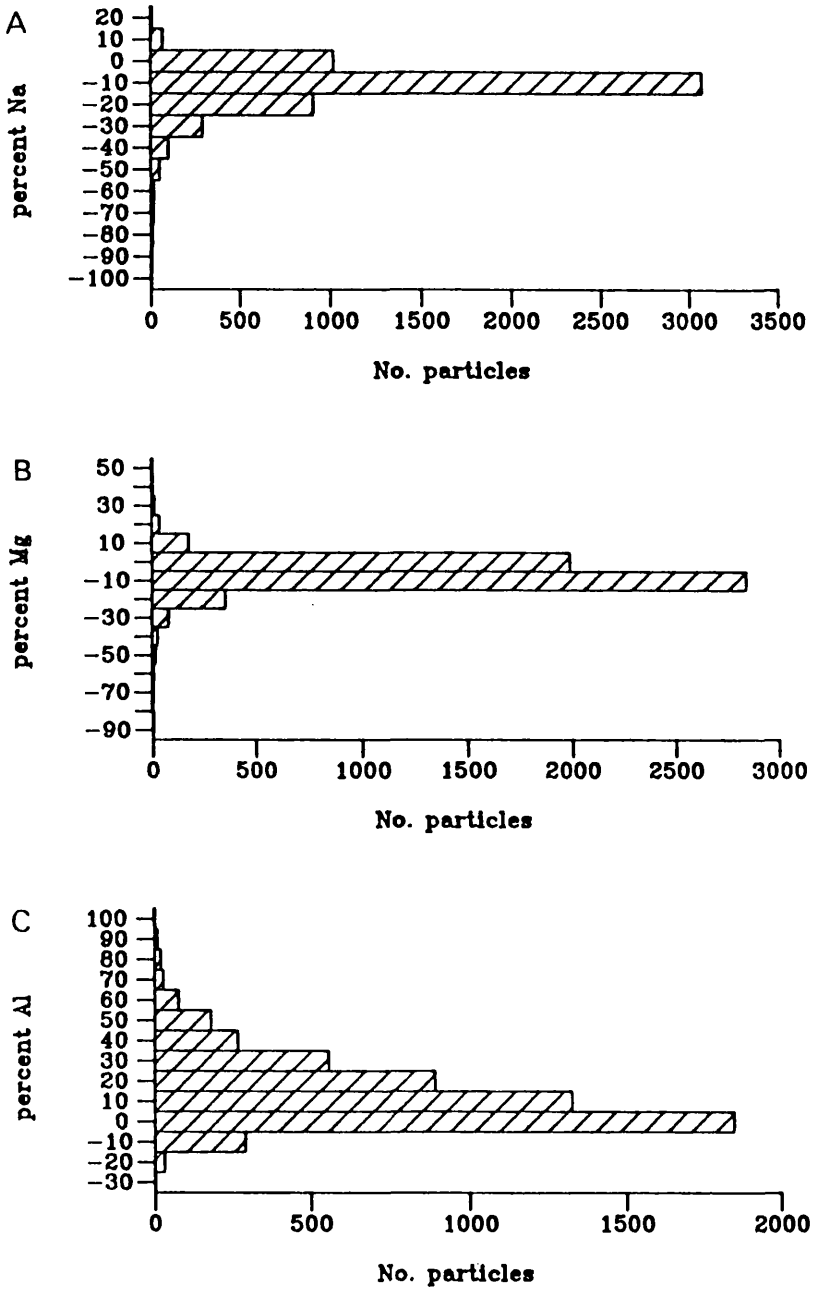

Figure 3.4. (cont.) (d) silicon, (e) phosphorus and (f) chlorine.

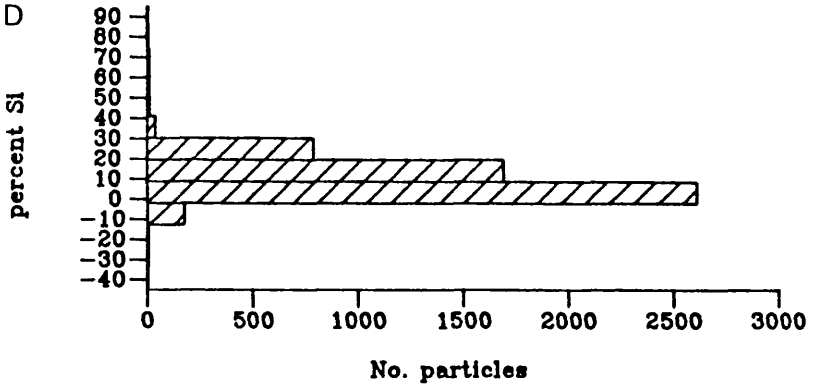

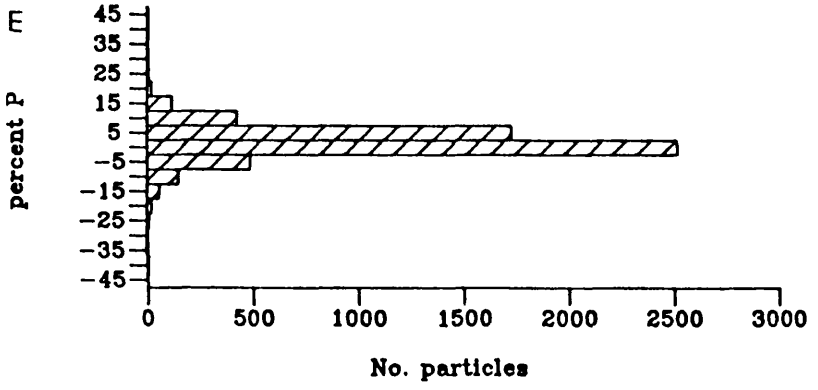

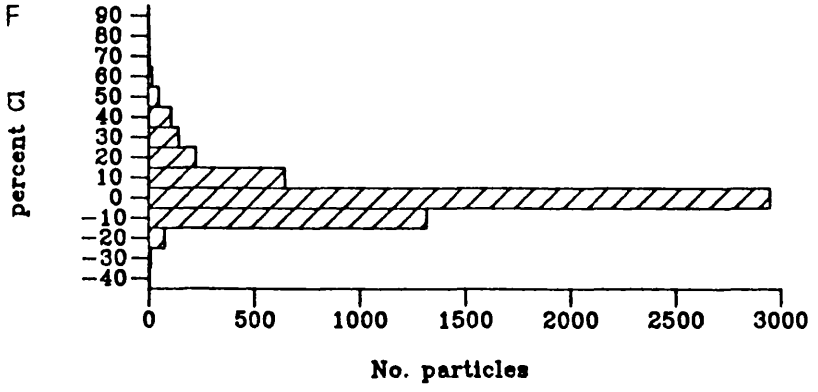

Figure 3.4. (cont.) (g) potassium, (h) calcium and (i) titanium.

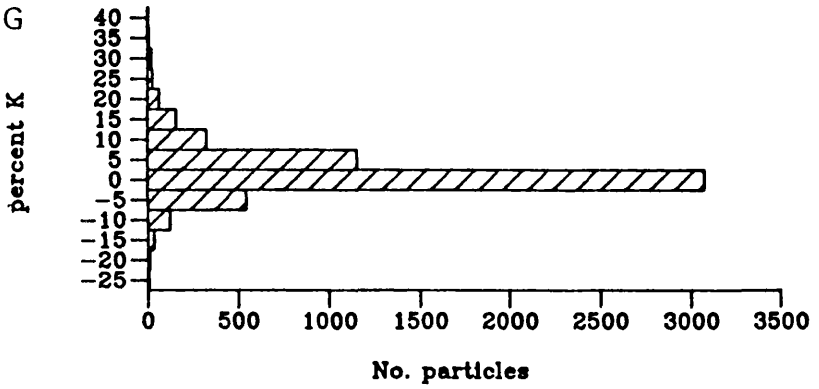

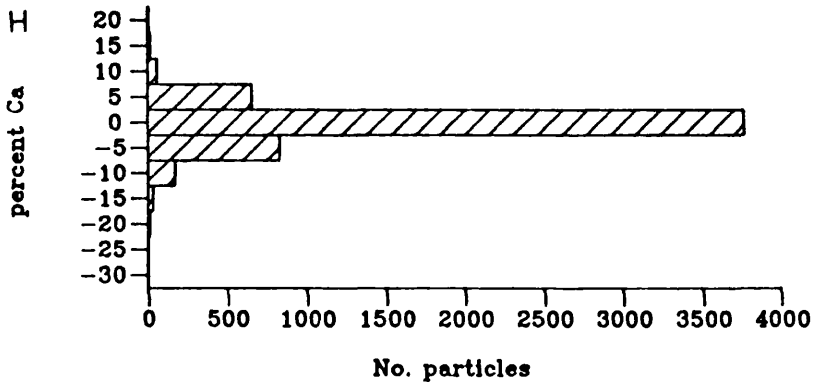

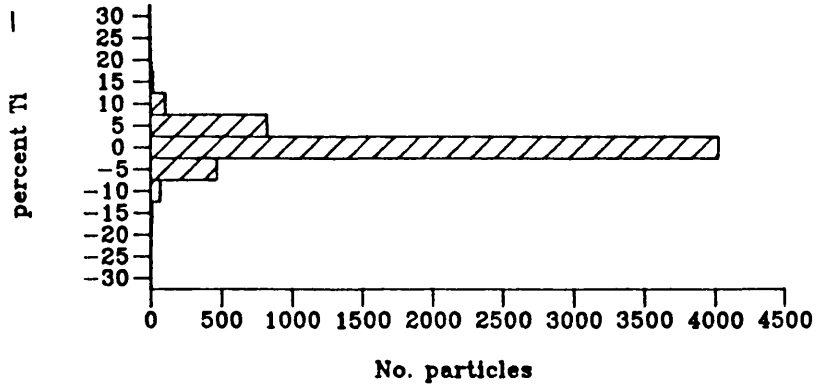

Figure 3.4. (cont.) (j) zinc, (k) chromium and (l) manganese.

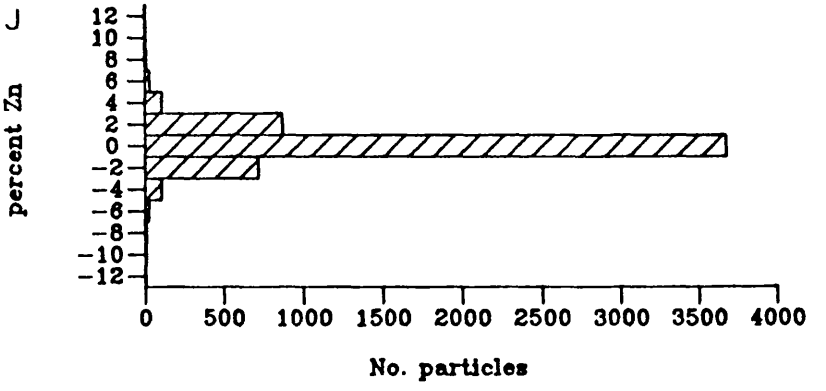

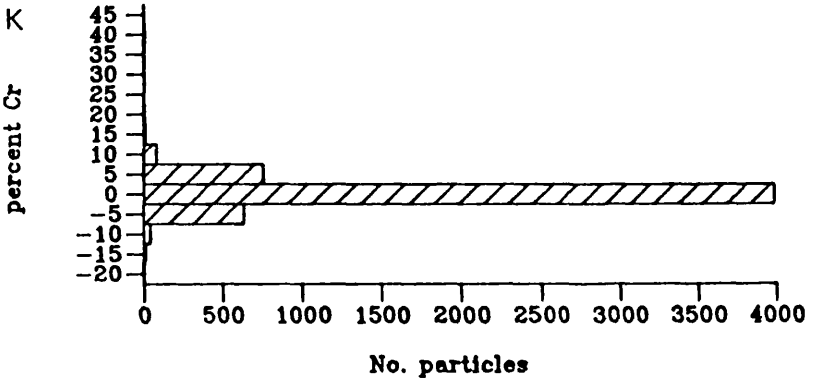

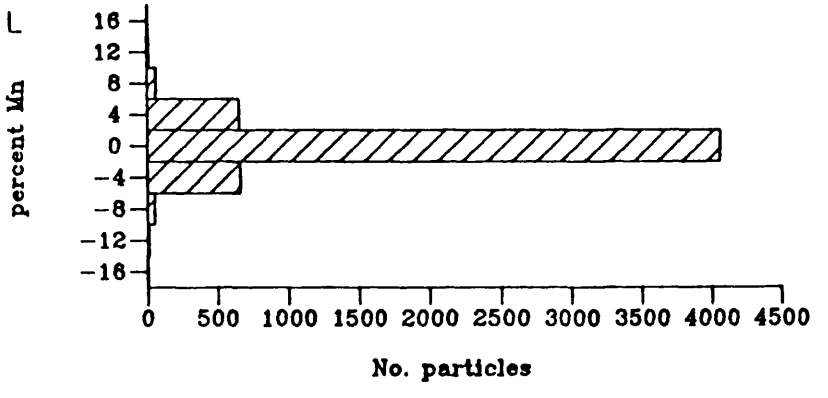

Figure 3.4. (cont.) (m) nickel and (n) copper.

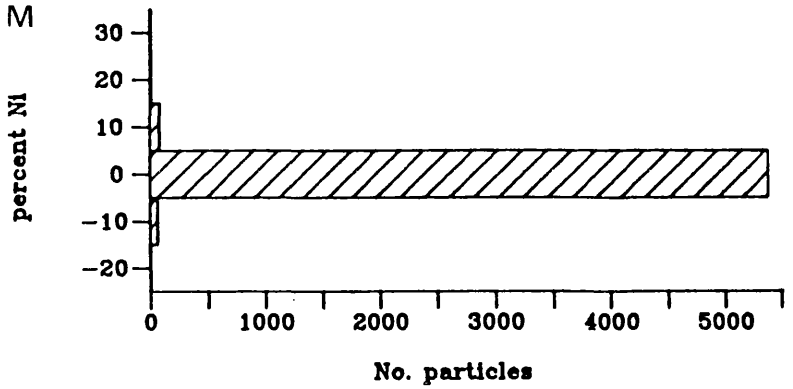

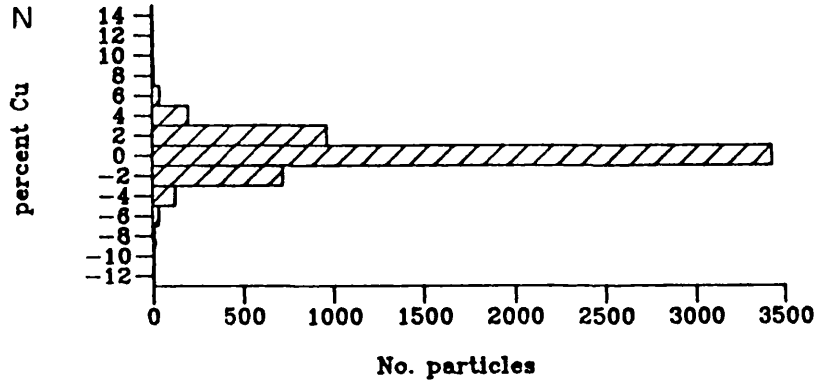

Figure 3.5. Distributions of sulphur composition in (a) the total reference data-set (b) coal reference particles only and (c) oil reference particles only, showing that the bi-modal distribution in the oil data causes the full data-set to be bi-modal.

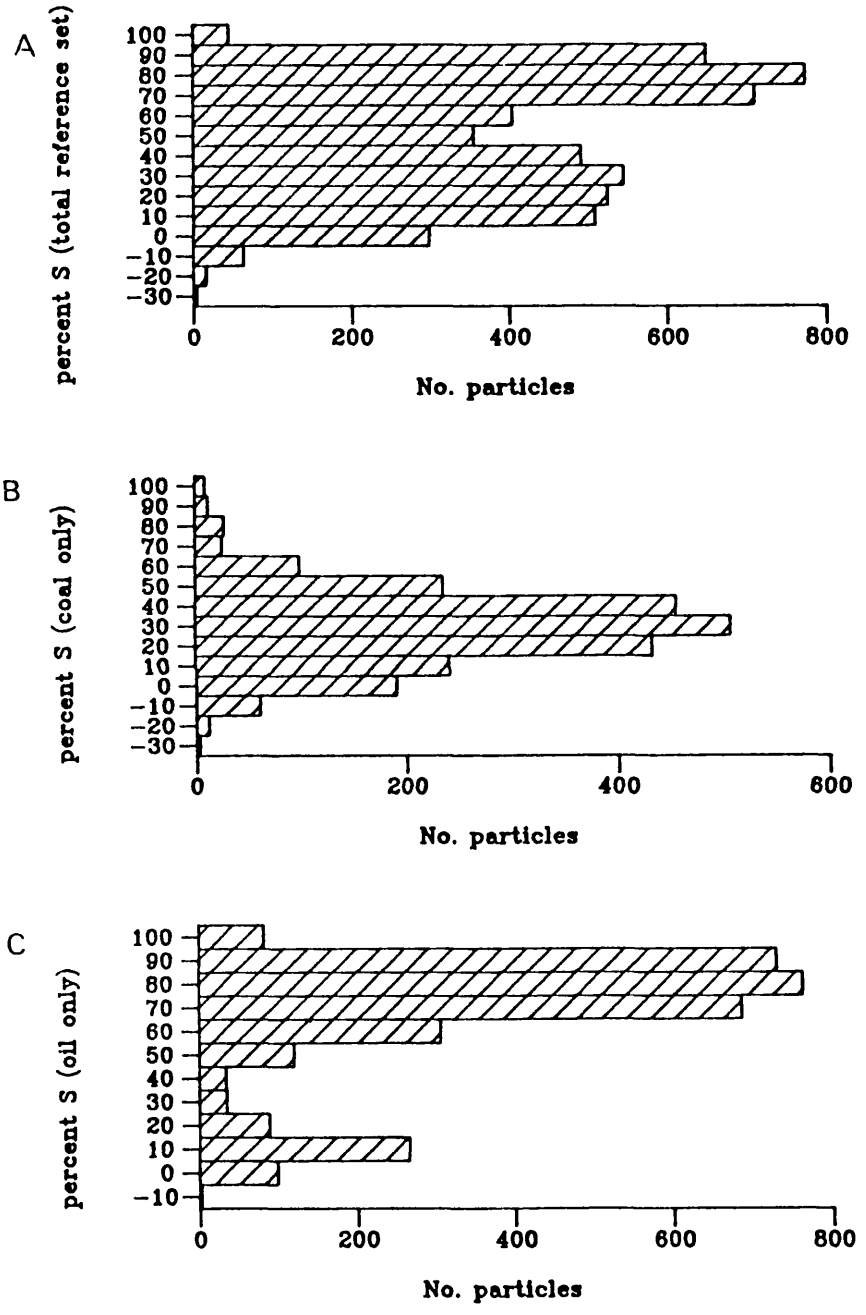

Figure 3.6. Distributions of vanadium compostion in (a) the total reference data-set, (b) coal reference particles only and (c) oil reference particles only, showing that the bi-modal distribution in the oil data causes the full data-set to be bi-modal.

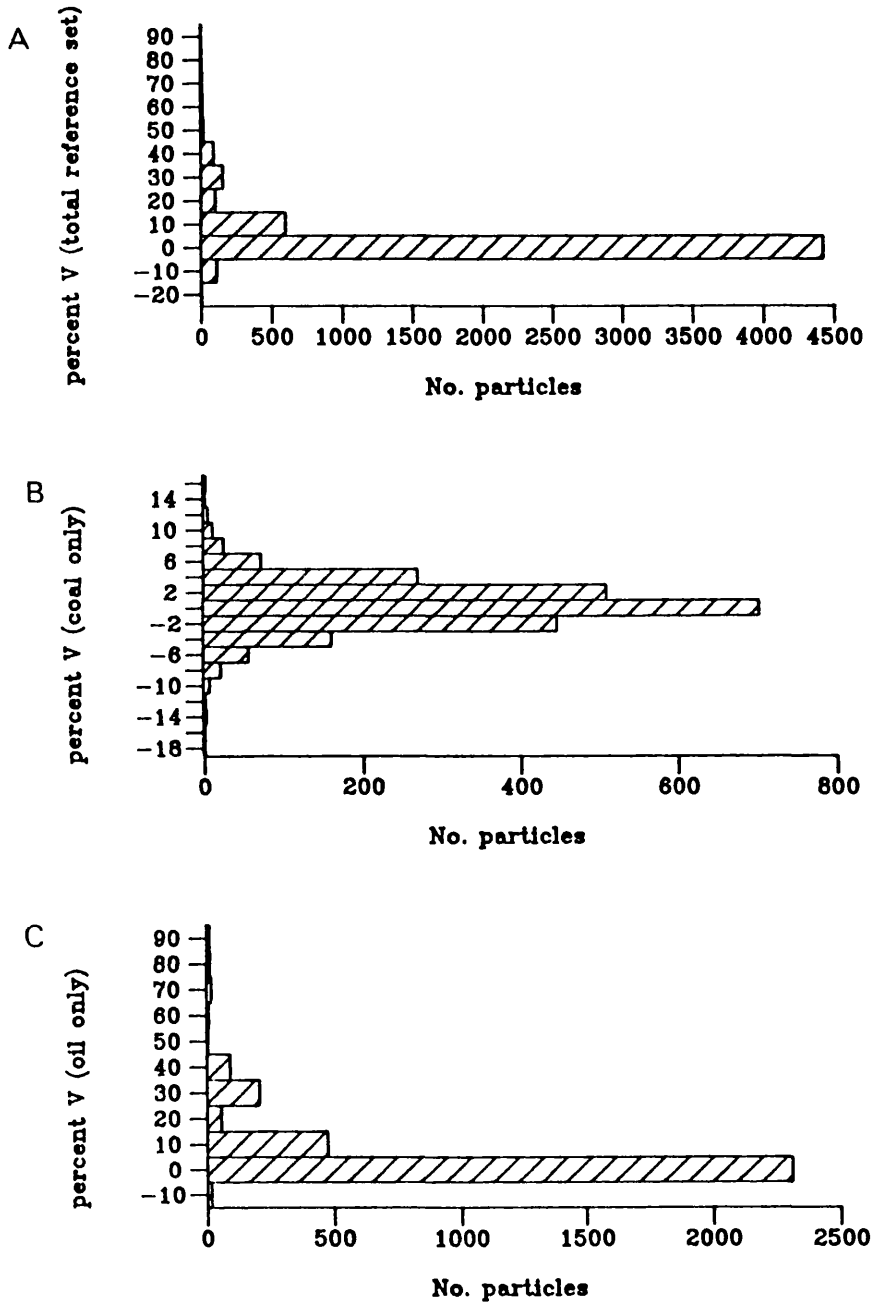

Figure 3.7. Distributions of iron composition in (a) the total reference data-set, (b) coal reference particles only and (c) oil reference particles only, showing that the skewed distribution in the oil data causes the full data-set to be skewed.

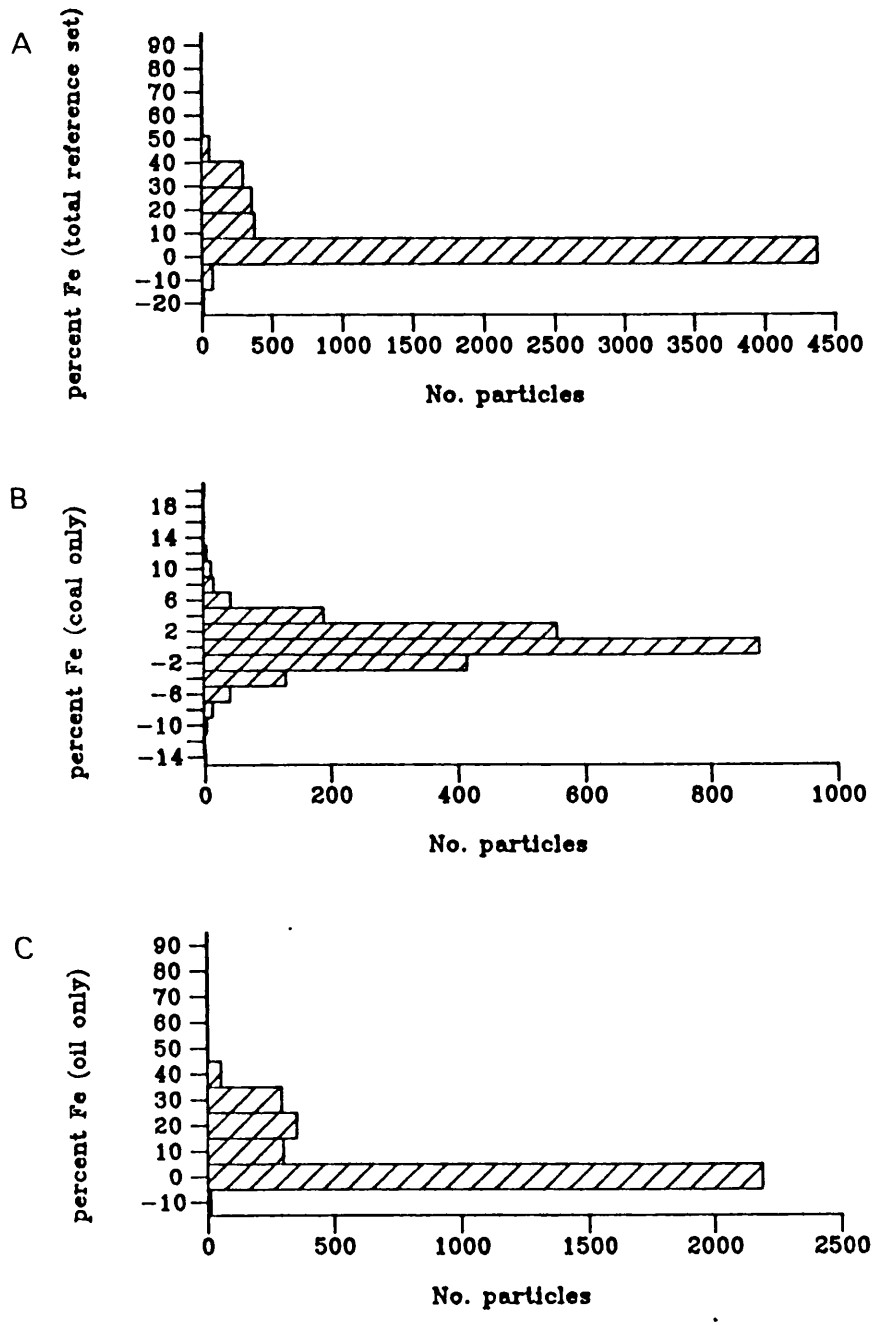

i) Both coal and oil distributions are normal around the same point resulting in a normal distribution for the full reference data-set. These elements are: P, K, Ca, Ti, Cr, Mn, Ni, Cu, Zn.

ii) One fuel-type has a bi-modal distribution and the other is normally distributed, resulting in a bi-modal distribution for the full reference data-set. This occurs for two elements, S (see Figure 3.5) and to a much lesser extent V (see Figure 3.6). In both instances it is the oil particles that show the bi-modal distribution.

iii) One fuel-type is normally distributed and the other has a skewed distribution, resulting in a skewed distribution for the full reference data-set. These elements are: Na (coal skewed), Mg(coal), Al(oil), Si(oil), Cl(coal), Fe(oil). For example Figure 3.7 shows the distribution of Fe for the full reference data-set, and for coal and oil separately, indicating how the skewed distribution of Fe in oil particles produces a skewed distribution for the full data-set.

For the peat data, all the elements show normal distributions, except for Na, Si and Ca which show slightly skewed distributions.

3.7. Preliminary data analysis of EDS data.

3.7.1. MIDAS analysis using data from Ironbridge, Pembroke and Gweedore power stations.

A preliminary analysis using a subset of the reference data-set (i.e. the data from one coal station, Ironbridge, one oil station, Pembroke and one peat station, Gweedore) was done using MIDAS to ascertain the potential for fuel-type separations using the EDS chemistry data.

Using MIDAS, subdivisions can be made by examination of the distribution of single elements using quantile plots, and pairs of elements using scatter plots. In each case the values for the elements for every particle in the data sub-set are plotted. Use is made of any obvious clusters in the scatter plots (e.g. Figure 3.8a) and discontinuities shown by breaks in slope on the quantile plots (e.g. Figure 3.8b)

Figure 3.8. Preliminary particle separations. (a) Scatter plot showing particle clusters, and (b) quantile plot showing breaks in slope which indicate different particle sub-populations.

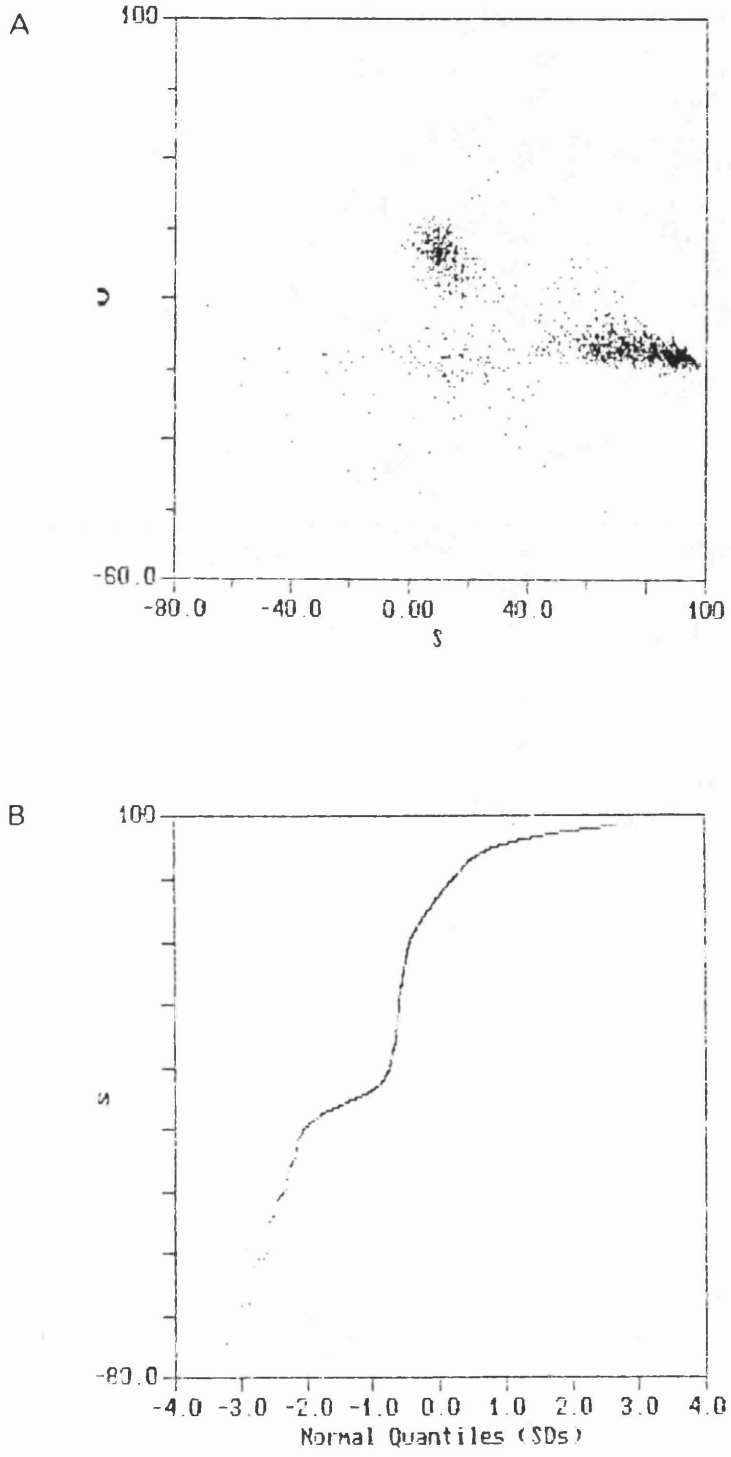

to split the data into various sub-populations. These sub-populations are then examined to assess the homogeneity of the groups and to split them further if necessary.

In this preliminary analysis the 1,205 particles from Ironbridge, 1,041 from Pembroke and 397 from Gweedore were mixed together in turn and separated to produce a classification scheme using this clustering procedure. The resulting dendrograms for each pair, coal/oil, oil/peat and coal/peat appear in Figures 3.9, 3.10 & 3.11 respectively. In each case an initial series of scatter plots for pairs of elements revealed those elements which would best separate the fuel-types. The most effective separator was found to be sulphur in each case. This element alone accounted for 88%, 91% and 83% of the correct assignments for coal/oil, peat/oil and peat/coal respectively. Vanadium and iron were also found to be important where oil particles were involved. Gross count rate (GCR) was used in two instances (this is a valid parameter when the electron beam settings and acquisition times are the same) in the particle analysis. For the peat/oil classification 97.2% of the particles were correctly allocated and 98.2% for peat/coal. The coal/oil separation was the least effective with only 86.6% of particles being correctly allocated. This was due to a group of particles representing 11.1% of the total for which no separation was found. This group probably contained the highly porous or 'lacy' particles with little surface area, as the Tcount for these was generally low. Apart from this group, only 2.3% of the particles were actually misclassified into the wrong fuel-type.

These three classification schemes were then amalgamated into one (Figure 3.12), separating the particles into 12 groups each with a characteristic chemistry to which a single fuel-type was allocated except for the one coal/oil group. Of the 2,643 particles in the classification, 85.8% were correctly allocated a fuel-type, 9.6% were in the unclassified coal/oil group and only 4.6% were allocated the wrong fuel-type.

This scheme appeared to work especially well for peat particles. However, particles extracted from United Kingdom lake sediments are most likely to be of either coal or oil origin and it was this separation which was the least satisfactory in this analysis. Also, this provisional classification was constructed using only one

Figure 3.9. Dendrogram for the separation of coal (Ironbridge) and oil (Pembroke) reference particles using MIDAS.

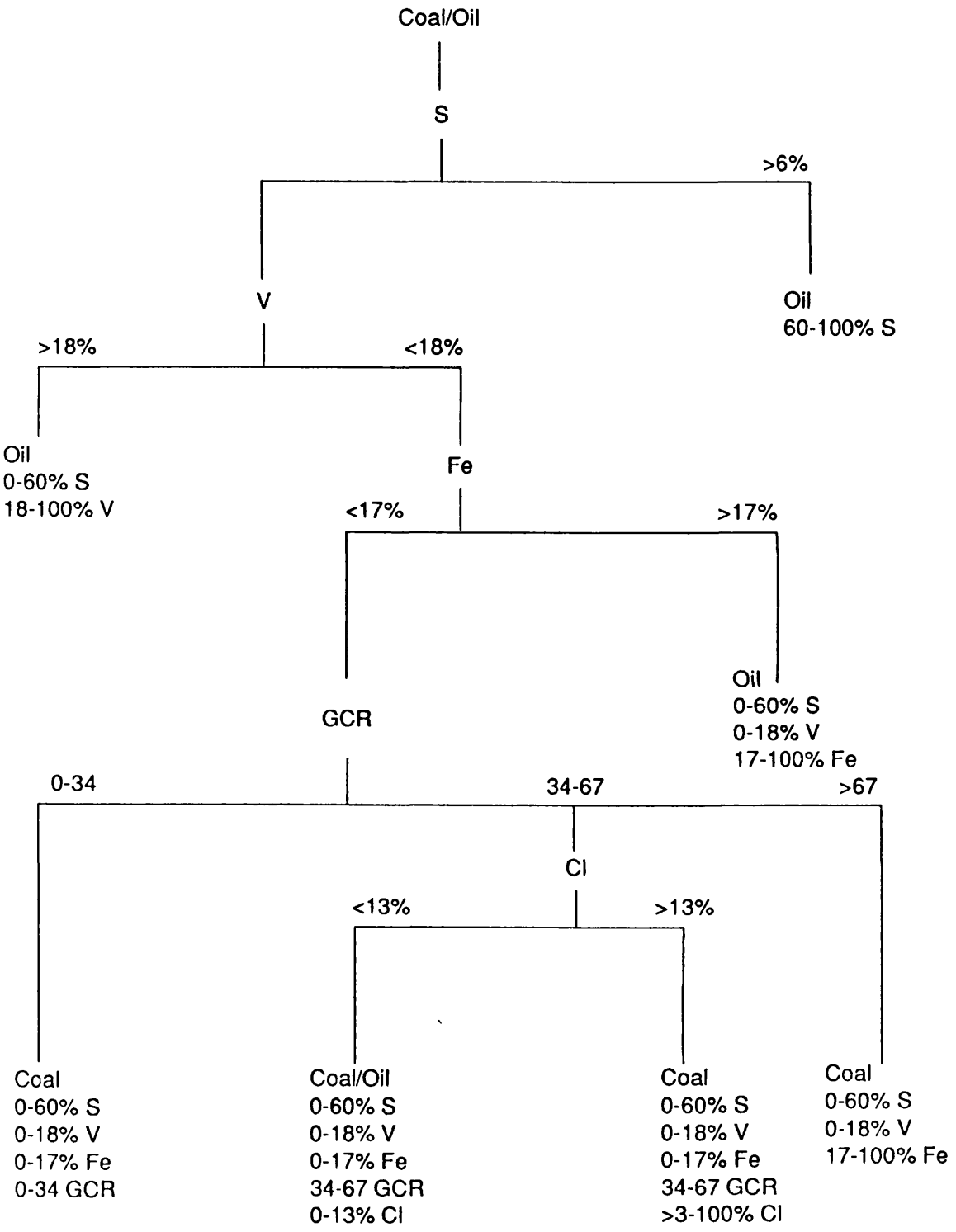

Figure 3.10. Dendrogram for the separation of peat (Gweedore) and oil (Pembroke) reference particles using MIDAS.

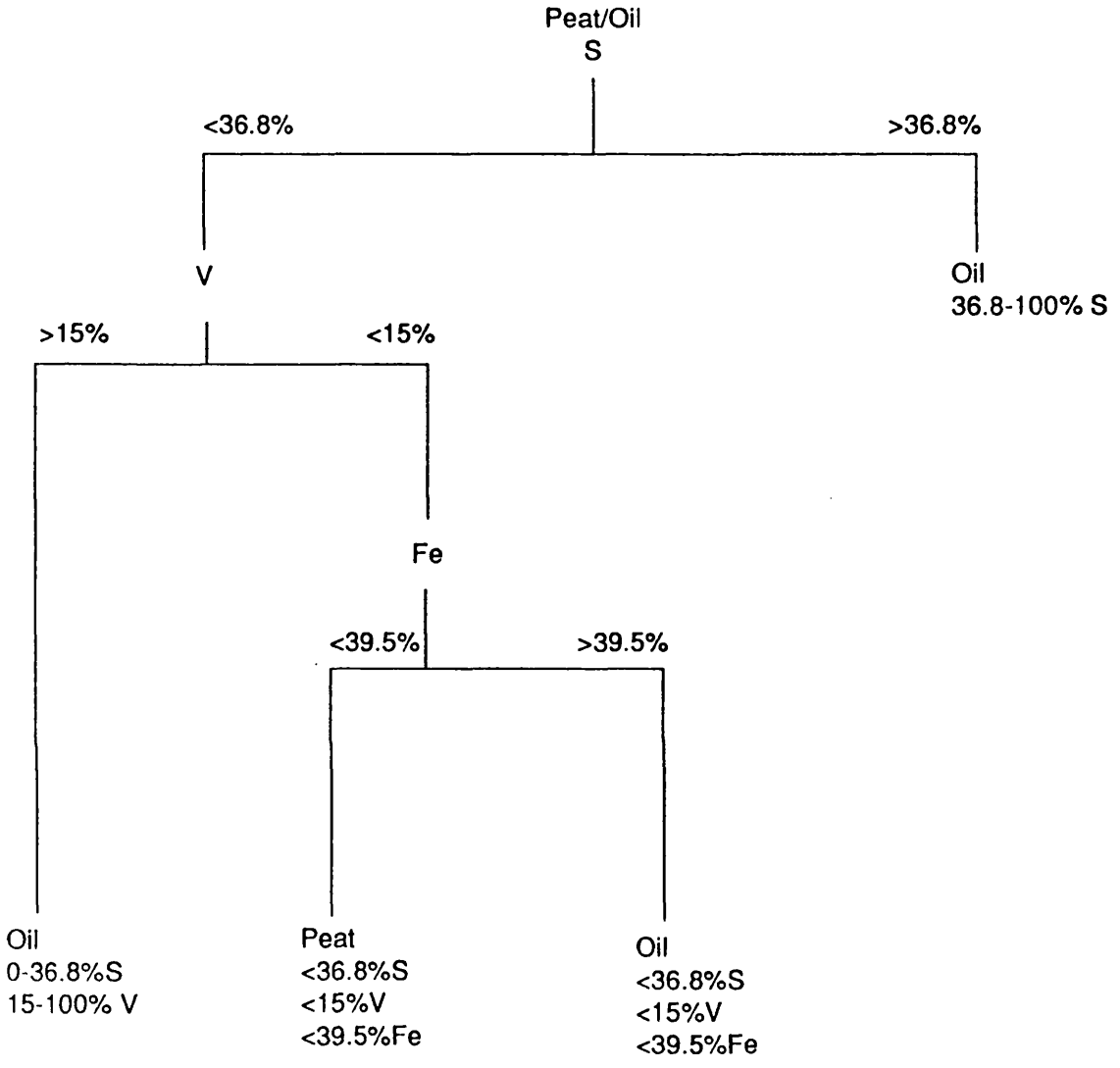

Figure 3.11. Dendrogram for the separation of peat (Gweedore) and coal (Ironbridge) reference particles using MIDAS.

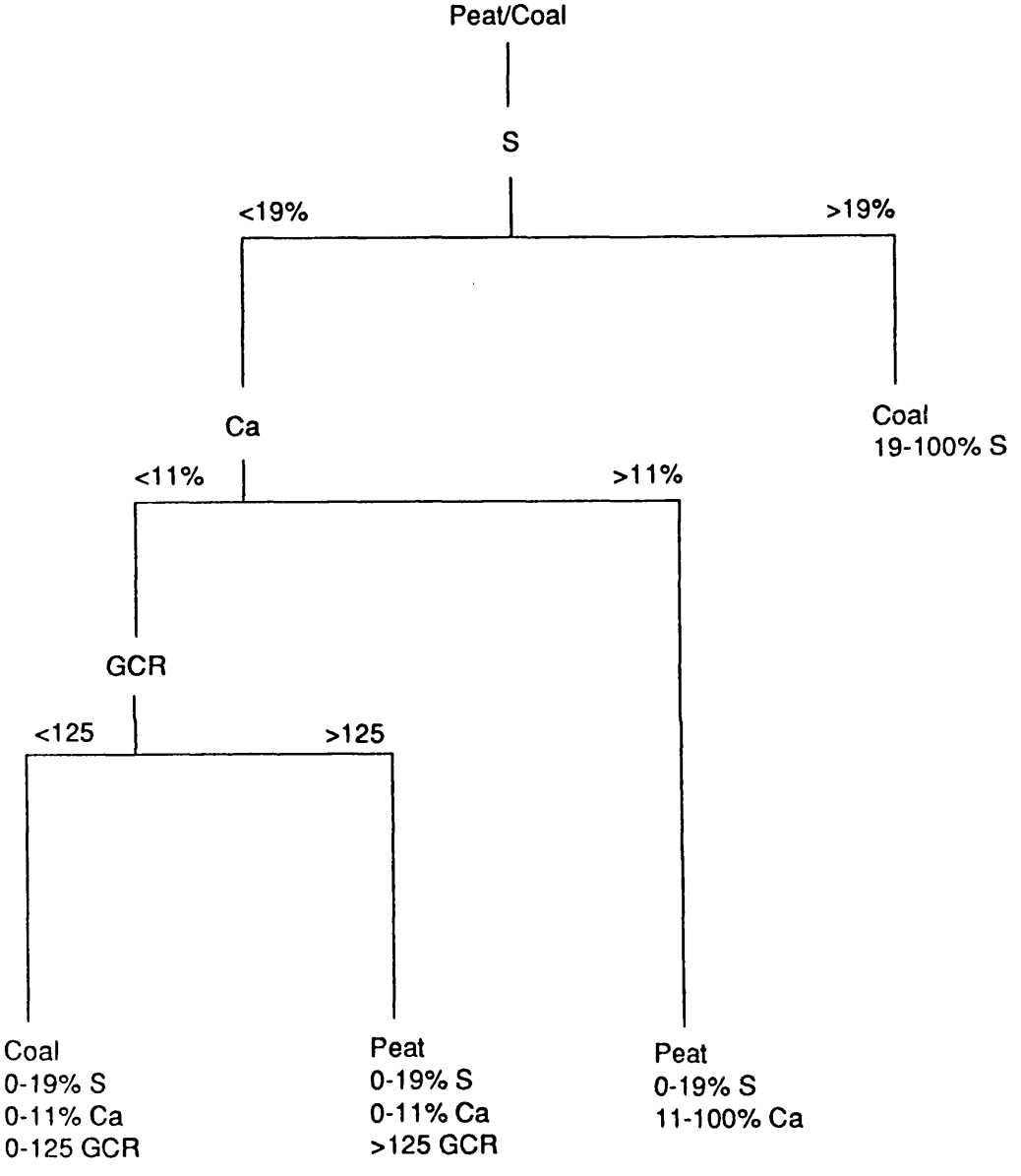

Figure 3.12. Amalgamation of the coal/oil, peat/oil and peat/coal dendrograms into a single classification scheme.

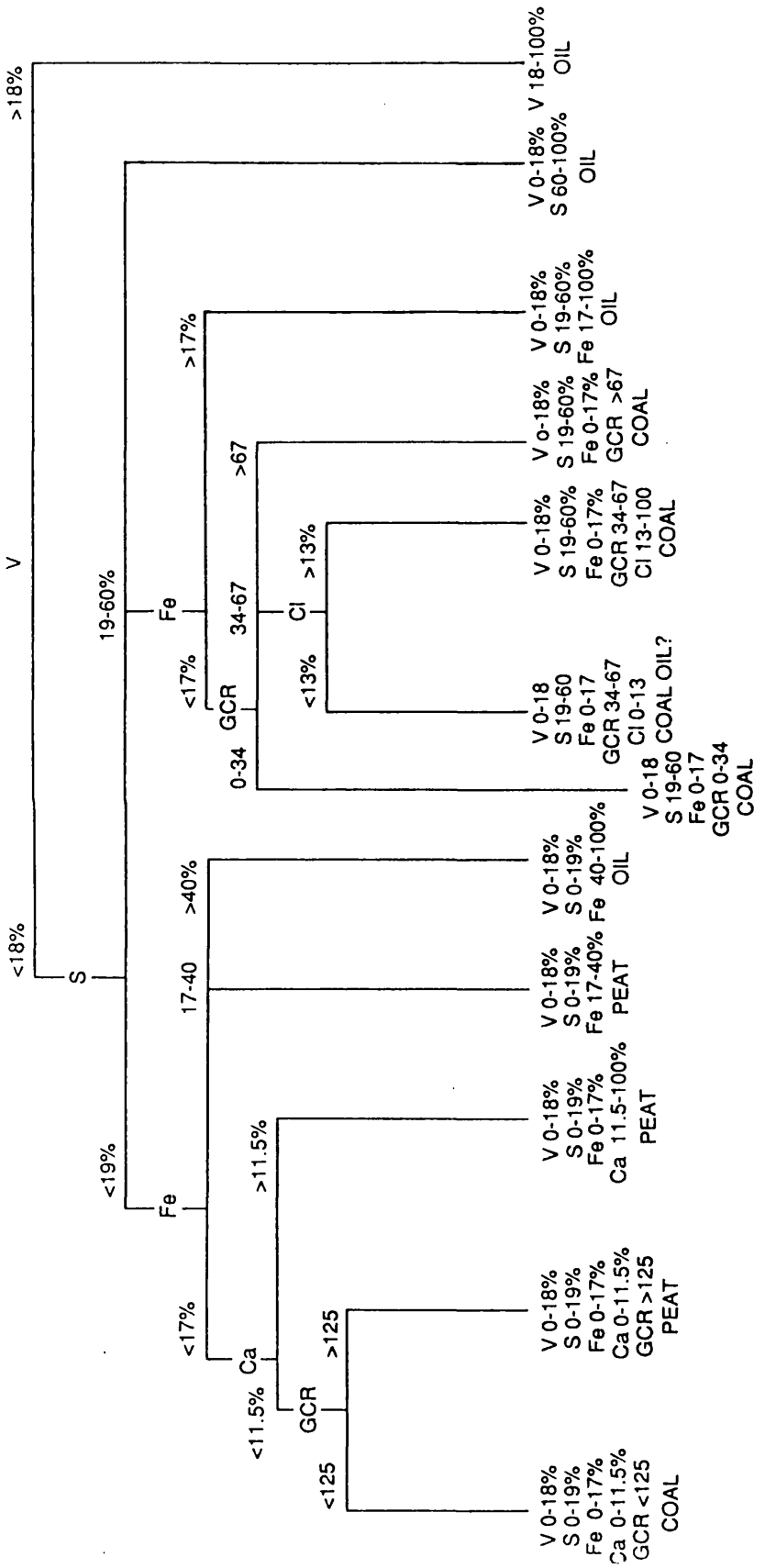

ash of each fuel-type. Since 'within fuel-type' variations are likely to be larger than 'within power station' variations for the same elements, these results are probably over-optimistic. They do, however, show that there is considerable potential for the development of a fuel-type separation using particle surface chemistry.

3.7.2. Multivariate analysis using data from Ironbridge and Pembroke power stations.

The simple technique used above allocated 85% of the particles to the correct fuel-type. However, with data on 17 elements available for each particle, it seemed that multivariate approaches which use more or all of these data were likely to produce an even better separation. Consequently, an initial multivariate analysis was carried out with the data from the Ironbridge and Pembroke ashes using stepwise discriminant analysis.

All 25 measured variables (17 elements, 6 morphological, Tcount and GCR) were included in a stepwise discriminant analysis to separate the Ironbridge and Pembroke ashes using the BMDP-7M program for this procedure.

Stepwise discriminant analysis (SDA) produces an F statistic for each variable which is a measure of how well the variable separates the groups. The F statistic is defined as S_g^2 / S_w^2, where S_g^2 is the variance between the groups, and S_w^2 is the variance within the groups. Consequently, the bigger the value of F, the better that variable is at group separation. The initial F statistics for the 25 variables are shown in Table 3.12a.

Aluminium had the highest value of F in the analysis of variance and so the first classification function produced used only aluminium values. As aluminium was now included in the classification function, the F values for the remaining variables were recalculated and so changed (Table 3.12b). This was because the F values represent the separating power of each variable taking into account the separation already possible by the variable(s) included in the classification function (at the moment just aluminium). Consequently, the F values for those variables highly correlated (either positively or negatively) to aluminium, such as sulphur and silicon, drop and the F

Table 3.12. *F statistics for the analysis of variance for the variables in the discrimination analysis (a) initially, (b) after removal of aluminium, and (c) after removal of aluminium and MaxFer.*

	F to enter (a)	F to enter (b)	F to enter (c)
Variable			
Na	49.887	102.006	66.555
Mg	2.887	87.644	52.634
Al	751.850	-	-
Si	353.065	84.191	93.773
P	4.280	0.292	0.516
S	580.959	158.338	150.929
Cl	361.697	328.738	310.384
K	24.260	44.973	36.050
Ca	0.080	1.240	1.560
Ti	8.932	7.191	8.454
V	50.116	43.300	22.976
Cr	11.392	0.097	0.047
Mn	1.581	1.707	4.271
Fe	125.616	49.030	11.322
Ni	34.821	25.243	11.591
Cu	0.212	0.086	0.678
Zn	0.470	0.007	0.478
Tcount	50.909	37.250	8.266
GCR	1.505	0.006	48.306
MinFer	256.969	291.252	69.492
MaxFer	523.402	535.361	-
MidFer	444.459	464.477	75.893
Aspect	36.191	14.210	2.421
CxArea	55.845	88.488	565.325
TrArea	42.678	75.504	520.046

values for the variables not correlated to aluminium, such as the size data, stay much the same or increase. The next most important variable at separating the groups was therefore MaxFer, so this was then included in the classification function and the F values were once again recalculated to determine which variable was the next most important. This was CxArea (see Table 3.12c).

The stepwise formation of the classification function continued to add variables in this way until all the variables whose recalculated F-to-enter values were above the set threshold (4.000) had been added. Variables could also be removed from the classification function if their F-to-remove value (also recalculated at each step) fell below the threshold (3.996). This is what happened to sodium, added to the classification function as its F-to-enter value became the highest, and removed from the function again when iron was added and the F-to-remove value of sodium was recalculated below the threshold. When the F-to-enter values for all the remaining variables not included in the classification function were too low to be included, and the F-to-remove values for the variables added to the classification function were all above the threshold, the function was complete.

The completed classification function included all but six of the variables. These were Na, P, Cr, Cu, Zn, and MidFer. Table 3.13 shows the variables in the order they were added to the classification function and the Wilks' Lambda for each additional step. Wilks' Lambda is a test statistic which measures the optimisation of the group separations. As separation improves the value of Wilks' Lambda decreases until optimal separation is achieved at its minimum. It can be seen from Table 3.13 and Figure 3.13 that all the added variables improved the value of Wilks' Lambda although the improvement was very slight after the addition of TrArea.

The classification function was then applied to the particle data and a classification score was produced for each particle in the form of a Mahalanobis distance. This is a measure of dissimilarity of the particle from the group (coal and oil) centroids, taking into account and reducing the influence of highly correlated variables (perfect correlation would be similar to using the same variable twice), and variables with large within-group variance (since individual values from the same group may vary

greatly). Hence the smaller the Mahalanobis distance, the higher the probability that an individual carbonaceous particle will belong to that group. A probability is given for each particle for each group and the particle is allocated to the group with the highest probability. At this stage there was no 'unclassified' group and a particle was allocated to either coal or oil in every instance unless the probability of allocation was exactly 0.5000.

Table 3.13. *Order of the variables added to the classification function in the preliminary analysis, and the subsequent Wilks' Lambda.*

Variable	Rank	Wilks' Lambda
Al	1	0.6585
MaxFer	2	0.4809
CxArea	3	0.3458
Cl	4	0.2925
Aspect	5	0.2565
Si	6	0.2462
GCR	7	0.2405
Tcount	8	0.1410
MinFer	9	0.1361
TrArea	10	0.1284
K	11	0.1255
V	12	0.1233
Ti	13	0.1212
Mg	14	0.1191
Ca	15	0.1171
S	16	0.1163
Fe	17	0.1140
Ni	18	0.1130
Mn	19	0.1127

Figure 3.13. Improvement in Wilks' Lambda upon addition of successive variables to the classification function.

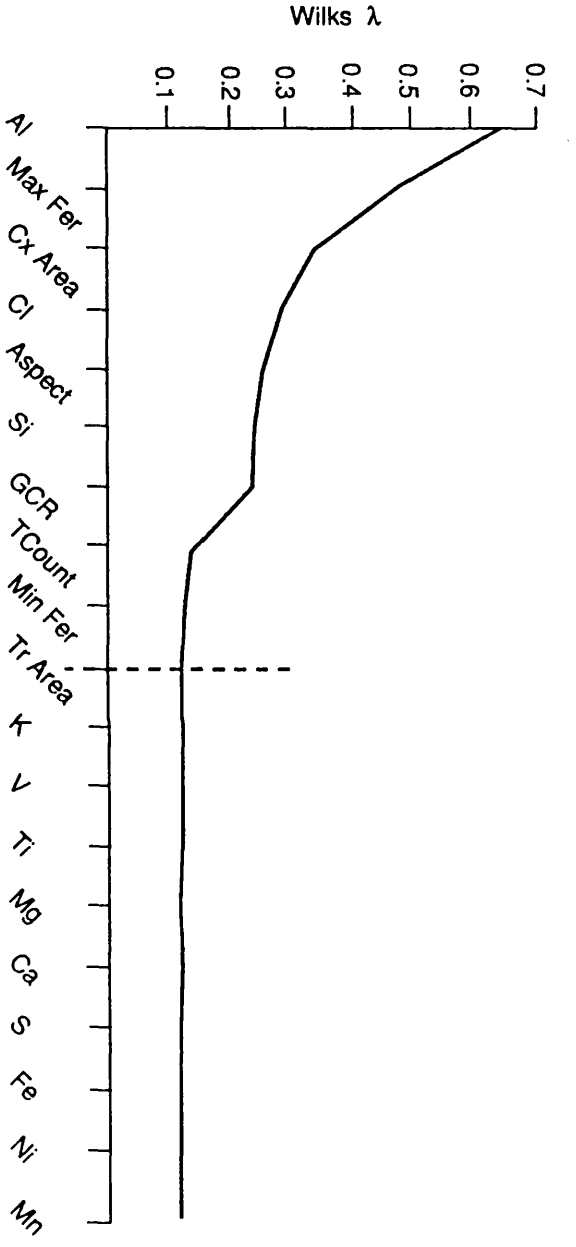

This classification worked very well with 98% of the particles being allocated to the correct fuel-type. However, this can again be regarded as an over optimistic view of the approach for the following reasons.

i) the particles being allocated to the groups were the same particles whose data formed the classification function and so it would be expected that this analysis would perform well;

ii) as in the MIDAS analysis, only data from one coal and one oil power station ash were used, and the variation for each parameter is likely to be higher between power stations of the same fuel-type than between particles in a single power station ash;

iii) morphological data have been used in the construction of the classification function, and Table 3.13 shows these variables to be important. However, as section 3.5.4 shows, these data may not accurately reflect the true particle dimensions and this may affect the discriminatory power of these variables.

3.8. Multivariate analysis of the full reference data-set.

The preliminary studies described in section 3.7 showed that the multivariate approach was better at separating coal particles from oil particles than the MIDAS approach. Therefore, the next step was to apply multivariate techniques to the full 5,539 particles of the reference data-set to produce a classification function which takes into account the variability within the data from a range of power stations of each fuel-type, rather than just one of each as in the preliminary studies.

Before this classification function was produced the data were analysed using principal components analysis to ascertain in a qualitative way the extent to which the coal and oil particles were separable and which were the best elements to use in such a separation. Stepwise discriminant analysis was used to see whether all the elements improved the separation, or whether some were redundant i.e. they make no difference, or reduce the efficiency of the separation. Both of these procedures were done on the 5,539 particles of the reference data-set. Once these

key elements were identified, a linear discriminant function using only those elements which improve the separation was produced.

3.8.1. Principal components analysis

Principal components analysis (PCA) can be regarded as an ordination technique for reducing multivariate data into fewer dimensions. This has been used extensively in the literature as a method of reducing the number of variables in a study or to screen data in order to identify those variables (or combination of variables) which have close associations within a data-set, or which can be used to separate groups. For example, PCA has been applied to chemical data to distinguish between mineralogical species (Webb & Briggs, 1966), geochemical compositions of tektites to estimate the composition of the parent material from which they were derived (Miesch et al., 1966), determination of the variability within and between basic magma types (Le Maitre, 1968), differences in paraffinicity of crude oils and similarity of foraminifera species used to define a biostratigraphic zone (McCammon, 1966) and so on.

PCA transforms the original data-set of 17 variables into a new set of 17 principal components. Although there are as many principal components as original variables the transformation is such that the first one or two principal components account for a larger proportion of the total variance than an equivalent combination of the original variables, giving a more representative idea of the total data variation. PCA is performed by extracting eigenvectors and eigenvalues from the original data. The first eigenvector defines the direction of maximum variability of the data cluster and its eigenvalue is the length of this axis. The second eigenvector defines the maximum variability of the data cluster at right angles to the first eigenvector. The third eigenvector is at right angles to the first two and so on. These eigenvectors (or principal components) have a loading from each variable and so it is possible to see which elements are responsible for the majority of the variance in the data (i.e. those that have a high loading on the first principal component). The loadings for the elements on the first two principal components are shown in Table 3.14 and the elements with the highest loadings are shown in bold type.

Table 3.14. Variable loadings for first and second principal components after PCA of reference data-set.

Variable	1st PC Loading	2nd PC Loading
Na	**0.377**	**-0.401**
Mg	0.167	**-0.314**
Al	**-0.461**	-0.177
Si	**-0.392**	-0.246
P	0.078	-0.215
S	**0.465**	**0.370**
Cl	-0.271	-0.198
K	-0.099	-0.167
Ca	0.146	-0.158
Ti	-0.081	-0.069
V	0.127	-0.289
Cr	-0.077	0.140
Mn	-0.098	0.179
Fe	0.194	-0.241
Ni	0.104	0.154
Cu	-0.148	0.251
Zn	-0.167	0.299

From Table 3.14 it can be seen that no single element was responsible for the variance explained by the first principal component. Rather, it was a combination of Na, Al, Si, and S, although S and Al appear to be the most important. Na, Mg and S are the most important elements on the second principal component. These first two principal components represent 27.5% (15.8% + 11.7%) of the total variance of the data which is reasonably high considering the number of variables in the analysis.

Using the loadings given in Table 3.14, each particle was given a score for each

principal component e.g.

Score on PCA_1 = 0.377Na + 0.167Mg - 0.461Al - 0.392Si + 0.078P + 0.465S - 0.271Cl.....

Score on PCA_2 = -0.401Na - 0.314Mg - 0.177Al - 0.246Si - 0.215P + 0.370S - 0.198Cl.....

These were then plotted on the principal component axes (see Figure 3.14 where oil particles are plotted in yellow and coal in red). The first principal component appears to separate the two fuel-types quite effectively, the oil particles clustering tightly higher up the axis than the coal particles. This is due to the oil particles being higher in sulphur and lower in aluminium and silicon than coal particles, making their first principal component scores higher. The second principal component shows that the oil particles were split into two groups, and from the loadings for this principal component (Table 3.14), the smaller cluster probably represents the low sulphur, high vanadium group of oil particles seen in section 3.7.1, as they would have a lower score on this second axis. There was some degree of overlap between the two groups, a few coal particles plotting in the centre of the oil cluster. Particles of this type are discussed further in section 3.8.3.

The influence of individual elements on the first and second principal components can be expressed more clearly on a correlation bi-plot of the covariance matrix. A problem with using data expressed in percentage form, is that the variables are not independent even if, as in this case, the values do not sum to 100% and this can disrupt the covariance matrix making the bi-plot difficult to interpret (Stokes & Lowe, 1988). This problem is usually overcome by a logarithmic transformation (Aitchison, 1983; Stokes & Lowe, 1988), but with more than about 6 variables the advantages of transforming are small (Juggins, pers. comm.) and in these instances, such transformations have little effect on the results (Stokes & Lowe, 1988). It is more important that the variable data are normally distributed, and consequently, no transformations were done on the element data before PCA. However, some of these elements are not normally distributed (see section 3.6.2.), but in separations involving only two classes, where variable distribution is removed from normal for

Figure 3.14. Plot of first and second principal component scores for particles of the reference data-set (oil in yellow and coal in red).

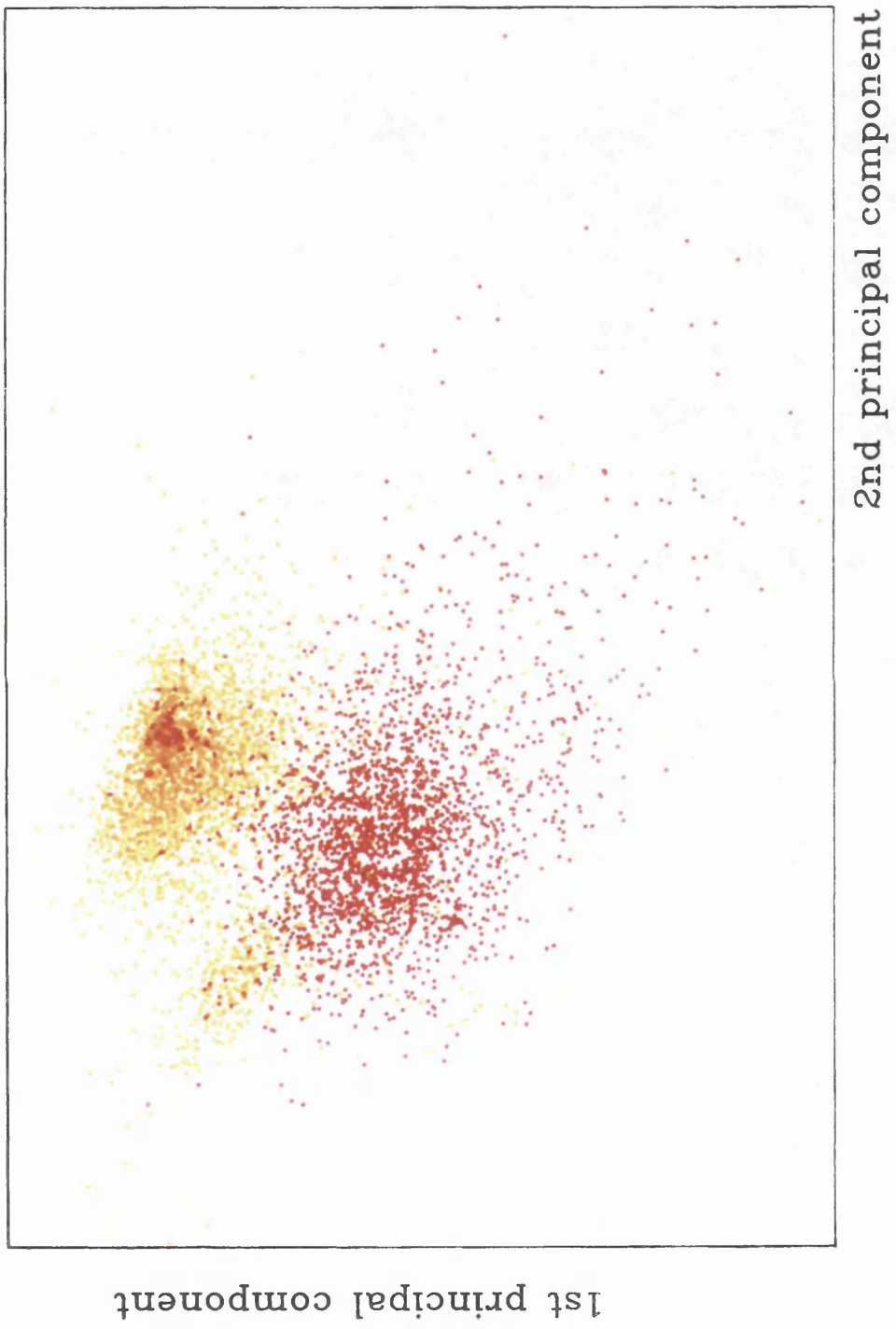

Figure 3.15. Bi-plot of element loadings on the first two principal components for 500 randomly selected particles from the reference data-set.

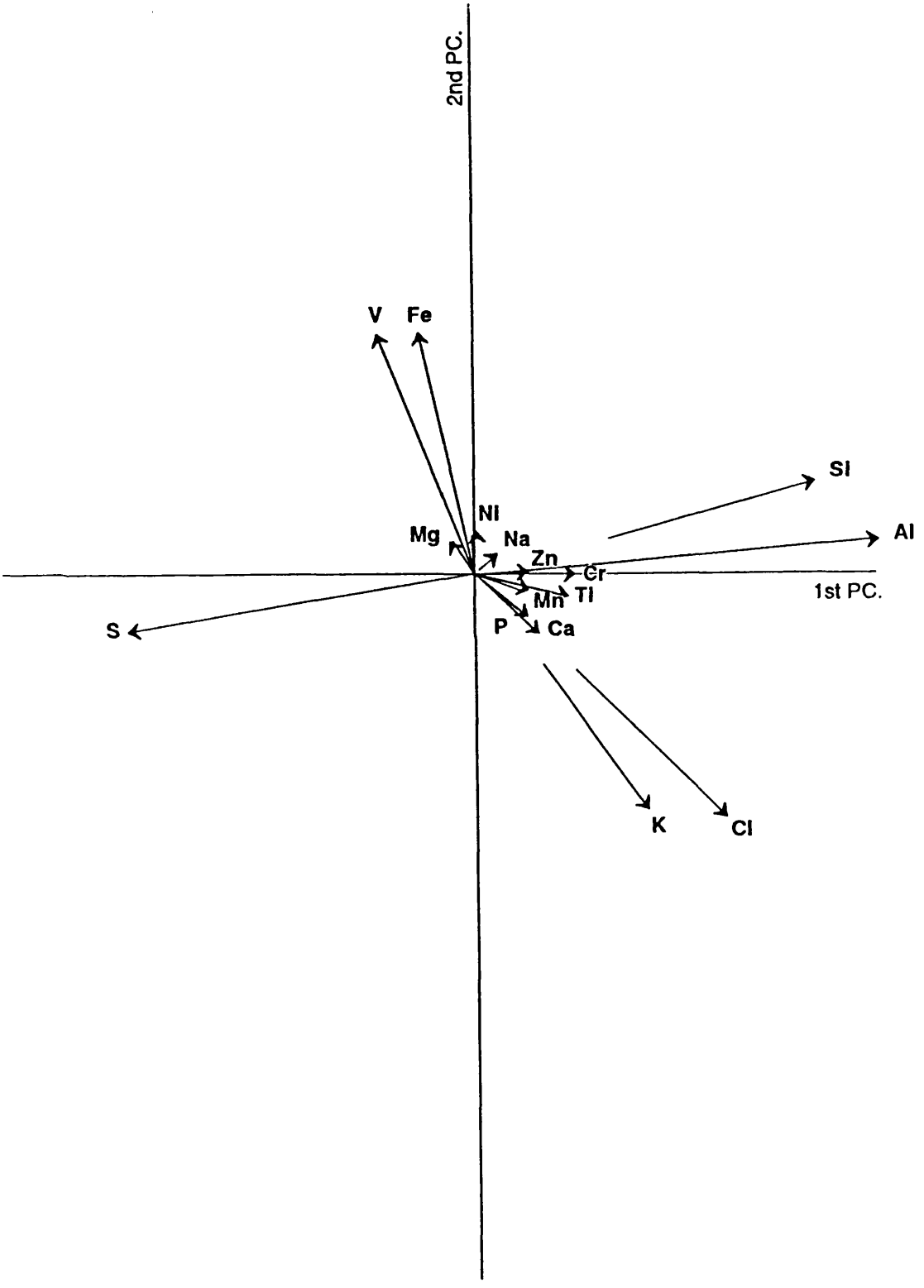

only one class, these variables are often important (Srivastava & Carter, 1983). In the case of coal and oil separation, these elements are sulphur, vanadium and iron.

Figure 3.15 shows a bi-plot for 500 randomly selected particles from the reference data-set and each element is described on the diagram by a vector, the direction and length of which show how important the element is to the principal components on the axes. The Figure confirms some of the points made above. Sulphur and aluminium show their importance to the first principal component, and their strong negative correlation. The second principal component is dominated by vanadium and iron confirming that the second oil group split off by the second principal component is the high vanadium group identified above. Vanadium and iron (generally more abundant in oil particles) are seen to be negatively correlated to potassium and chlorine (higher in coal) and the remainder of the elements appear to have little bearing on the first two principal components and cluster around the origin.

If the analyses from the peat-fired power station at Gweedore are introduced into this analysis, the results are much the same. The first two principal components explain a similar amount of the total variance (26.7%), as they did for the reference data alone and the same elements are again important (see Table 3.15).

The scores for the reference data and the peat particles (shown in blue) are plotted in Figure 3.16. The coal and oil particles are split on the first principal component, and the separate high vanadium/low sulphur oil group again appears (although this time further along the second principal component axis as the vanadium loading is positive and the sulphur loading is negative - see Table 3.15). Peat is separated out from oil on the first principal component (as like coal it will be higher in silicon and aluminium and lower in sulphur and iron) and from coal on the second principal component (again lower in sulphur but higher in sodium, magnesium and calcium). These results are consistent with those obtained in constructing the dendrograms in section 3.7.1. There is very little overlap between peat and oil particles, but more between coal and peat. This would be expected as coal and peat are fairly similar substances, both originally derived from plant material.

Figure 3.16. Plot of first and second principal component scores for the particles of the reference data-set and the reference peat data from Gweedore. (oil in yellow, coal in red and peat in blue)

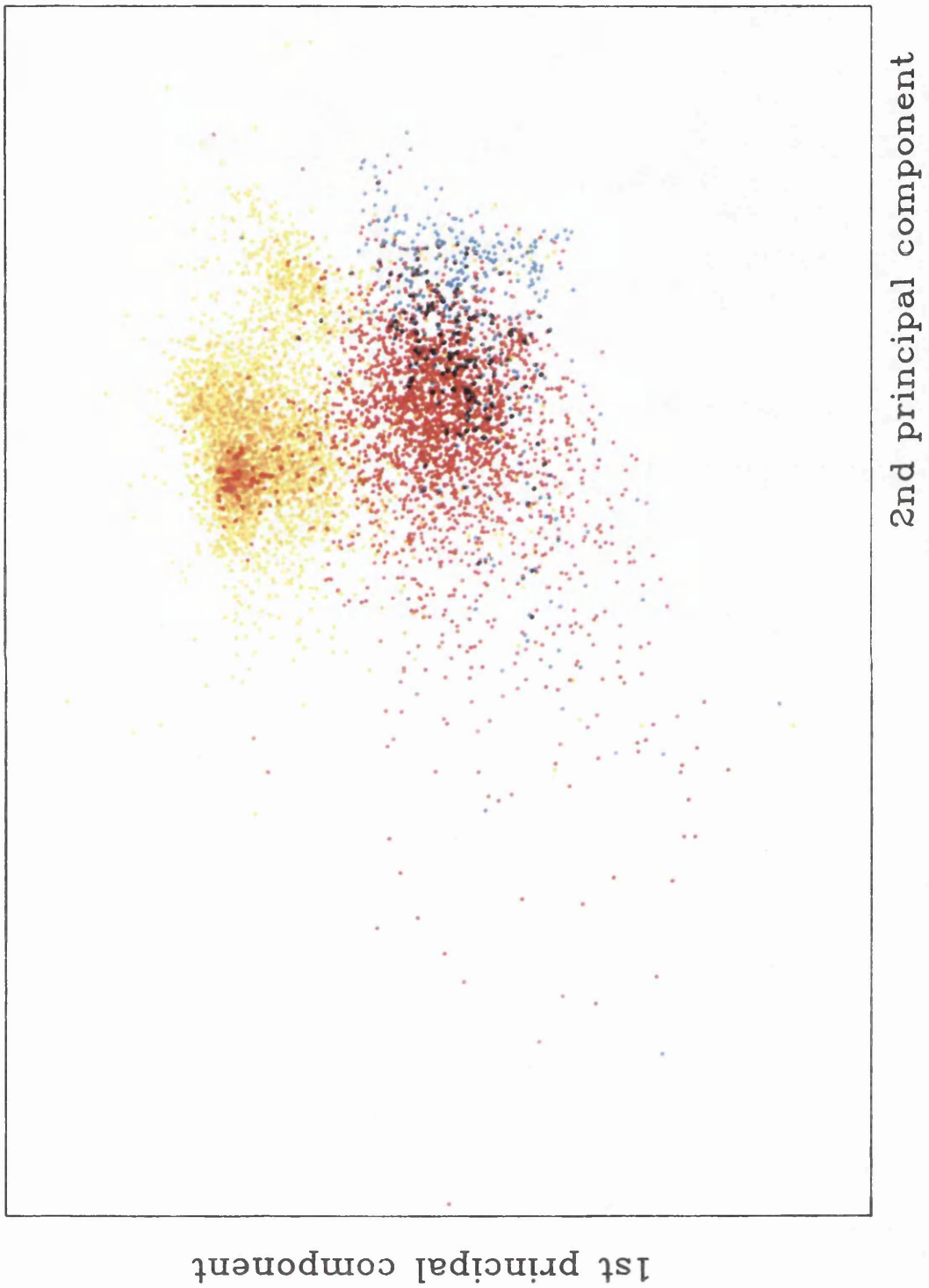

Table 3.15. Variable loadings on the first two principal components for the reference data-set including the particles from the Gweedore peat-fired station.

Variable	1st PC Loading	2nd PC Loading
Na	**0.319**	**0.480**
Mg	0.074	**0.420**
Al	**-0.468**	0.109
Si	**-0.408**	0.245
P	0.017	0.192
S	**0.500**	**-0.298**
Cl	-0.303	0.125
K	-0.126	0.099
Ca	-0.047	0.231
Ti	-0.068	0.030
V	0.156	0.246
Cr	-0.069	-0.122
Mn	-0.091	-0.153
Fe	0.216	0.224
Ni	0.127	-0.113
Cu	-0.136	-0.239
Zn	-0.157	**-0.309**

3.8.2. Discriminant analyses on the reference data-set.

Discriminant function analysis (DFA) involves the determination of a linear combination of variables allowing the derivation of a single transformed variable, or variables, by which a number of mutually exclusive groups may be discriminated (Srivastava & Carter, 1983). One advantage of this method is that it results in a classification which may be applied to samples of unknown origin, allowing them to be allocated to one of the groups with a known probability of misclassification. This is one of the most widely used multivariate procedures and has been used extensively in the geological literature as a tool to separate and classify origins of material using morphological measurements (Davis, 1986) and chemical composition

data (Borchardt et al., 1971). This has been especially important in tephra studies where deposits from different sources need to be separated to be used as stratigraphic markers and chronological indicators (King et al., 1982; Beaudoin & King, 1986; Stokes & Lowe, 1988).

Stepwise discriminant analysis (SDA) is a variant of DFA and elements important in fuel-type separations can be identified as shown in the preliminary study. Using the element data of the 5,539 particles of the reference data-set, an element ranking was produced using the F-to-enter criterion as described in section 3.7.2.

The SDA was done using the SOLO (Hintze, 1988) program and, as would be expected, sulphur and aluminium showed the highest initial F-values (see Table 3.16). That of aluminium was marginally higher, however, and was the first selected into the classification function (now called the linear discriminant function or LDF). As sulphur and aluminium were highly negatively correlated in the reference data-set (Pearson's correlation coefficient = -0.694, N = 5,539 $p \leq 0.001$), the value for sulphur decreased and ranked only tenth in the discrimination. Table 3.16 shows the element ranking, the percentage correct allocation to fuel-type for each element added to the LDF and Wilks' Lambda for each additional element (these values are also shown in Figure 3.17). Best separation is achieved at the optimal Wilks' Lambda, in this case when all 17 elements are used. However, very little improvement is caused by adding elements after sulphur (only another 27 particles out of the 5,539 correctly allocated) and a cut-off might be considered here in the interests of speed during an analysis.

The SOLO program (unlike the BMDP-7M program used in section 3.7.2) gives the operator the option of which variable to select (although this is usually the one with the highest value) once the F-to-enter values have been recalculated. This means that an alternative element ranking can be produced by selecting sulphur as the first element to enter the LDF and then taking the elements in their F-to-enter order. In this case the ranking produced is as follows: S > V > Fe > Mg > Ti > Cl > Cr > Al > K > Si > Na > Mn > Ni > P > Zn > Ca > Cu.

Figure 3.17. Graph showing the improvement in (a) Wilks' Lambda and, (b) percentage correct allocation of particles with the addition of successive elements to the linear discriminant function.

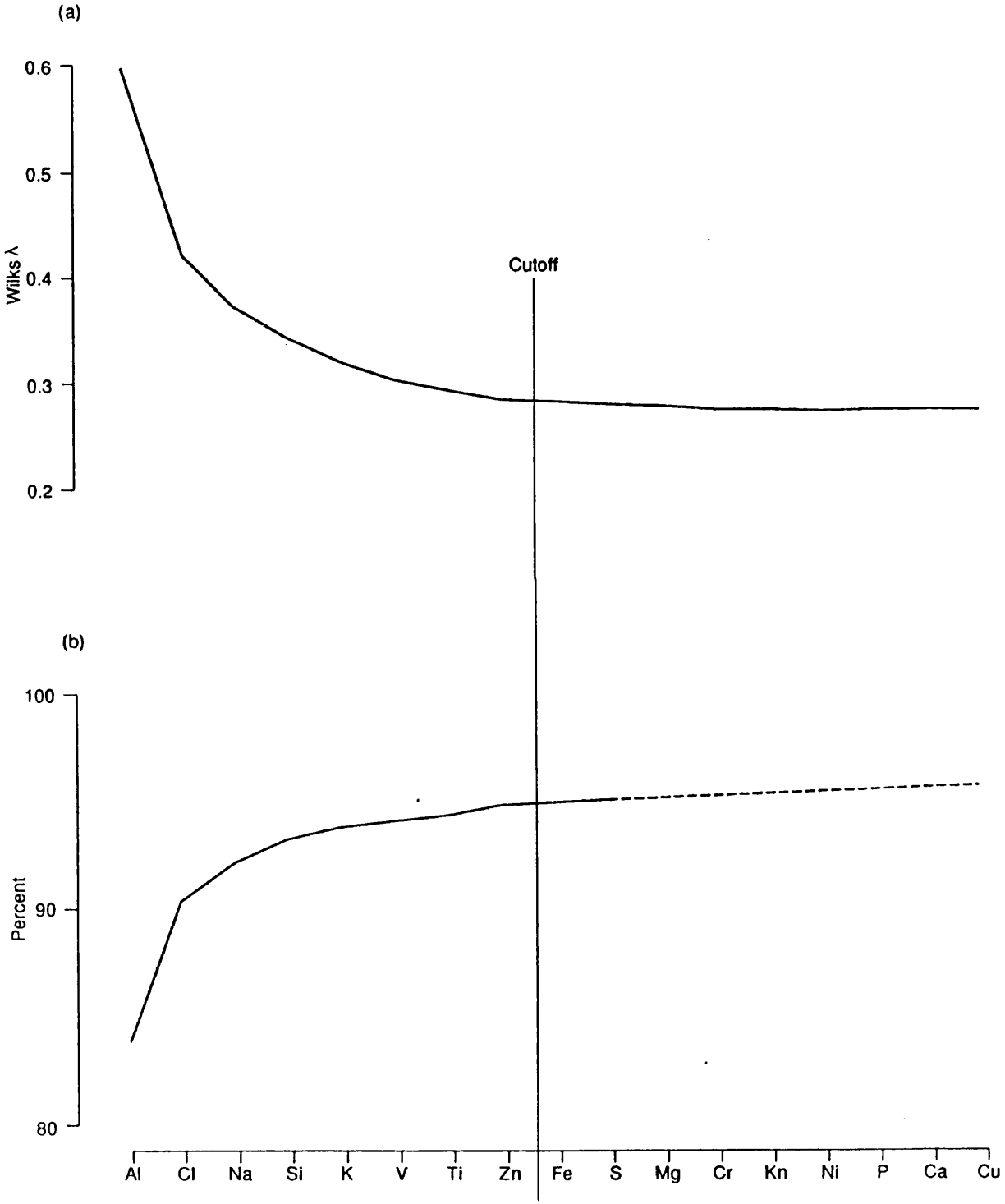

Table 3.16. Element ranking, initial F values, the % of particles correctly allocated with each added element and the respective Wilks' Lambda for a SDA on the 5,539 particles of the reference data-set.

Rank No.	Initial F value	Selected Element	% Correctly Allocated	Wilks' Lambda
1	3748.0	Aluminium	83.9	0.5963
2	1913.2	Chlorine	90.4	0.4231
3	972.2	Sodium	92.2	0.3715
4	1748.7	Silicon	93.3	0.3433
5	576.1	Potassium	93.8	0.3178
6	546.7	Vanadium	94.2	0.3005
7	134.7	Titanium	94.4	0.2909
8	7.9	Zinc	94.8	0.2844
9	832.8	Iron	94.9	0.2807
10	3329.4	Sulphur	95.0	0.2759
11	244.5	Magnesium	95.1	0.2729
12	5.3	Chromium	95.1	0.2708
13	85.2	Manganese	95.2	0.2697
14	144.9	Nickel	95.2	0.2680
15	6.4	Phosphorus	95.2	0.2671
16	21.6	Calcium	95.3	0.2671
17	9.6	Copper	95.3	0.2671

A LDF was created using the aluminium data alone and applied to the 5,539 particles of the reference data-set, of which 83.9% were correctly allocated to their fuel-type. 25.7% of coal particles and 9.2% of oil particles were misallocated and these combined, represented 16.1% of the total reference set. The next LDF was created using aluminium and chlorine data and 90.4% of the reference particles were correctly allocated. The amount of misallocated coal particles dropped to 14.9%, and oil particles to 5.8% which gave a total misallocation of 9.6%. The rest of the elements in the aluminium ranking were then used in this way and the results are shown in Table 3.17(a). This procedure was also followed for the sulphur ranking and these results are shown in Table 3.17(b).

Table 3.17. Comparison of correctly classified and misclassified particles (% of the total data-set, % coal particles and % oil particles) for linear discriminant functions produced using (a) the aluminium ranking and (b) the sulphur ranking.

Variable(s) in LDF.	% Correctly classified	% Misclassified total	coal	oil
(a)				
Al	83.9	16.1	25.7	9.2
Al+Cl	90.4	9.6	14.9	5.8
+Na	92.2	7.8	12.2	4.7
+Si	93.3	6.7	8.9	5.2
+K	93.8	6.2	8.2	4.8
+V	94.2	5.8	7.3	4.8
+Ti	94.4	5.6	6.9	4.7
+Zn	94.8	5.2	6.2	4.5
+Fe	94.9	5.1	5.8	4.6
+S	95.0	5.0	5.7	4.5
All 17	95.3	4.7	5.6	4.1
(b)				
S	84.2	15.8	13.6	17.3
S+V	92.6	7.4	9.1	6.1
+Fe	93.7	6.3	7.0	5.7
+Mg	94.5	5.5	5.6	5.3
+Ti	94.6	5.4	5.6	5.2
+Cl	94.8	5.2	6.3	4.7
+Cr	94.9	5.1	6.1	4.7
+Al	94.9	5.1	6.2	4.3
+K	95.0	5.0	6.0	4.3
+Si	95.1	4.9	5.8	4.3
All 17	95.3	4.7	5.6	4.1

It can be seen that at every stage the sulphur ranking is more successful at allocating particles to their fuel-type than the aluminium ranking. The misallocations are also interesting. With only aluminium added to the LDF, a higher percentage of coal particles are misclassified than oil, and this continues for the whole of the aluminium ranking. With only sulphur added, a higher percentage of oil are misclassified than coal, although once vanadium, the next element, is added, coal is once again the more misclassified fuel-type. The PCA of the reference data-set (Figure 3.14 above) shows the reasons for this. The coal particles have a much broader range of chemistries than the oil particles and this is shown by the scatter on the diagram, and so it might be expected that a higher percentage of the coal particles would be misallocated in most instances. Figure 3.14 also shows that the oil population is split into two parts, a high sulphur/low vanadium group and a smaller high vanadium/low sulphur group and so using only sulphur in the LDF would probably misallocate this latter group to coal causing the percentage of oil particles that are misclassified to be higher than coal. Once vanadium is added, both these groups become classified as oil, and the coal particles again have a higher percentage of misallocations.

Using all 17 elements to create a classification scheme, and then to use such a scheme for thousands of particles extracted from lake sediments takes a considerable amount of computer time. As there is very little improvement in particle allocations using all the elements, a more efficient characterisation may be achieved by reducing the number. The multivariate procedures described above point to the sulphur ranking as the marginally more successful separation method and so reducing the number of elements in the discriminant function to the top 5 or 6 of this series may be more efficient.

3.8.3. Probabilities of allocation.

So far, using the discrimination procedures described above, all analysed particles have been allocated to the fuel-type to which they fall nearest, regardless of how little they resemble either group. The SAS package used for the discrimination, produces a probability of allocation to coal and to oil for each particle. These probabilities can then be used to set a post-probability, the minimum probability

level that a particle must achieve to be allocated into a group. For example, with two groups such as coal and oil, if the post-probability is set at 0.5000, then all the particles will be allocated into one group or the other, even if the probability for doing so is only 0.5001. In such a case, the confidence that this particle has been correctly allocated must be very low. Some features, however, will have been analysed which are not carbonaceous particles, especially when this is applied to particles extracted from lake sediments, when mineral fragments may survive the extraction procedures (see section 3.5.4). Raising the post-probability may help remove these from the analysis.

Figure 3.18a shows the probability that a given particle in the reference data-set is allocated 'coal'. There are two main peaks, the 0.0 - 0.1 peak representing the majority of the oil particles and the 0.9 - 1.0 peak representing the majority of coal particles. Consequently, the post-probability can be set quite high and most of the particles will still be included. Those particles with probabilities falling below the set level are allocated to an unclassified group. However, Figure 3.18b shows the probability of allocation of all the misallocated particles and shows that 48% have a probability of allocation of over 0.9, and so the setting of the post-probability at a higher level would still include most of the misallocated particles.

Table 3.18. *The effect of different post-probability settings on the misallocation of particles.*

Post-Probability	No. Misallocated	No. in Unclassified	No.Misallocated in Unclassified
0.5	261 (4.7%)	0	0
0.6	216 (4.0%)	96	45
0.7	171 (3.2%)	209	90
0.8	147 (2.9%)	331	114
0.9	125 (2.5%)	588	136

With a post-probability of 0.5 (i.e. the lowest possible with only two groups), 261 particles are allocated to the wrong fuel-type and this corresponds to 4.7% of the

Figure 3.18. (a) Probability of allocating particles in the reference data-set to 'coal', and (b) the probability of allocation of mis-allocated particles.

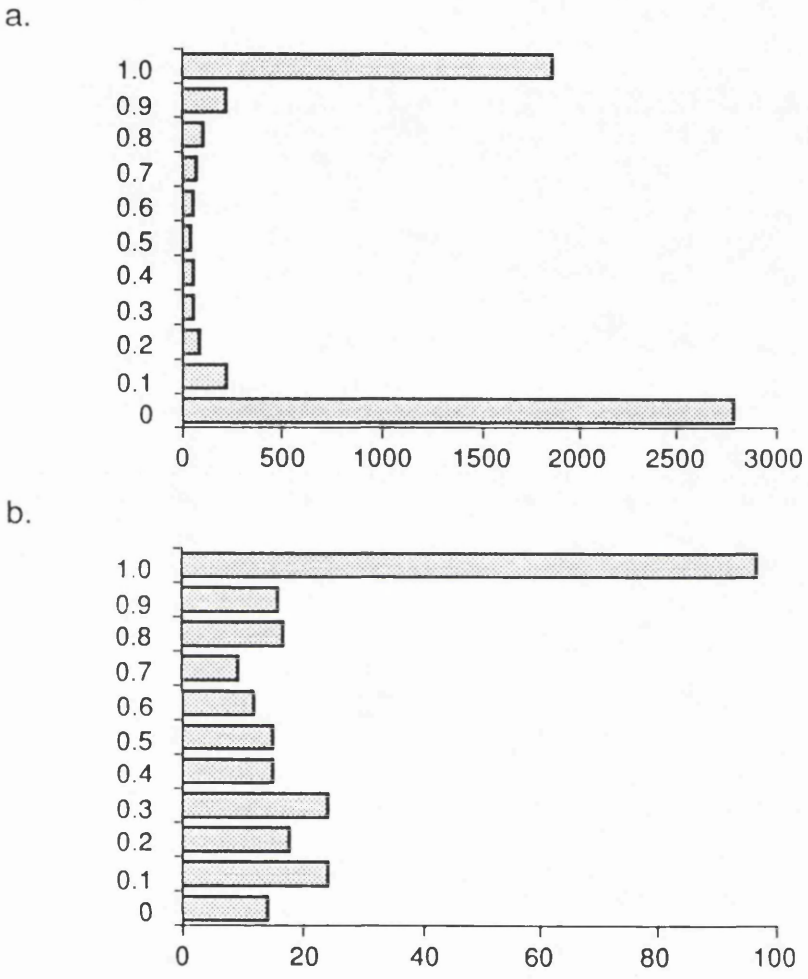

total data-set. When the post-probability is set to 0.6, 96 particles are allocated to the unclassified group. Of these 96 particles, 45 were originally misclassified, but 216 misclassified particles (4.0% of the remaining particles) are still included in the analysis. This means that of the particles allocated a fuel-type, 96% are correctly allocated. This can be done with different post-probability settings and the results appear in Table 3.18. Therefore, if the post-probability is set at 0.9, 97.5% of the particles allocated to a fuel-type are allocated correctly. However, because the unclassified group is now so large, this only represents 89% of the total data-set, and perhaps a post-probability of 0.8 would be a better compromise where 94% of the data-set are allocated a fuel-type, 97.1% correctly.

3.8.4. Derivation of a coal/oil discriminant function.

An effective classification of carbonaceous particles into coal and oil fuel-types can be achieved using the elemental surface chemistry of the particles as determined by EDS analysis. If the elements giving the best separation are determined by stepwise discriminant analysis, then little improvement (less than 0.7% more particles correctly allocated to their fuel-type) in this separation is achieved after the first six elements have been included in the LDF. The reduction in the number of elements is desirable, firstly to remove redundant elements (i.e. those which are contributing little or nothing to the discrimination), and secondly to speed up the process of characterising material extracted from sediments when thousands of particles are to be analysed. Sulphur and aluminium are initially the most important elements in producing a separation, but they are highly negatively correlated and so inclusion of one of these elements in a LDF severely reduces the usefulness of the other. Consequently, two unrelated LDFs are produced depending on which of these elements is first included. Table 3.17 shows that until all 17 elements are included, the sulphur ranking is marginally more successful, at every stage.

When principal component analysis is performed on the particles of the reference data-set, sulphur has a marginally higher loading than aluminium on the first principal component. This loading is increased when peat particles are included in the analysis, and increased still further when particles from sediments are included (see Chapter 4). The most efficient method to separate coal from oil using these

data would thus appear to be a LDF containing the top six elements in the sulphur ranking, i.e. S, V, Fe, Mg, Ti and Cl. The coefficients for this linear discriminant function are given in Table 3.19.

Table 3.19. *Coefficients for the linear discriminant function produced using the top six elements of the sulphur ranking.*

	Coal	Oil
Constant	-2.429	-10.265
S	0.097	0.249
V	0.102	0.309
Fe	0.074	0.279
Mg	-0.107	-0.008
Ti	0.089	-0.042
Cl	0.115	0.039

Using these coefficients, a score is given to each particle for both fuel-types. e.g.

Coal score = 0.097S + 0.102V + 0.074Fe - 0.107Mg + 0.089Ti + 0.115Cl - 2.429

Oil score = 0.249S + 0.309V + 0.279Fe - 0.008Mg - 0.042Ti + 0.039Cl - 10.265

The particle is then allocated to the group for which the score is most positive and, using the 5,539 particles of the reference data-set, this is done correctly 94.6% of the time.

The probability of allocation (correct or not) for most of the particles is high, but a post-probability level can be set so that some of the misallocated particles falling below this level are put into an unclassified group. If the post-probability is set too high many correctly allocated particles also fall into this group and the most effective level is 0.8 where of the 94% of the population allocated a fuel-type, 97.1% are correct.

A PCA was then carried out on the reference data-set using only those 6 elements

now used in the LDF. The loadings for the first two principal components are shown in Table 3.20, and a plot of 1st principal component versus 2nd principal component is shown in Figure 3.19.

Table 3.20. Loadings on the first two principal components for a PCA using only the six elements present in the final linear discriminant function.

Element	Loading on 1st P.C.	Loading on 2nd P.C.
S	-0.496	-0.489
V	0.631	-0.239
Fe	0.561	-0.341
Mg	0.095	-0.248
Cl	0.143	0.682
Ti	0.109	-0.739

Figure 3.19 shows a few differences from Figure 3.14 (the PCA for the reference data-set using all 17 elements). The separation of the fuel-types is fairly similar, but there appears to be less scatter within the coal particle cluster when fewer elements are used. The coal particles still appear as a single population, but the high vanadium/low sulphur oil group separates totally from the main oil group on the first principal component axis. The main oil group and the coal separate on the second principal axis, showing that the high vanadium oil group is accounting for a large proportion of the variability in the data cluster. The loadings on the first principal component show that this axis is dependant on just three elements S, V and Fe, all elements which have been shown to be present in higher amounts in oil particles (see section 3.7.1.). Therefore the coal particles do not have much distribution along this axis. The main variability in the coal cluster appears along the 2nd principal component axis, which from the loadings appears to be a Cl/Ti axis. These are elements generally associated with coal and hence there is little variability within the oil cluster on this axis. However, the loadings on this axis are such that coal particles with high titanium will plot lower down and could become mis-allocated as oil. This is particularly interesting when it is considered that it was

Figure 3.19. Plot of first and second principal component scores for the particles of the reference data-set, using only the six elements present in the final linear discriminant function (oil in yellow, coal in red).

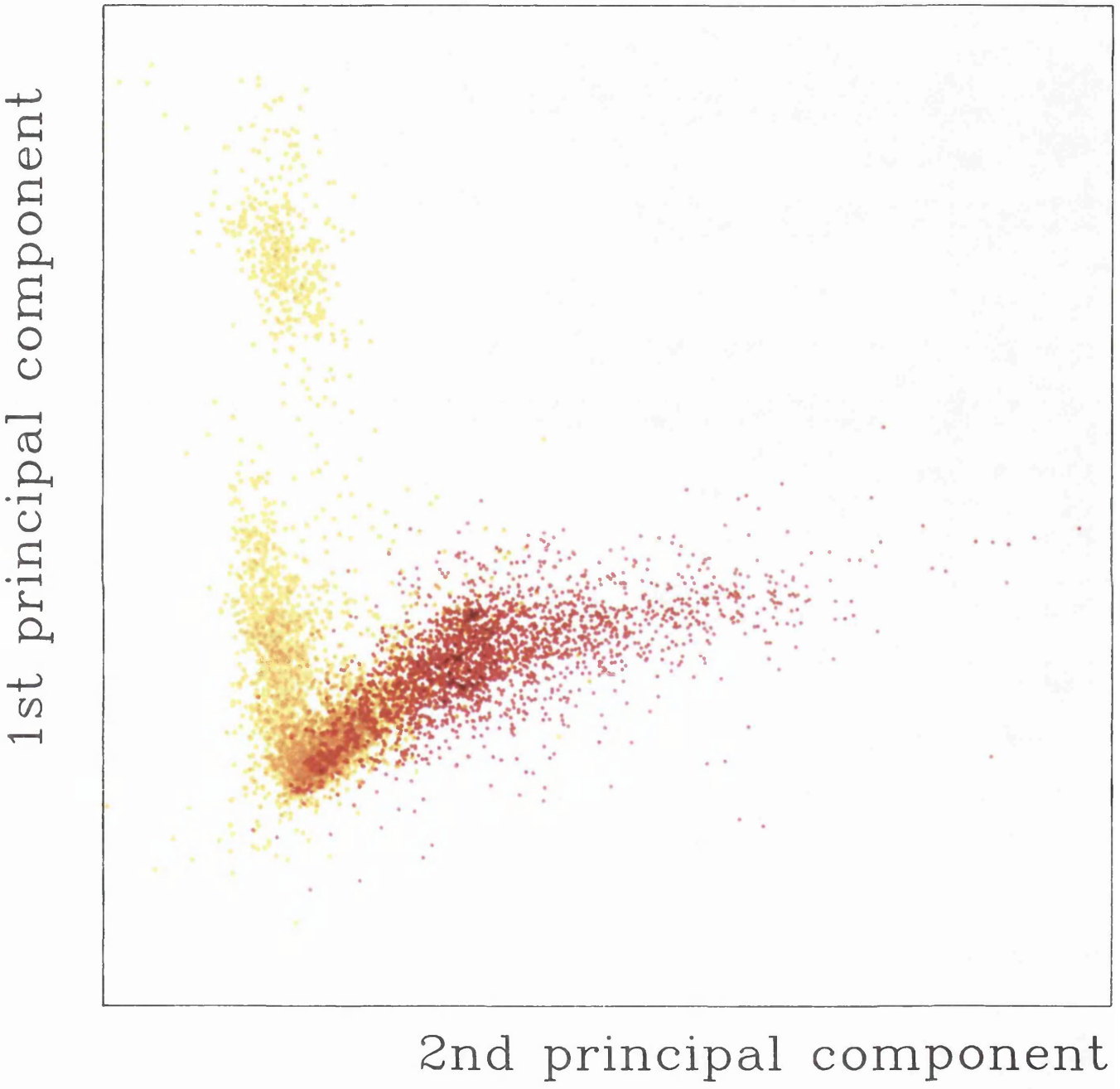

titanium that was used as a coal indicator in previous studies (Shen et al., 1976; Cheng et al., 1976).

3.9. Extensions to the characterisation technique.

3.9.1. Power station allocation.

Carbonaceous particles can be allocated to a fuel-type with a fairly high degree of confidence, but it remains to be seen whether it is possible to successfully characterise them to individual power stations within a single fuel-type. About 150 particles from each of seven power stations, five coal (Blyth, Drax, Eggborough, Ironbridge & Rugeley) and two oil (Pembroke & Tarbert) were randomly selected from the reference data-set, and a discriminant analysis was run using the chemical data from all 17 elements. Initially, no post-probability was set, the particle being allocated to the station with the highest probability, even though this could theoretically be as low as 0.143 (i.e. just higher than one seventh, or equal probability for each station). The results appear in Table 3.21a and show that most of the particles are allocated to the correct power station, although there is some overlap between stations within a fuel-type (e.g. Blyth and Drax).

Table 3.21b shows the same discrimination but with the post-probability set at 0.5. The oil-fired stations appear to separate better than the coal, with over 70% of the particles from both Tarbert and Pembroke being correctly allocated. The coal-fired stations, with the exception of Eggborough do not separate well, with the majority of the particles remaining unclassified. Blyth shows very poor allocation with none of its particles being put into the correct station.

Classification into the correct fuel-type remains very good. When no post-probability is set (making it easier to allocate incorrectly), less than 9% of particles in each case are put into stations which are of the wrong fuel-type. When the post-probability is set at 0.5, for those particles allocated to a station (i.e. not put into unclassified) less than 3.5% are allocated to a station which is a different fuel-type.

In some instances, power station allocation appears to be quite promising, but

Table 3.21. Probabilities of power station allocation.

a) No post-probability

	Percent Classified into Station.						
From Stn.	blyt	drax	eggb	iron	pemb	ruge	tarb.
blyt	31.71	24.39	6.10	17.07	0.61	18.90	1.22
drax	14.55	49.70	4.85	10.91	1.21	11.52	7.27
eggb	4.35	6.83	77.64	6.83	0.62	2.48	1.24
iron	26.85	21.48	6.71	21.48	0.67	17.45	5.37
pemb	0.00	5.68	0.00	1.70	71.02	0.57	21.02
ruge	11.03	15.17	1.38	15.17	0.00	52.41	4.83
tarb	0.74	2.22	2.96	2.22	1.48	0.00	90.37

b) Post-probability = 0.5

	Percent classified into Station							
From Stn.	blyt	drax	eggb	iron	pemb	ruge	tarb	unclass
blyt	0.00	4.88	2.44	0.00	0.61	10.98	0.61	80.49
drax	0.00	7.88	2.42	0.00	1.21	9.09	1.21	78.18
eggb	0.00	0.62	70.81	0.00	0.00	1.24	0.00	27.33
iron	0.00	4.03	5.37	2.01	0.67	10.74	2.68	74.50
pemb	0.00	1.14	0.00	0.00	70.45	0.00	17.61	10.80
ruge	0.00	0.69	0.69	0.00	0.00	41.38	1.38	55.86
tarb	0.00	0.00	2.96	0.00	1.48	0.00	84.44	11.11

once again the particles being allocated to the stations are also the ones used to form the discriminant function and this artificially raises the number of particles correctly allocated to their station. Also, the particles used to undertake this separation were produced over a short period of time, and presumably from one fuel

source. In reality, large power stations use fuels from many sources over a period of months (Street, pers. comm.) and the sediment record of carbonaceous particles is only resolvable in terms of years (see Chapter 4). To proceed with a power station characterisation for carbonaceous particles extracted from lake sediments, a number of ashes from each station covering a longer period of time would need to be collected and studied together. In this way, a classification based on station differences rather than fuel source differences may be produced. Even then, it may be that characterisation of power stations within a fuel-type proves impossible to do with any certainty.

3.9.2. Extension to other fuel-types.

Although the possibility of taking this particle characterisation a stage further to power station level seems unlikely, extending it to include other fuel-types commonly used in other parts of Europe seems highly plausible. The initial classification scheme generated in section 3.7.1, showed that peat particles can be separated from those of coal and oil quite readily and this was supported by the principal components analysis performed including the peat data (see Figure 3.16). This work has not been taken any further in the present study, but it seems very likely that an effective characterisation including peat could be produced. The work of Mejstrik & Svacha (1988), shows that fly-ash produced from power stations burning brown coal and lignite in Czechoslovakia is enriched in Co, Zn, Cr, Ni and Cd. If this is true of all brown coal and lignite ashes then there should be few problems in including these fuel-types in a future characterisation scheme.

The linear discriminant function produced here was used to allocate sources for both sediment core material (i.e. temporal distribution of coal and oil types) and surface sediment material (i.e. spatial distribution). These results are described and discussed in Chapters 4 & 5 respectively. With the inclusion of other fuel-types in some future classification, the potential exists to look at both spatial and temporal distribution of fossil-fuel derived particles from many different sources on a European scale.

CHAPTER 4. TEMPORAL DISTRIBUTION OF FLY-ASH PARTICLES IN LAKE SEDIMENTS.

4.1. Introduction

As lake sediments accumulate they record atmospheric pollutants deposited on to the lake and its catchment. These pollutants include carbonaceous particles and inorganic ash spheres. Analysis of a sediment core for these particles gives a record of the fossil-fuel combustion history for the region.

The first work of this kind was done by Griffin & Goldberg (1981) when a profile of percentage carbon by weight was produced for a box core taken from Lake Michigan. This was essentially a charcoal analysis, and the percentage carbon values of the >38μm fraction were produced using infra-red techniques. Consequently, there was a carbon record at all levels in the profile due to domestic wood burning and natural fires, and the industrial fossil-fuel record began at around 1900. This was shown by an increase in carbon levels and a change in particle morphology towards a more spherical nature. Carbon concentrations doubled in the periods 1900-1930 and 1930-1960 followed by a decline. It was concluded that the particles found in lake sediments produced by the high temperature combustion of fossil-fuels had the characteristic of sphericity, and that the change in concentrations of this type of particle reflected the changes in fossil-fuel consumption and the introduction and improvement of particle-arresting techniques at the combustion sources.

Profiles of carbonaceous spherule concentration from Swedish lakes (Renberg & Wik, 1984, 1985a & 1985b) similarly reflected the historical development of coal and oil burning on a regional scale. These profiles showed the beginning of particle deposition to be around the middle of the 19th century, due to increased coal burning in the Industrial Revolution. There was a steady rise in particle concentration after this, followed by a sharp increase after the Second World War due to increased oil consumption. A peak value occurred around 1970, immediately before the oil crisis, and this was followed by a general decline in particle

concentration. This pattern emerged so consistently that it became possible to use these carbonaceous particle profiles as an indirect dating method for sediment cores (Renberg & Wik, 1985a).

The first carbonaceous particle profile for a British lake sediment core was produced for the Round Loch of Glenhead by Darley in 1985 and this correlated strongly with the history of fossil-fuel combustion in Britain (Darley, 1985). The particle record began in the mid-19th century at the time of the Industrial Revolution and there was a sharp increase after the Second World War due to the rapid expansion of the electricity generation industry. This was followed by a steady increase in particle concentration to the sediment surface. A peak value just before the time of the oil crisis was not observed because the British electricity generating industry was, and still is, dominated by coal rather than oil combustion (see Figure 4.1). Additional cores analysed by Natkanski (formerly Darley) showed a decline in concentration in the uppermost sediment levels. This was not seen at all sites, being more common in cores taken from more northerly locations (Wik & Natkanski, 1990). This work is discussed further below.

This chapter describes the temporal trends of non-differentiated carbonaceous particle concentrations (i.e. no coal/oil separation) in British lake sediments and discusses regional differences in these patterns. The distribution of carbonaceous particles characterised according to fuel-type down a sediment core is also described for one site and the potential for using this technique to add extra dating levels to a sediment core is assessed. Finally, the temporal trends of inorganic ash spheres are discussed.

The locations of the sites considered in this chapter are shown in Figure 2.2. The particle concentrations on the profile diagrams are expressed in per gram dry mass of sediment (gDM^{-1}) and where error bars are shown, these are 95% confidence limits on the statistical counting error. The data for all the sediment profiles analysed for this study are shown in Appendix B.

Figure 4.1. Consumption of coal and oil in the electricity generation industry in England Wales 1920 - 1988.

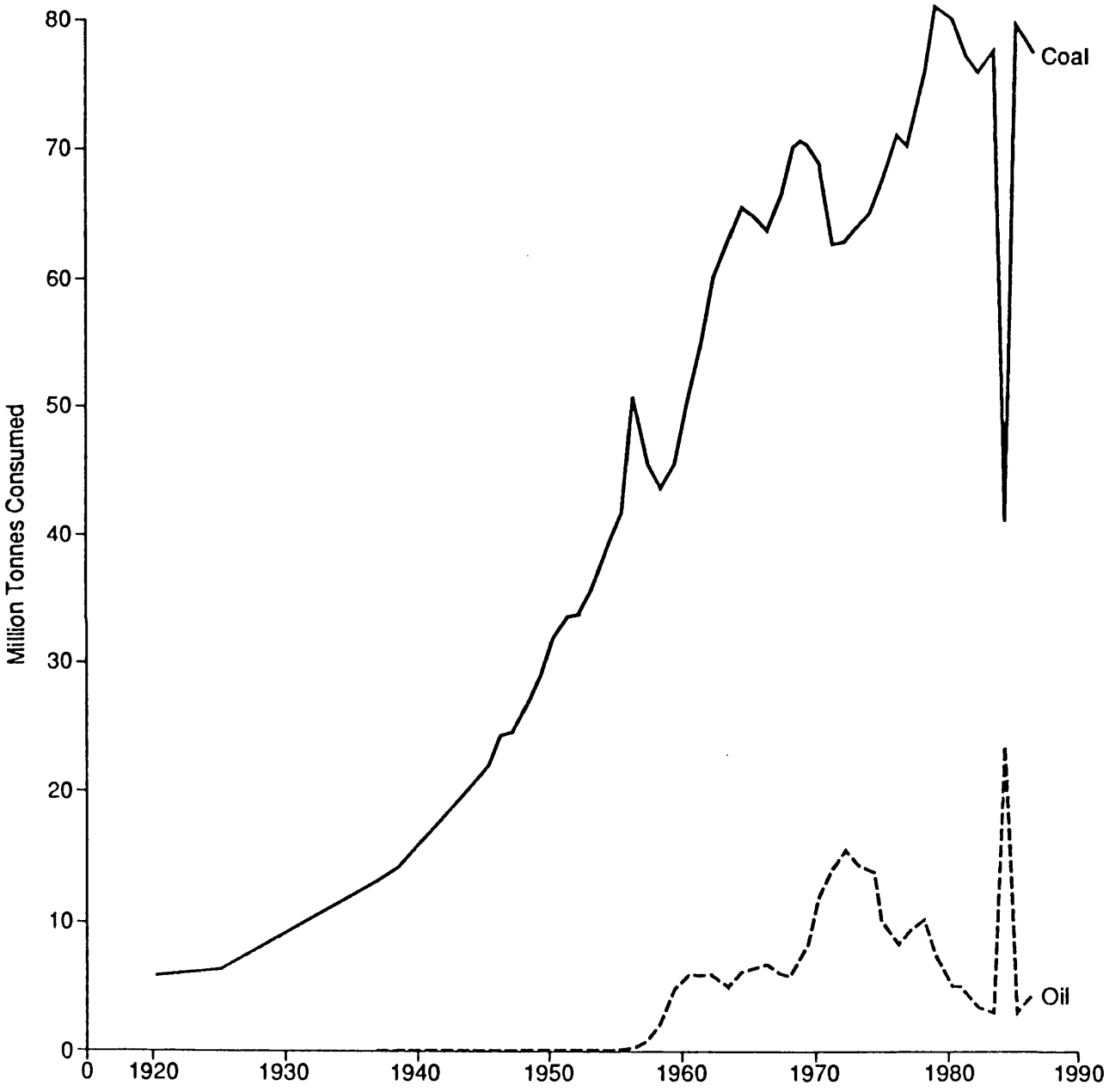

(From Electricity Council Statistics, 1988)

4.2. Temporal trends in carbonaceous particle profiles in lake sediments.

4.2.1. Scotland.

The carbonaceous particle profiles for sediment cores from six Scottish lochs were produced as described in section 2.4. These were Loch na Larach (site 55), Long Loch of Dunnet Head (56), Loch Teanga (57), Loch Coire nan Arr (58), Loch Uisge (60) and Loch Doilet (61). All these cores were ^{210}Pb-dated. Loch Tinker (66) was also analysed and this has been discussed in section 2.4. In addition, the Round Loch of Glenhead and Loch Fleet were re-cored after an interval of several years and these were used to assess the most recent changes in carbonaceous particle concentrations. In these instances, the earlier cores were analysed using the method described by Renberg & Wik (1984), and the later cores as described in section 2.4. For these cores, only the earlier ones were ^{210}Pb-dated.

Loch na Larach.

The sediment core analysed was LAR8 taken in June 1986. The results are shown in Figure 4.2. The particle record starts in the 1860's and increases until the 1890's. This is followed by a period of decrease in concentration until the 1930's. Particle concentrations increase from this time until the mid-1970's, with a plateau in the 1940's/1950's and a sharp increase in concentration in the early 1960's. There is a peak particle concentration of 3,336 gDM^{-1} in 1976 (± 2 years) after which there is a general decline to the surface.

Long Loch of Dunnet Head.

The sediment core analysed was LON2 taken in June 1986. The results are shown in Figure 4.3. The particle record begins earlier than the first ^{210}Pb date, probably around 1810-1820. There is a steady increase in particle concentration until the turn of the century when there is a sharp increase. This is the result of only one datum point however, and may appear exaggerated due to the low particle concentrations throughout the profile. Apart from this point there is a steady increase in concentration up until the late-1960's when there is a sharp increase to a peak of 3,839 gDM^{-1} in 1975 (± 2 years). This is a similar peak concentration to that of Loch na Larach and both are situated near the north coast of Scotland. After the

Figure 4.2. Carbonaceous particle profile for Loch na Larach (core LAR8) taken in June 1986.

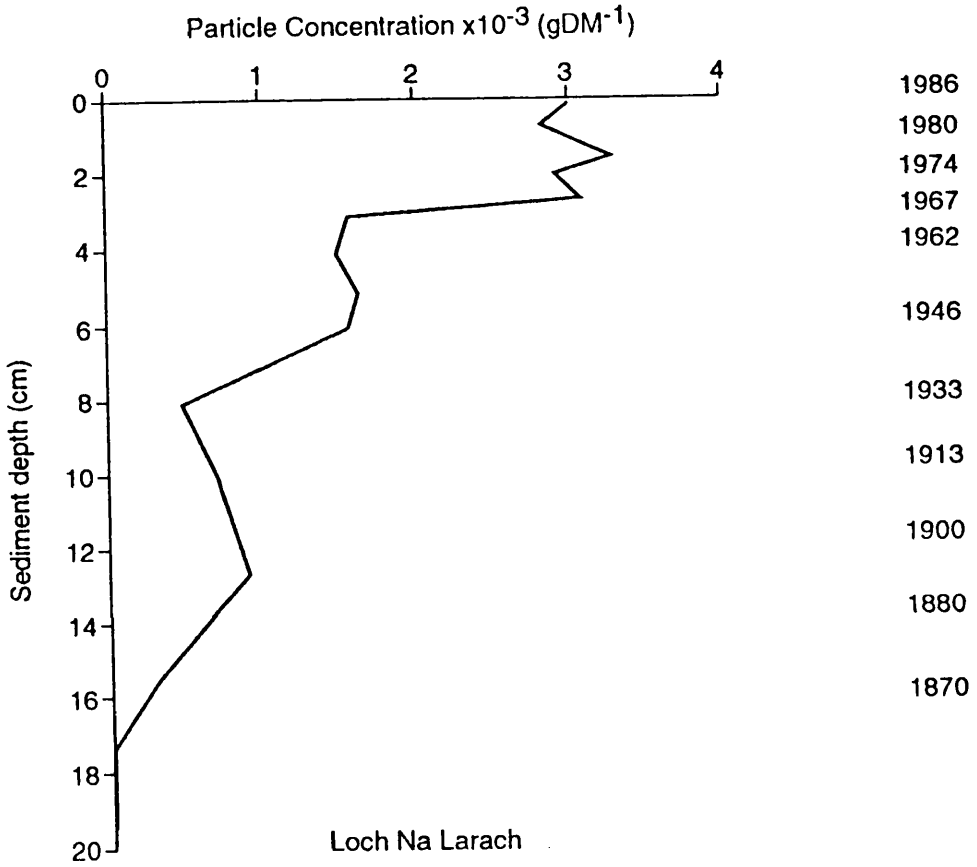

Figure 4.3. Carbonaceous particle profile for Long Loch of Dunnet Head (core LON2) taken in June 1986.

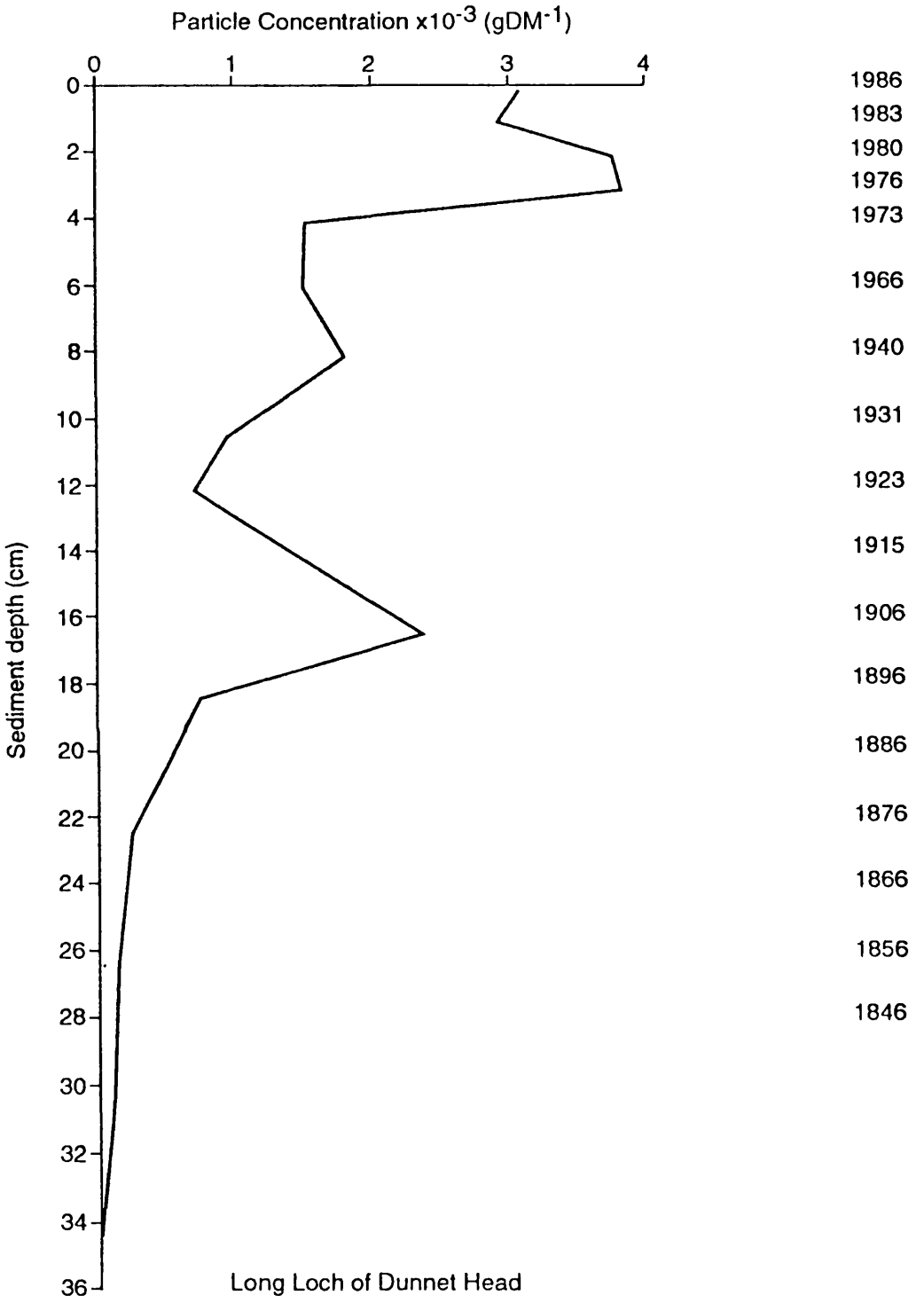

peak there is a general decline in particle concentration to the surface.

Loch Teanga.

The sediment core analysed was TEAN5 taken in September 1987. The results are shown in Figure 4.4. The particle record begins in the 1890's, later than the cores mentioned above. There is generally a steady increase until the early-1960's when the concentration curve steepens and this continues to the surface of the sediment. Although there is no decrease the curve begins to flatten in the uppermost levels (this is supported by inorganic ash sphere evidence - see section 4.4). Loch Teanga is situated on South Uist in the Outer Hebrides and the highest concentration of 3,040 gDM^{-1} is very similar to other sites in the far north of Scotland.

Loch Coire nan Arr.

The sediment core analysed was ARR2 taken in June 1986. The results are shown in Figure 4.5. There are very low concentrations of carbonaceous particles throughout this core although the concentration does not fall to zero at the lowest depth analysed. With such low values it is difficult to interpret the profile. There is, however, a general increase in particle concentration up to the surface, and no recent decline is apparent. The surface particle concentration of 1,806 gDM^{-1} is amongst the lowest values found in contemporary British sediments.

Loch Uisge

The sediment core analysed was UIS1 taken in June 1986. The results are shown in Figure 4.6. There is a long low particle concentration record at the bottom of this core and the values do not fall to zero. If the accumulation rate has not varied, the carbonaceous particle record starts close to the beginning of the nineteenth century. This is an unusually early date and is possibly an artefact due to core smearing (see section 2.4.6). Even so, there is a characteristically steady increase in concentration from the bottom of the profile to the 1950's when there is a sharp increase to a peak at 1975 (± 2 years) of 6,002 gDM^{-1}, followed by a decline to the sediment surface.

Loch Doilet.

The sediment core analysed was DOI2 taken in June 1986. The results are shown

Figure 4.4. Carbonaceous particle profile for Loch Teanga (core TEAN5) taken in September 1987.

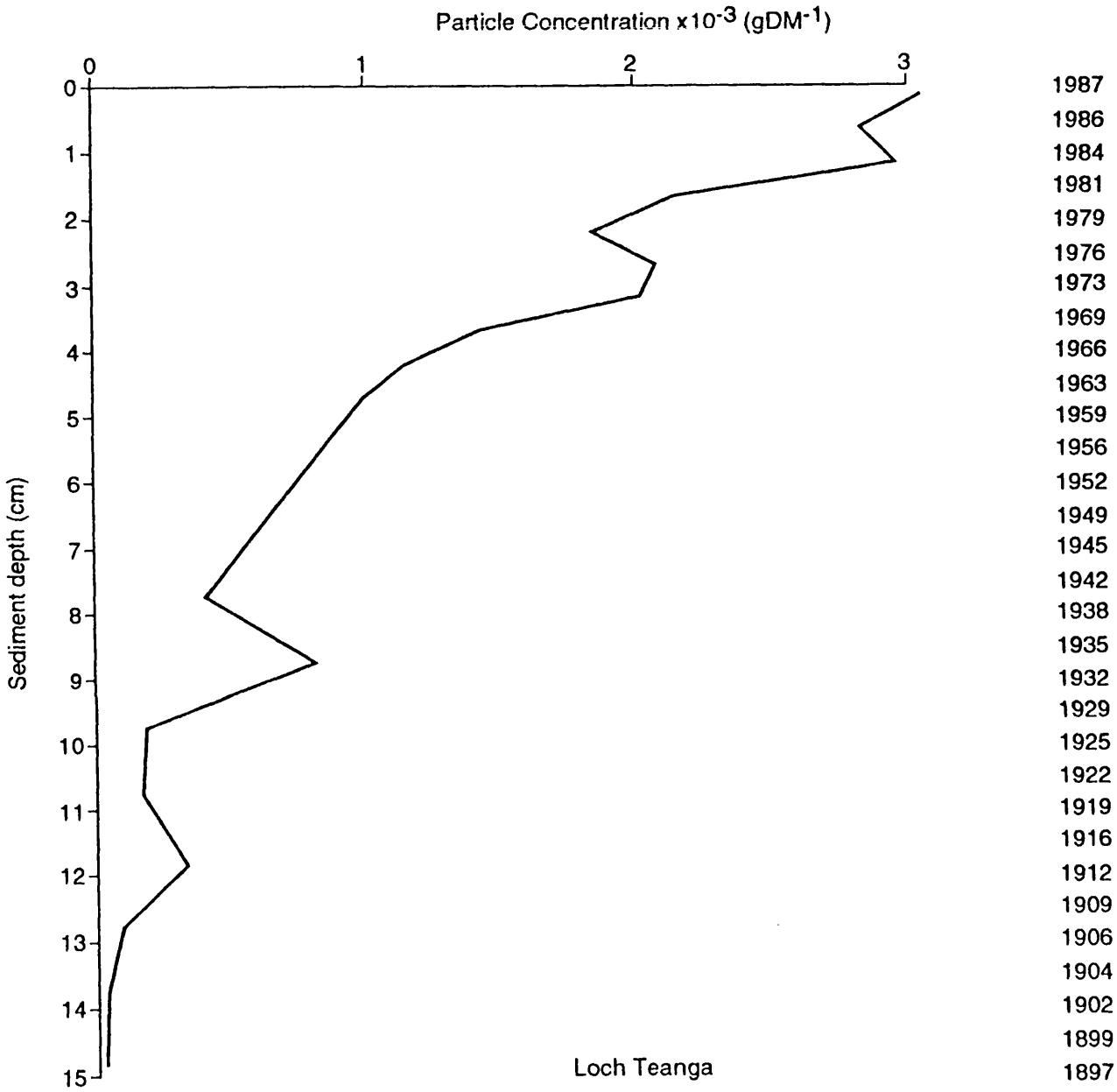

Figure 4.5. Carbonaceous particle profile for Loch Coire nan Arr (core ARR2) taken in June 1986.

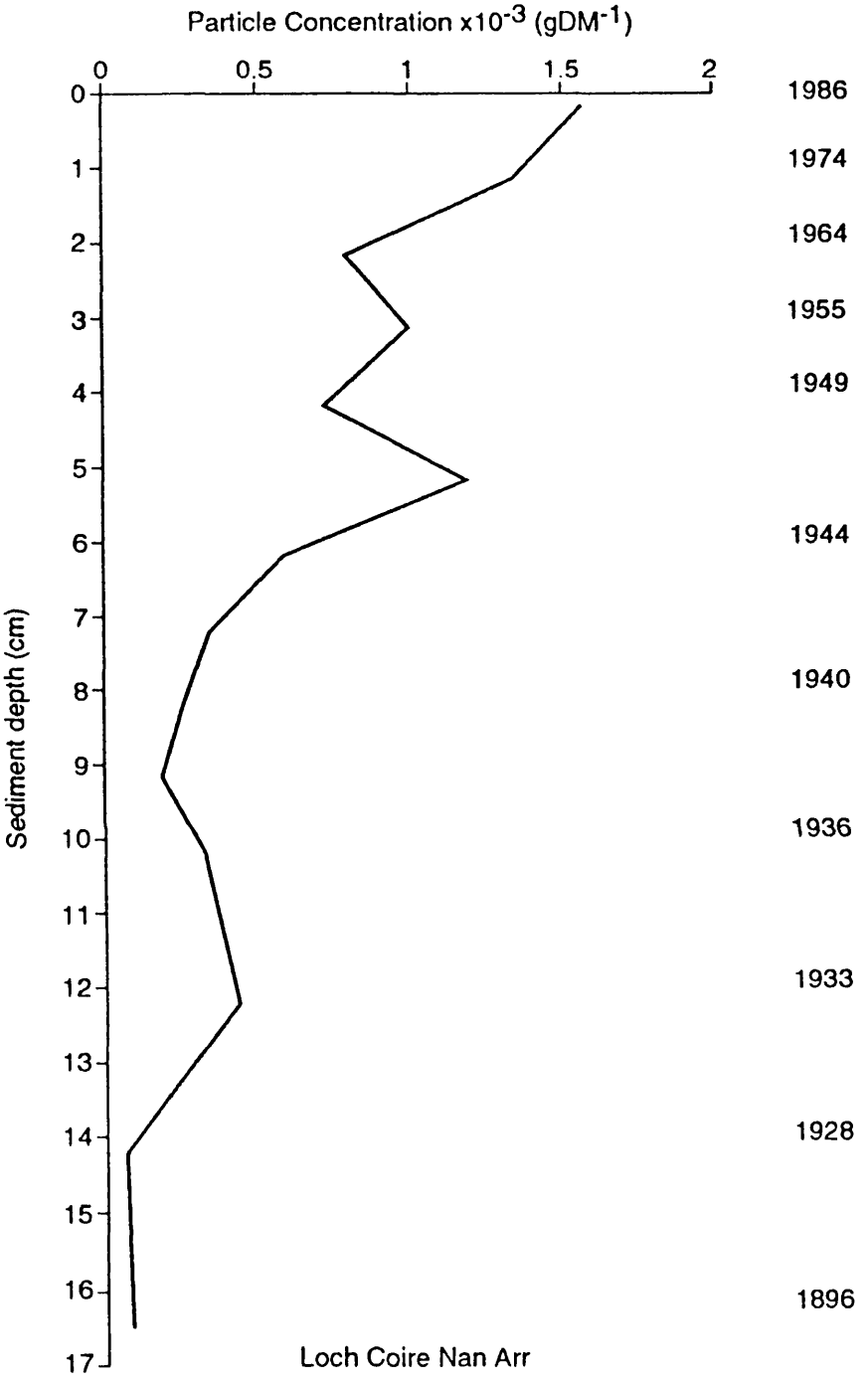

Figure 4.6. Carbonaceous particle profile for Loch Uisge (core UIS1) taken in June 1986.

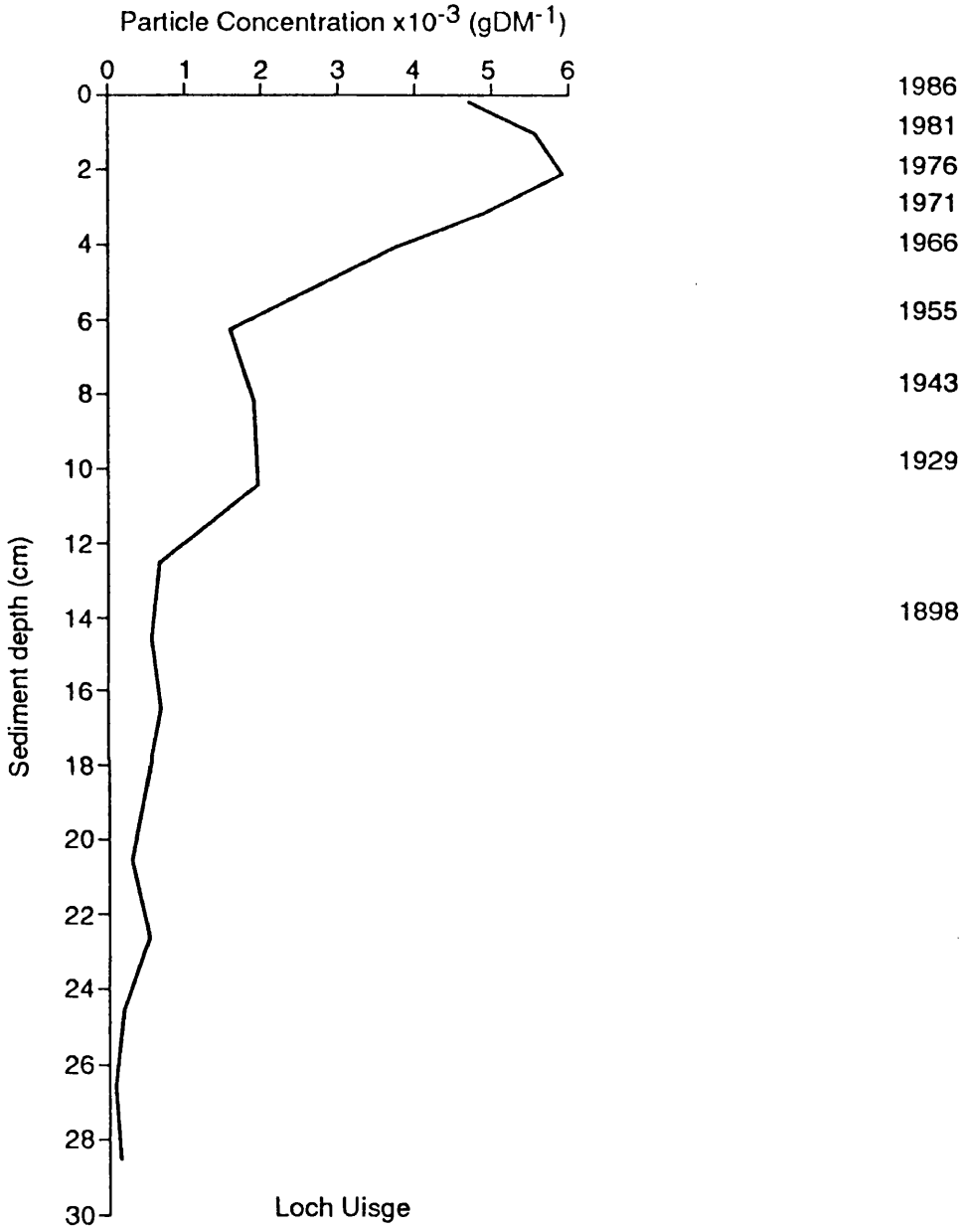

in Figure 4.7. As for the Loch Coire nan Arr profile, there are very low concentrations of particles throughout. The record begins in the 1890's, but the profile is too variable to identify any characteristic features.

Round Loch of Glenhead.

The first sediment core to be analysed for carbonaceous particles (RLGH3) was taken in May 1984 and analysed by Darley using the Renberg and Wik (1984) method. The results appear in Darley (1985). Carbonaceous particles were recorded in sediments dating from 1780, but these were in very low numbers and were probably due to core smearing. Figure 4.8a shows the post-1900 profile. Particle concentrations increased steadily until the 1930's when the concentration increased more rapidly up to the sediment surface where values are over 90,000 gDM^{-1}. Round Loch of Glenhead is situated in Galloway in the south-west of Scotland an area of high sulphur deposition (relative to the rest of Scotland) and this particle concentration is correspondingly one of the highest recorded for the region.

The core taken from Round Loch of Glenhead in 1988 was RLGH88 and was analysed for carbonaceous particles using the technique described in section 2.4. The results appear in Figure 4.8b and show a major decrease in the surface 1.5cm. If the accumulation rate of this core is similar to others taken from the loch (Flower et al., 1987; Jones et al., 1989) this peak is dated to around 1979-1980. A more recent ^{210}Pb-dated core taken in 1989, shows the surface levels to have a higher rate of accumulation (about 0.3cm yr^{-1}) which would put the peak at 1984, the date when RLGH3 was taken. The surface value of the 1984 core would then correspond to the peak in the 1988 core. The lower particle concentration in RLGH3 is probably due to the use of a technique which is not as sensitive to smaller carbonaceous particles as that used for the 1988 core (see section 2.4.8).

Loch Fleet.

The first sediment core to be analysed for carbonaceous particles from Loch Fleet was LF L3 taken in July 1985 and analysed by Darley using the Renberg and Wik (1984) method. The results appear in Anderson et al. (1986) and in Figure 4.9a. Due to the very high sediment accumulation rate for this core (Anderson et al., 1986)

Figure 4.7. Carbonaceous particle profile for Loch Doilet (core DOI2) taken in June 1986.

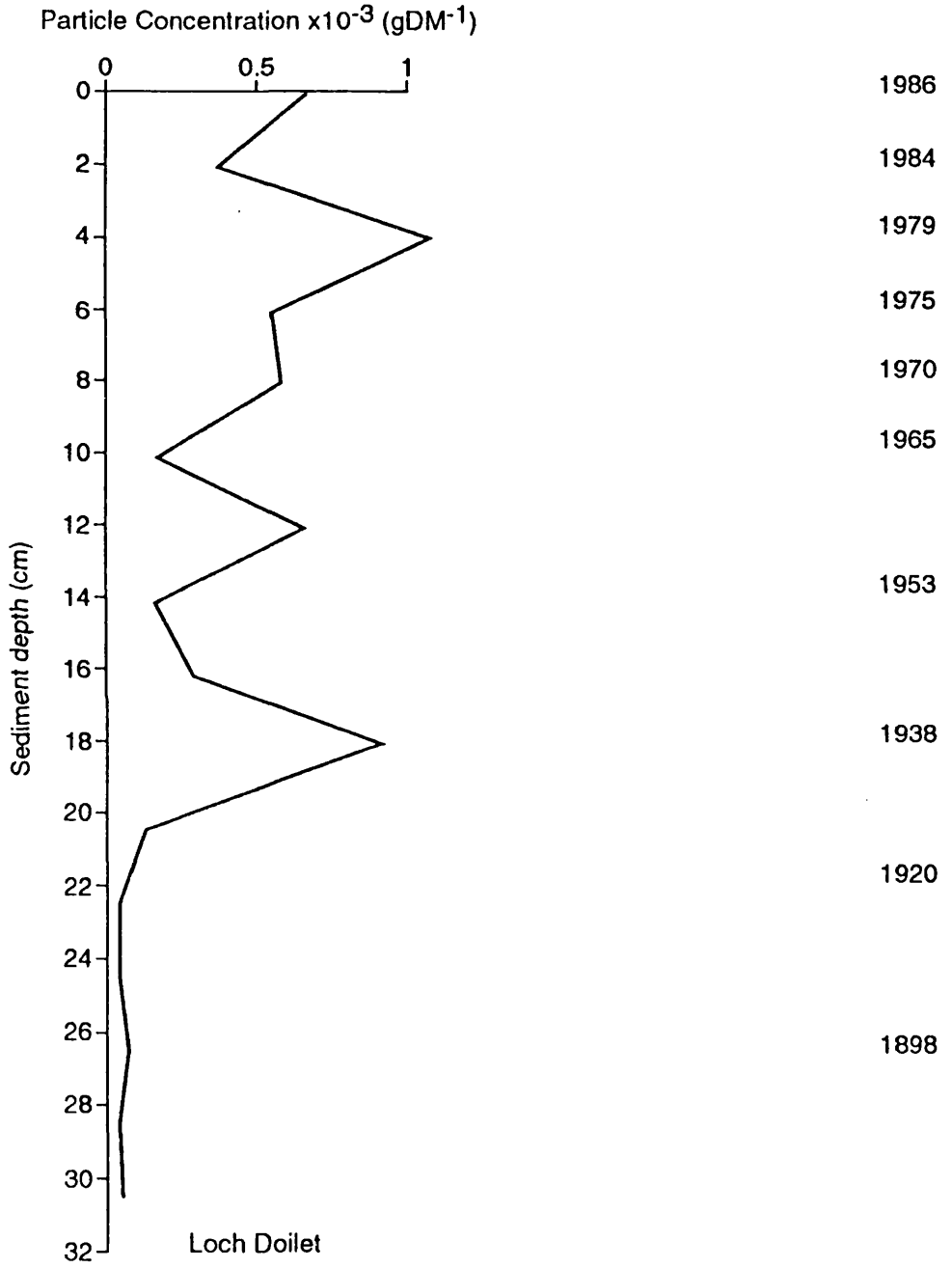

Figure 4.8. Carbonaceous particle profiles for Round Loch of Glenhead (a) core RLGH3 taken in May 1984, and (b) core RLGH88 taken in 1988.

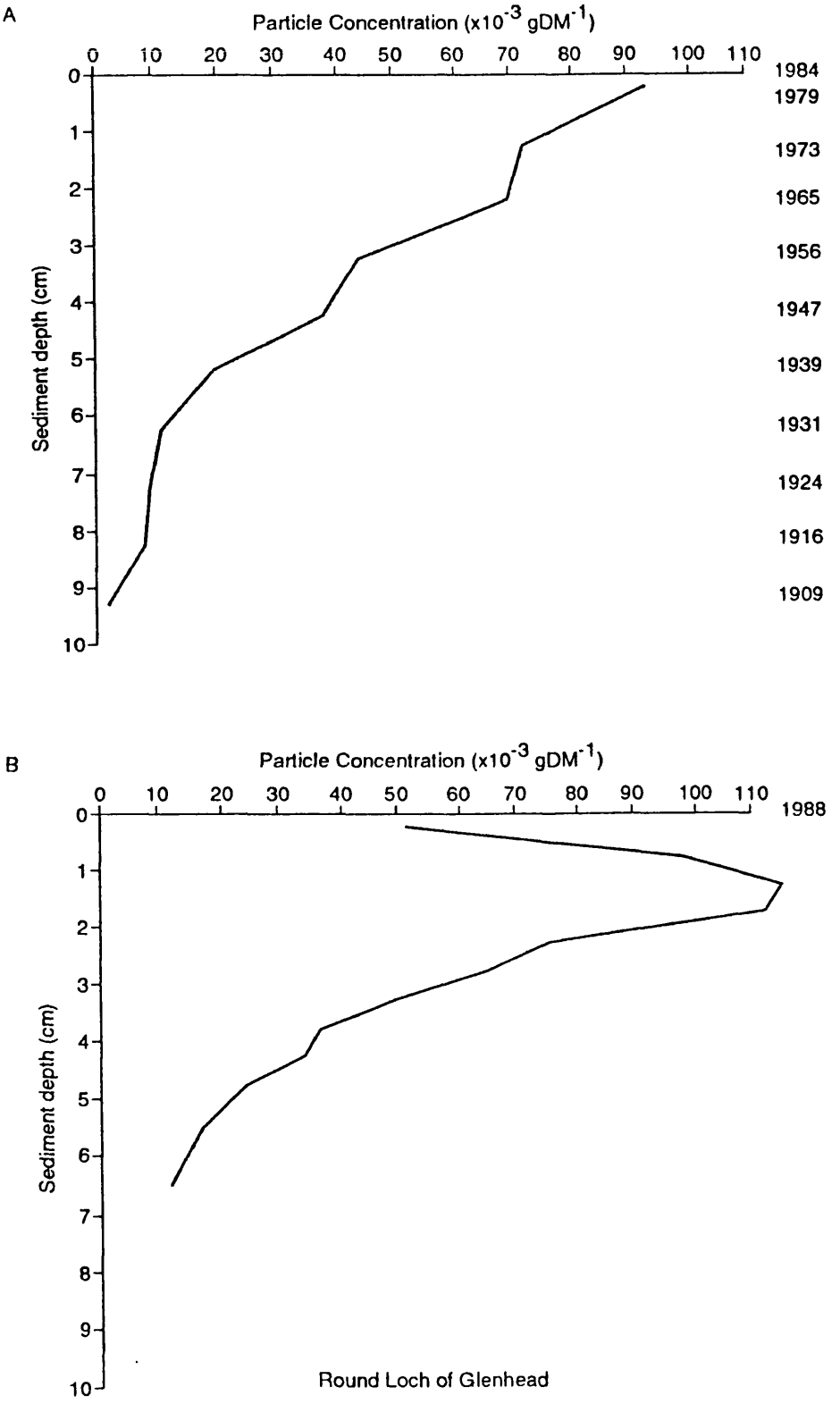

Figure 4.9. Carbonaceous particle profiles for Loch Fleet (a) core LF L3 taken in July 1985 and (b) core LFK90 taken in October 1990.

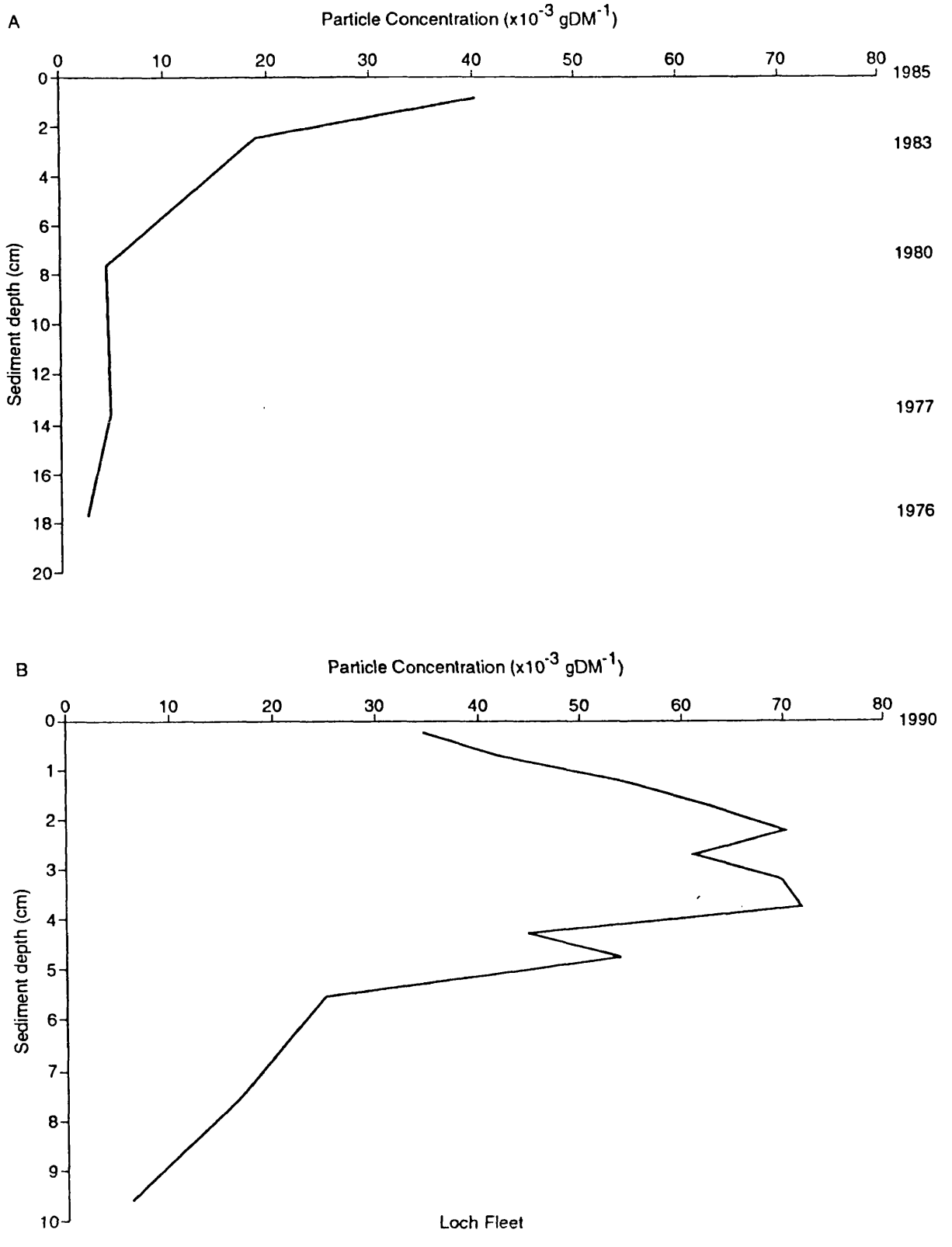

the particle concentrations remain low relative to other sites in the Galloway region until the late-1960's. Concentrations then increase steadily until about 1980 when they increase more sharply. This rapid and sudden increase may have been due, in part, to the slowing down of accumulation rate after a reduction in soil-inwash following catchment ploughing in the early 1960's. There is no surface decline in particle concentration.

Loch Fleet was re-cored in October 1990 (core LFK90) and analysed as described in section 2.4. The results appear in Figure 4.9b and, as for the Round Loch of Glenhead profile, they show a major decrease at the surface. The surface levels of the ^{210}Pb-dated 1985 core show the sediment accumulation rate to be approximately 1.4cm yr^{-1} (Anderson et al., 1986) and this would date the peak in the 1990 core at 1987. Recent studies (Cameron, unpub. data) show that the accumulation rate is still slowing down and so the carbonaceous particle peak may date a little earlier than 1987. Anderson (1990) has shown that there is considerable variability between sediment cores taken from Loch Fleet and so the date of the peak is somewhat uncertain.

Other Scottish sites previously described.

In addition to those described above, carbonaceous particle data are available from four other sediment cores from Scotland taken between 1984 and 1986. These were analysed by Natkanski (in Battarbee et al., 1988) using the Renberg & Wik (1984) method. These are briefly described below and their locations also shown on Figure 2.2.

Loch Urr, cored in May 1984, shows the start of the particle record at 1840, and a steady increase in concentration up to the 1950's when there is a sharp increase to the sediment surface. The surface particle concentration is 6,790 gDM^{-1}.

Loch Tanna, cored in June 1986, shows the start of the particle record in the 1870's. Concentrations remain low until the 1950's when there is a very rapid increase in particle concentration. A peak in concentration of 16,800 gDM^{-1} dates at about 1973.

Loch Laidon cored in July 1985, shows the start of the particle record to be unusually late, in the 1940's. However, it is probably that the Renberg & Wik technique used was not sensitive enough to detect particles present in lower concentrations in earlier sediments. The particle concentration record increases very rapidly up to a peak of 11,060 gDM^{-1} in the mid-late 1970's after which there is a slight decrease in concentration to the surface.

Lochnagar, cored in June 1986, shows the start of the particle record in the 1840's. Particle concentrations increase only slowly until the 1940's when there is a sharp increase in concentration up to a peak of 11,110 gDM^{-1} in the mid-1970's followed by a decline to the surface.

Other Scottish sites: presence and distribution of near-surface decline.

From the cores described above, it can be seen that a feature of carbonaceous particle profiles from sediment cores taken after 1985 is a decrease in particle concentration at the surface levels of the core. This decrease appears in cores from all the regions studied and therefore probably represents a real decrease in atmospheric deposition. Moreover, if this feature is synchronous between sites then it may be possible to use it as a new dating level in post-1985 cores.

A further seven sediment cores from Scottish lochs selected from areas of Scotland not represented by the lochs above were analysed for carbonaceous particles to ascertain the distribution of the surface decline. These sites were: Loch Saugh (1), Lily Loch (5), Loch Dallas (8), Loch Bran (14), Loch Arial (33), Loch Walton (37) and Loch Dubh Cadhafuaraich (85). The locations of these sites are shown in Figure 2.2 and the profiles are shown in Figures 4.10 - 4.16 respectively.

A surface decline occurs in all these cores except for one, Lily Loch. This loch has a very slow accumulation rate, with the whole carbonaceous particle profile occupying only the top 4cm, and a surface decline would not be expected in such a core. The extent to which the particle concentration decreases in the surface levels of the other cores is quite variable. The profiles from Loch Bran, Loch Walton and Loch Dubh Cadhafuaraich show a decrease in the uppermost level only and in the latter two the concentration does not decrease by very much. By contrast, the Loch

Figure 4.10. Carbonaceous particle profile for Loch Saugh (core SAUG1) taken in August 1989.

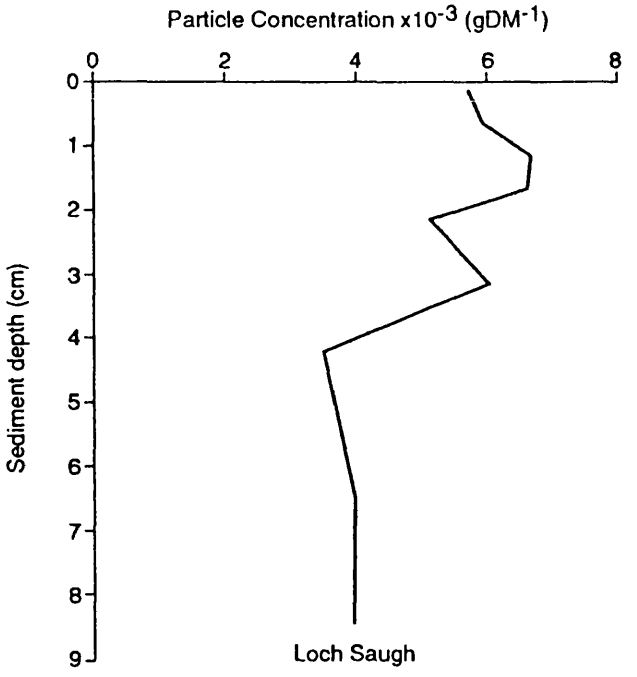

Figure 4.11. Carbonaceous particle profile for Lily Loch (core LILY1) taken in August 1989.

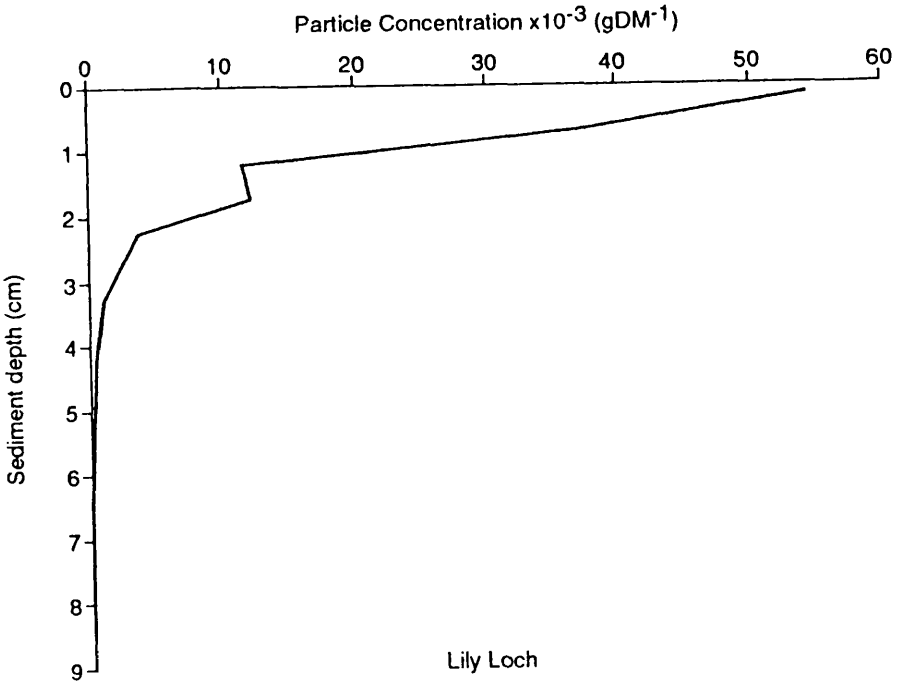

Figure 4.12. Carbonaceous particle profile for Loch Dallas (core DALL1) taken in August 1989.

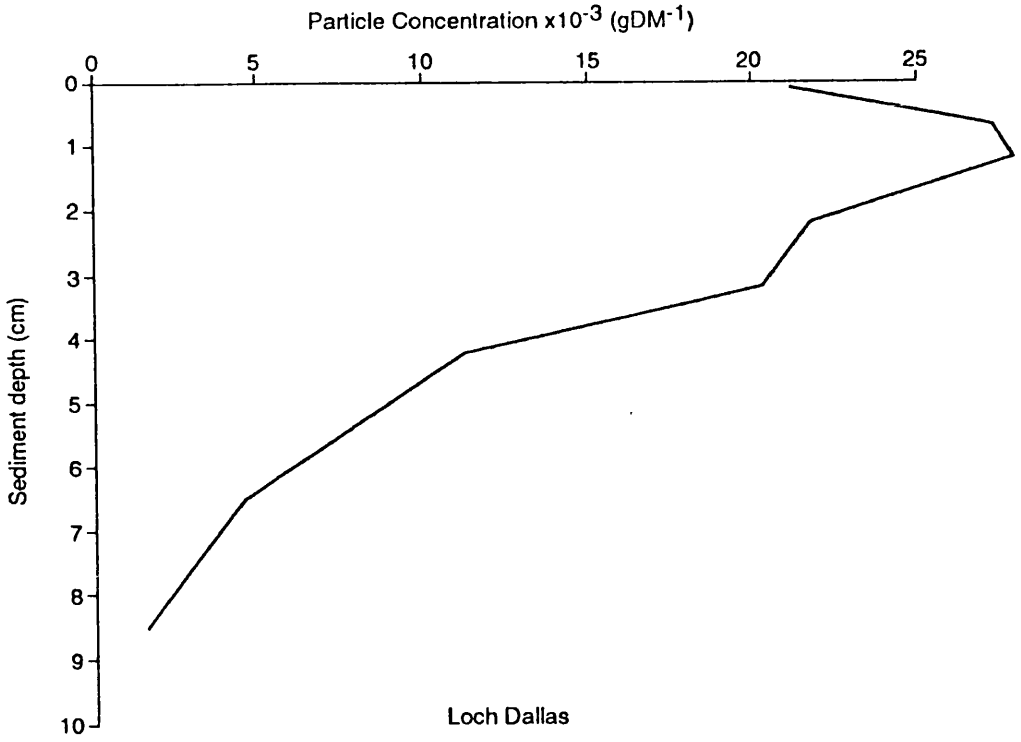

Figure 4.13. Carbonaceous particle profile for Loch Bran (core BRAN1) taken in August 1989.

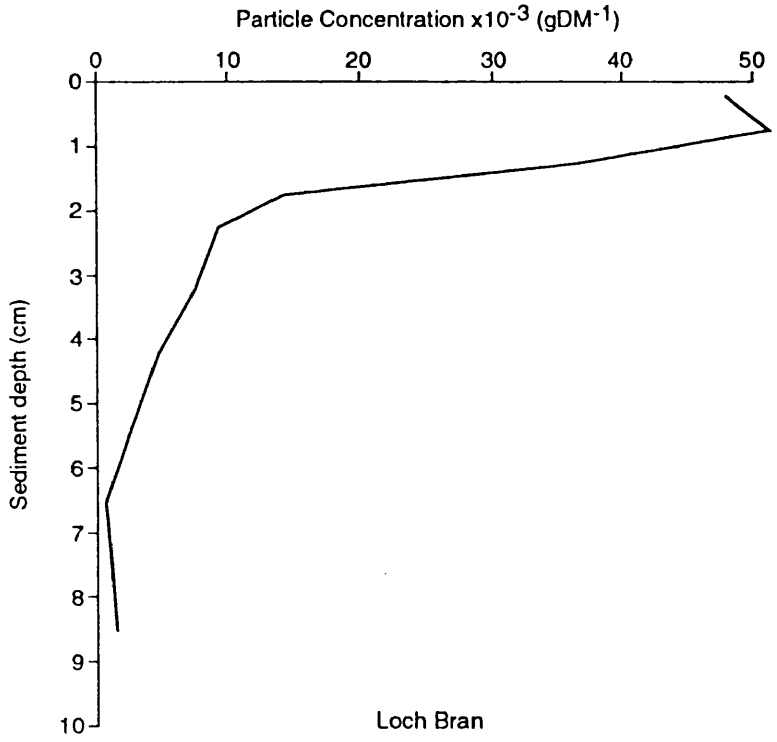

Figure 4.14. Carbonaceous particle profile for Loch Arial (core ARIA1) taken in September 1989.

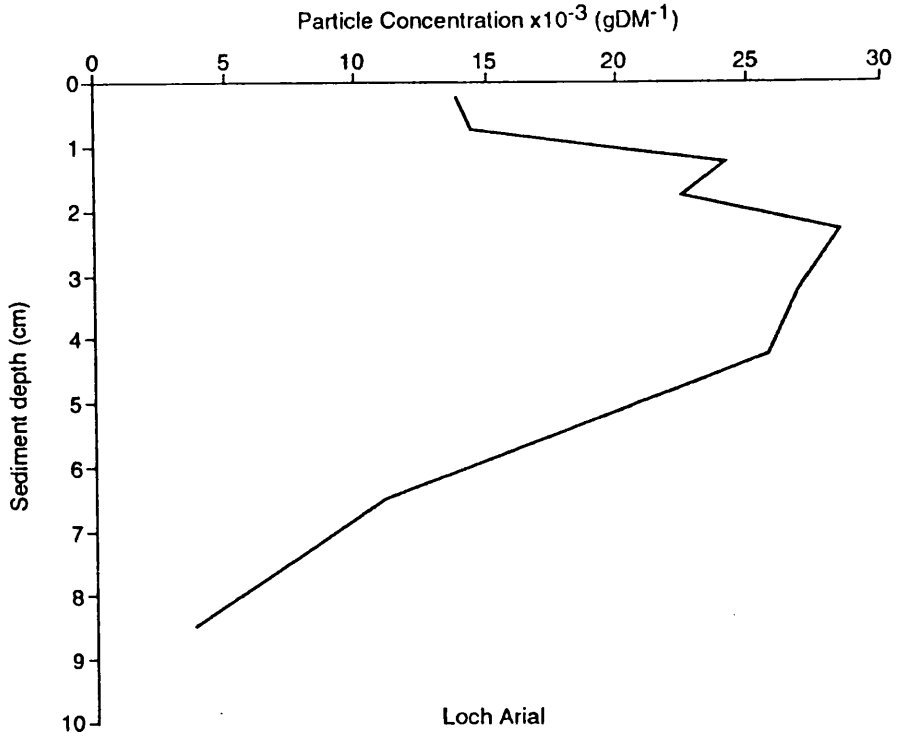

Figure 4.15. Carbonaceous particle profile for Loch Walton (core WALT1) taken in September 1989.

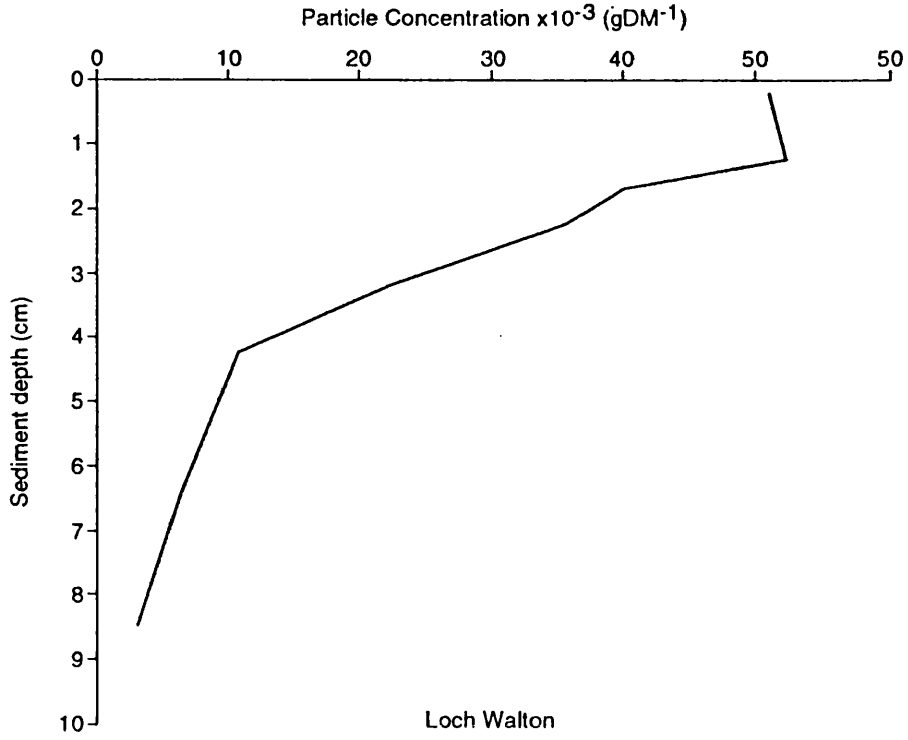

Figure 4.16. Carbonaceous particle profile for Loch Dubh Cadhafuaraich (core CADH1) taken in October 1989.

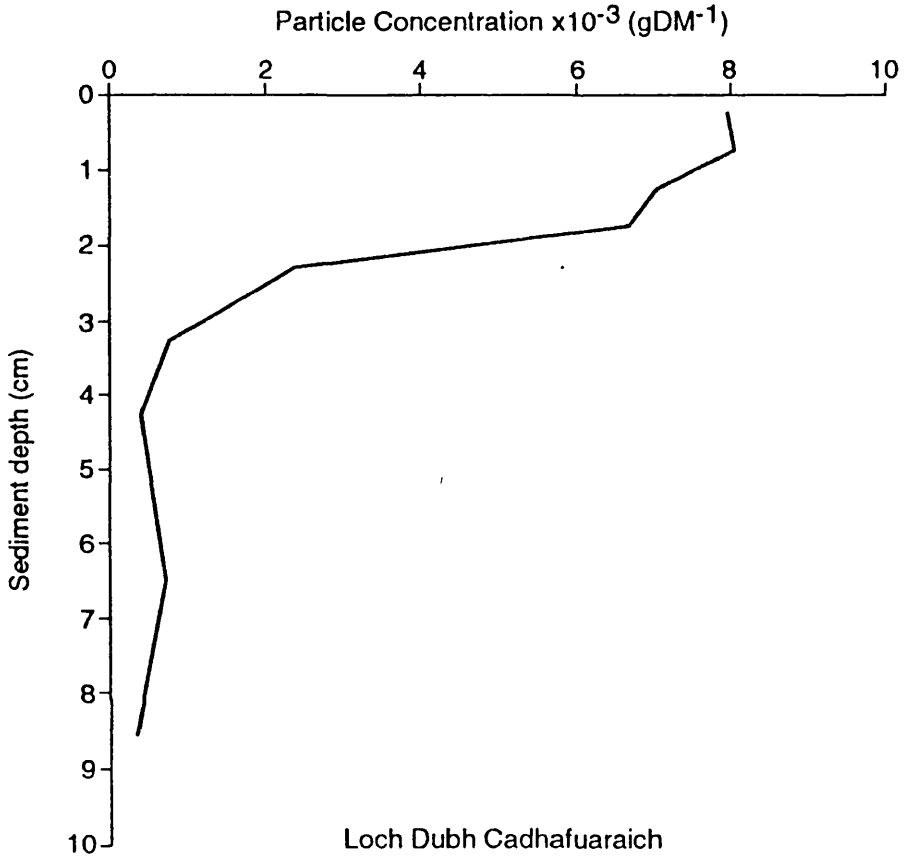

Dallas and Loch Arial profiles show major decreases at the surface involving several sediment levels. The profile from Loch Saugh also shows a decline in the two uppermost levels although the decline is less marked. These variations are most likely to be due to differences in sediment accumulation rates and it seems that a particle concentration peak is common in many post-1985 cores. Its potential as a dating horizon is discussed more fully below.

4.2.2. Wales.

Sediment cores were taken from three lakes in North Wales in 1987, Llyn Glas (site 96 - see Figure 2.2), Llyn Irddyn (97) and Llyn Conwy (98) and analysed for carbonaceous particles as described in section 2.4. All three were ^{210}Pb-dated. In addition Llyn Hir was cored twice, in 1984 and 1988, and the later core was used to assess more recent changes. As with the Scottish repeat cores, the earlier core was analysed by Natkanski using the Renberg and Wik method (1984) and the later core was analysed using the method described in section 2.4.

Llyn Glas.

The sediment core analysed was GLAS1. The results are shown in Figure 4.17. This shows the particle record starting early in the 19th century and the concentration increase gradually until the 1940's when there is a rapid increase. This continues until a peak in 1976 (± 2 years) of 5,334 gDM^{-1} after which there is a decline to the surface. Although Llyn Glas is situated in an area of high sulphur deposition, the carbonaceous particle values are unusually low. Since the sediment accumulation rate is also low these values are more likely to be the result of losses due to short water residence times in this small, high altitude lake.

Llyn Irddyn.

The sediment core analysed was IRD2 taken in May 1987. The results are shown in Figure 4.18. The particle record begins in the 1860's and the concentration increases slowly until the 1950's. After this, the concentration starts to increase more rapidly followed by a massive increase in the 1960's to a peak of 34,417 gDM^{-1} in 1980 (± 2 years). This is followed by a decline in concentration to the sediment surface.

Figure 4.17. Carbonaceous particle profile for Llyn Glas (core GLAS1) taken in 1987.

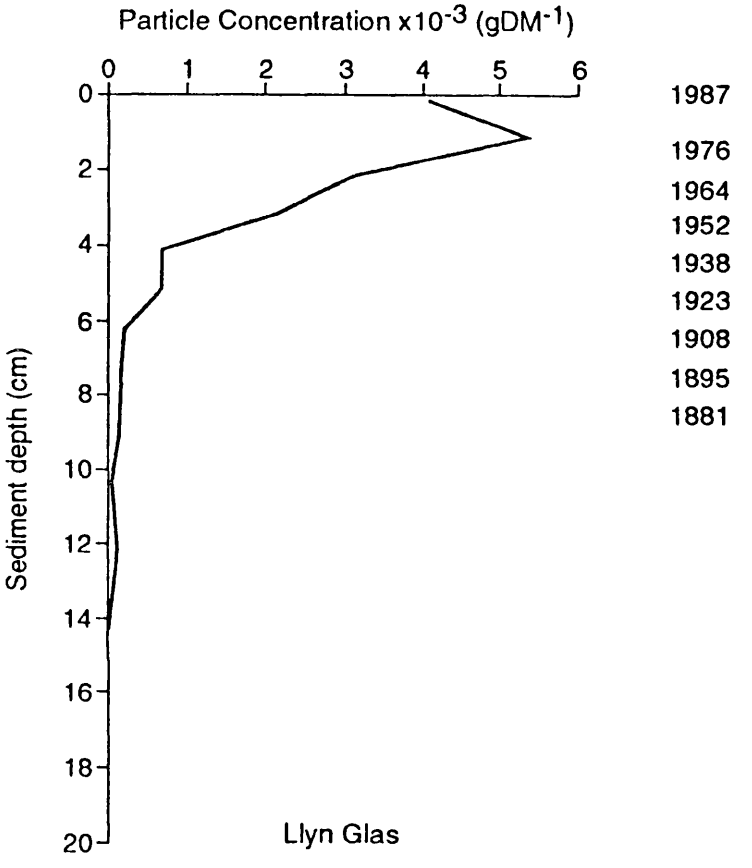

Figure 4.18. Carbonaceous particle profile for Llyn Irddyn (core IRD2) taken in May 1987.

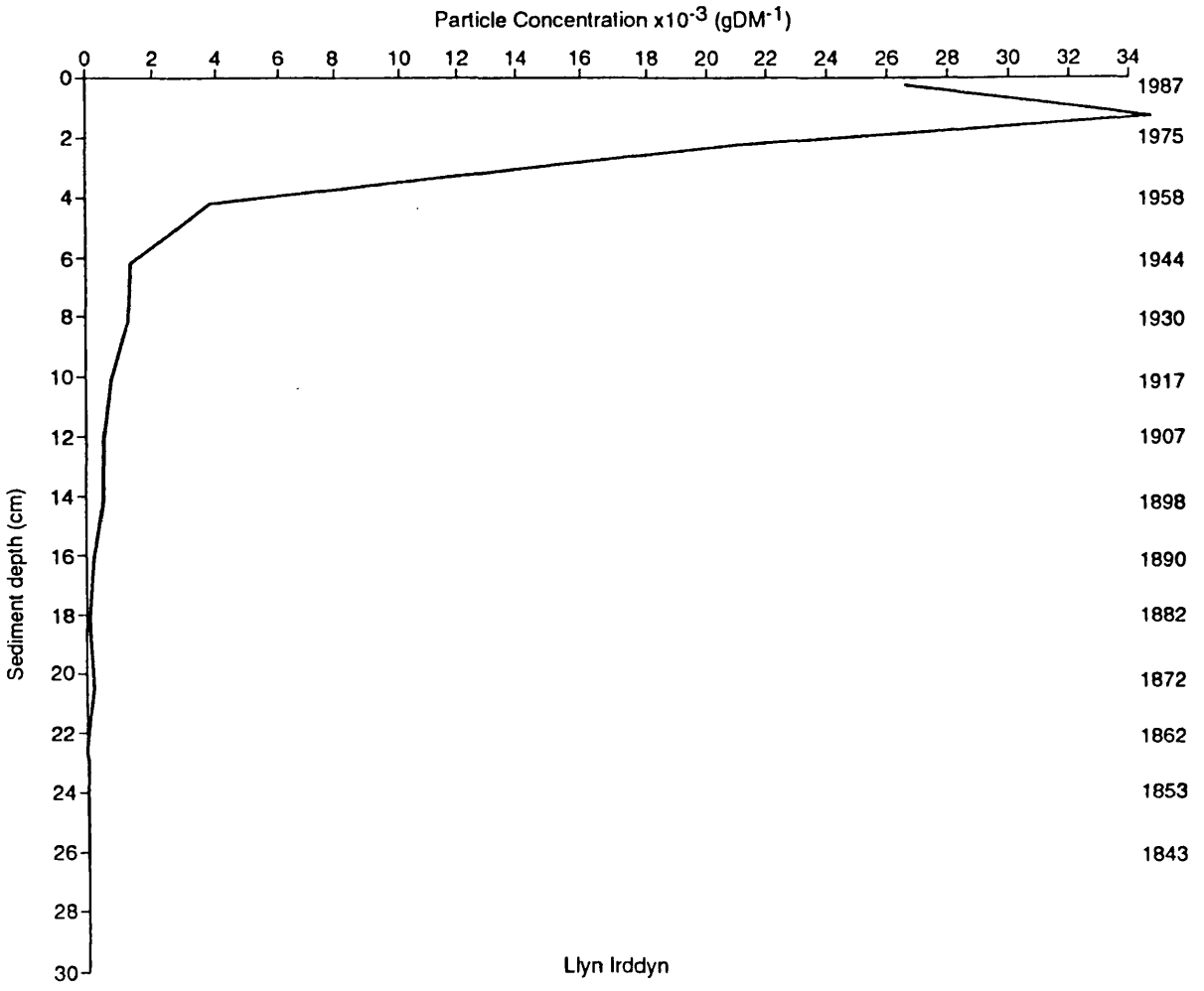

Llyn Conwy.

The sediment core analysed was CON4 taken on 25/5/1987. The results are shown in Figure 4.19. The particle record begins below the analysed section of the core, i.e. pre-1880's. The concentration generally increases up to the 1960's when there is a rapid increase up to a peak of 28,896 gDM^{-1} in 1971 (± 2 years). This is followed by a decline in concentration to the sediment surface.

Llyn Hir.

The results from the carbonaceous particle analysis of the 1984 core, HIR1, analysed by Natkanski are published in Fritz et al., (1986) and Battarbee et al. (1988) and appear in Figure 4.20a. The particle record begins in the 1850's and increases steadily until a rapid increase in the 1950's. Particle concentrations increase to 26,120 gDM^{-1} at the sediment surface although there appears to be a levelling off after about 1970.

Llyn Hir was re-cored in 1988. The results appear in Figure 4.20b and show a decrease in particle concentration at the sediment surface. The ^{210}Pb-dated 1984 core showed the accumulation rate to be slow, about 0.1cm yr^{-1}. This rate has been fairly consistent for several decades and if extrapolated to the 1988 core, the carbonaceous particle concentration peak is dated at about 1976.

The range of values observed for the surface sediments of Llyn Irddyn, Llyn Conwy and Llyn Hir (i.e. 25,000 - 35,000 gDM^{-1}) represents the value that might be expected for Llyn Glas were it not for the effect of water residence times on the particle accumulation.

Other Welsh sites.

Additional data for Wales are also available for five other Welsh sites analysed by Natkanski (in Battarbee et al., 1988).

Llyn Gynon, cored in 1985, shows that particle record beginning in the 1850's and concentrations increase slowly until a rapid increase in the 1950's. This continues to a peak of 19,390 gDM^{-1} in approximately 1980, followed by a surface decline.

Figure 4.19. Carbonaceous particle profile for Llyn Conwy (core CON4) taken in May 1987.

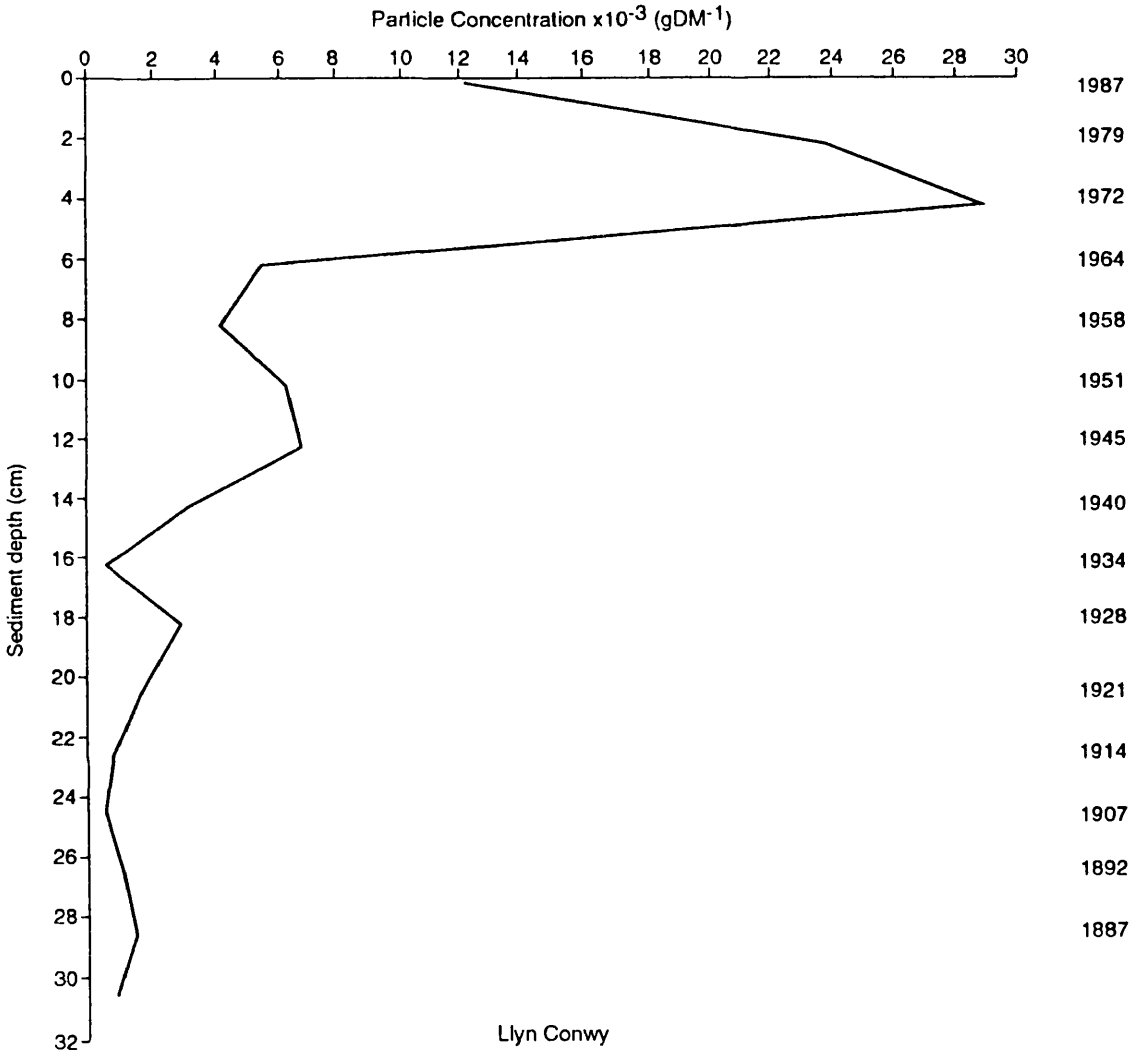

Figure 4.20. Carbonaceous particle profiles for Llyn Hir (a) core HIR1 taken in 1984 and (b) core HIR88 taken in 1988.

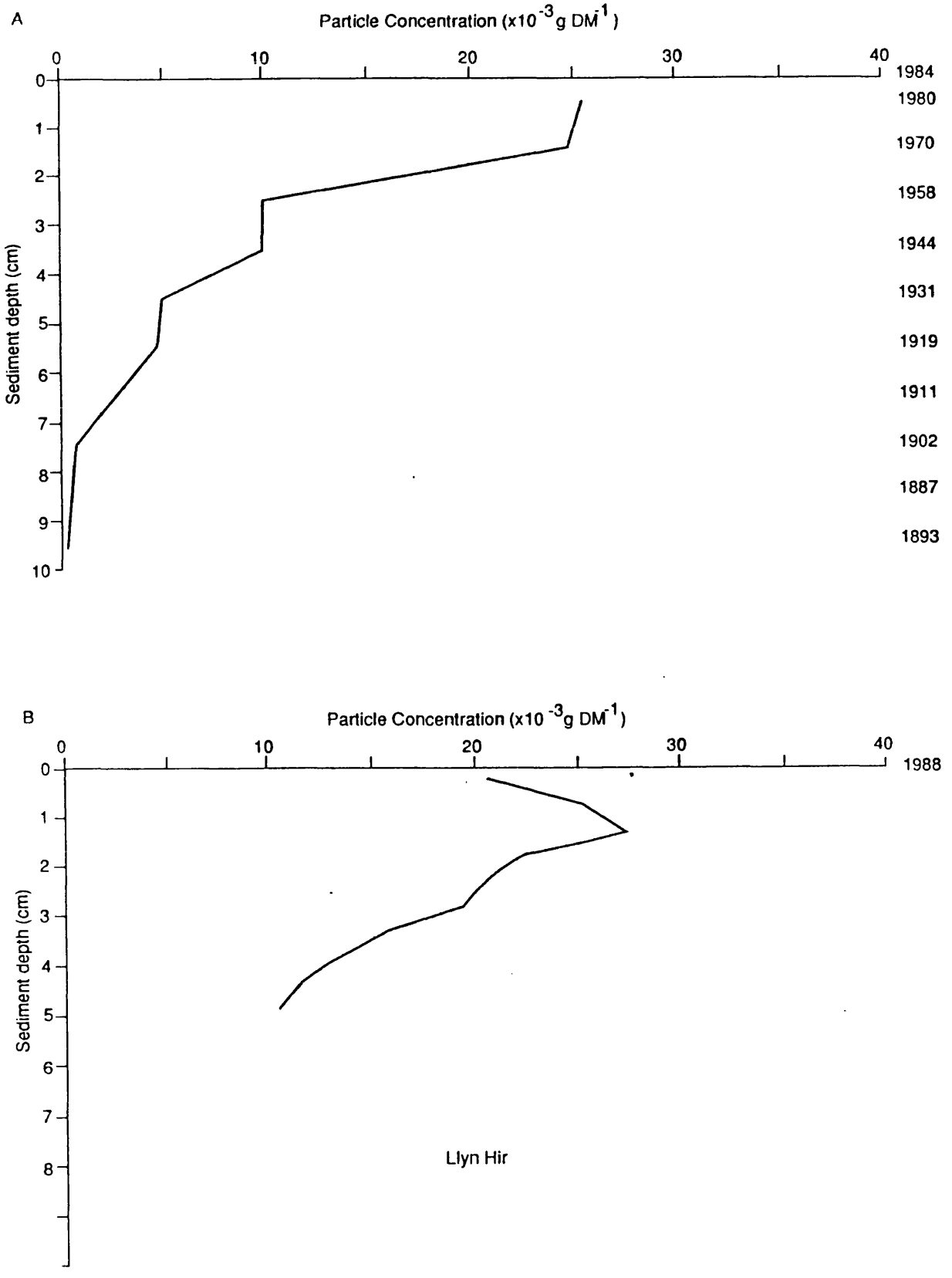

Llyn y Bi was cored in May 1985 and shows the particle record beginning in the 1850's. Particle concentrations increase to 20,580 gDM^{-1} at the surface of the core although unlike most other sites there is no point at which there is a rapid increase.

Llyn Dulyn, cored in August 1985, shows the start of the particle record in the 1860's. A rapid increase in concentration occurs in the 1940's and particle concentration continues to increase to 13,480 gDM^{-1} at the sediment surface.

Llyn Cwm Mynach, cored in May 1985, shows the start of the particle record in the 1840's. Concentrations increase slowly until a rapid increase in the 1950's. The concentration continues to increase to 26,330 gDM^{-1} at the sediment surface.

Llyn Llagi was cored in 1985 and shows the start of the particle record in the 1870's. A rapid increase in concentration in the 1960's continues to the top of the core and a surface value of 73,740 gDM^{-1}.

4.2.3. Ireland.

Cores were taken from five lakes in Ireland in 1988. Three were in County Donegal: Lough Veagh (site 99), Lough Muck (100) and Lough Maam (101), and two from further south, Lough Maumwee (102) in County Galway and Lough Nammina (103) in County Clare. Of these, all except the Lough Nammina core were ^{210}Pb-dated.

Lough Veagh.

The sediment core analysed was VEAGH2 and the results are shown in Figure 4.21. The particle record begins in the 1890's and the concentration increases steadily until a rapid increase in the 1950's. This rapid increase continues up to a peak concentration of 11,840 gDM^{-1} in 1982 (± 2 years) after which there is a major decline to the surface.

Lough Muck.

The sediment core analysed was MUCK2 taken in May 1988, and the results are shown in Figure 4.22. The start of the particle record pre-dates the 1860 base of the

Figure 4.21. Carbonaceous particle profile for Lough Veagh (core VEAGH2) taken in May 1988.

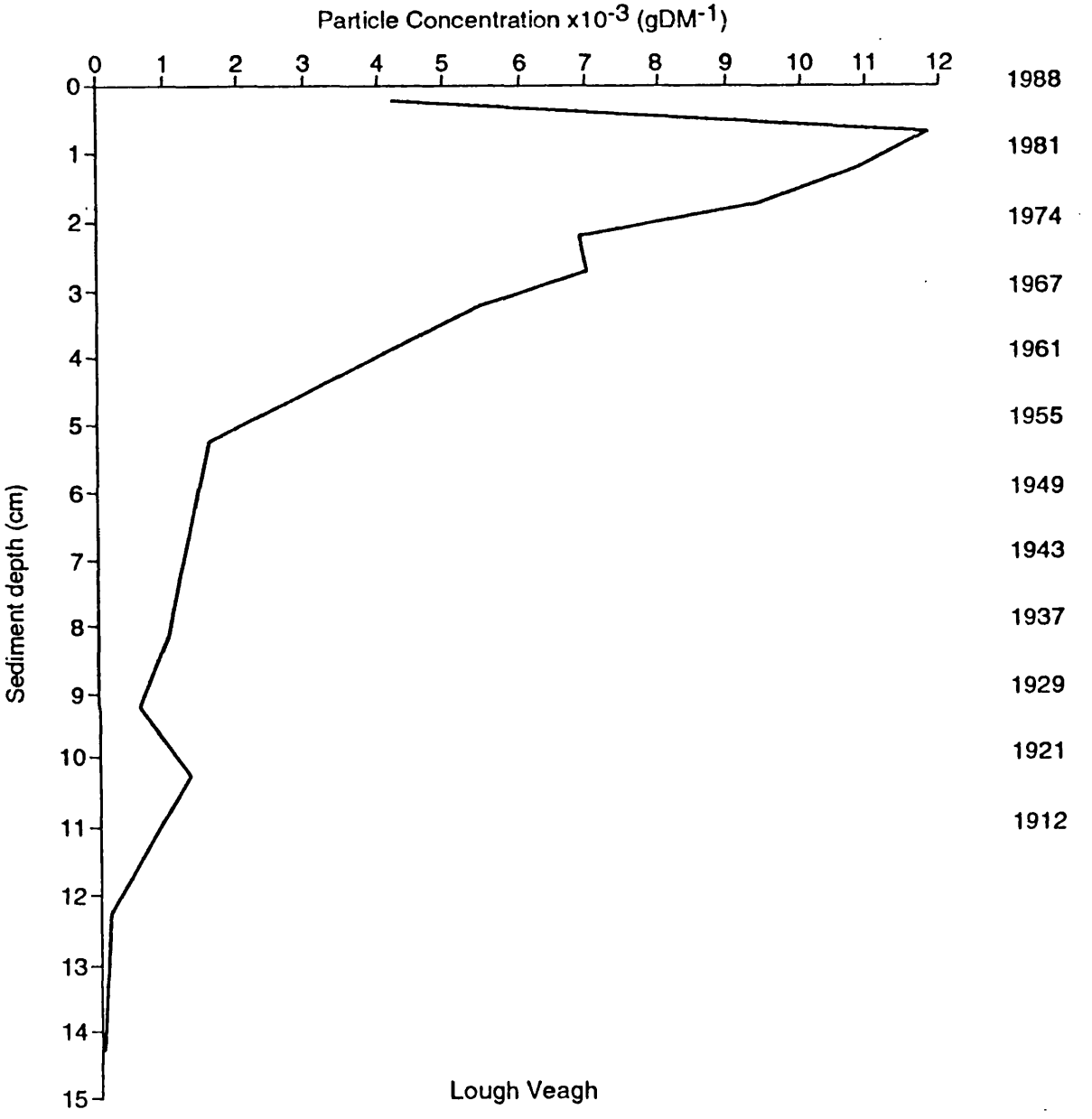

Figure 4.22. Carbonaceous particle profile for Lough Muck (core MUCK2) taken in May 1988.

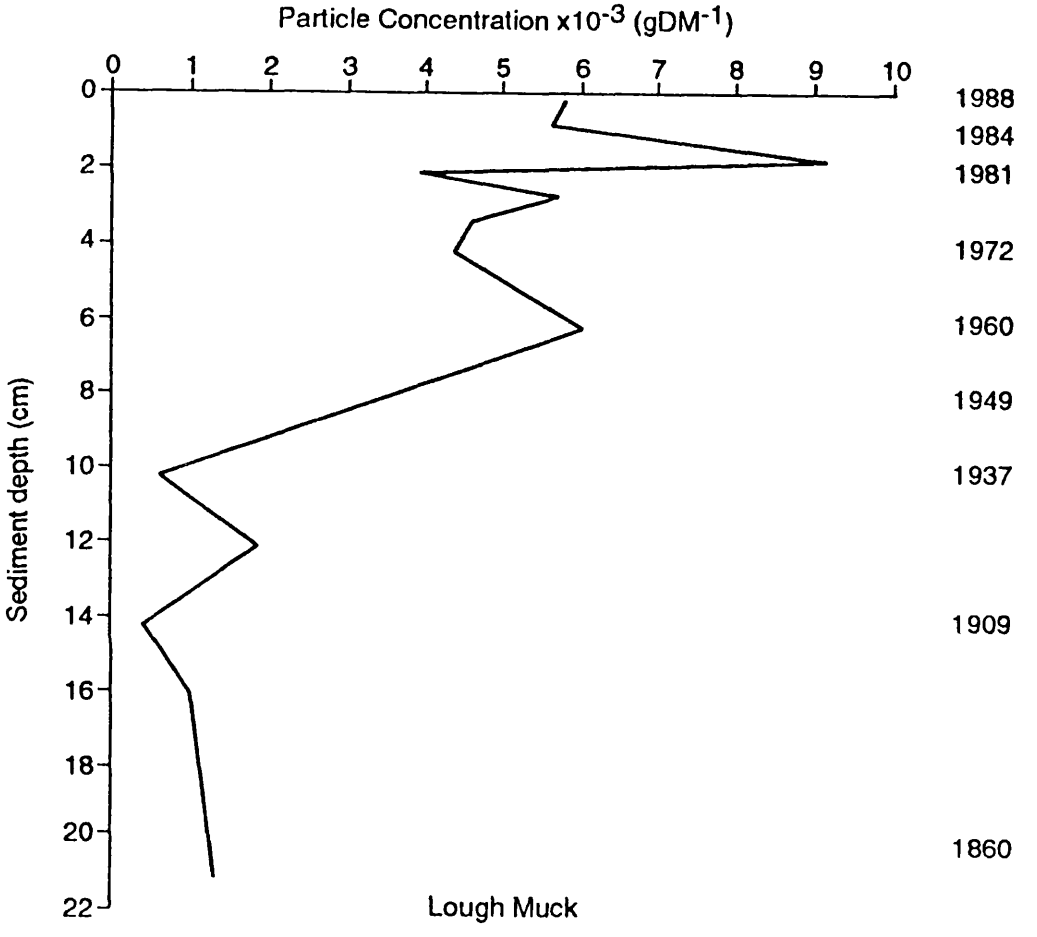

core analysed. There is a certain amount of variability within the profile, but there is a general increase up to a peak of 9,174 gDM^{-1} in 1982 (± 2 years), with more rapid increases in the 1940's and late-1970's. After the peak, there is a decrease to the sediment surface. Lough Muck has a massively eroded blanket peat catchment and the loss-on-ignition results for this core show considerable variability in the top 15cm. Consequently, the variations in the carbonaceous particle profile are probably related to periodic peat inwashes.

Lough Maam.

The sediment core analysed was MAAM3 taken in May 1988, and the results appear in Figure 4.23. The start of the particle record is quite late at 1910 - 1920, then there is a steady increase in concentration from this time up to the 1970's, followed by a rapid increase to a peak of 8,840 gDM^{-1} at 1981 (± 2 years). There then follows a slight decline in concentrations up to the sediment surface. The error bars on the diagram show the 95% confidence limits and illustrate the variation possible when low particle numbers are counted. However, the trends in the particle profiles remain consistent.

Lough Maumwee.

The sediment core analysed was MAUW1 taken in May 1988 and the results are shown in Figure 4.24. The particle record begins in the 1880's and the concentration increases slowly up to the early-1970's when there is a rapid increase up to a peak of 4,821 gDM^{-1} in 1981 (± 2 years) followed by a decrease to the surface.

Lough Nammina.

This core was taken in May 1988 and was not dated. The site was selected due to its proximity to the power stations at Moneypoint and Tarbert on the River Shannon. The results appear in Figure 4.25. These results again show the rapid increase and surface decline in particle concentrations and, from the results obtained in the above dated cores, the peak could be given the date 1981-1982 (± 2 years). The peak concentration of 6,043 gDM^{-1} shows there is little or no obvious influence from the local power stations.

Figure 4.23. Carbonaceous particle profile for Lough Maam (core MAAM3) taken in May 1988.

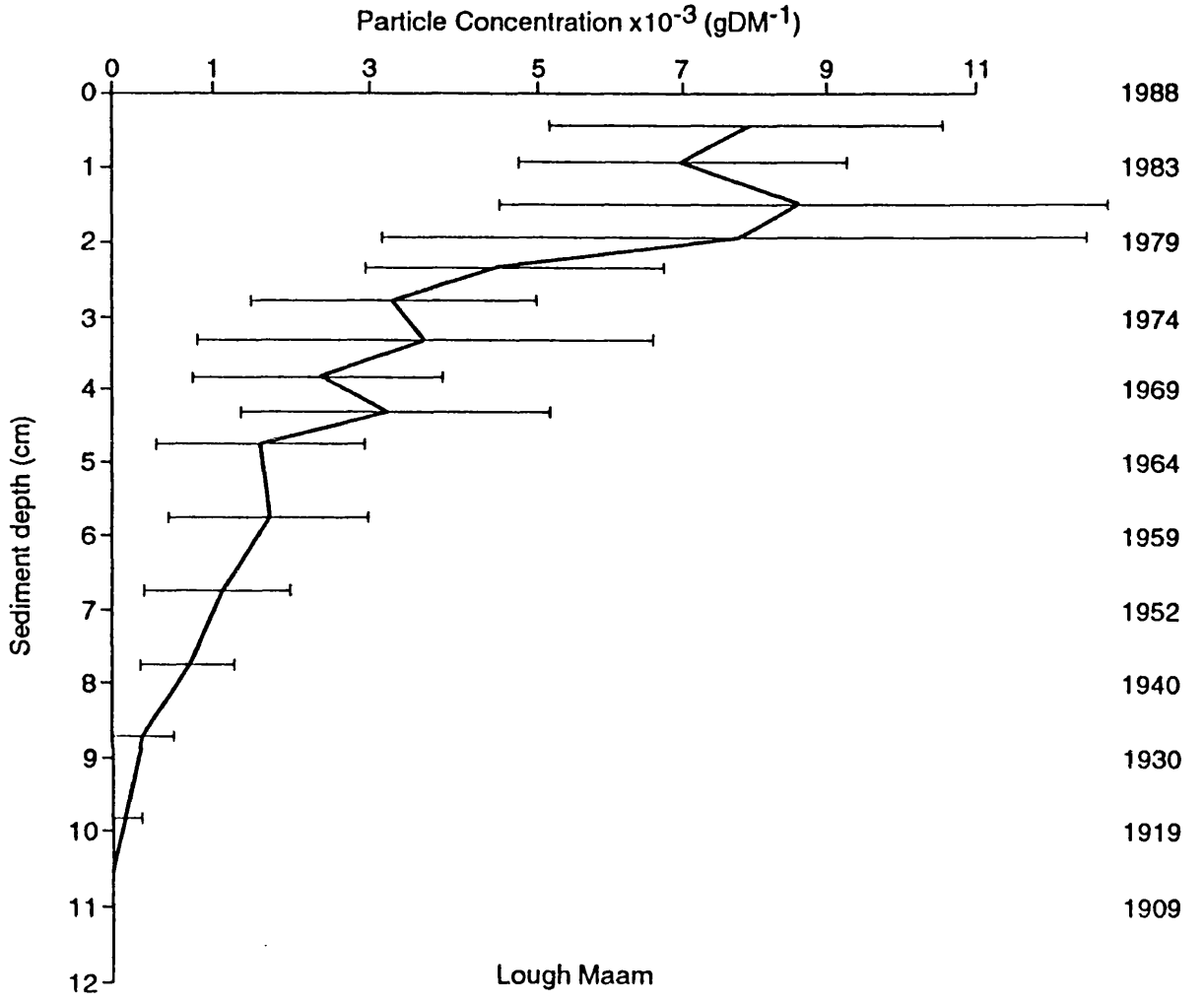

Figure 4.24. Carbonaceous particle profile for Lough Maumwee (core MAUW1) taken in May 1988.

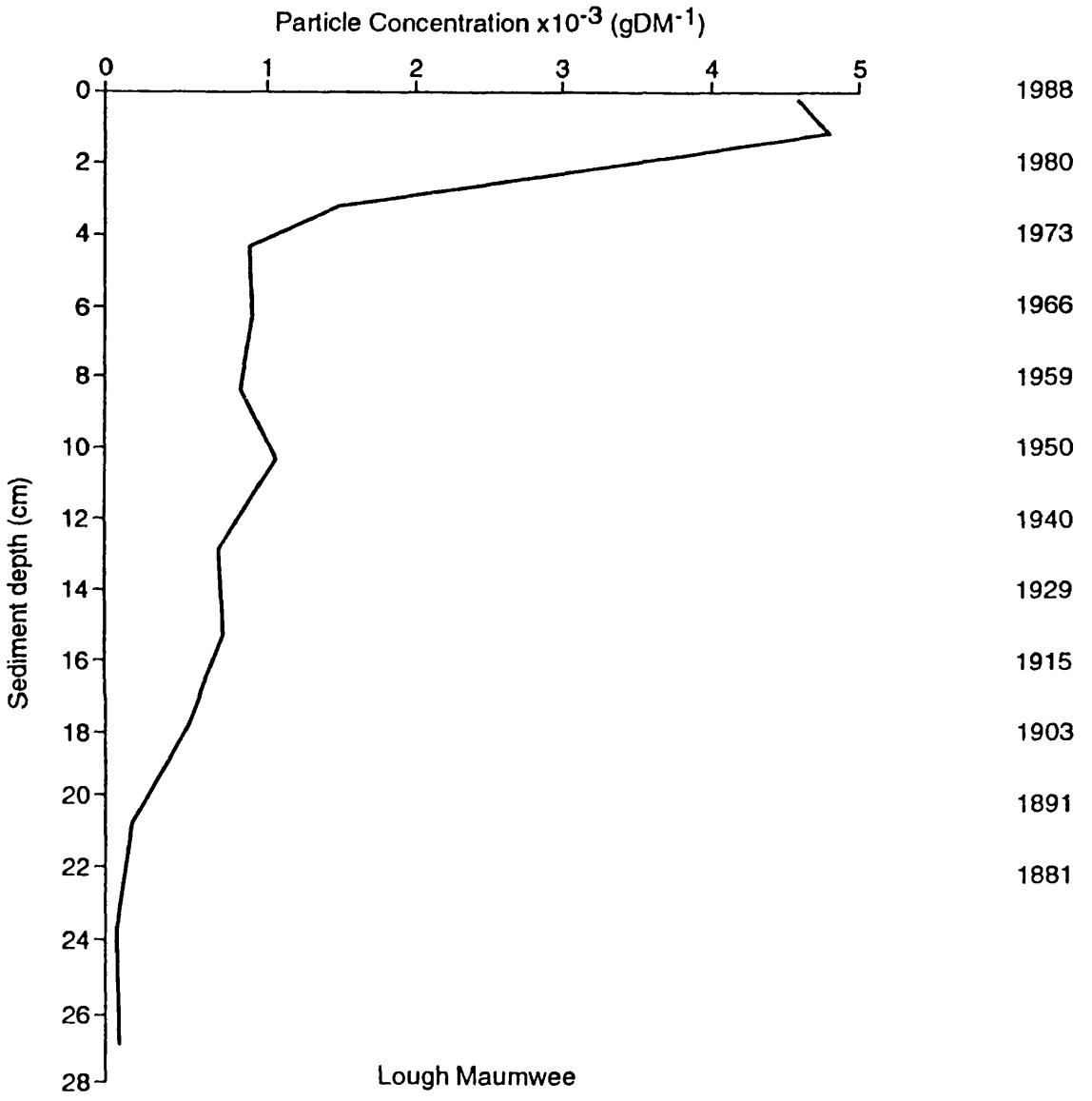

Figure 4.25. Carbonaceous particle profile for Lough Nammina (core NAMM1) taken in May 1988.

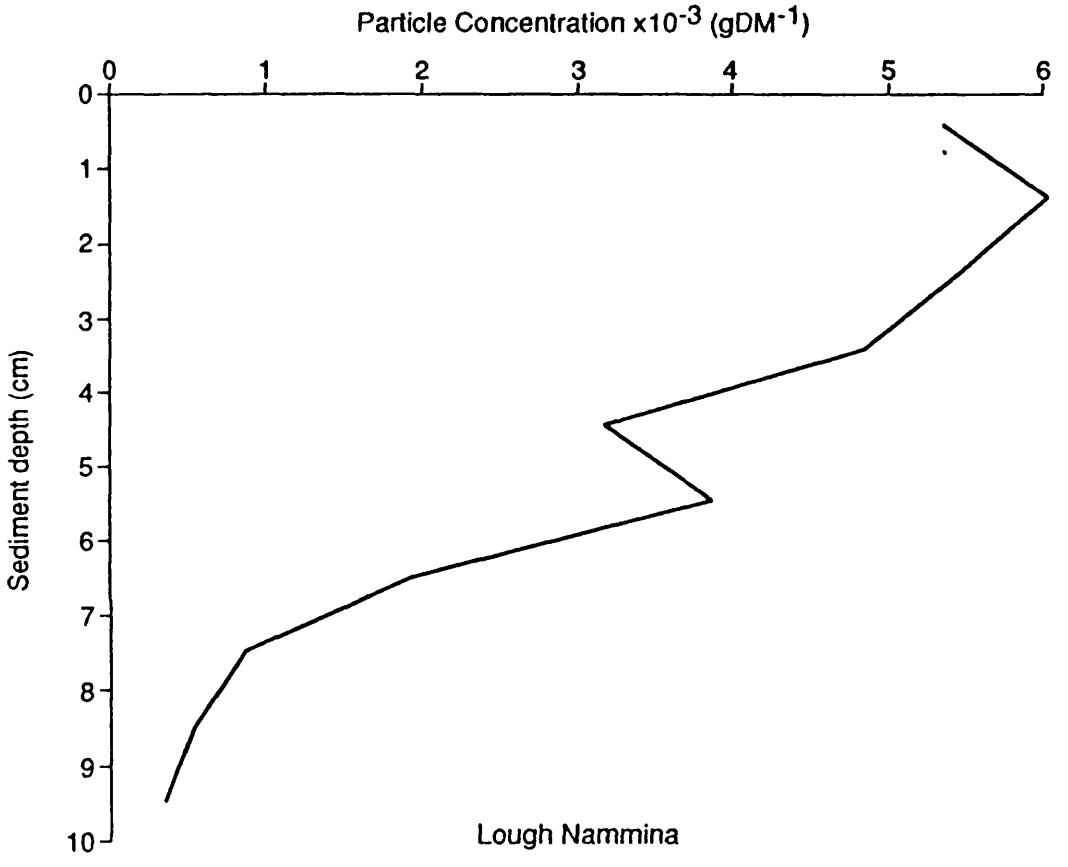

4.2.4. England.

Four cores were taken from lakes and reservoirs in England. These were Whitfield Lough (site 82), Malham Tarn (104), Tunnel End Reservoir (114) and the Men's Bathing Pond on Hampstead Heath (105) in North London. These sites were chosen for a variety of different reasons in association with other projects. Only the Tunnel End and Hampstead Heath cores were ^{210}Pb-dated.

Tunnel End Reservoir.

The sediment core analysed was TUNN2 taken in 1989. The results are shown in Figure 4.26. The sediment accumulation rate is more rapid at the top of the core (1.65cm yr^{-1}) than at the base (0.15cm yr^{-1}). The profile is very variable and this may be due to erosion events within the catchment although the loss-on-ignition results do not show an unusual amount of variation. There is a sharp increase in the late-1930's/early-1940's, and a peak occurs in the 1950's/1960's followed by a general decrease in concentration to the sediment surface, although this may be due to the increase in sediment accumulation rate. Converting these particle concentrations to fluxes still shows considerable variability within the profile and adds little information on the surface decrease as 2.0cm is the uppermost ^{210}Pb-dated level.

Men's Bathing Pond - Hampstead Heath.

The sediment core analysed was MEN2, taken in October 1987. The results are shown in Figure 4.27. The accumulation rate is very rapid at over 2.0cm yr^{-1}. There is a slow increase in particle concentration from the bottom of the core to the 1950's, followed by a rapid increase up to a peak of 123,642 gDM^{-1} which occurs in 1969. This peak is followed by a general downward trend in particle concentration to the sediment surface. Concentrations throughout, despite the rapid accumulation rate, are extremely high due to the location in central London and long water residence times.

With a rapidly accumulating core such as this, there is a danger of over-interpretation. It is tempting to assign every peak and trough in the particle profile to a specific historical event. For example, the ten values in the 0-10cm region only

Figure 4.26. Carbonaceous particle profile for Tunnel End Reservoir (core TUNN2) taken in June 1989.

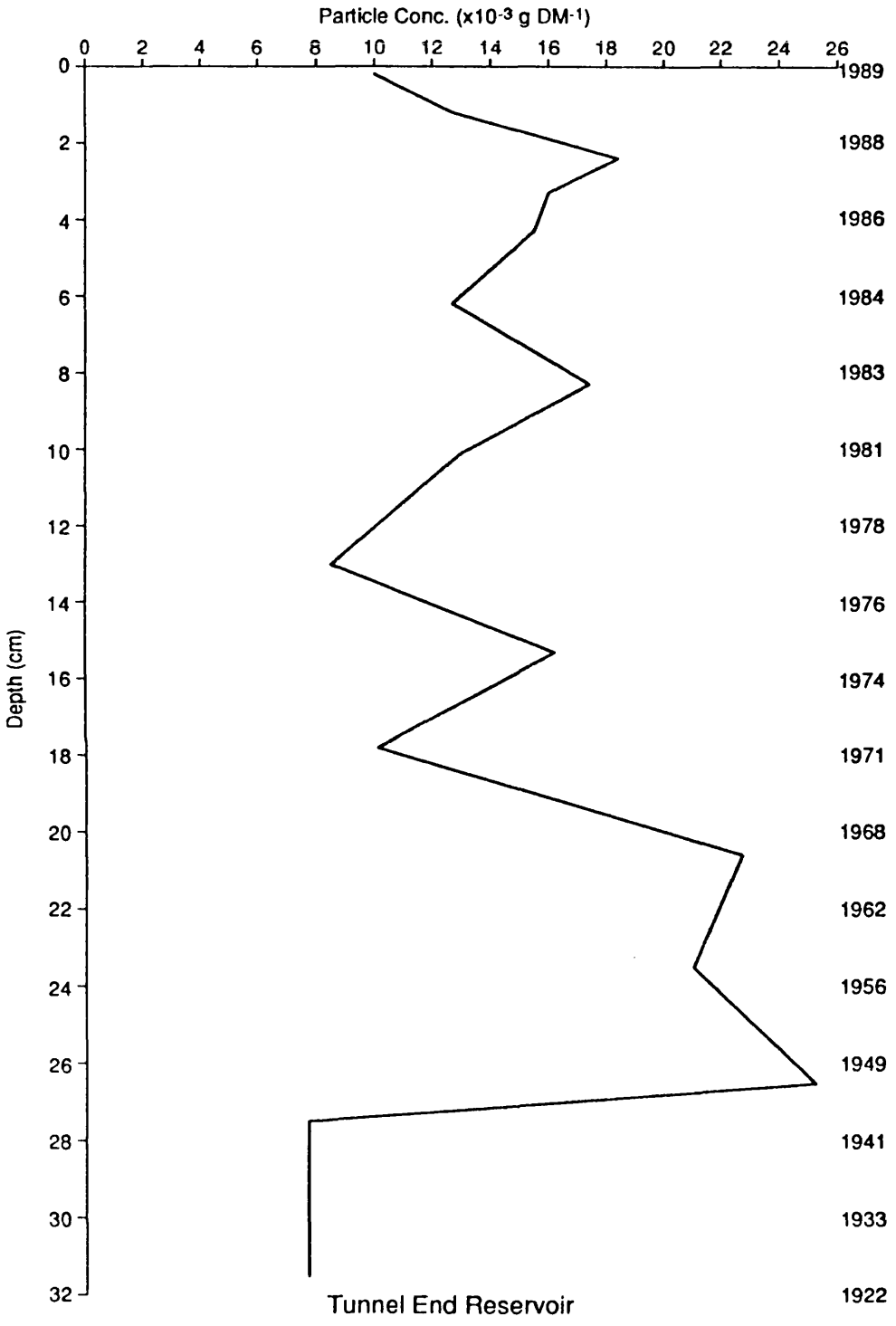

Figure 4.27. Carbonaceous particle profile for the Men's Bathing Pond on Hampstead Heath (core MEN2) taken in October 1987.

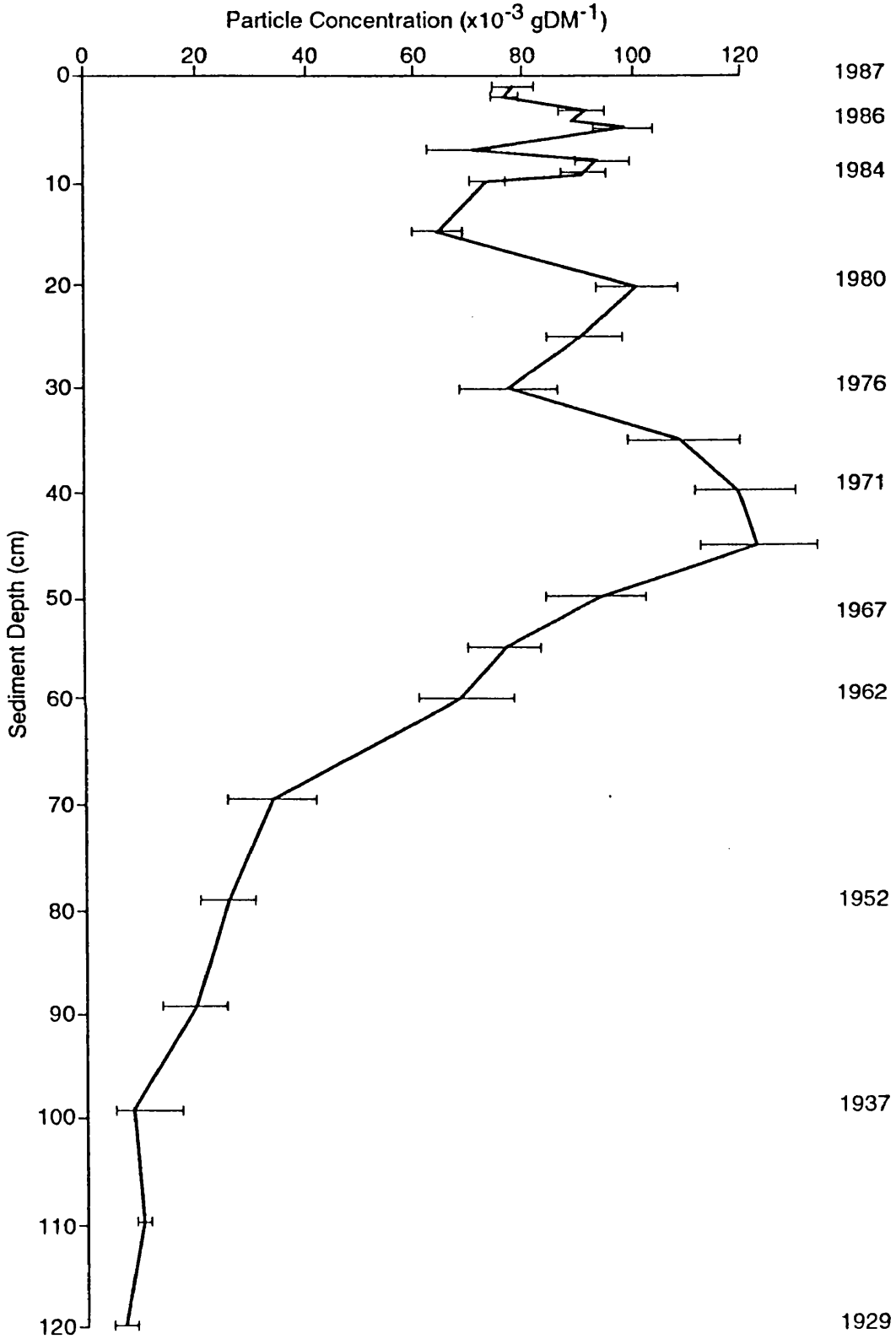

cover a period of 3 or 4 years and it would be easy to interpret this spikiness as high winter and low summer values in electricity generated for heating and lighting. In reality, it is more likely to be due to natural variation caused by episodic atmospheric deposition due to meteorological phenomena. The error bars showing the 95% confidence limits on the statistical counting error shown in Figure 4.27 indicate that the variation in the surface levels may be real rather than an artefact of the analytical techniques.

Whitfield Lough.

This core was taken in June 1989 and the results appear in Figure 4.28. The core was not dated, but shows a similar profile to many of the cores described so far. There is a steady increase in particle concentration which becomes more rapid at about 4cm depth. A peak of 37,300 gDM^{-1} occurs at 0.5cm and this is followed by a slight decline in concentration at the surface.

Malham Tarn.

This was a Kajak core taken in October 1988 and the results are shown in Figure 4.29. The particle record begins at 16-17cm and there is a steady increase followed by a rapid increase above 12cm to a peak value at 4-5cm. There appears to be a second peak at 1-2cm followed by a decrease in concentration to the surface.

Other English sites.

Natkanski (in Battarbee et al., 1988) analysed a sediment core from another Yorkshire reservoir, Watersheddles, cored in May 1986. This reservoir was built in 1877 and so the core is only a record of late-19th and 20th century deposition. Similar to the Tunnel End Reservoir, the profile shows high variability, but a peak concentration of 24,860 gDM^{-1} can be seen in the 1950's followed by a general decline to the sediment surface.

4.2.5. Sites in Norway and France.

During the course of this study several cores were taken in Norway and France and these were also analysed for carbonaceous particles.

Figure 4.28. Carbonaceous particle profile for Whitfield Lough (core WHIF1) taken in June 1989.

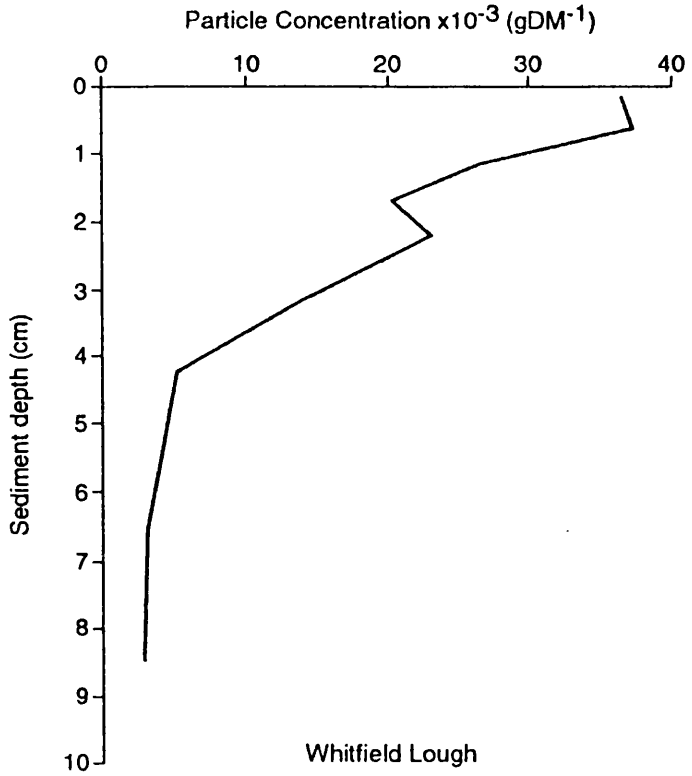

Figure 4.29. Carbonaceous particle profile for Malham Tarn (core MALH1) taken in October 1988.

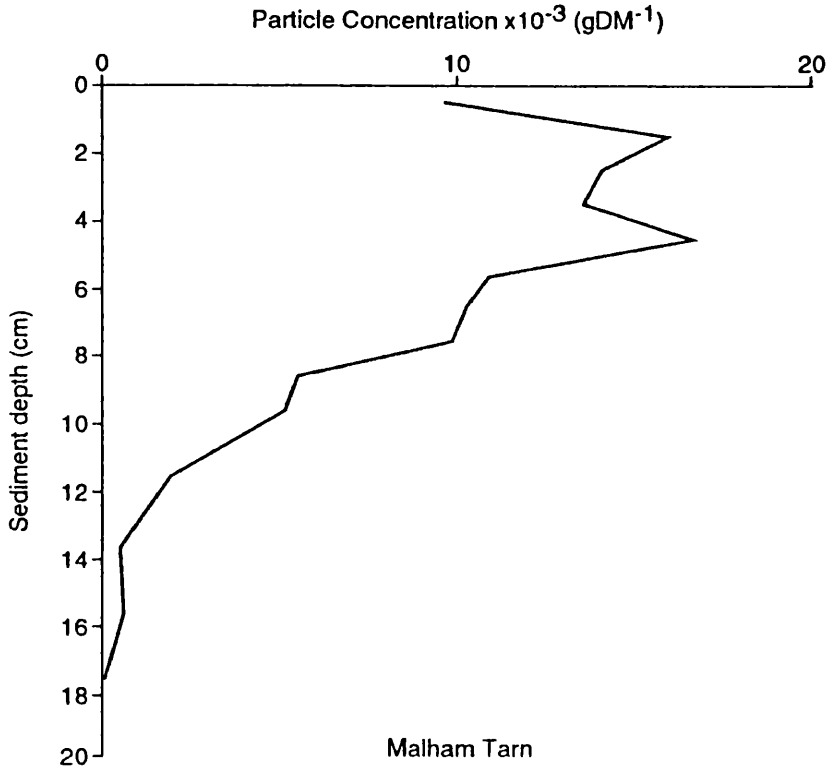

Norway

Short cores were taken from three lakes in the Höylandet region of mid-Norway in 1988, Röyrtjörna, Langtjörna and an unnamed lake known as "Granite A". All had very low concentrations of carbonaceous particles similar to, or less than, the lowest values found in Britain (i.e. 1,000 - 1,500 gDM^{-1}).

Röyrtjörna.

The particle profile is shown in Figure 4.30, and shows all the features of the British cores: the steady increase in concentration, followed by a more rapid increase to a peak and a subsequent decline to the sediment surface. This peak had been found in an earlier core and dated at 1969 (Wik & Natkanski, 1990).

Langtjörna and Granite 'A'.

The profiles are shown in Figures 4.31 and 4.32 respectively. Both profiles show the rapid increase in particle concentration, but no surface decrease. Höylandet is in a relatively 'clean' area of Norway as far as particle deposition is concerned, and the low concentrations and short sediment record probably account for the lack of surface decline in these cores.

France

Cores were taken from two sites in the Vosges region of France in 1987, Lac des Corbeaux and Lac de Gerardmer. ^{210}Pb chronology is only available for the Lac des Corbeaux core.

Lac des Corbeaux.

The particle profile is shown in Figure 4.33. The particle record starts well before the ^{210}Pb chronology probably in the late 18th century. There is a steady increase in particle concentration from this time until the 1940's when there is a more rapid increase to a maximum of 9,142 gDM^{-1} at the sediment surface. There is no surface decline.

Lac de Gerardmer.

This profile, shown in Figure 4.34, shows low particle concentrations from the start of the record at 35cm, to 5 - 10cm where there is an enormous increase up to a

Figure 4.30. Carbonaceous particle profile for Röyrtjörna (core ROY1) taken in July 1988.

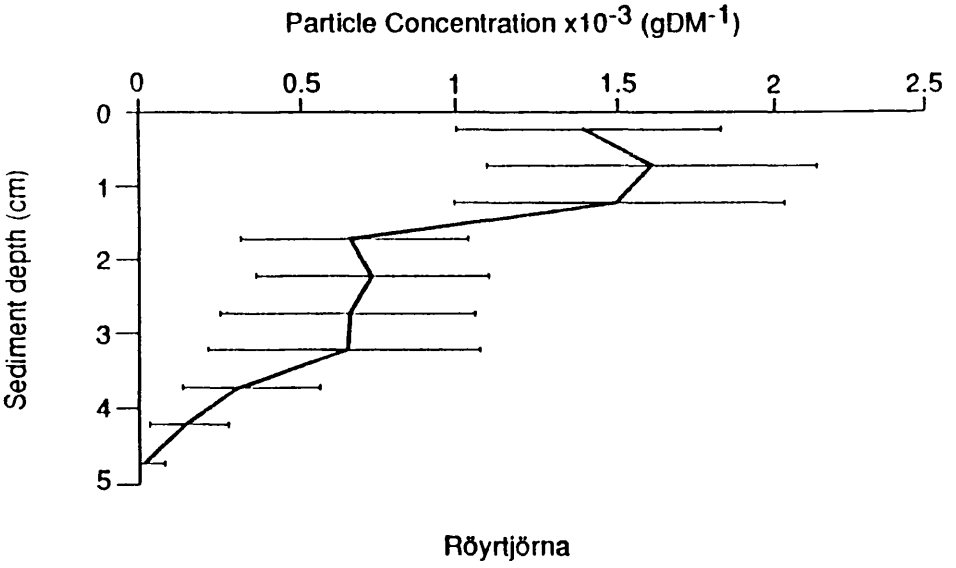

Figure 4.31. Carbonaceous particle profile for Langtjörna (core LAG1) taken in July 1988.

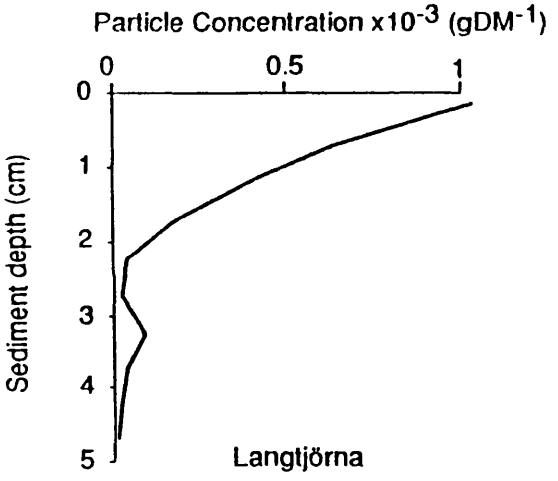

Figure 4.32. Carbonaceous particle profile for 'Granite A' (core GRNA1) taken in July 1988.

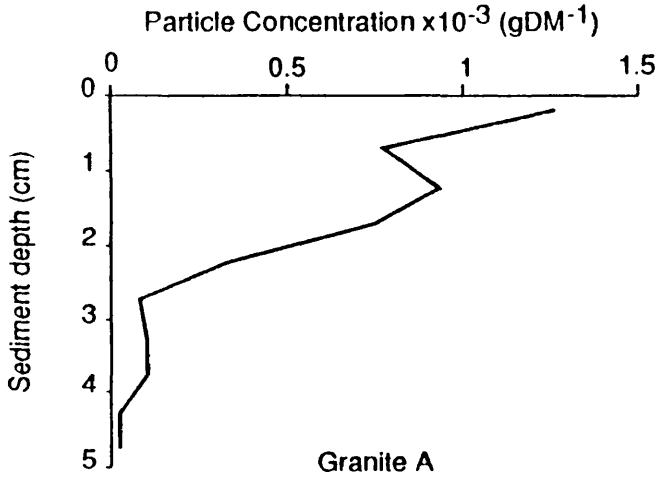

Figure 4.33. Carbonaceous particle profile for Lac des Corbeaux (core CORB1) taken in 1987.

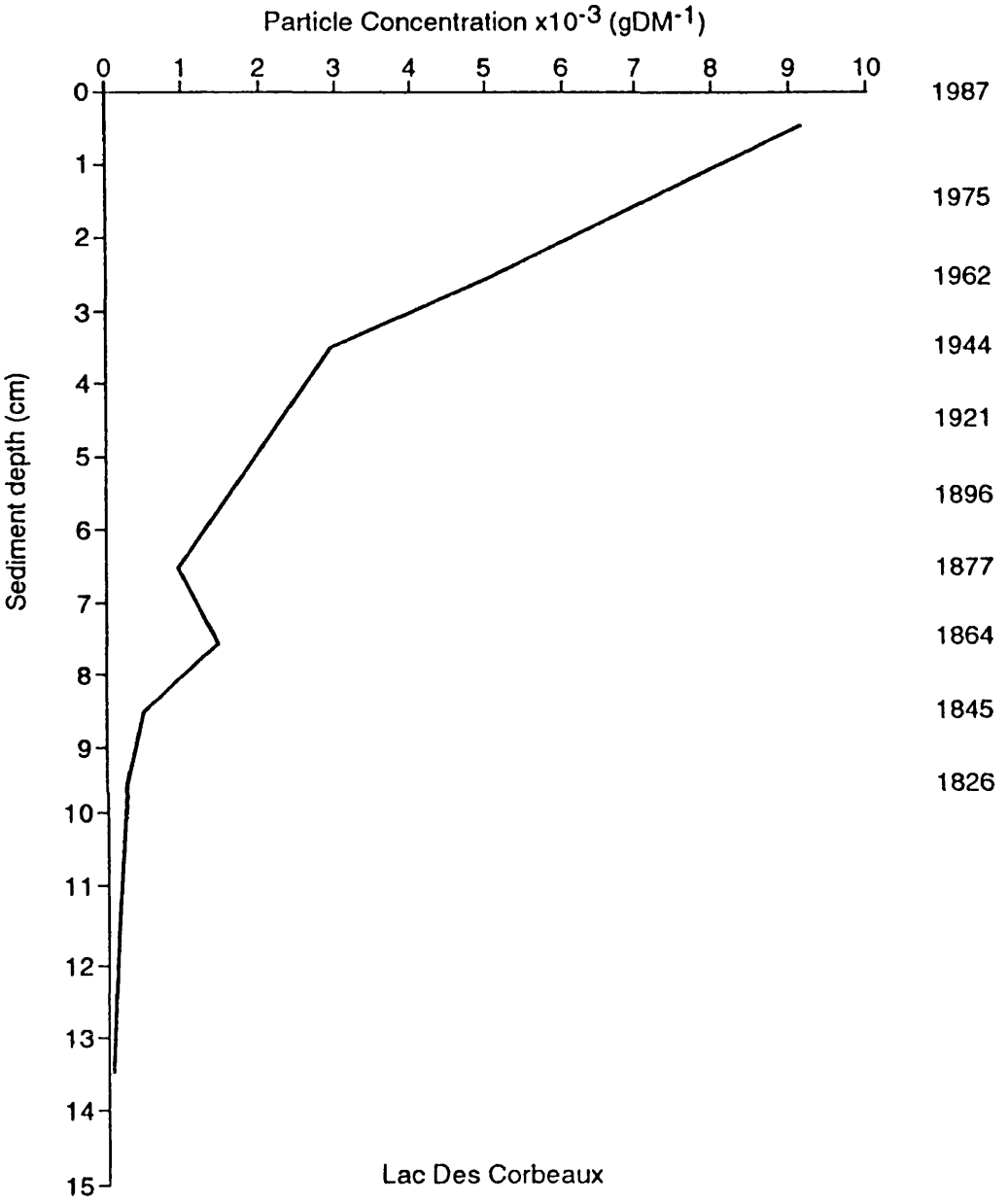

Figure 4.34. Carbonaceous particle profile for Lac de Gerardmer (core GERA1) taken in 1987.

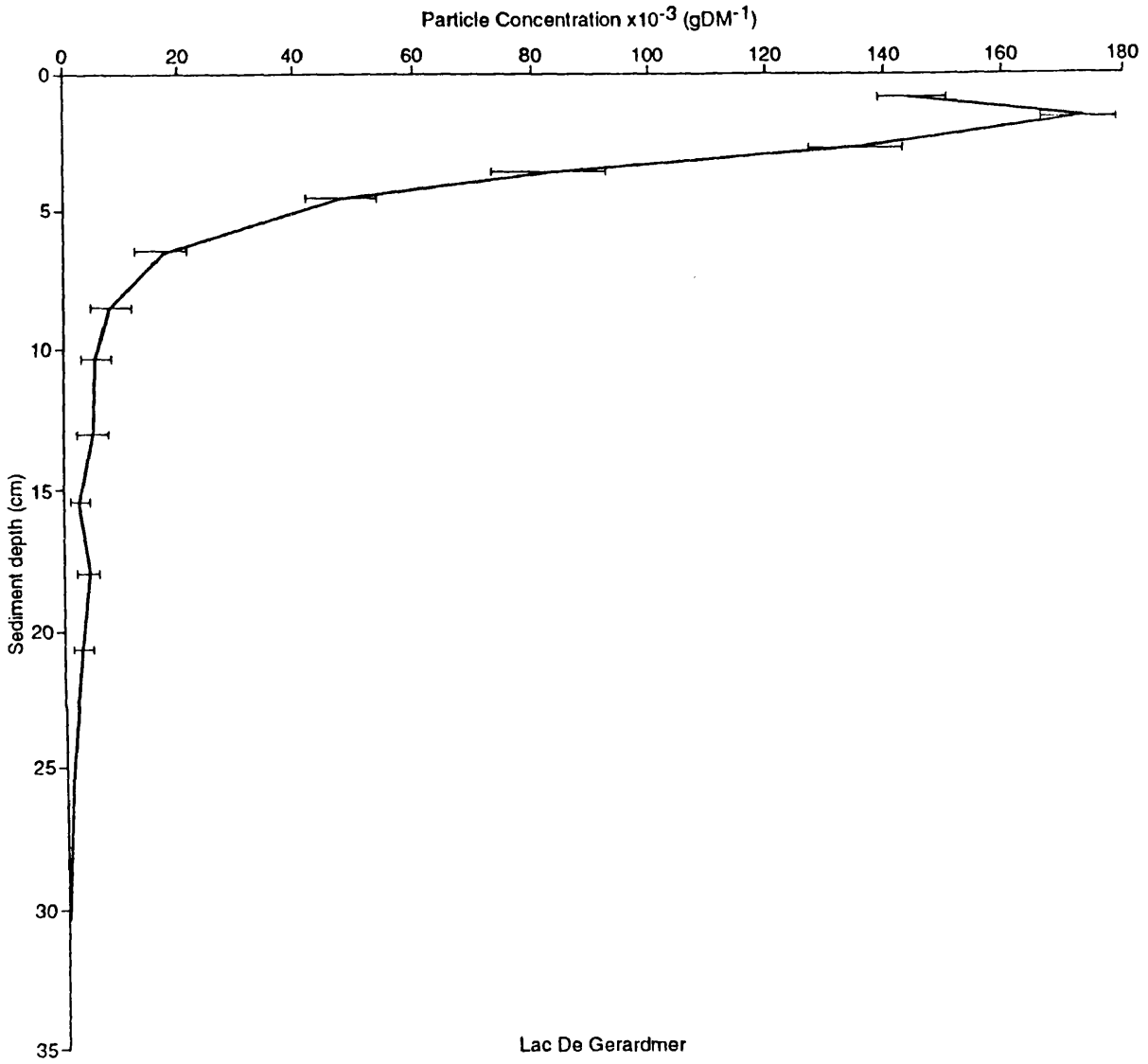

concentration peak at 1-1.5cm where the values are over an order of magnitude greater than at Lac des Corbeaux. Concentrations decline to the sediment surface. These features cannot, unfortunately, be dated as the ^{210}Pb chronology is not yet available.

4.3. Characterisation of carbonaceous particles extracted from lake sediments.

In most instances, it is sufficient to know the extent to which a lake and its catchment have been affected by atmospheric deposition through time, by constructing fly-ash particle profiles in the ways described in sections 2.4 and 2.5. Apart from being useful as indirect dating techniques, these profiles have made a major contribution to the debate on the causes of surface water acidification, by their correlation with diatom inferred pH trends. Similarly, the more recent near surface decline in particle concentration probably represents a combination of the post-1970 decrease in acid deposition and the introduction and development of particle arresting techniques. At sensitive sites this may indicate where recovery from acidification is occurring. However, now that carbonaceous particle characterisation into fuel type is possible with a high degree of confidence, more information can be obtained from these particle records. This takes the form of possible sources for the particles found in the sediments and the possibility of identifying extra dating levels associated with the introduction of different fuel types, especially oil.

4.3.1. Extending particle characterisation to 'fossil' material.

The carbonaceous particles extracted from lake sediments were put through the same procedures as the reference material (i.e. extraction as described in section 2.4 and characterisation as described in Chapter 3). The sources of these particles should be either coal or oil and so their chemistries should be similar to those of particles in the reference data set. In section 3.8.1, principal components analysis of data from the reference data set and from peat particles was used to highlight the differences between the three fuel types. A similar analysis, but including the extracted 'fossil' particles was carried out here to assess whether the fossil particles clustered with the reference material rather than formed a separate group.

The data from 1500 analyses of lake sediment particles were added to those of the reference material. These were taken from the upper levels of the Hampstead Heath core and so were all post-1970 particles. The loadings of the variables on the first two principal components are shown in Table 4.1 and the scores resulting from these are plotted in Figure 4.35.

Table 4.1. *Loadings on the first two principal components for a PCA on the reference data set and 1500 particles extracted from a sediment core using all 17 elements.*

Variable	1st PC Loading	2nd PC Loading
Na	0.188	-0.541
Mg	-0.037	-0.375
Al	-0.331	0.217
Si	-0.363	-0.022
P	-0.009	-0.200
S	0.496	0.041
Cl	-0.387	-0.142
K	-0.311	-0.311
Ca	-0.234	-0.366
Ti	-0.157	-0.127
V	0.177	-0.083
Cr	-0.058	0.108
Mn	-0.092	0.118
Fe	0.246	-0.075
Ni	0.100	0.029
Cu	-0.130	0.269
Zn	-0.142	0.316

The extracted particles cluster with the reference particles to a certain extent. However, PCA by its very nature shows this clustering to its least advantage as the

Figure 4.35. *Plot of first and second principal component scores for the particles of the reference data-set and 1500 'fossil' particles extracted from a lake sediment core. (oil in yellow, coal in red and fossil in green).*

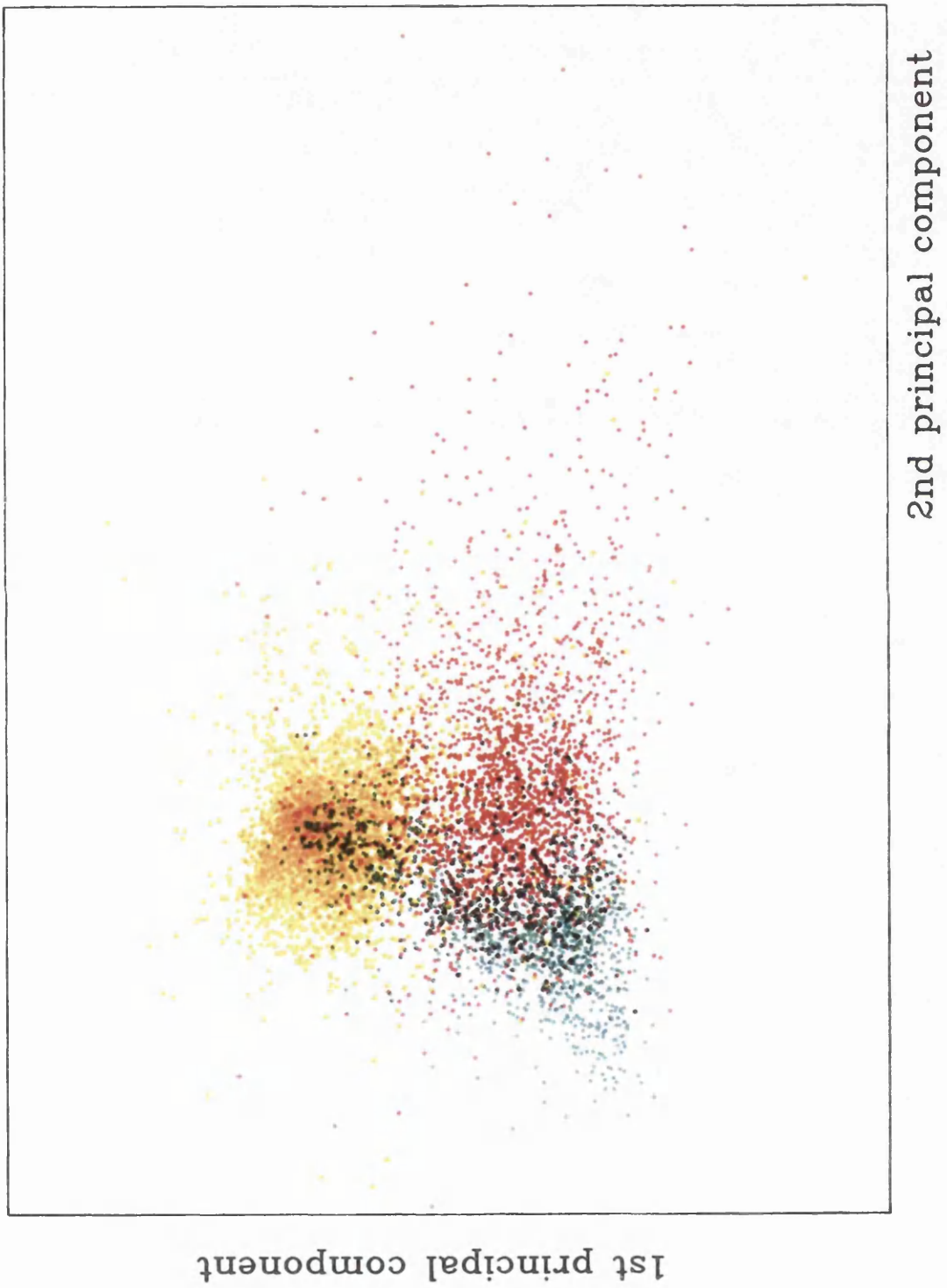

analysis tries to maximise the differences between particle types. There is no difference between the reference and 'fossil' particles on the first principal component axis, but the 'fossil' particles tend to cluster lower down on the second axis. As the particles have all been through the same chemical procedures this difference may be due to some process occurring in the sediment. From Table 4.1, increases in the amounts of Na, Ca, Mg and K would all reduce the second principal component. Mamane & Pueschel (1979), show that fly-ash particle surfaces are important in adsorption reactions in the atmosphere and this has also been found to be the case on stone surfaces (Del Monte et al., 1984). It may be that adsorption of Na, Mg, Ca and K from minerals in the sediment or pore water onto the particle surfaces is causing the results obtained above.

If a PCA is done on these same 1500 'fossil' particles and the reference data set, using only those elements in the final linear discriminant function of Chapter 3 (i.e. S, V, Fe, Ti, Cl and Mg), then the effect of all the elements, except Mg, which appear to be causing the 'fossil' particles to plot away from the reference material, are removed from the analysis. The loadings on the first two principal components are shown in Table 4.2 and it can be seen that Mg is the least important element on both axes.

Table 4.2. Loadings on the first two principal components for a PCA on the reference data set and 1500 particles extracted from a sediment core, using the 6 elements of the final linear discriminant function.

Variable	1st PC Loading	2nd PC Loading
S	-0.051	-0.702
V	-0.628	0.281
Fe	-0.658	0.164
Mg	-0.032	0.144
Cl	0.368	0.538
Ti	0.182	0.302

The particle scores on the first two principal components are shown in Figure 4.36 and it is now apparent that the 'fossil' material plots on top of the reference material and not slightly removed from it as in Figure 4.35. This means that the probability of allocation for particles extracted from lake sediments are likely to increase when using only 6 elements in the linear discriminant function. It is also interesting to note that the loading on the first principal component for sulphur in Table 4.1, is much higher than that of aluminium when 'fossil' particles are included compared with when only reference data were included (see Table 3.14) and the loadings were fairly similar. This increases the confidence that the best element selection was chosen to produce the linear discriminant function in Chapter 3.

4.3.2. Application of particle characterisation to a sediment core.

The characterisation technique was then applied to carbonaceous particles extracted from the sediment core taken from the Men's Bathing Pond on Hampstead Heath in North London. This site was selected as described in section 2.1.2. The core was ^{210}Pb-dated and the total carbonaceous particle profile is shown in Figure 4.27. 7504 carbonaceous particles from 18 levels were characterised using the discriminant function derived from the EDS generated S, V, Fe, Mg, Ti and Cl values and a post-probability set at 0.8 as discussed in Chapter 3. The results are shown in Figure 4.37 and in Table 4.3. When the analysis was also performed using the 17 elements of the full data set there was less than 1% difference in particle allocation between the two methods at any one level.

These results fit very well with the known combustion histories of coal and oil. Before the 1920's fossil-fuel consumption in Britain was almost exclusively coal based, although from this time onwards the use of oil increased rapidly from 3 million tonnes in 1920 to 160 million tonnes in 1972. This was principally due to an influx of cheap fuel oil after the Second World War. As a response to this the first major power station specifically designed to be oil-fired was opened in 1952 on the River Thames at Bankside. Oil consumption increased rapidly in the late 1950's / early 1960's and continued to increase until the oil crisis in 1974. Since

Figure 4.36. *Plot of the first two principal component scores for the particles of the reference data-set and 1500 'fossil' particles extracted from a lake sediment core using only the six elements present in the final linear discriminant function (oil in yellow, coal in red and fossil in green).*

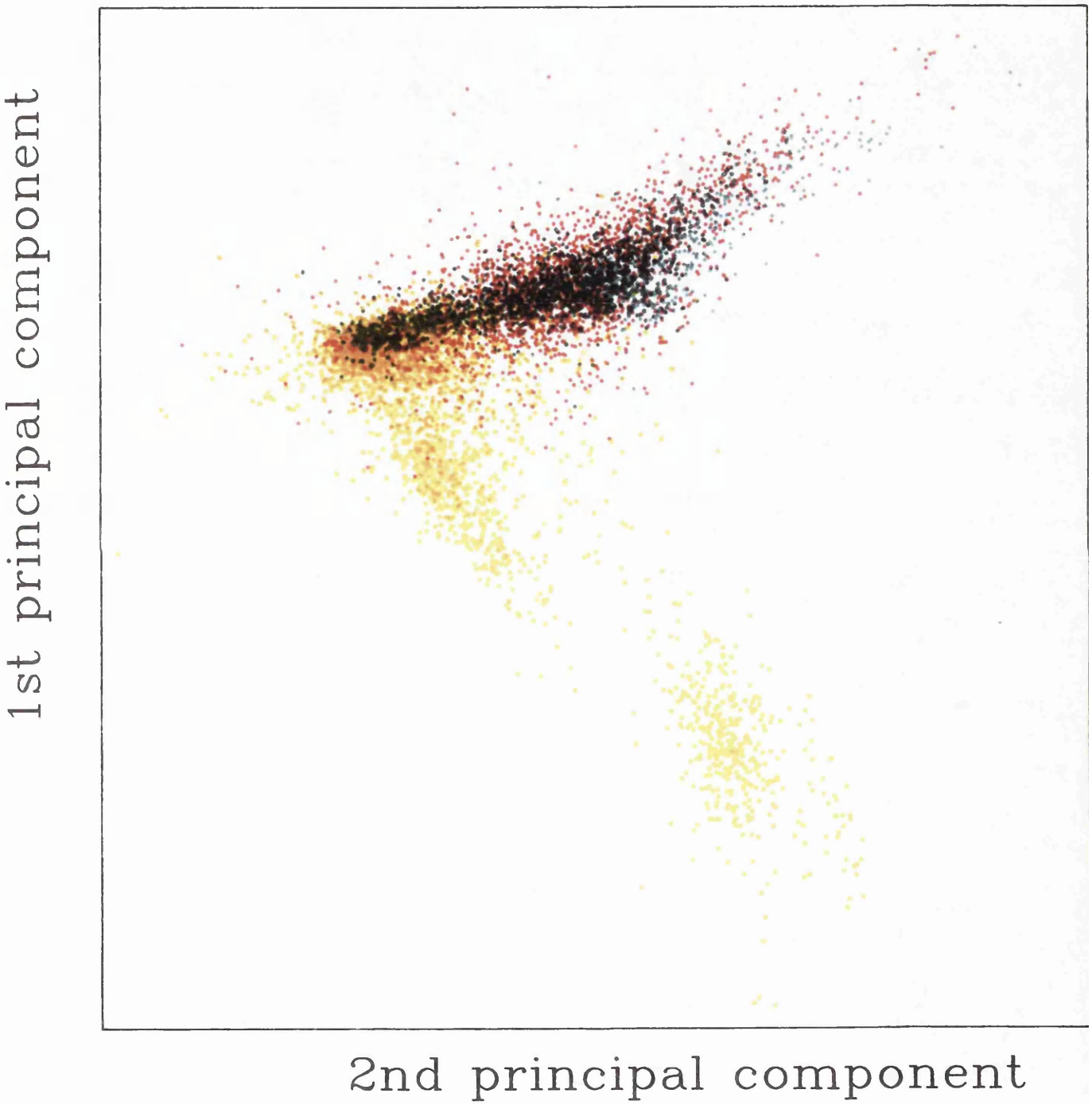

Figure 4.37. Concentrations of 'coal', 'oil' and 'unclassified' carbonaceous particles in the Men's Bathing Pond core, as proportions of the total particle concentration.

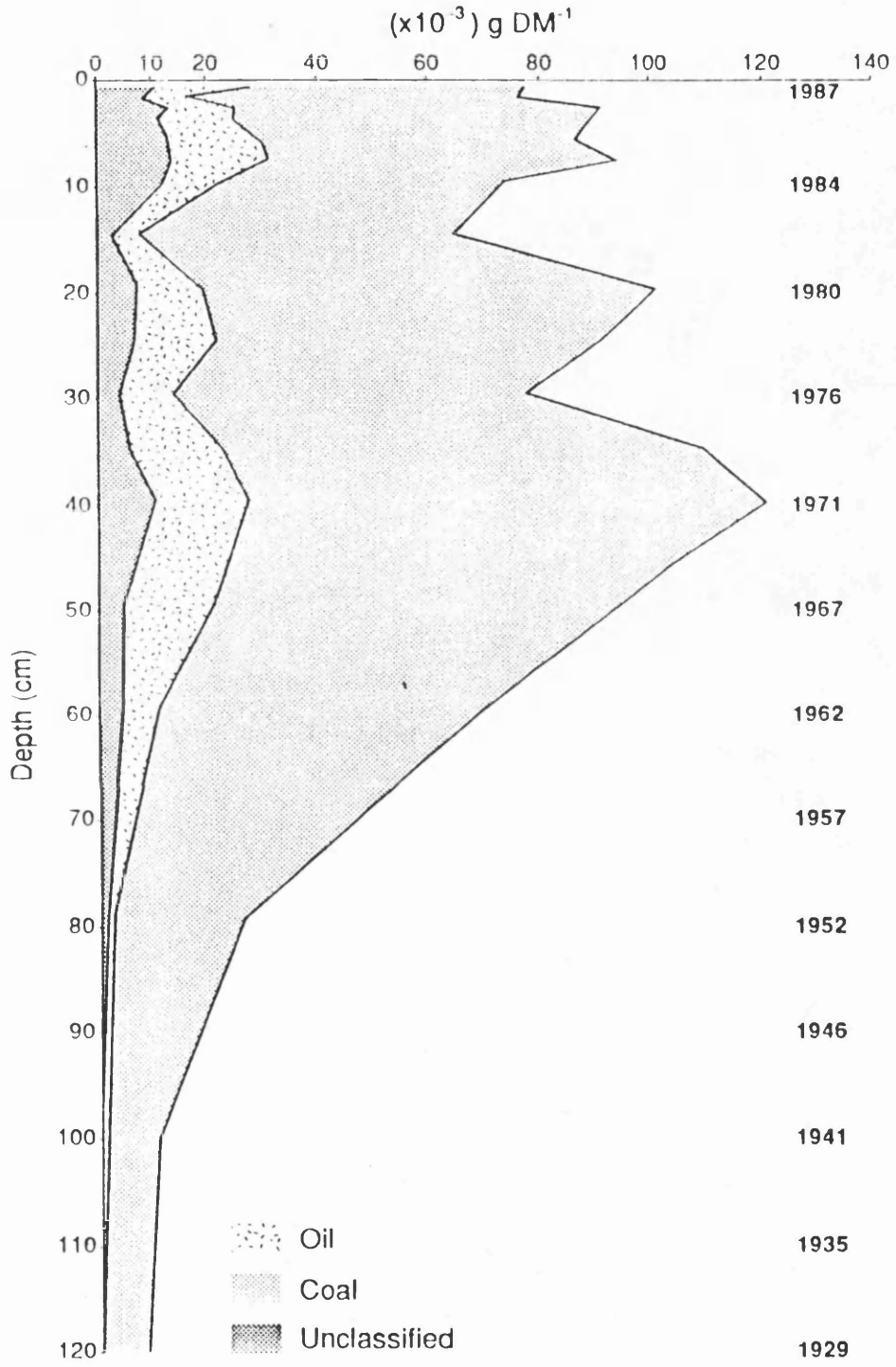

Table 4.3. Fuel type allocation for the Hampstead Heath core.

Depth (cm)	Date	% coal	% oil	% unclassified
0-1	1987	63.8	22.8	13.4
1-2	1987	79.0	9.3	11.7
2-3	1986	72.6	13.0	14.4
3-4	1986	72.5	14.7	12.8
5-6	1986	65.4	19.3	15.3
7-8	1985	67.1	18.4	14.5
9-10	1984	68.9	14.6	16.5
14-15	1982	88.5	7.4	4.1
19-20	1980	80.9	11.9	7.2
24-25	1978	76.1	17.1	6.8
29-30	1976	82.6	12.4	5.0
34-35	1974	79.6	15.6	4.8
39-40	1971	77.6	14.1	8.3
49-50	1967	78.0	17.4	4.6
59-60	1962	84.7	9.3	6.0
79-80	1952	92.4	3.3	4.3
99-100	1941	94.7	2.1	3.2
119-120	1929	99.8	0.0	0.2

then, there has been a general decrease in oil consumption with the exception of 1984/85 during the miners' strike (Figure 4.1). Coal, however, has remained the dominant fuel throughout.

Despite the limited number of data points, most of these events seem to be reflected by the results shown in Figure 4.37, and Figure 4.38 which shows the coal and oil profiles separately. There are very few oil particles until the 1950's, a sharp increase at the end of that decade, and a steady increase until the mid-1970's, when the number generally decreases except for a peak at about 1984.

Figure 4.38. Concentrations of 'coal' and 'oil' carbonaceous particles in the Men's Bathing Pond core.

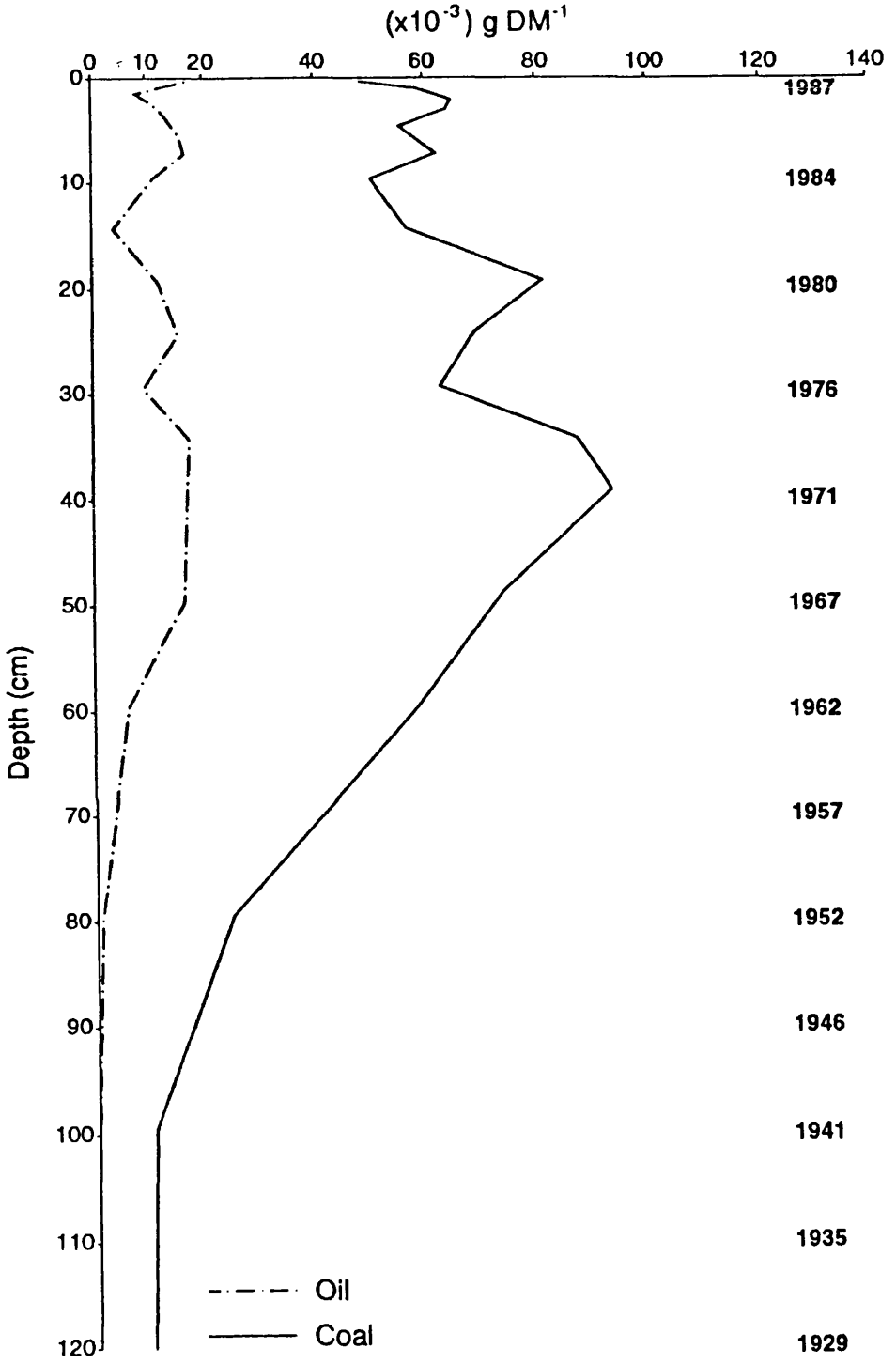

The classification scheme developed in Chapter 3 was produced using reference data from modern power station ash. However, the particles from the Hampstead Heath core were produced up to sixty years ago, and it might be suggested that a discriminant function based on modern particle data should misallocate more of the older particles than modern ones. From the results of the Hampstead Heath core, this does not appear to be the case, as the oldest particles characterised are from a time when there was almost exclusively coal combustion, and the results concordantly show 99.8% coal particles, 0.2% unclassified and 0.0% oil. The reason for this probably lies in the chemical composition of coal and oil. Being fossil-fuels, the chemistry of the coals and oils burned today in power stations will not differ greatly from those burned 50 years ago, or in the case of coal 100 years ago. The most variation will probably occur between different sources of coal and oil, and, as modern power stations now burn much more fuel from more sources than they did 50 years ago, modern fuel ash probably exhibits a much broader range of particle chemistries. This would explain why, despite using five different coal station ashes and five different oil station ashes in producing the discriminant function, there are more lake extracted particles allocated 'unclassified' in the modern samples than in the older ones. It also serves to illustrate that a classification to individual power station level is very unlikely.

One major change that has occurred is in burning techniques. Today, all the major coal-fired power stations use pulverised fuel. In the past, chain grate, travelling grate and spreader stoker furnaces were all used extensively. Falster & Jacobsen (1982), found that different furnace types produced particles of different sizes and so morphological characteristics, would be of little use in fuel type allocations through time, even if they were suitable for modern samples. A chemical technique, by contrast, appears to allocate well both modern and 'fossil' particles.

4.4. Trends in inorganic ash sphere profiles.

As coal has been the major fossil-fuel burned in Britain throughout history, it would be expected that inorganic ash spheres, produced almost exclusively from coal combustion, would follow the same trends in a sediment profile as carbonaceous particles. Full sediment profiles from three sites, Loch Tinker (site 66 - see section

2.5.12) and Loch Teanga (57) in Scotland and the Men's Bathing Pond on Hampstead Heath (105) were analysed for inorganic ash spheres and the results are shown in Figures 2.6, 4.39 and 4.40 respectively. As was briefly mentioned in section 2.5.12, it is quite clear that the trends for both types of particle are similar.

The main difference between the two particle types is the presence, in the inorganic ash profile, of a low, continuous background value, present at all pre-industrial sediment depths. These 'naturally produced' particles will still be present in levels corresponding to industrial times but their presence is obscured by the vast numbers of industrially produced particles. When this 'background' value is removed from the diagrams, the industrial ash sphere record begins at the same depth/date as the carbonaceous particle record.

There are two possible sources for these 'natural' spheres, volcanoes and micro-meteorites. Lefèvre et al. (1986), estimated that approximately 1.6 tonnes of microspherules (1-5μm in diameter) were produced per day from a single summit crater of Mount Etna during moderate recurring activity. These volcanic particles are siliceous (47-98% SiO_2) and may be hollow or filled with other spheres much like industrial ash. Morphologically, meteoritic dust spheres are also very similar but their chemical and isotopic composition is totally different (Wohletz & McQueen, 1984). Handy & Davidson (1953), calculated that the annual global deposit of meteoritic dust (5 - 200μm in diameter), is about 2 million tons, corresponding to about 40g ha^{-1} yr^{-1} distributed evenly over the Earth's surface. Both these types of particle will contribute to the 'background' concentration of spheres accumulated in lake sediments.

Both Loch Tinker and Loch Teanga show much higher concentrations of inorganic ash spheres than carbonaceous particles. This is probably because fossil-fuel fired power stations in Scotland have been virtually exclusively coal-fired, the only major oil-fired station being at Inverkip in Glasgow which operated between 1970 and 1987. Consequently, the inorganic ash sphere to carbonaceous particle ratios are high, approximately 5.8:1 at the surface of Loch Tinker and 7:1 for Loch Teanga, and this reflects the ratios of these particles found in coal-fired ash.

Figure 4.39. Inorganic ash sphere profile for Loch Teanga (core TEAN5) taken in September 1987.

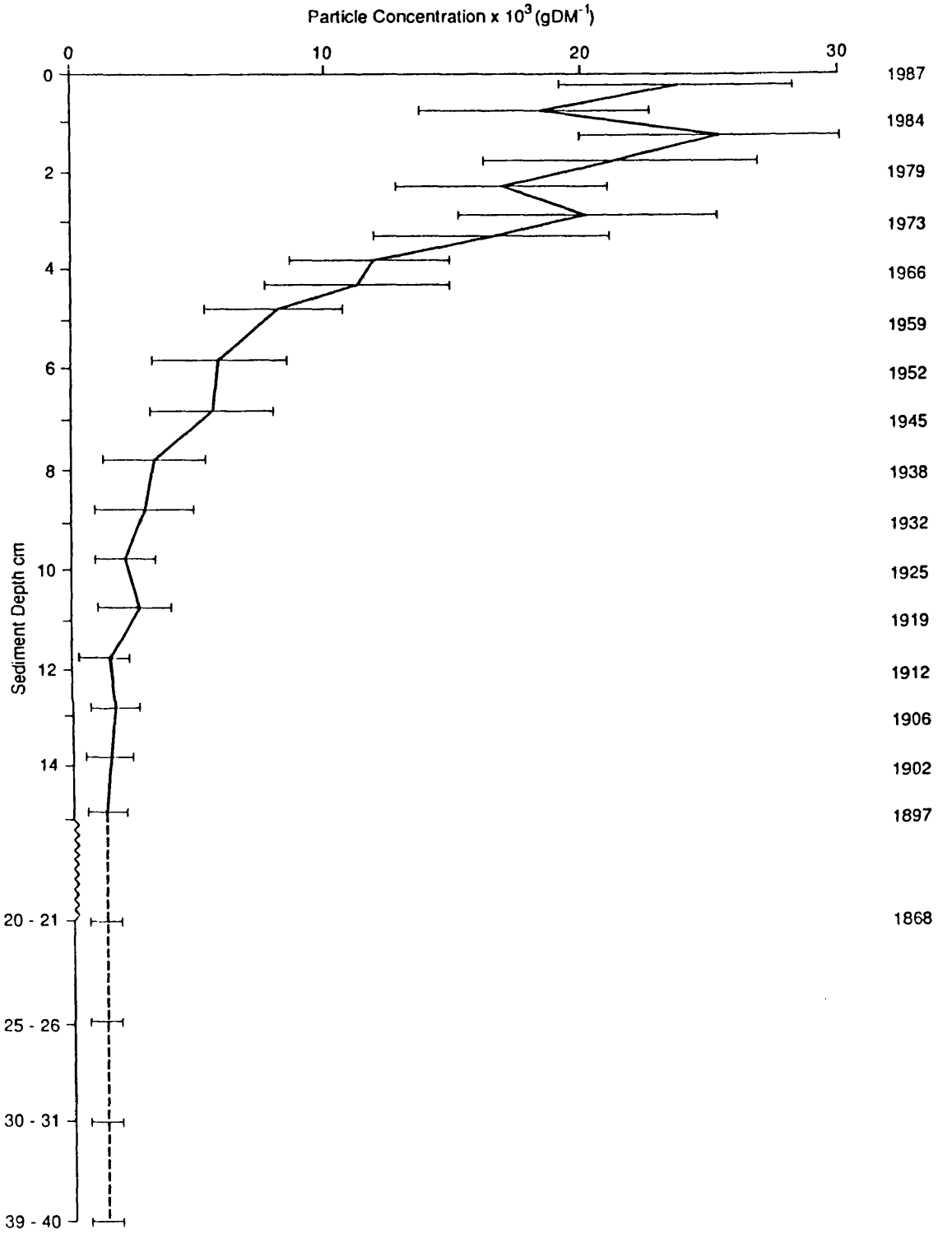

Figure 4.40. Inorganic ash sphere profile for the Men's Bathing Pond on Hampstead Heath (core MEN2) taken in October 1987.

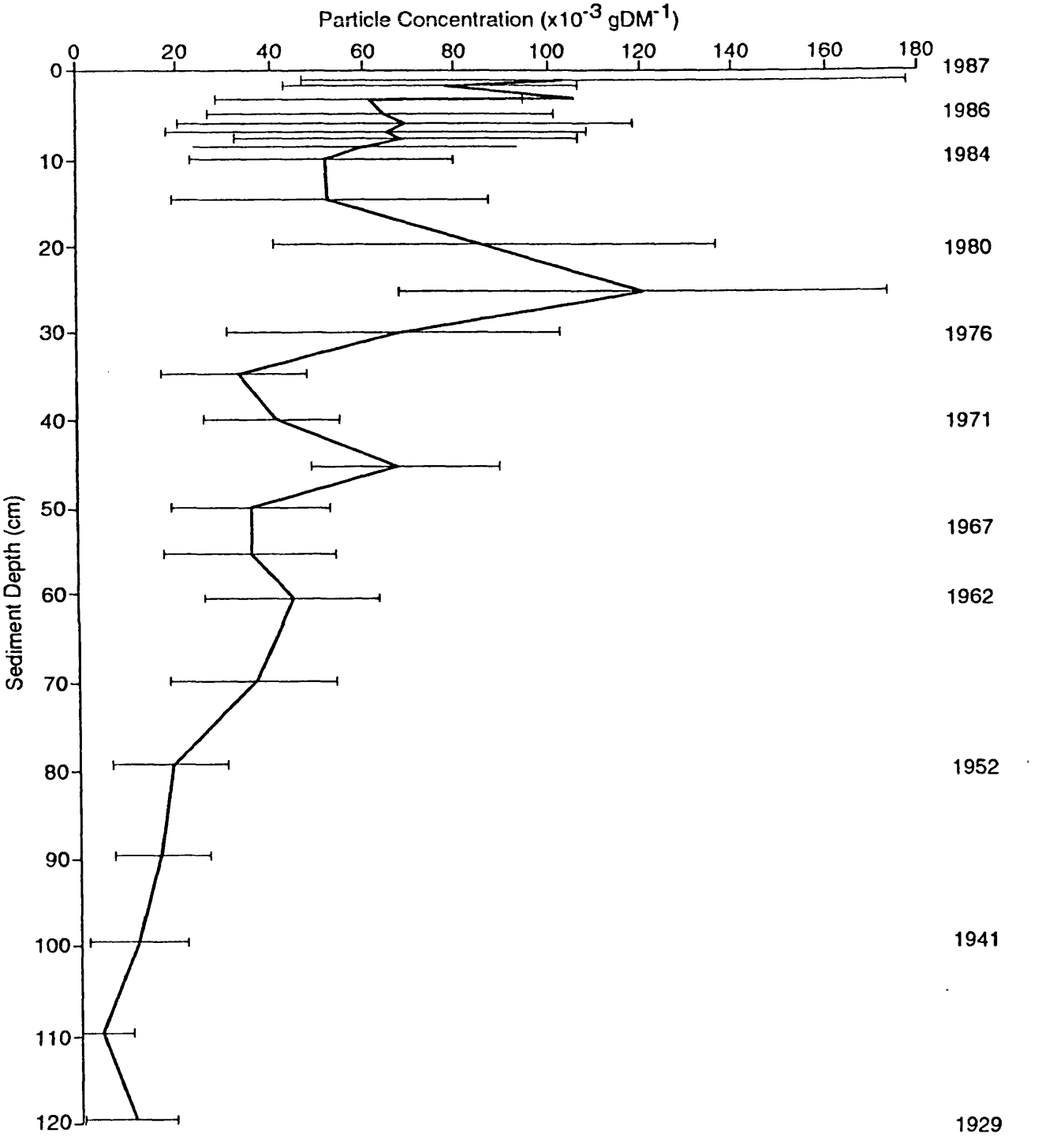

The carbonaceous particle profile for Loch Teanga showed a 'levelling off' at the top of the core, possibly indicating the start of a downturn in the particle record. This is reinforced by the inorganic ash sphere profile, where a peak occurs just below the sediment surface at the point where the levelling off of the carbonaceous particle record began.

By contrast to these Scottish sites, the inorganic ash sphere to carbonaceous particle ratio throughout the Hampstead Heath core is much lower, between 0.5 and 2:1 and this probably reflects the much greater influence that oil-fired power stations have had in the south-east of England. It may be that this ratio of particles can be used in future to give some indication of the relative influence of coal and oil combustion on a lake and its catchment, especially when this information is used in association with the characterisation of carbonaceous particles. This is discussed more fully in Chapter 5.

4.5. Discussion.

4.5.1. Trends in particle deposition 1800 - 1980.

The start of the carbonaceous particle record in the mid-nineteenth century is generally attributed to the effect of the Industrial Revolution and the combustion of larger quantities of coal at higher temperatures. The Industrial Revolution in Britain began in the early years of the eighteenth century with the development of a pumping engine by Savery, Papin and Newcomen, but it was not until the late nineteenth century and the work of Faraday and Gramme that the industrial generation of electricity finally became practicable. The first fossil-fuelled power station supplying electricity to the public was situated at Holborn Viaduct in London and began generation on 12th January 1882, and by the end of the century most large towns had their own electricity generating stations. The start of the carbonaceous particle record in lake sediments therefore pre-dates the first power generating station and during this period probably reflects the combustion of coal in industry as a whole. This may account for the variability in the start of the particle record both within and between regions, as local industries would have a large impact on the atmospheric input. The start of the particle record for the Irish

sites is generally 10-20 years later than those in Wales and Scotland (no available data for England) and this is probably due to the relative remoteness of these sites from the majority of British industry and the small amounts of coal and oil burned for electricity generation.

From the 1920's and 1930's onwards, the consumption of coal continued to increase, and this accelerated after the Second World War due to a considerable increase in total energy demand. An abundance of cheap fuel-oil also became available at this time and led to the first oil-fired power station at Bankside, in 1952. During this period of expansion and increased consumption in the power generation industry (see Figure 4.1), there was a substantial reduction in coal consumption in other industrial markets and the railways. Particle emission legislation was also limited at this time as the Clean Air Act was not passed until 1956. The carbonaceous particle record for this period shows a rapid increase in most sediment cores and it seems probable that this mainly reflects the fuel consumption of the electricity generation industry (Darley, 1985). This rapid increase has been attributed to the increase in oil consumption alone (Battarbee et al., 1988), however, due to the rapid increase in consumption of both coal and oil at this time and the dominance of coal in electricity generation (Figure 4.1) this seems unlikely.

Coal consumption continued to increase until the 1980's, whilst that of oil increased until 1973 when the massive price increases imposed by OPEC (Organisation of Petroleum Exporting Countries) and the oil shortage caused by the Arab oil embargo of 1973-1974, caused consumption to decrease again and long term fuel strategies to return to a coal basis.

Starting in the 1930's, the Central Electricity Board, followed by the Central Electricity Authority and the Central Electricity Generating Board continued a policy of creating fewer, larger and more efficient power stations. This increase in combustion efficiency and the implementation of more rigorous pollution control legislation meant that, despite the continued increase in fuel consumption in the 1960's and 1970's, the increase in particle emission was slowing down, until a peak in particle deposition occured in 1976 (Vallack & Chadwick, 1989). The particle record in lake sediments for this period shows a continued increase in concentration

to a peak, dating in the 1970's / 1980's. In a similar way to the start of the particle record, both the rapid increase in particle concentration and the concentration peak occur later in the Irish sites than in the Scottish and Welsh sites, and this delay in response is again probably due to the remoteness of these sites from historical and contemporary particle sources.

4.5.2. Causes of a decrease in particle deposition.

Coal consumption in Britain as a whole has not changed significantly in recent years. With the exception of the 1984/85 miners' strike, consumption in England and Wales has been reasonably steady since the late-1970's (Electricity Council, 1988) (see Figure 4.1), and in Scotland has decreased from about 6 million tonnes in the late-1970's to about 3 million tonnes in 1985 (mainly due to the reduction in heavy industry) since when it has remained steady (I.Anderson, Scottish Power, pers. comm.). Oil consumption throughout Britain has decreased in that time. The recent reduction in the number of carbonaceous particles reaching lake sediments throughout the British Isles is therefore probably due to a combination of two factors. Firstly, the small decrease in fossil-fuel consumption (probably more significant in Scotland than elsewhere) and secondly, improvements in the removal of particulates from flue gases before they are emitted to the atmosphere and to the more widespread use of these techniques, caused by the implementation of more stringent air pollution legislation.

Following the deaths of over 4,000 people in London during the 'Great Smog' of December 1952 (Wilkins, 1954) and the subsequent report of the Beaver Committee published in 1954, the Clean Air Act was passed by Parliament in July 1956. There were four main objectives of the Clean Air Act (with subsequent amendments in the Control of Pollution Act, 1974 and the Health and Safety at Work Act, 1974).

1. Control of unacceptable ground level concentrations of effluent gases especially sulphur dioxide.

This was to be done by a system of approved chimney heights. Legislation was put into the hands of the local authorities which could decide upon a minimum height of discharge, after consideration of matters that would affect the ground level

concentration of sulphur dioxide. In addition to ground level concentrations, the Control of Pollution Act, 1974 limited the sulphur content of fuel oils in parallel with the rest of the EEC.

2. Control of low-level smoke emissions from domestic sources.

For the first time domestic sources were to be regulated and this was done by empowering local authorities to make smoke control areas.

3. Control of smoke emissions from any chimney on industrial and trade premises.

Section 1 of the Act made it an offence to allow dark smoke to be emitted from a chimney on any building. Sections 19 & 20 made similar restrictions on railway engines and ships in certain U.K. territorial waters. The Dark Smoke (Permitted Periods) Regulations, 1958, imposed limits on the time in which dark smoke may be emitted for soot blowing etc.. The emission controls did not extend to emissions other than from chimneys, although this was amended in Section 1 of the Clean Air Act, 1968, where emission of dark smoke from industrial and trade premises, from other than a chimney was prohibited. There were certain exceptions to these controls and these were outlined in the Clean Air (Emission of Dark Smoke)(Exemption) Regulations, 1969, but they did not concern the combustion of fossil-fuels.

4. Control of emissions of particulate matter from chimneys.

In the Clean Air Act, 1956, there was a policy of requiring modifications only in situations of major potential emissions. This control was extended by the Clean Air Act, 1968 and by the Clean Air (Emission of Grit and Dust from Furnaces) Regulations, 1971, to control emissions from both pulverised and solid fuel furnaces burning fuel at a lower rate of 100lb/hr (45.3kg/hr) or more, and emissions from liquid and gaseous fuelled furnaces at a rate of over 1.185×10^6kJ/hr. Regulations also specified the amount of grit (particles of diameter greater than 75μm) permitted in effluent gases before requiring the installation of grit and dust arresting equipment. Limits established by the Alkali and Clean Air Inspectorate in 1974, specify that power stations built before 1958 may emit up to 0.46g m^{-3}, while coal-fired power stations in the 2,000 - 4,000 MW range may only emit up to 0.115g m^{-3}.

Following the Clean Air Act (1956), the Central Electricity Authority started equipping all new power stations with dust extraction equipment and tall chimney stacks. This was continued by the Central Electricity Generating Board until by 1961 all power plants under the C.E.G.B.'s control had either been fitted with some sort of particle arrestor or converted to oil, as oil combustion was more efficient and emitted less fly-ash to the atmosphere. This included obsolete plants used only for a few hours a year at peak times (C.E.G.B. Annual Report, 1960/61).

The multitude of small, old power stations was gradually replaced by fewer, larger stations starting in the late-1960's. These stations were fitted with more efficient particle arrestors (electrostatic precipitators which were to be at least 99.8% efficient), and were subject to the more stringent regulations of 1974, and it seems to be this gradual conversion that caused the decline in particle deposition.

Yearly mean rates of dust deposition in the United Kingdom, as measured by British Standard gauges are available for the period April 1973 to March 1982 from the Department of Trade & Industry's Warren Spring Laboratory. Over 400 gauges were measured monthly, including a number of sites "in open country to catch general deposit" and a summary of the results appears in Table 4.4 (from Vallack & Chadwick, 1989). It can be seen that there is a clear downward trend in deposition between 1976 and 1982.

4.5.3. Reasons for the delay in sediment response to the decrease in atmospheric particle deposition.

The particle concentration decrease only appears to be present in cores taken after 1985 and, if this really is recording the particle deposition decrease starting in 1976/77, then there is an apparent 8-9 year delay in the response of the sediment record to this atmospheric event. Lake sediments are affected by many post-depositional processes which could cause mixing of the surface levels. These include biological factors such as bioturbation as well as physical processes such as resuspension and degassing. Moreover, cores taken in the early 1980's were sliced at 0.5cm or 1cm intervals and insufficient sediment would have accumulated since 1975 to resolve this decline.

Table 4.4. Summary of deposit gauge rates of dust deposition for the U.K. from 1973-1981 for sites in open country. Values in mg m^{-2} day^{-1}. (from Vallack & Chadwick, 1989).

Year	Mean	Std. Devn.
Oct 1973 - Mar 1974	59.3	41.7
Apr 1974 - Mar 1975	53.3	33.7
Apr 1975 - Mar 1976	56.5	27.5
Apr 1976 - Mar 1977	57.3	27.1
Apr 1977 - Mar 1978	44.7	18.3
Apr 1978 - Mar 1979	41.6	22.0
Apr 1979 - Mar 1980	34.8	15.5
Apr 1980 - Mar 1981	40.2	28.3
Apr 1981 - Mar 1982	31.6	16.0

The feeding, burrowing and locomotory activities of sediment dwelling animals cause significant mixing of lake, river and ocean sediments. The influence of any given species on sediment properties will depend on size, mobility, depth and rate of feeding and particle size selectivity as well as the population density at which the species occurs (Aller, 1978). Tubificid worms ingest sediment at 5-8cm depth and then expel at the sediment/water interface (Fisher et al., 1980). The worms move both laterally and vertically causing sediment to slump into vacated burrows and dragging particles with them whilst burrowing. Davis (1974) produced a model which predicted that due to tubificid feeding 36% of surface pollen would be greater than 30 years old and 5% greater than 90 years. Carbonaceous particles are in the same size range as pollen grains and there is no reason to assume that these particles would be treated any differently. Davis also suggested that with additional factors, such as the affect of water currents and gas bubbles, it would often not be possible to distinguish events shorter than a decade or two, a time scale which would certainly explain the observed delay in response to the reduction in particle deposition.

The continuous mixing of surface sediment layers therefore has a 'time averaging' effect on the particle record. Episodic deposition events such as periods of high particle deposition due to unusual wind patterns, may be mixed with sediments from

low deposition periods, smoothing what would otherwise be an unusual peak in the sediment record. Clark (1988) suggested that a moderate amount of mixing is sufficient to obscure a high signal as the sediment of several consecutive years will be reworked before it is buried below the mixing layer. Similarly, at the beginning of the particle record, mixing may move particles down to earlier sediment levels making the record appear longer than it really is. The delay in distinguishing a particular event, therefore depends on the balance between the rate of sediment input, the duration of the event and the intensity of the mixing of the sediment.

4.5.4. Dating.

The carbonaceous particle record in lake sediments has been used as an indirect dating technique in Sweden (Renberg & Wik, 1984 & 1985a). The approach relies on relating consistent particle trends in undated cores to those which have previously been dated using a reliable technique such as ^{210}Pb chronology or varve counting. Until recently, this indirect dating approach has been limited in British sediments as there have been only two dates that could be assigned to the profile. These are the start of the particle record, and the sharp increase in particle concentration. From sections 4.2.1 - 4.2.4 it can be seen that these features are nearly always present in a sediment profile. There should always be a start to the particle record if the core is long enough and analyses are carried out to a sufficient depth. Only Loch Coire nan Arr and Loch Doilet failed to show a rapid increase in particle concentrations probably due to the very low particle concentrations present at all depths within the profile. However, although these features are consistently present, the evidence from a comparison of the dated profiles shown above suggests that they fall within quite broad periods of time and to a certain extent there are regional differences in date. In cores taken most recently, a third feature representing a particle concentation maximum can also be used as a dating horizon.

The dating of the start of the particle record is probably the most vague of the features. In Scottish sites this falls between the 1840's (Long Loch of Dunnet Head, Loch Urr, Lochnagar) and the 1890's (Loch Doilet and Loch Teanga); for Welsh sites, from the early 19th century (Llyn Glas) to the 1880's (Llyn Conwy, Llyn Gynon, Llyn y Bi), and for Irish sites from the 1860's (Lough Muck) to the 1910's

(Lough Maam). However, if the doubtful usefulness of the Loch Coire nan Arr and the Loch Doilet profiles is taken into account and Loch Teanga is treated as a special case (its profile appears more similar to the Irish sites than the Scottish ones and this may be due to its remoteness on South Uist in the Outer Hebrides), then it is possible to suggest a range of dates for this feature in the different regions (see Table 4.5). There are no dated sites at present in England with a complete particle record, and so it is not possible to add this region to the table.

Table 4.5. Range of dates for the start of the carbonaceous particle record (feature A) for different geographical locations.

Scotland	:	1840's - 1870's
Wales	:	1850's - 1880's
Ireland	:	1860's - 1910's

The rapid increase in particle concentration which characterises the second useful dating feature is less vague and is usually associated with the post-War expansion in the electricity generating industry. As such it usually dates to the late 1940's - 1950's, although it is later in some cores e.g. 1960's in Long Loch of Dunnet Head, Loch Larach, Loch Teanga, Llyn Irddyn, Llyn Conwy, and the 1970's in Lough Maam and Lough Maumwee. It is present in every core analysed except for three, Loch Doilet and Loch Coire nan Arr, the profiles of which were discussed earlier, and Llyn y Bi, which shows a smooth concentration curve without any one single point of rapid increase. The cores from France and Norway also show this feature, and for Lac des Corbeaux, the only one ^{210}Pb-dated, the increase occurred in the late-1940's (see Figure 4.33). Further work is required to confirm this dating in European cores. However, it is possible to put a range of dates on the feature for each British geographical region as shown in Table 4.6.

Battarbee et al. (1988) took the mean particle fluxes from all their analysed sites in Wales and in Scotland and showed that both the start of the particle record and the rapid increase in the Welsh sites occurred later than in the Scottish ones. To a certain extent this is supported by the above, although the variability within a region is such that for an undated profile, a range of dates such as those suggested here

should be allocated for each feature.

Table 4.6. Range of dates for the rapid increase in carbonaceous particle concentration (feature B) for different geographical locations.

Scotland	:	1940's - 1960's
Wales	:	1940's - 1960's
Ireland	:	1940's - 1970's
England	:	1940's - 1950's

The third feature which can now be found in most recent sediment cores throughout Britain is the peak in carbonaceous particle concentration. In one or two cases, such as the profiles from Loch Fleet (Figure 4.9b) and Malham Tarn (Figure 4.22), double peaks are present and it may be difficult to positively identify the right one, but in most cases there should be no confusion.

In the same way that the start of the particle record and the sharp increase in concentration vary between one part of the country and another so the peak appears to differ by a few years in different regions. All the post-1985 cores from Scotland show a concentration peak except for three, Loch Coire nan Arr, Loch Doilet and Loch Teanga. The reasons for these cores differing from other Scottish cores have been discussed earlier. For the dated cores which show a surface decline, the peak appears to occur remarkably consistently. For the Long Loch of Dunnet Head and Loch Uisge cores the ^{210}Pb date for the peak is given as 1975 ± 2 years and for the Loch Larach core 1975 ± 1 year. The peaks for the Loch Tanna, Loch Laidon and Lochnagar cores date in the mid-late 1970's (Battarbee et al., 1988).

All the Welsh post-1985 cores show a surface decrease in particle concentration, but the date of the peak is less consistent than the Scottish cores, and this is probably because the analyses were not done on continuous slices throughout the profile. Llyn Glas gives a peak date of 1976 ± 2 years, Llyn Irddyn 1980 ± 2 years and Llyn Conwy 1971 ± 2 years, but due to the sampling interval this latter peak should probably date later, somewhere between 1971 and 1979. Generally it would

appear that the peak in particle concentration in Welsh lakes occurs a little later than those in Scotland and this would agree with previous results that Welsh lakes are influenced by, or respond to, atmospheric events later than those in Scotland. The Welsh cores analysed by Natkanski (in Battarbee et al., 1988) were all taken in 1985 and only one, Llyn Gynon, shows a peak dating at 1980.

All the Irish cores show a sub-surface peak in particle concentration, and this again occurs at a consistent date with respect to the ^{210}Pb chronologies. Lough Muck and Lough Maam both give a peak date at 1982 ± 2 years and Lough Veagh and Lough Maumwee 1983 ± 2 years. This is a later date than for both Welsh and Scottish lakes and it may be that Irish sites are influenced by atmospheric events even later than the Welsh sites being further from the main area of British industry.

On the basis of the limited data available, a peak also occurs at English sites but much earlier than for the other regions. This is the result of only two dated cores, Tunnel End Reservoir where the peak occurs in the 1960's, and the Hampstead Heath Bathing Pond which has a peak dating at 1969 ± 2 years. This early decrease may be due to the C.E.G.B.'s power station closure programme, which reduced the number of power stations in England and Wales from 233 in 1964 to 168 in 1975 and to just 90 in 1984, preferentially in the southern regions (C.E.G.B. Annual Reports). It may be that the peak also reflects local sources and therefore would be more variable in timing which might be expected the closer the site is to industries and cities. Further work is needed to confirm this English peak date. Regional dates for the particle concentration peak are shown in Table 4.7.

Table 4.7. *Range of dates for the peak in particle concentration (feature C) for different geographical locations.*

Scotland	:	1974 - 1980
Wales	:	1975 - 1982
Ireland	:	1980 - 1983
England	:	1960's (?)

Figure 4.41. Schematic carbonaceous particle profile for a recent sediment core, showing the three dating features, A - the start of the particle record, B - the rapid increase in concentration, and C - the concentration peak.

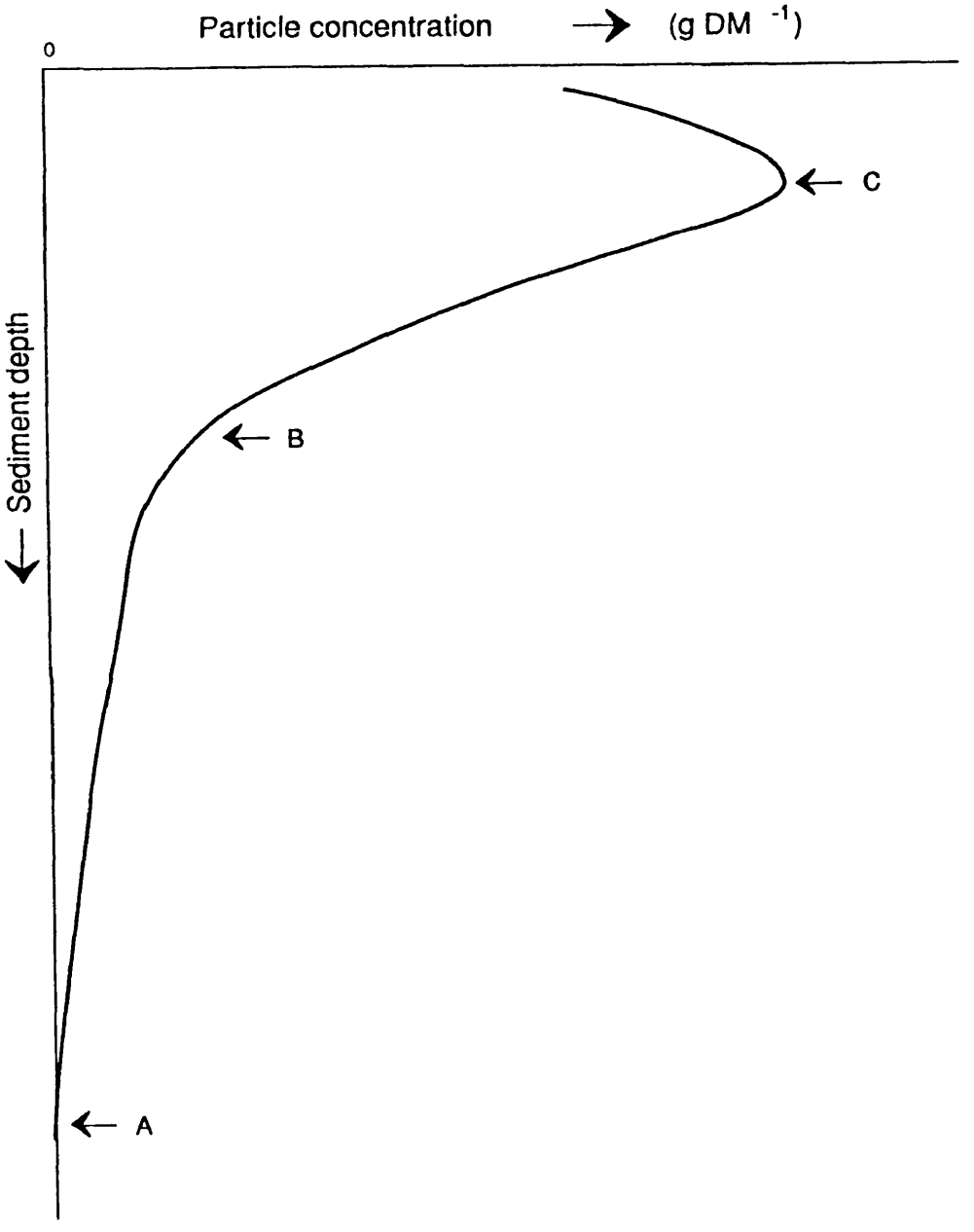

A schematic carbonaceous particle profile for a recent sediment core is shown in Figure 4.41. This pattern is now found in lake sediments throughout the United Kingdom and Ireland and the features A (the start of the particle record), B (the rapid increase in concentration) and C (the peak in particle concentration) can be used to indirectly date the core depending on the location of the site, using the dates in Tables 4.5 - 4.7.

Other dates can possibly be added to carbonaceous particle profiles using the results of oil/coal characterisation. The commissioning of new power stations and other particle sources are well documented, and where new particle types appear in the profile, a date should be readily available. For example, using the Hampstead Heath core, oil particle concentrations closely follow the oil consumption trends through time (see Figure 4.42), and dates for the 1972/73 peak and subsequent decline in oil consumption would only be a year or two out when transferred to the carbonaceous particle diagram. The same is not so true of coal, where although the trends are roughly the same (Figure 4.43), there are some differences, especially in more recent times. This is probably due to the majority of coal consumption taking place further north in an area remote from the site, enforcing the need for local information when interpreting these diagrams.

Inorganic ash sphere analyses add little to normal core dating, but may give more information on a longer time scale. As mentioned in section 4.4, there is a continuous background concentration of ash spheres at all pre-industrial depths corresponding to the natural input of these particles from volcanic and extra-terrestrial sources. If the accumulation rate of the lake sediment remains roughly constant, then any major departure from this background level will probably correspond to atmospheric emissions by major volcanic eruptions in the region. These too have been well documented through history, and it may be that inorganic ash sphere analysis on long cores can give extra dates in this way, especially in regions of high volcanic activity.

4.5.5. Particle allocations through time.

The allocations of carbonaceous particles extracted from the Hampstead Heath core

Figure 4.42. Oil consumption in England and Wales compared to the concentration of oil carbonaceous particles in the Men's Bathing Pond core from 1920 to 1984.

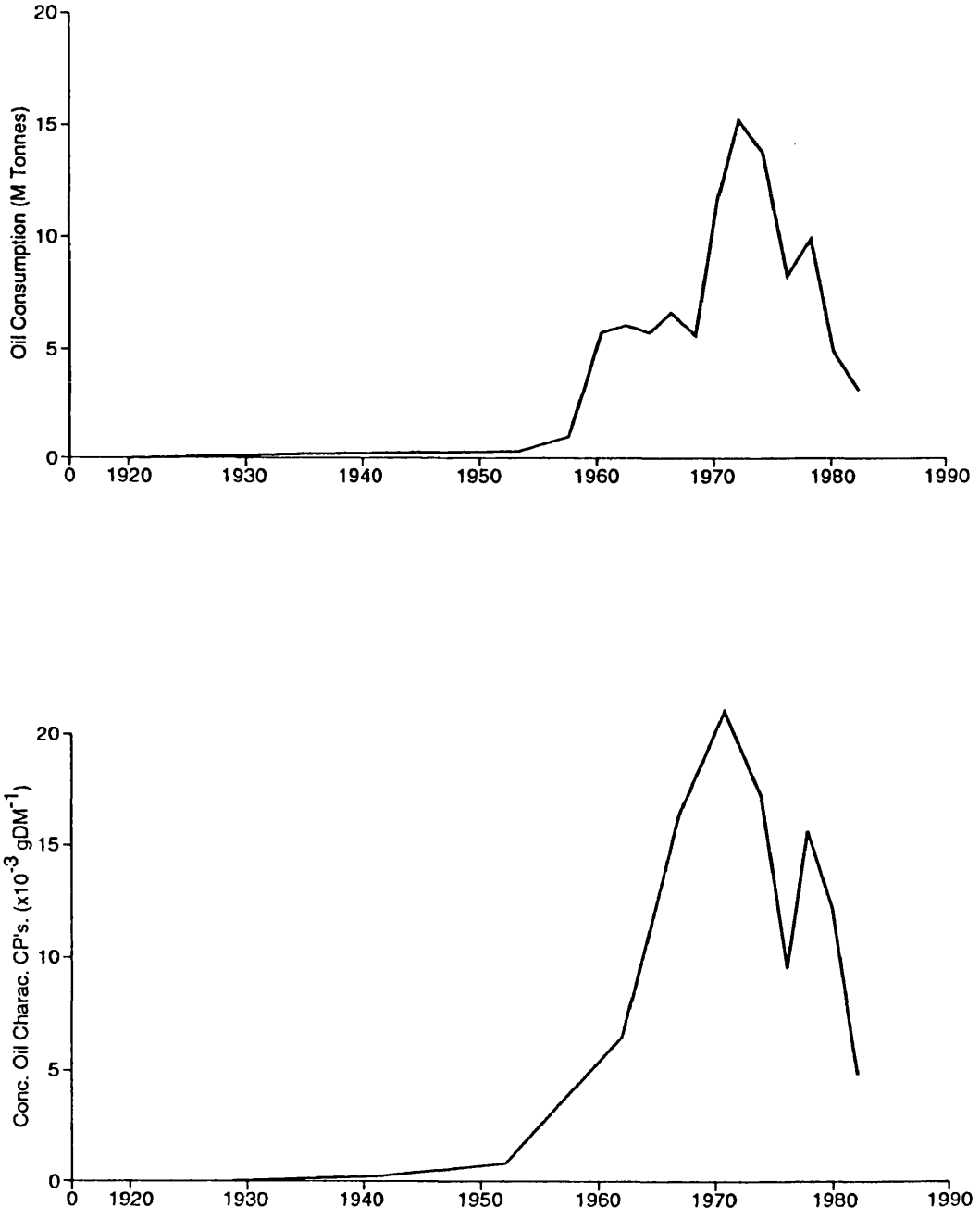

Figure 4.43. Comparison of inorganic ash sphere concentration and coal carbonaceous particle concentration in the Men's Bathing Pond core, to coal consumption in England and Wales from 1925 to 1984.

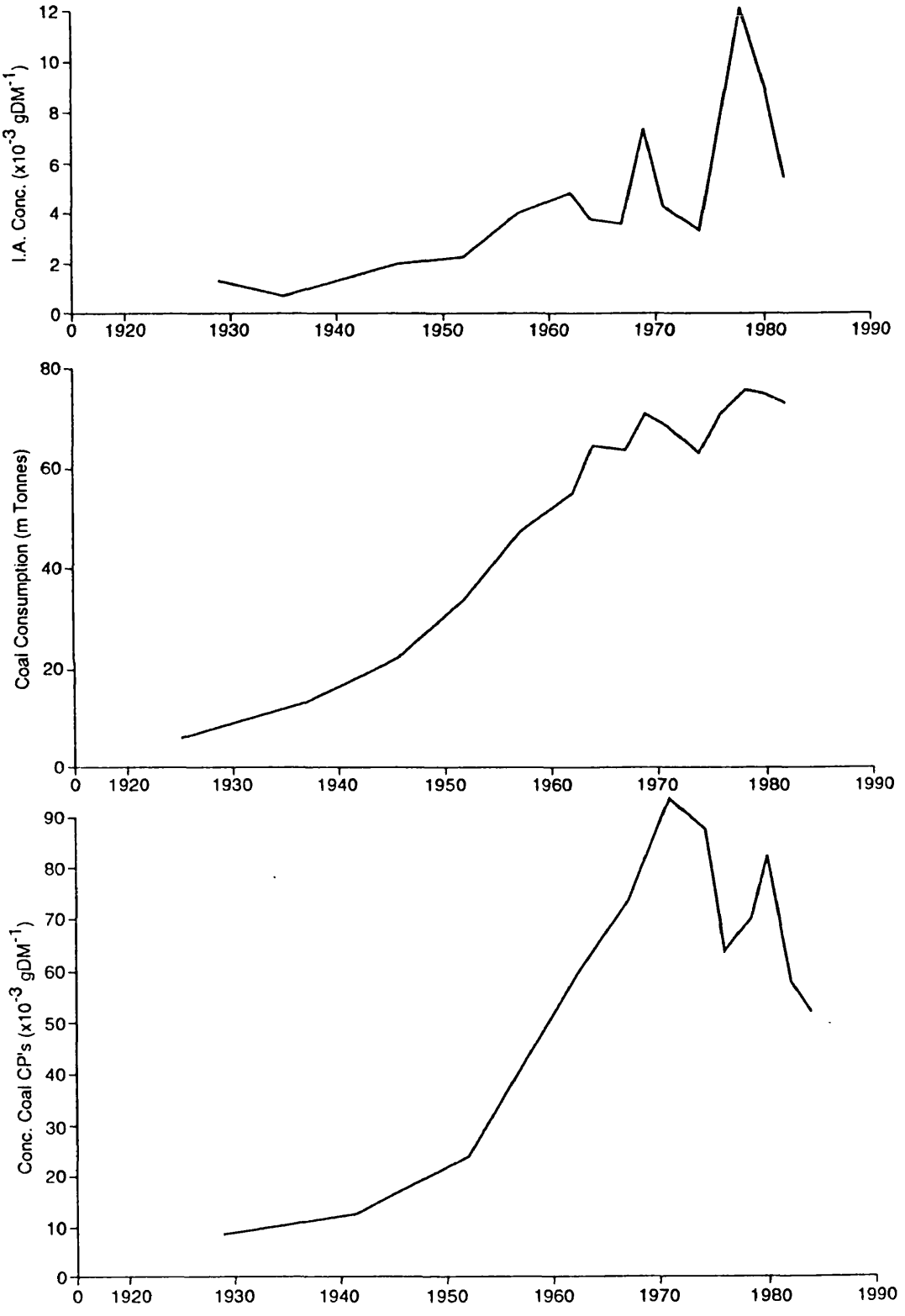

to fuel type compare well with known combustion histories, and thus increases the confidence in the particle characterisation procedure. Inorganic ash sphere analysis can, and in this instance does, support these allocations by correlating well with those particles allocated to coal (Figure 4.43). Where a close correlation of the two particle profiles is seen, this suggests a coal source for the majority of the deposited particles, especially where the ratio of the inorganic ash spheres to carbonaceous particles is high, for example, Loch Teanga and Loch Tinker. Consequently, using the information gained from both characterising carbonaceous particles and from inorganic ash sphere analysis, it is possible to get a good idea of the impact that the combustion of different fossil-fuels have had on a lake and its catchment through time.

CHAPTER 5. SPATIAL DISTRIBUTION OF FLY-ASH PARTICLES IN LAKE SEDIMENTS.

5.1. Introduction

It has been shown that the carbonaceous particle record in lake sediments corresponds well with fossil-fuel burning histories in countries such as Britain, Sweden, Norway (Wik & Natkanski, 1990) and the U.S.A. (Griffin & Goldberg, 1981). The spatial distribution of fly-ash particles has been studied on a local scale, by collection in deposition gauges (Vallack & Chadwick, 1989, 1990), but in Britain, the combination of these two ideas, and using surface sediments to provide a picture of contemporary geographical deposition from the atmosphere, has not been tried.

In Sweden, the distribution of carbonaceous particles has been studied on a provincial scale using lake surface sediments (Renberg & Wik, 1985) and forest soils (Wik & Renberg, 1987) and on a national scale, again using lake surface sediments (Renberg & Wik, in prep.). The results show that the spatial distribution of these particles, like the temporal distribution, follows industrial patterns.

In this study an attempt has been made to map the distribution of particles in Scotland. Using the cores taken from the sites selected in section 2.1.1, there are 92 sites in Scotland and 2 sites in the north Pennines that can be used. All these cores were taken between 1986 and 1989 with the exception of Loch Tinker, Loch Laidon and Loch na h'Achlaise which were cored in June 1985. For this particular study it would have been ideal to have taken all these cores at the same time. However, a degree of mixing occurs in the surface levels of the sediment (see section 4.5.3), and concentrations derived from particle analysis will be time-averaged over several years. Distribution patterns, therefore, should not be too greatly affected by the time difference between the dates of coring.

A major reason for using Scotland is its steep sulphur gradient with values ranging from 1.6g S m^{-2} yr^{-1} in the south to 0.4g S m^{-2} yr^{-1} in the north (Battarbee, 1990). High temperature fossil-fuel combustion plants are major sources of both

kinds of fly-ash particles and of the sulphur and nitrogen oxides that cause lake acidification. It is known that in areas of high sulphur deposition, carbonaceous particle concentrations in the surface sediments of lakes are also high (Battarbee, 1990). Consequently, Scotland is a good region to ascertain whether there is any relationship between fly-ash particle concentrations in lake surface sediments and sulphur deposition values.

5.2. The spatial distribution of fly-ash particles in Scottish surface sediments.

5.2.1. Carbonaceous particles.

Carbonaceous particle analysis was carried out on the 0 - 0.5cm level of the 94 Scottish and north Pennine sediment cores as described in section 2.4. The results are given in Appendix A and the distribution of these values is shown in Figure 5.1. The overall pattern shown by this distribution is for high carbonaceous particle concentrations in the south and south-west of the region around Galloway and Glasgow, decreasing towards the north-west with the lowest values in Sutherland and the Outer Hebrides.

One problem which becomes immediately apparent when studying these data is the considerable variability of particle concentrations between lakes which are relatively close together and which therefore should receive similar deposition. For example, Whitfield Lough (site 82) and Tindale Tarn (83) in the north Pennines are only 12km apart, but the carbonaceous particle concentration in the surface sediment differs by a factor of 7. The lochs in the Galloway region show similar variability with a range of 6,800 - 51,000 gDM^{-1} within a fairly small area. Lakes in close proximity to each other do not receive deposition at these different rates and the variability in concentration is due to 'within-lake' processes such as sediment accumulation rates and water residence times. A fast sediment accumulation rate will dilute the particle concentration and conversely a very slow rate will concentrate particles from many years in a short depth of sediment.

An example of this is seen in the surface concentrations of the lochs on the east coast of Scotland (Figure 5.1). There were five lochs sampled in this region: Policy

Figure 5.1. Carbonaceous particle concentrations for the surface levels of the 94 Scottish and north Pennine sediment cores. (Values in gDM^{-1})

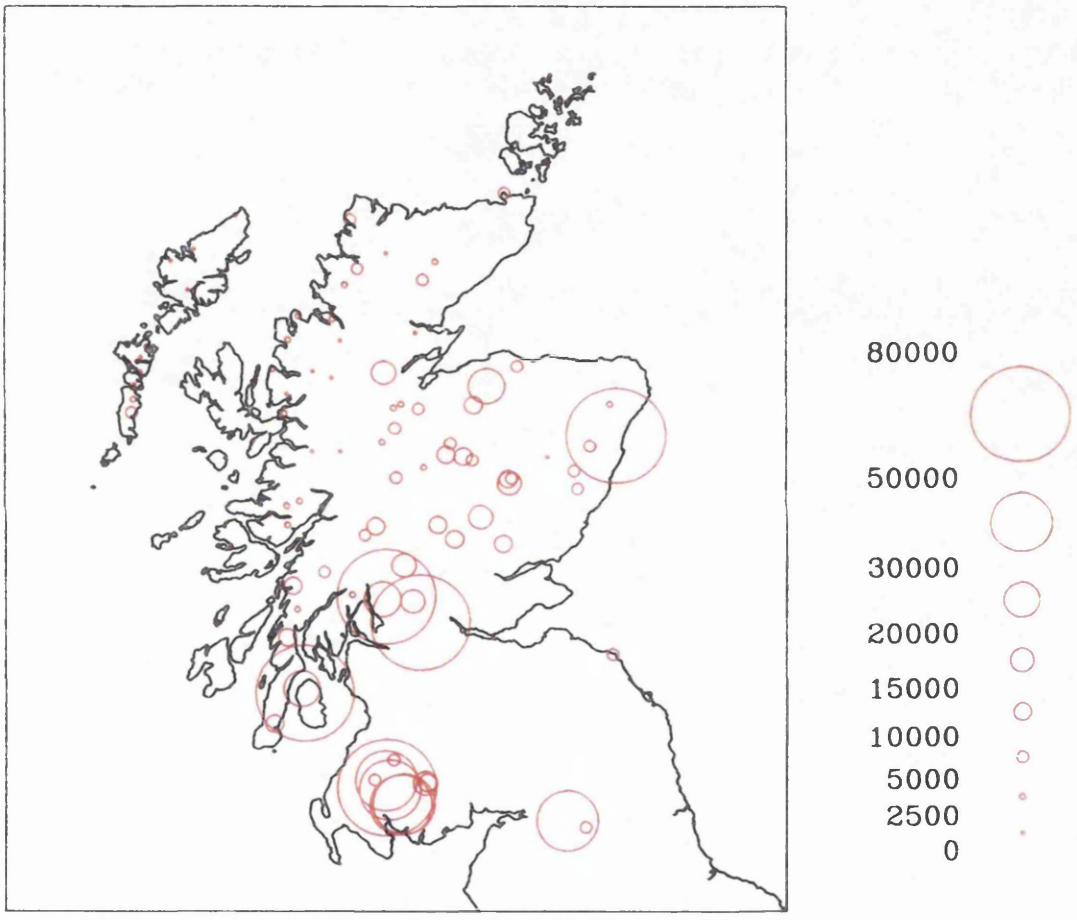

Loch (site 4), Kelly Lake (6), Loch Saugh (1), Unnamed 'H' (2) and Lily Loch (5). The first four sites have similar surface concentrations of carbonaceous particles, 9,722 (± 1,580), 3,203 (± 1,305), 5,771 (± 1,204) and 7,281 (± 1,051) gDM^{-1} respectively, and so other lochs in the area might also be expected to have values in this range. Lily Loch, however, has a surface concentration of 54,225 gDM^{-1} (± 6043) and this is probably due to an unusually slow sediment accumulation rate resulting in a high particle concentration in the surface levels (see section 4.2.1 and Figure 4.11). One way to overcome the accumulation problem is to date the cores and use particle flux rates instead of concentrations. Unfortunately this was not possible; radio-isotope dating is both expensive and time consuming and to date all the cores in this way was outside the scope of this study. The cores were not varved, and indirect dating using carbonaceous particles to determine the fluxes would lead to a circular argument.

Lake water residence times will also affect particle concentrations, a short residence time reducing the number of particles reaching the sediment, and a long residence time allowing the majority of the particles to accumulate. It was not possible to calculate water residence times at all the sites, because this requires bathymetric, water volume and lake discharge data which were not available. In the absence of dating and particle flux rates, concentrations must be used in such a way that the effect of between-lake differences in accumulation rate and water residence times on particle concentrations are reduced as much as possible.

There are several ways to approach this. The MAPICS computer graphics package can fit a surface to a height-gradient grid file (in this case where 'height' is carbonaceous particle concentration), and this will interpolate values between grid points, 'filling in' areas with no data and smoothing out some of the variability within a region. This produces a contoured diagram of carbonaceous particle concentration from the original data (Figure 5.2). The diagram shows high values in the south and south-west decreasing sharply away from this area but isolated high values still obscure regional trends. The high value for Lily Loch still shows up and in the absence of any more data, the computer package indicates a high region to the east of Aberdeen, in the North Sea.

Figure 5.2. Contour map of carbonaceous particle concentration in Scotland using individual site data. (All values x 10^{-3} gDM^{-1})

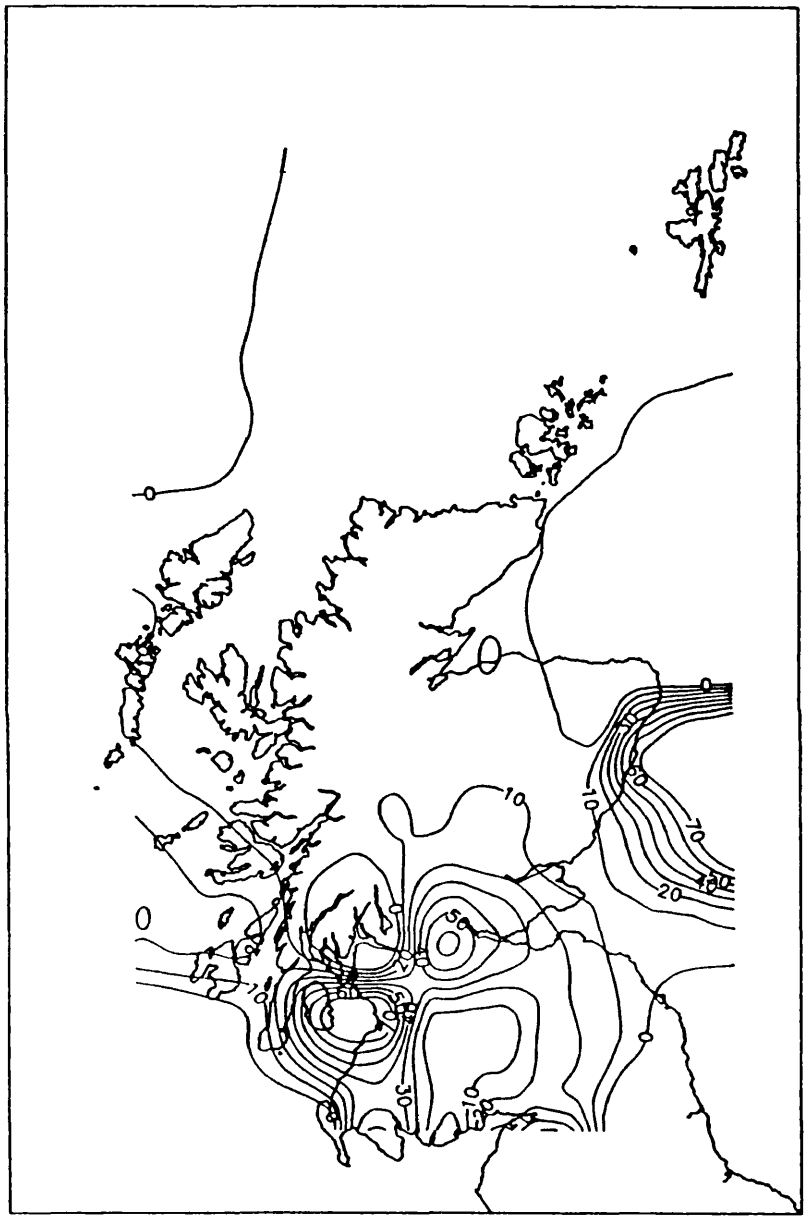

An alternative approach is to take the mean of the concentration values within a given area. This should reduce the effects of natural variation (or 'noise') within a region and the effects of exceptionally high or low values, enabling regional trends to be seen more clearly. For this exercise, a 50km x 50km grid was used based on the National Grid Reference System and the mean taken of the surface concentrations of the lakes falling into each square. Between 0 and 6 lakes were present in each grid square and the results are shown in Figure 5.3. Once again the general trend of high values in the south and south-west declining northwards is observed, the lowest values appearing in the Outer Hebrides and in the Shetland Isles. However, there are some problems with this method, as some of the squares only contain one value and where this is a high one, such as Loch Walton (square 25 65) this averaging approach is unsatisfactory. This can be seen more clearly if the data generated for the 50km x 50km squares are now contoured (Figure 5.4). Here, the effect of the high Lily Loch value is much reduced from Figure 5.2, but most of the contouring is now centred on the single high value for Loch Walton. Since the accumulation rate of this loch does not appear to be exceptionally slow (Figure 4.15) the concentration may be naturally high due to the loch's proximity to the power generating stations on the Clyde, and in Glasgow.

Both the above approaches partially solve the problem of local variability, reducing the effect of outlying high or low values to reveal regional trends. However, these extreme values still have a significant impact on the distribution diagrams. Either these values must be eliminated in some way, or the averaging can be done on a broader scale.

i) Removal processes

Not all the sediment cores whose surface layers have been used here, have been fully analysed for carbonaceous particles and it is therefore difficult to ascertain which have atypical sediment accumulation rates. Even if a full analysis had been carried out on every core, it would be a very subjective way to reject lakes. A more statistical approach is called for which can be applied to all values, so that the 'outliers' are selected on a more objective basis.

Figure 5.3. Carbonaceous particle concentration map for Scotland using the mean values for 50km x 50km grid squares. (Values in gDM $^{-1}$)

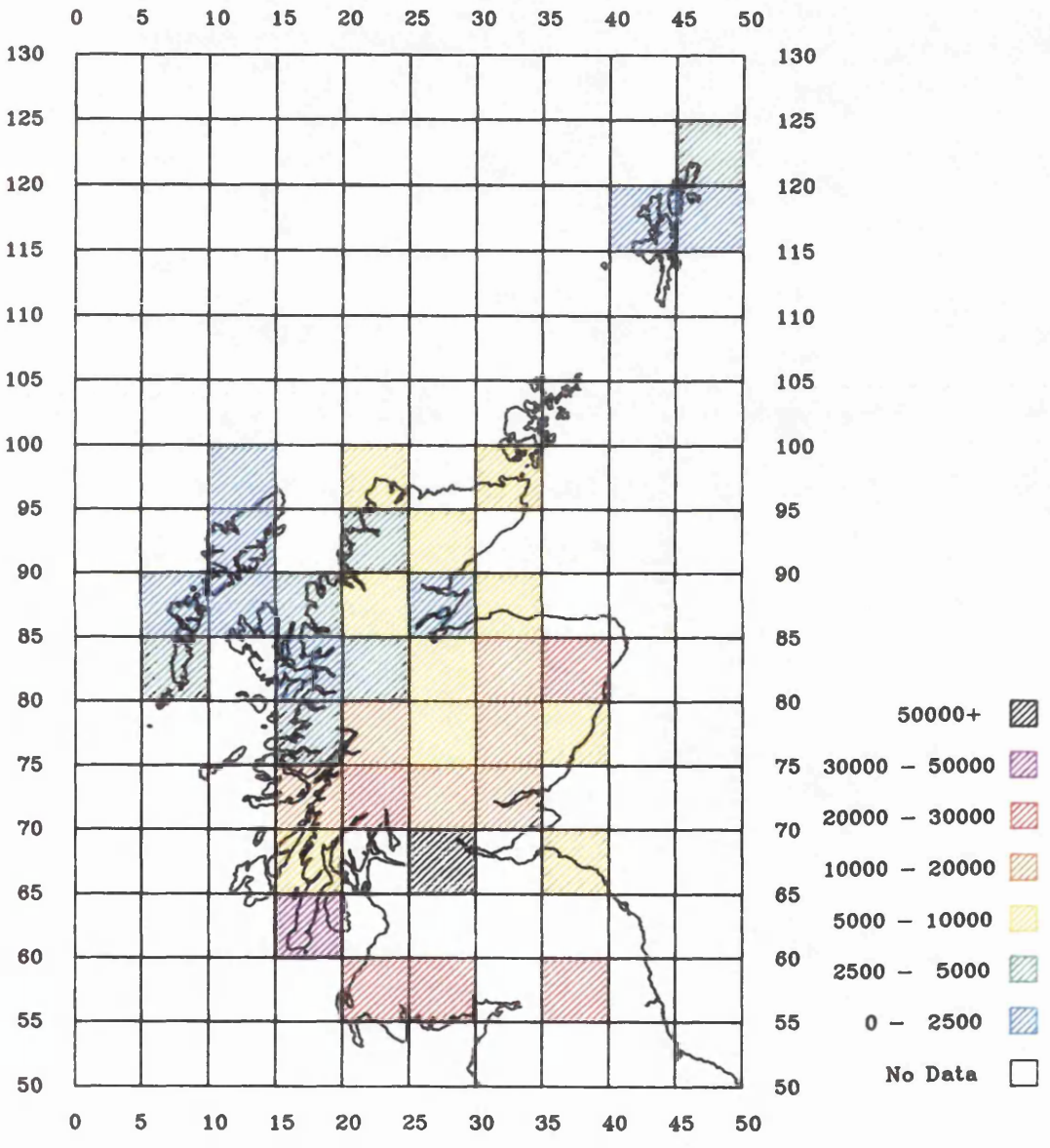

Figure 5.4. Contour map of carbonaceous particle concentration in Scotland using the mean values for the 50km x 50km grid squares. (All values x 10^{-3} gDM^{-1})

Ideally, this would involve fitting confidence limits onto the surface generated by the MAPICS contouring program, so that outliers which fell outside the 'confidence volume' produced could by identified and removed. This would require changes to be made to the contouring algorithm of the MAPICS program which has not been possible for this study. However, this can be done in a provisional way. Instead of treating the region as one surface, the country can be divided into smaller areas and each one treated as a small surface, from which outliers in that area can be identified.

If the 50km x 50km squares are used as these smaller areas, then the mean of the particle concentrations that fall within that square could be considered to be the fitted surface for that area, and values over two standard deviations from the mean of the remaining values considered outliers. If this is done, 11 sites are removed (Lochs' Tanna, Tinker, Bad an Losguinn, Braeroddach, Dallas, Lily, Camalochan, Unnamed U, Lhighe Bhig, Bealich na h-Uidhe and Unnamed 7), leaving 83 with which to generate a new distribution map shown in Figure 5.5. This solves some of the outstanding problems and the distribution shows a much smoother decrease from south to north-west, as might be expected. However, this solution is only partially successful due to the low number of sites in each square, and in the 16 of the 37 squares which only contain 1 or 2 sites there can be no change at all. Contouring these data (Figure 5.6) gives little extra information and only emphasises the influence that the single point representing Loch Walton has on the map. If this single point is removed, then the diagram is much simplified and shows a single high area in the Galloway region. However, there is no sound reason for removing this point from the analysis.

ii) Regional values.

If the size of the grid squares within which the particle concentrations are averaged is increased to 100km x 100km then in most cases the outlying values are diluted still further to show a regional pattern (Figure 5.7). For looking at broad country-wide trends this is an improvement on Figure 5.3, as there is less influence from squares with only a single value. Unfortunately, the square (20 60) still only contains Loch Walton so there is no improvement on the removal method (Figure

Figure 5.5. Carbonaceous particle concentration map for Scotland using mean values for 50km x 50km grid squares after removal of outlier values. (Values in gDM^{-1}).

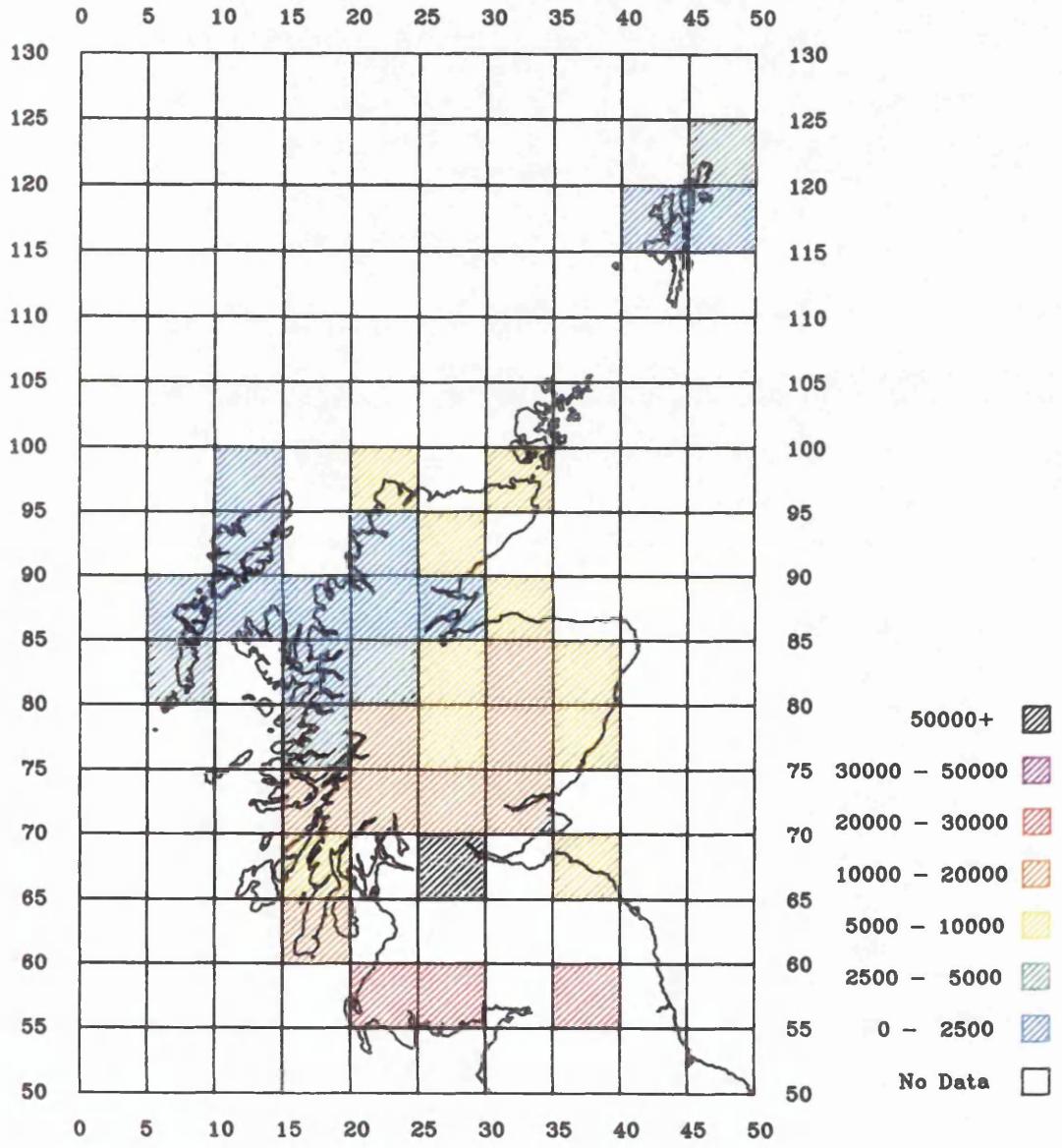

Figure 5.6. Contour map of carbonaceous particle concentration in Scotland using the mean values for the 50km x 50km grid squares after removal of outlier values. (All values x 10 $^{-3}$ gDM $^{-1}$)

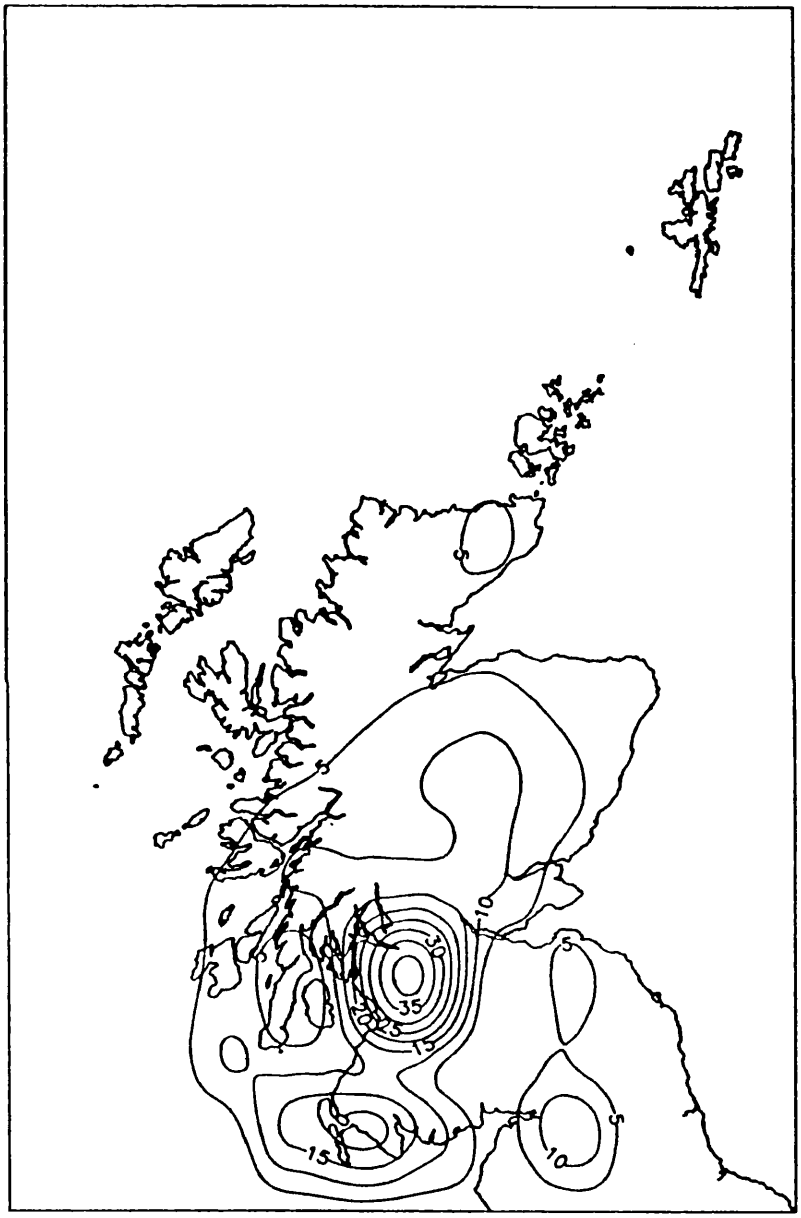

Figure 5.7. Carbonaceous particle concentration map for Scotland using mean values for 100km x 100km grid squares. (Values in gDM^{-1})

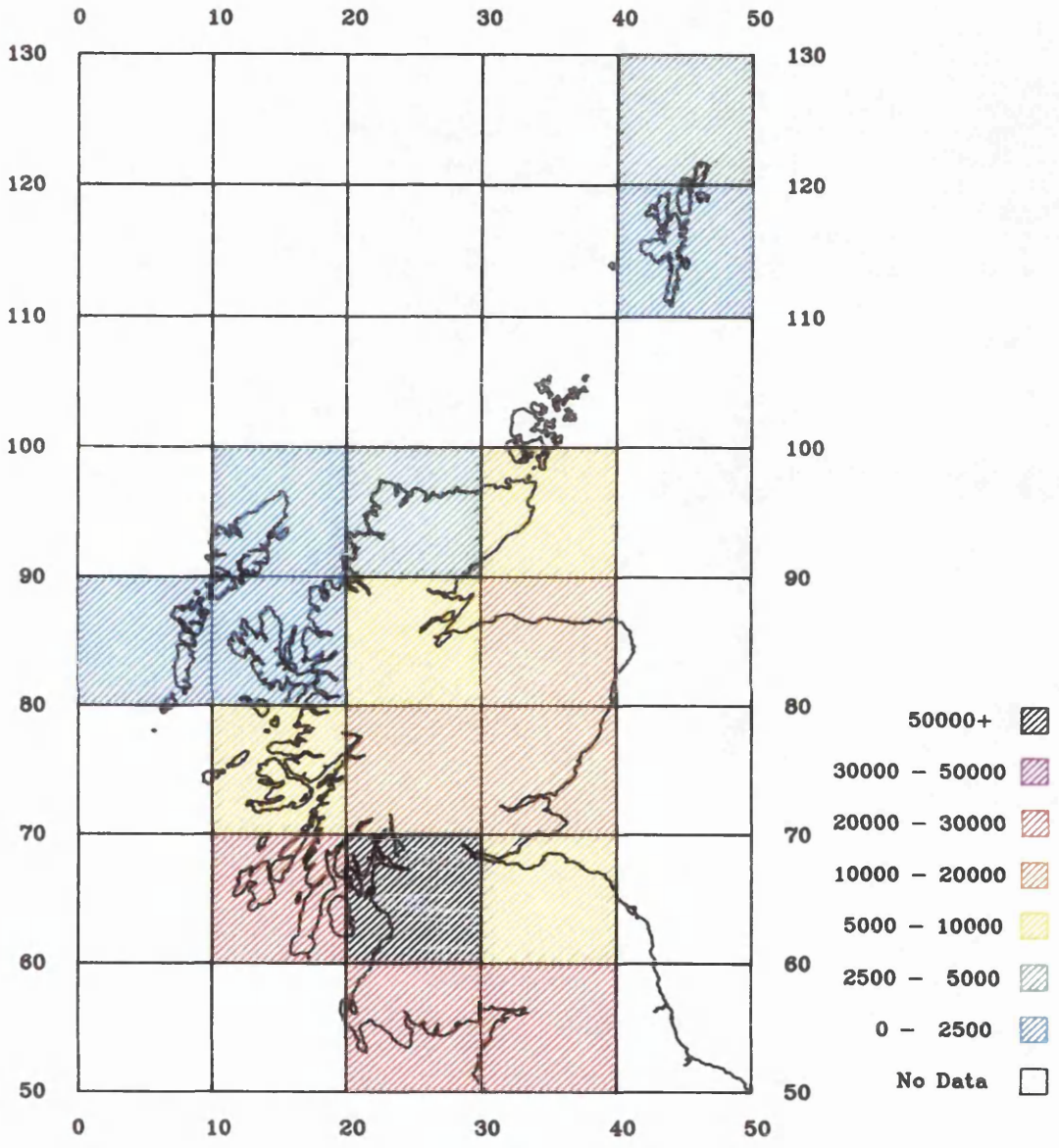

5.5). This could be changed by altering the 100km x 100km boundaries, but this then leaves other squares in the north containing only one site. Contouring these data (Figure 5.8) gives little useful information and only illustrates the need for more data points if a more meaningful diagram is to be produced.

The above methodology shows that the concentrations of carbonaceous particles in the surface sediments of lakes can be used as an indication of the trends in atmospheric deposition on a regional basis. Although particle concentrations at individual sites within a region can show considerable variation due to 'within-lake' processes, smoothing operations on these data such as interpolation and averaging over an area reveal obvious regional patterns. Too much data manipulation, on the other hand (for example, the contouring of the 100km x 100km data), leads to meaningless values, with little or no relevance to any real distribution.

5.2.2. Inorganic ash spheres

The geographical distribution of contemporary carbonaceous particle deposition in Scotland must be mainly due to coal combustion and so the regional patterns shown above should also be present in inorganic ash sphere distributions.

Inorganic ash sphere analysis was carried out on the 0 - 0.5cm level of the 94 sites. The data are shown in Appendix A and in Figure 5.9. As might be expected in a coal-dominated region, the concentrations of these particles are generally higher than the carbonaceous particle concentrations, and again the highest values are around the Glasgow area. These data have been treated in a similar way to the carbonaceous particle data, and the contoured map of these raw values (Figure 5.10) shows one or two differences between the two particle types. Despite the low accumulation rate that singled out Lily Loch in the carbonaceous particle analysis, the inorganic ash sphere concentration is not exceptional and agrees well with the other lochs in the area. The Galloway sites which were also high for carbonaceous particles are also now relatively low. This suggests that these areas may be more influenced by oil combustion (generating carbonaceous particles but not so many ash spheres) than other areas in Scotland, and particle characterisation confirms this (see section 5.3). Apart from the Glasgow region, the only other high concentration is

Figure 5.8. Contour map of carbonaceous particle concentration in Scotland using the mean values for the 100km x 100km grid squares. (All values x 10^{-3} gDM^{-1}).

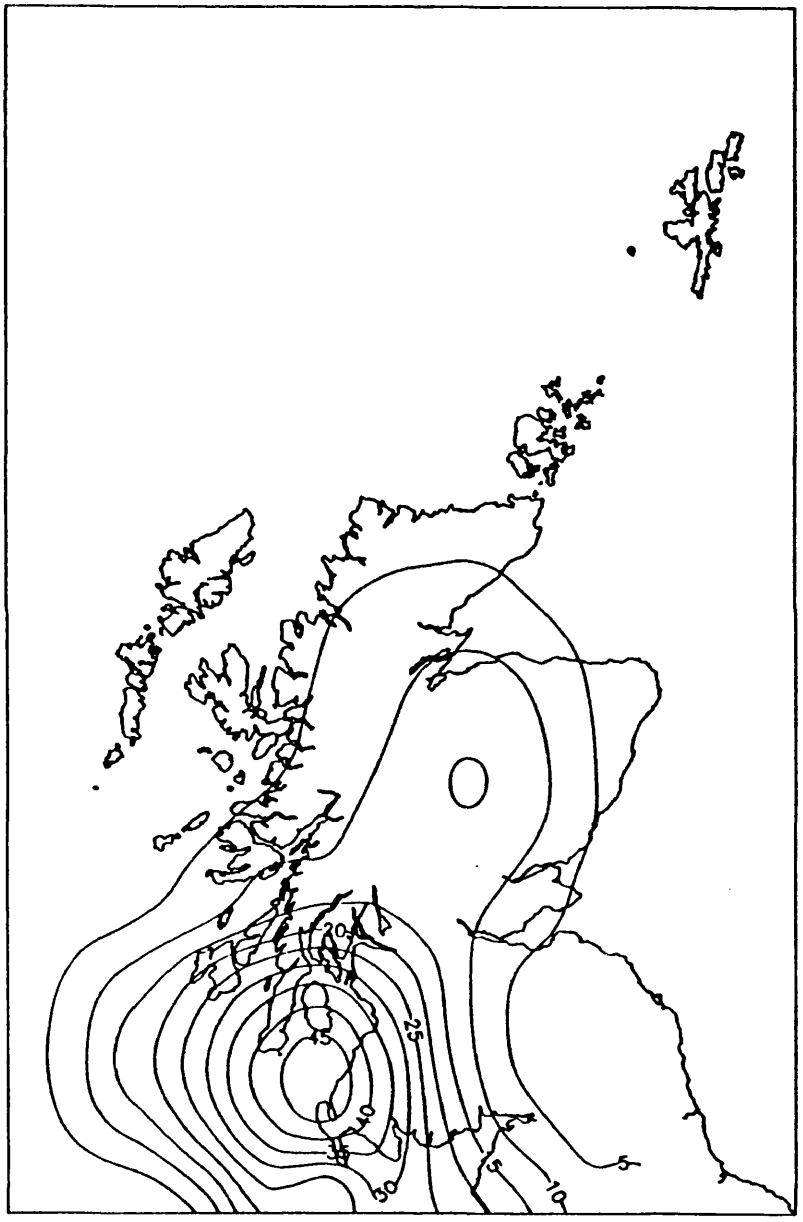

Figure 5.9. Inorganic ash sphere concentrations for the surface levels of the 94 Scottish and north Pennine sediment cores. (Values in gDM $^{-1}$)

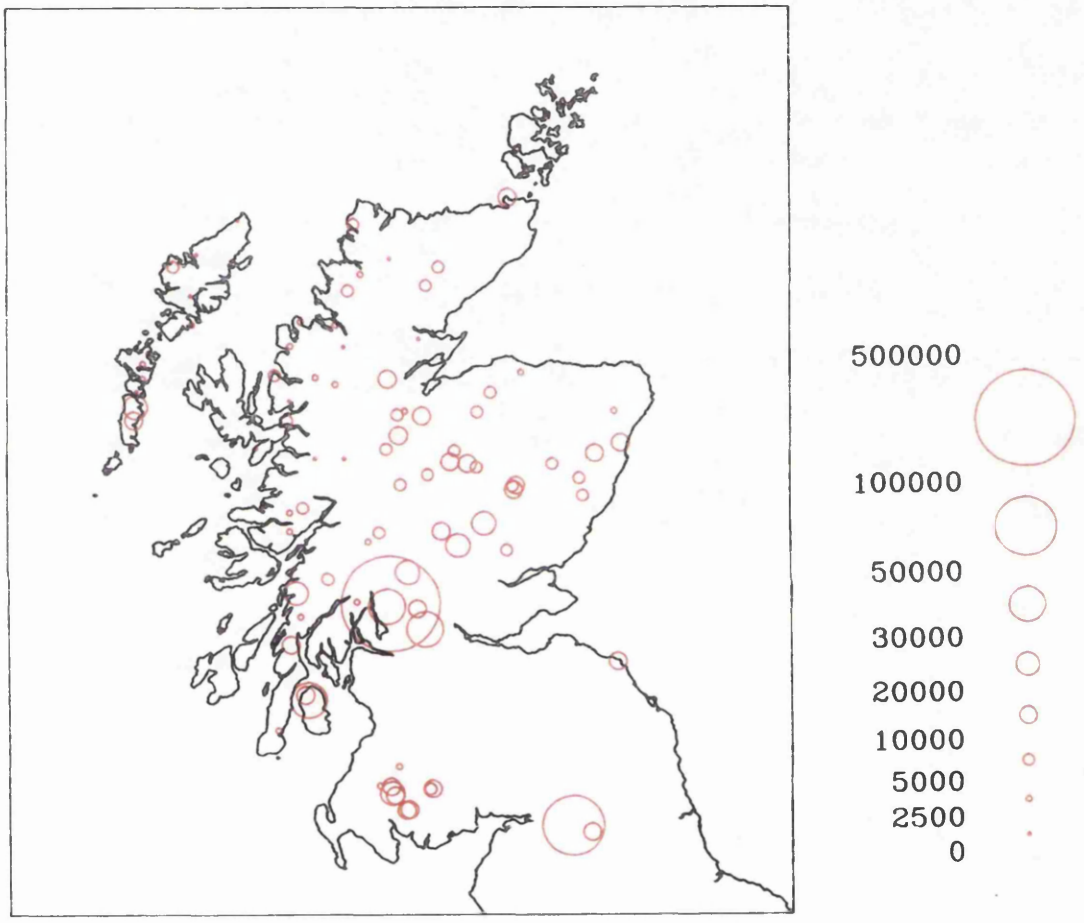

Figure 5.10. Contour map of inorganic ash sphere concentration in Scotland using individual site data. (All values x 10^{-3} gDM^{-1})

at Whitfield Lough (site 82), in the north Pennines, and this may be the influence of emissions from the large power generating stations in Yorkshire (Drax, Ferrybridge, Eggborough etc..), blowing northwards. The diagrams show a decrease again further south than Whitfield Lough, which would not be expected if these particles were travelling from a source in England. However, this is an artefact of the mapping program as no sites were included further to the south.

Further manipulation, such as averaging over 50km x 50km squares (Figure 5.11) and the contouring of these data (Figure 5.12), and averaging over 100km x 100km squares (Figure 5.13), add little further information except to confirm the high points identified above. The removal of outliers (Figure 5.14) also adds little information, except to produce a curious high region over South Uist and Barra, in the Outer Hebrides. A source of particles for this area is hard to explain, especially when surrounding squares are quite low and the coal-fired power stations on the Clyde, and in Belfast are quite remote.

5.3. The spatial distribution of carbonaceous particles in Scottish surface sediments according to fuel-type.

To study the impact of the combustion of different fossil-fuels on Scottish lochs, the carbonaceous particles extracted from the surface levels of 17 of the Scottish sediment cores were characterised using the methods described in Chapter 3 (i.e. the discriminant function contains 6 elements, post-probability = 0.8). The results appear in Table 5.1. This analysis was also done using all 17 elements analysed by the EDS in the discriminant function, and as with the temporal characterisation, the two sets of results were within 1% of each other.

A further six surface samples that were analysed were found to contain too few particles to use the automated EDS and multivariate statistical procedures. These sites were Loch Bharranch (20), Aucha Lochy (32), Lochan Dubh (62), Loch na h'Achlaise (63), Coldingham Loch (80) and Loch na h-Airbhe (91). Of these, only the Aucha Lochy material contained more than 10 carbonaceous particles, and the EDS spectra of these were found to be relatively high in sulphur and vanadium suggesting that they may be derived from oil combustion. Aucha Lochy is situated

Figure 5.11. Inorganic ash sphere map for Scotland using the mean values for 50km x 50km grid squares. (Values in gDM $^{-1}$)

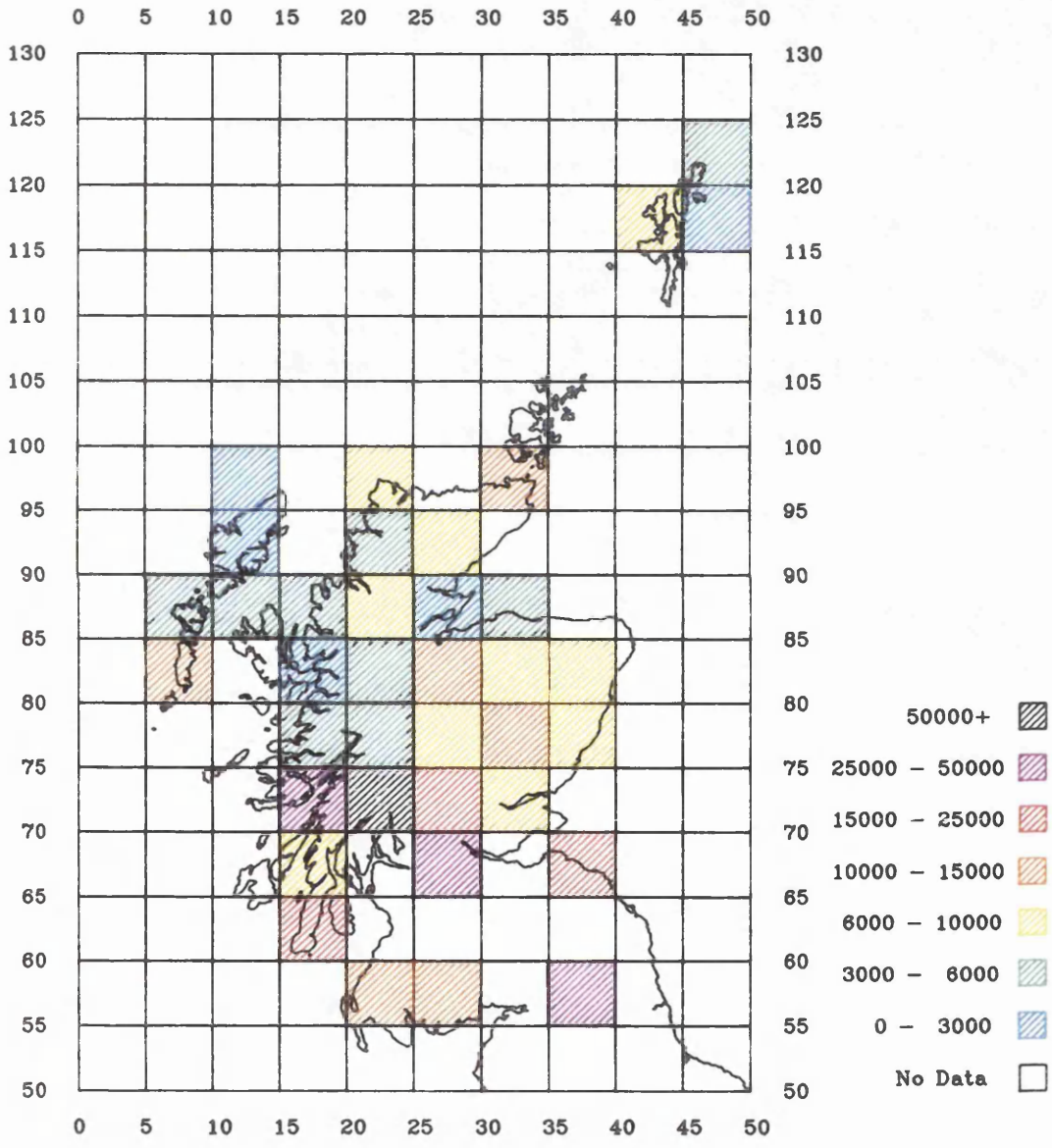

Figure 5.12. Contour map of inorganic ash sphere concentration in Scotland using the mean values for the 50km x 50km grid squares. (All values x 10^{-3} gDM^{-1}).

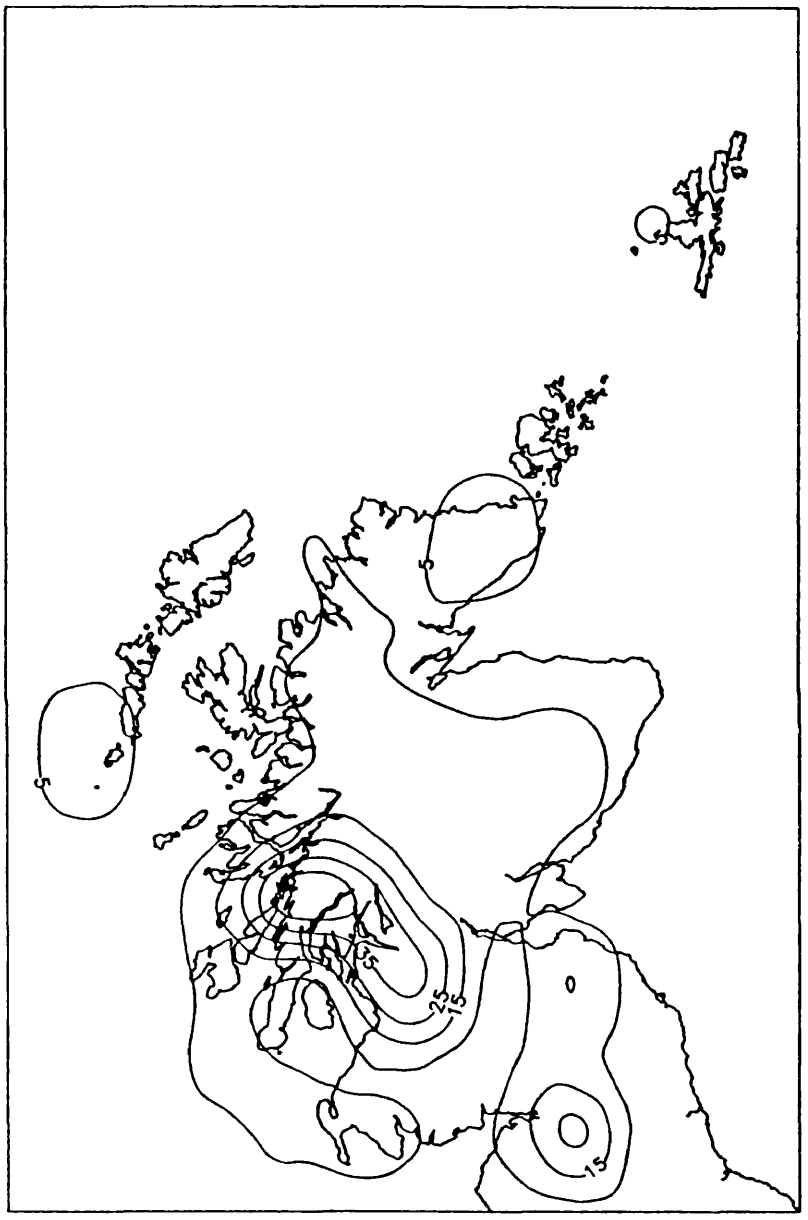

Figure 5.13. Inorganic ash sphere concentration map for Scotland using mean values for 100km x 100km grid squares. (Values in gDM $^{-1}$)

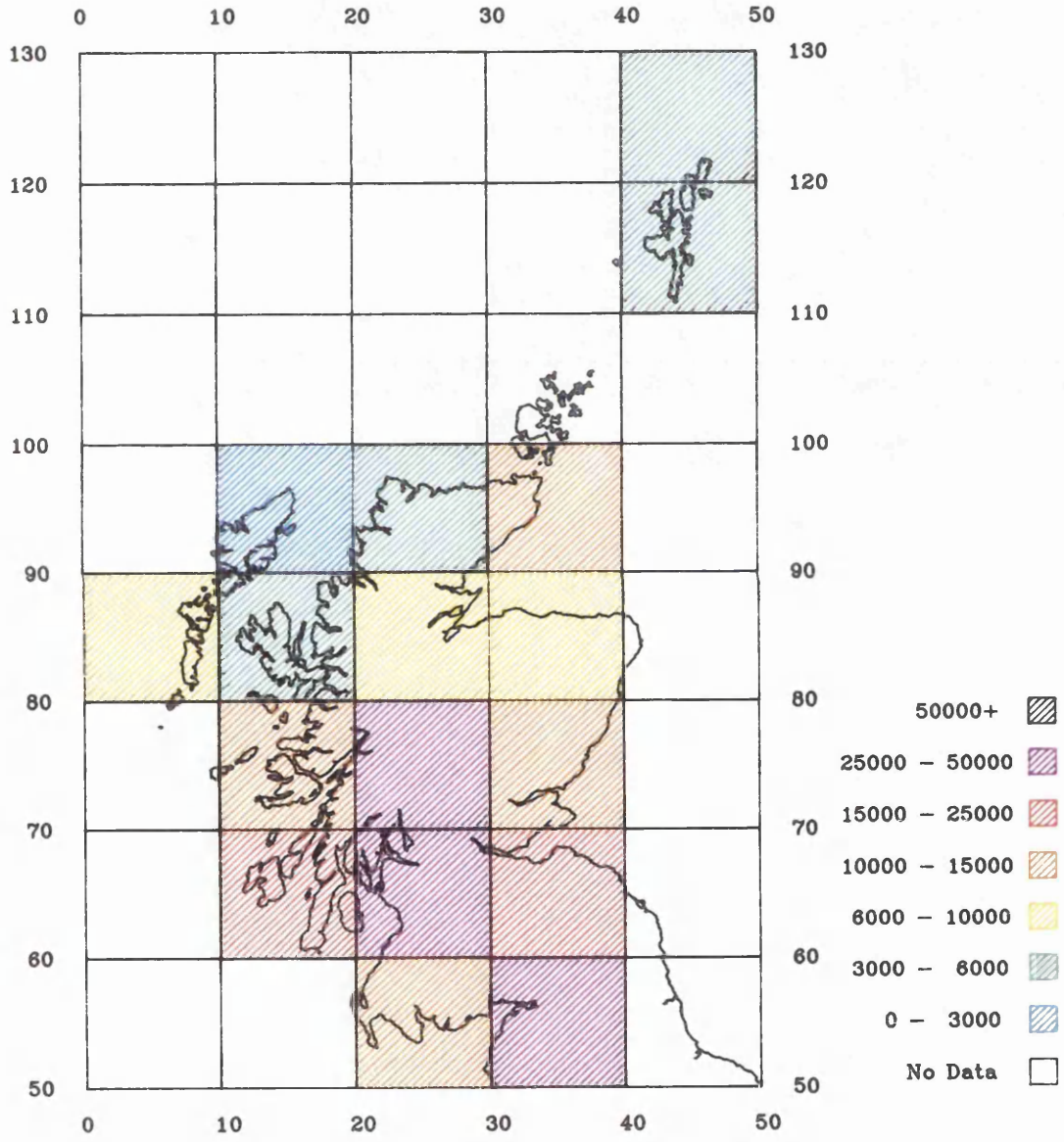

Figure 5.14. Inorganic ash sphere map for Scotland using mean values for 50km x 50km grid squares after the removal of outliers. (Values in gDM $^{-1}$)

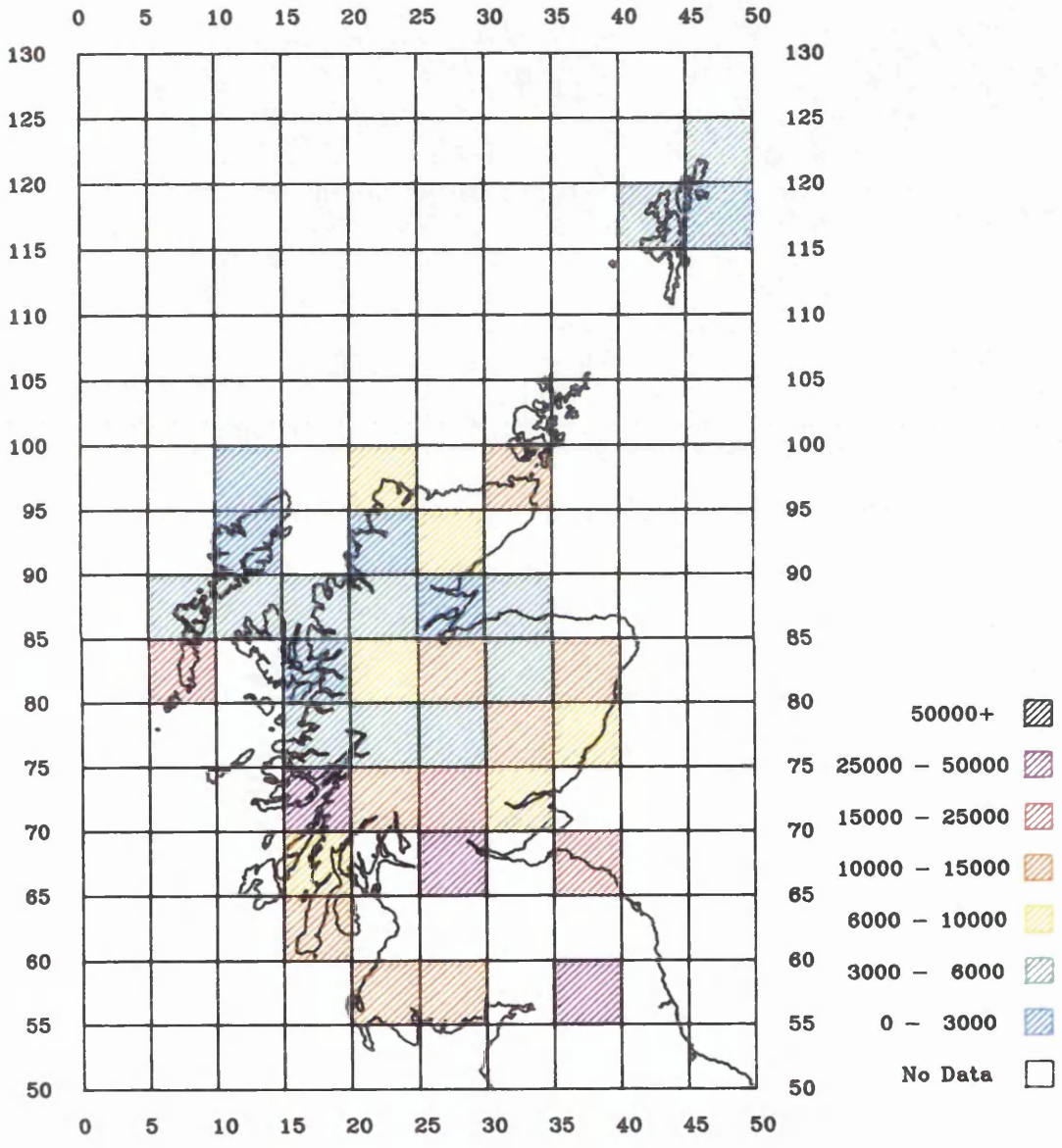

Table 5.1. The results of characterising carbonaceous particles extracted from Scottish surface sediments.

Site	No.	% coal	% oil	% unclassified
Loch Achilty	18	93.30	5.80	0.89
Loch Arial	33	95.45	2.27	2.27
Loch Bealich na h-Uidhe	88	99.36	0.64	0.00
Loch Bran	14	99.13	0.00	0.87
Loch Dubh Cadhafuaraich	85	98.48	1.27	0.25
Loch Curran	26	93.94	6.06	0.00
Loch Dallas	8	92.10	4.81	3.09
Loch Iain Oig	22	99.58	0.10	0.31
Lily Loch	5	87.44	11.79	0.77
Long Loch of Dunnet Head	56	98.30	1.36	0.34
Loch Bad an Losguinn	24	98.80	0.00	1.20
Round Loch of Glenhead	73	91.75	5.54	2.71
Loch Tanna	72	95.28	4.25	0.47
Loch Tinker	66	89.00	9.20	1.80
Uath Lochan	11	99.39	0.12	0.48
Loch Walton	37	92.44	4.56	3.00
Whitfield Lough	82	99.78	0.22	0.00

at the southern tip of Kintyre, just north-west of Galloway, and so would expect to receive deposition from the same sources as other sites in that region.

As expected, the results show that coal is the dominant fossil-fuel, with over 87% of the characterised particles allocated to coal at every site. However, the east coast and south-west of Scotland appear to be areas where there is more oil influence than might be expected in a region in which there are now no oil-fired power stations. Figure 5.15 shows a contour map of percentage oil particles interpolated from the above data.

The high point around Glasgow is due to the value for Loch Tinker. This may be

Figure 5.15. Contour map of percentage oil carbonaceous particles in Scottish surface sediments.

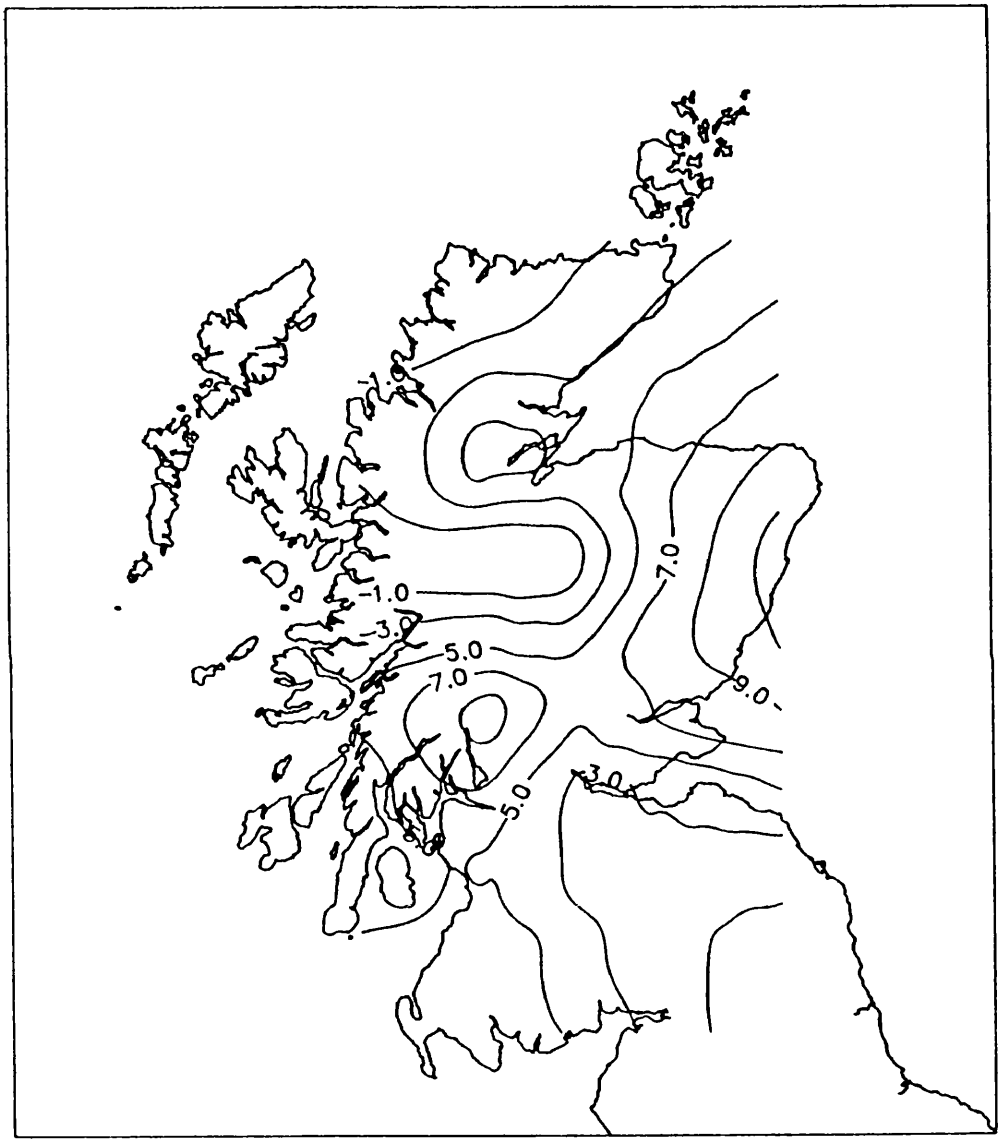

higher than expected, because it is from a core taken in June 1985, at a time when the Inverkip oil-fired power station in Glasgow, only 40km away, was still functional. Inverkip closed down in 1987 and it may be that characterisation of particles extracted from the surface level of a core taken from Loch Tinker now, would show a lower oil value. Apart from these areas there appears to be very little oil influence (less than 3%) over the rest of the country.

The oil particles deposited in these higher (5-12%) oil areas must have their origins outside the country. Oil percentage contours decline to the south of Galloway with the value for Whitfield Lough in the north Pennines being only 0.22% and this suggests that oil-derived particles are not being transported northwards from England. The oil-fired power station furthest north in England is Ince 'B' on Merseyside about 200km away. Since this is not a major plant the alternative sources for the oil particles in the south-west are the oil-fired power stations at Coolkeragh and Ballylumford in Northern Ireland.

Sources for the east coast oil particles are not so clear. Although Scotland contains no oil-fired power stations, this coast is the terminus for many of the pipelines from the North Sea oil-fields. The burning off of wastes may produce some particles, although whether they would be in sufficient quantity to account for these results is doubtful. Other sources for these oil particles could be low-level industrial sources around Aberdeen, and possibly emissions from the power generation and other industries in Scandinavia, where oil is the major fossil-fuel consumed. It should be remembered however, that these results are only generated by 17 points, and although there is more than one site with 'high' oil in each of these regions, the map is far from conclusive. A further 20 sites concentrated around these two areas are in the process of being characterised and it is hoped that these results will help to confirm these findings.

5.3.1. Characterised carbonaceous particles and the IA:CP ratio.

It was suggested in section 4.4 that there may be some relationship between the fuel-type allocations of characterised carbonaceous particles and the ratio between inorganic ash sphere and carbonaceous particles concentrations. Figure 5.16 shows

Figure 5.16. Contour map of inorganic ash sphere to carbonaceous particle ratios for the 94 Scottish and north Pennine sites.

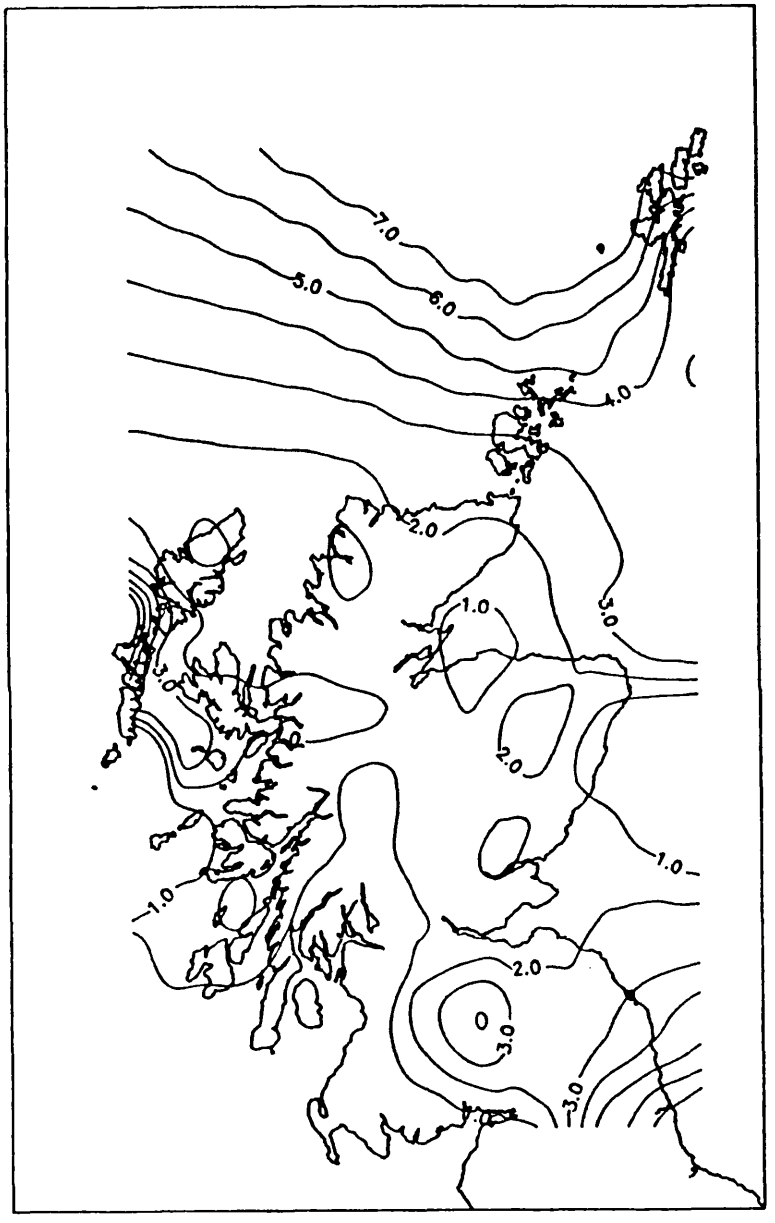

a contour map of inorganic ash sphere to carbonaceous particle (IA:CP) ratios for the surface levels of the 94 Scottish and north Pennine sites. Low ratios (below 1.0) represent areas where inorganic ash concentrations are lower than carbonaceous particle concentrations and it was suggested that these might represent a higher oil influence. It is interesting to note, therefore, that these areas do correspond to the 'high' oil areas identified in Figure 5.15, i.e. the south-west and east coast. High ratios appear to be present in the south Scotland/north England region, probably due to coal emissions blowing north from the major industrial centres in Yorkshire etc.. High ratios are also present in the more remote sites such as the Outer Hebrides and the Shetland Isles. This cannot be due to any industrial centres, and so is likely to be due to the physical differences between the particle types. Inorganic ash spheres are generally smaller than carbonaceous particles and so would be expected to travel further in air streams before being deposited. If this is the case, then the further away from any source a site is, the higher the IA:CP ratio will be.

Regional patterns in both percentage oil particles and IA:CP ratios appear to be similar, but there is no direct numerical relationship and the correlations between % oil, coal:oil ratio and oil concentration (in gDM^{-1}) with the IA:CP ratio are low. (Pearson's correlation coefficient = 0.108, 0.159 and 0.291 respectively; N = 17, p = not significant in each case). It therefore seems that although the IA:CP ratio may give an idea of the relative influences of coal and oil combustion in an area, it is no substitute for carbonaceous particle characterisation.

5.4. The relationship between fly-ash particle concentrations and sulphur deposition.

Sulphur from non-marine sources is a direct indicator of acid deposition on a lake and as such has been measured in some sediment profiles (Nriagu & Coker, 1983; Holdren et al., 1984; Giblin et al., 1990). However, because sulphur sedimentation processes such as sulphate reduction change in efficiency as lake conditions change, polycyclic aromatic hydrocarbons (PAH) have been used as a more reliable record (Rippey, 1990). The main source of PAHs is fossil-fuel combustion and so other products of burning such as fly-ash particles should also give a reliable record. The relationship between PAH and carbonaceous particle deposition has been studied and

significant correlations found (Broman et al., 1990), but the relationship between sulphur and fly-ash particles is uncertain. However, were it determined, then it may be possible to reconstruct sulphur deposition histories with more confidence than by measuring sulphur in sediments directly, as these particles remain unchanged in the sediment. As mentioned previously, the steep sulphur gradient that exists in Scotland makes this an ideal place to study this relationship.

5.4.1. The sulphur deposition data.

Both modelled and measured sulphur deposition data were obtained for the year 1987. The Review Group on Acid Rain report (RGAR, 1990) states that for the period 1978 to 1987 there was no significant change in the deposition of non-marine sulphate over northern Britain. Consequently, values obtained representing deposited sulphur for the year 1987 will be reasonable figures to use in this study despite the slight difference in coring date. Values are obtained on a 'per year' basis and this smooths the 'within-year' variability caused by episodic deposition events.

The modelled data were obtained from Dr R. Derwent, (then of AERE at Harwell). There was not a satisfactory treatment for deposition onto sea surfaces in the model and this resulted in an unknown amount of sulphur being available for deposition on the more remote islands. Consequently, the 5 sites from the Shetlands were not included and the available data consisted of dry, wet and total sulphur deposition values for the remaining 89 surface sites.

The model used was that outlined in the RGAR 1987 report. Dry deposition values were obtained from the product of near-surface SO_2 concentration and a velocity of deposition appropriate to the area. This area is the 20km x 20km grid square in which the site falls, classified into one of five broad land use categories, and this is used to determine the atmospheric transfer of SO_2 to the surface. The wet deposition in a grid square is produced by summing the contribution from sources in each of the other grid squares. The influence of such sources depends on the probability that the wind transports material from the source into the square and the probability that sulphur is not lost by dry or wet deposition on the way. These probabilities depend on the average occurrence of meteorological conditions at a

typical site in Central England (RGAR, 1987).

The measured data were obtained from Dr G. Campbell, at the Warren Spring Laboratory. These measured values also used the RGAR 1987 model but used measured data interpolated to 20km grid squares, rather than the modelled emission and trajectory based values. Data were obtained for the whole country rather than just the lake sites, but again the Shetland Isles were not included.

The modelled data for the 89 sites were treated in the same way as the particle concentration data and averaged on a 50km x 50km grid square basis. These values are not greatly different from the individual site values as the deposition does not vary greatly over a grid square of this size. These modelled total, dry and wet sulphur deposition values are shown in Figures 5.17, 5.18 and 5.19 respectively. The measured values are shown on the 20km x 20km grid for which the data were provided, the total, dry and wet sulphur depositions appear in Figures 5.20, 5.21 and 5.22 respectively. All values are in g S m^{-2} yr^{-1}.

The two sets of data should give the same results for each site, and although there is good general agreement there are some differences. Figure 5.23a shows that the measured and modelled total sulphur deposition values for the 89 sites give similar results. These values are derived from the addition of dry and wet sulphur depositions and it is these that differ more significantly. For dry deposition (Figure 5.23b), modelled values are higher than the measured values, and this is reversed for wet deposition (Figure 5.23c). The Pearson's correlation coefficients for the two sets of total, dry and wet deposited sulphur values are 0.655, 0.728 and 0.519 (all $N = 89$, $p \leq 0.001$) respectively.

5.4.2. Particle concentrations and modelled sulphur deposition.

The modelled sulphur deposition data for Scotland shows a steady decrease in concentration from the south to the north and, being based on a 20km x 20km, grid, is fairly uniform over a 50km x 50km area. It has been shown that over a similar area both carbonaceous particle and inorganic ash sphere concentrations can vary greatly (see section 5.2), and so a good correlation between sulphur deposition and

Figure 5.17. *Modelled total sulphur deposition for 89 Scottish and north Pennine sites. (Harwell data) (Values in g S m $^{-2}$ yr $^{-1}$)*

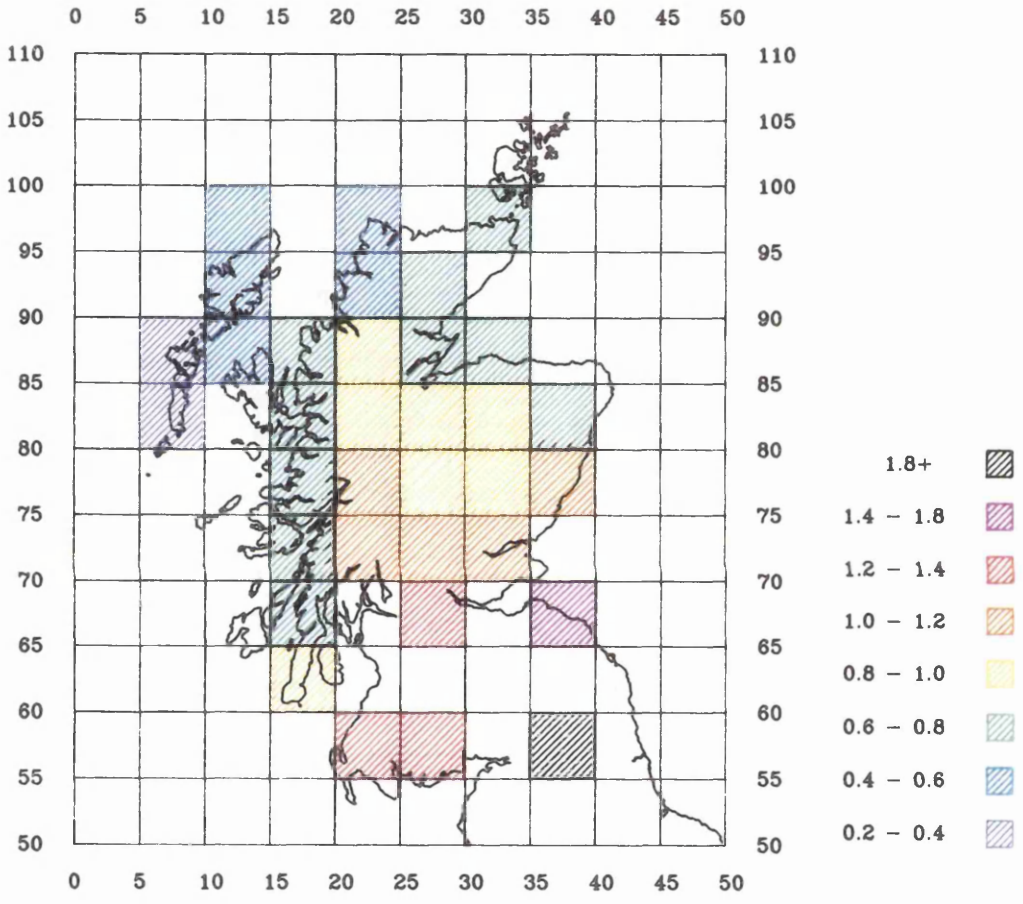

Figure 5.18. Modelled dry sulphur deposition for 89 Scottish and north Pennine sites. (Harwell data). (Values in g S m $^{-2}$ yr $^{-1}$)

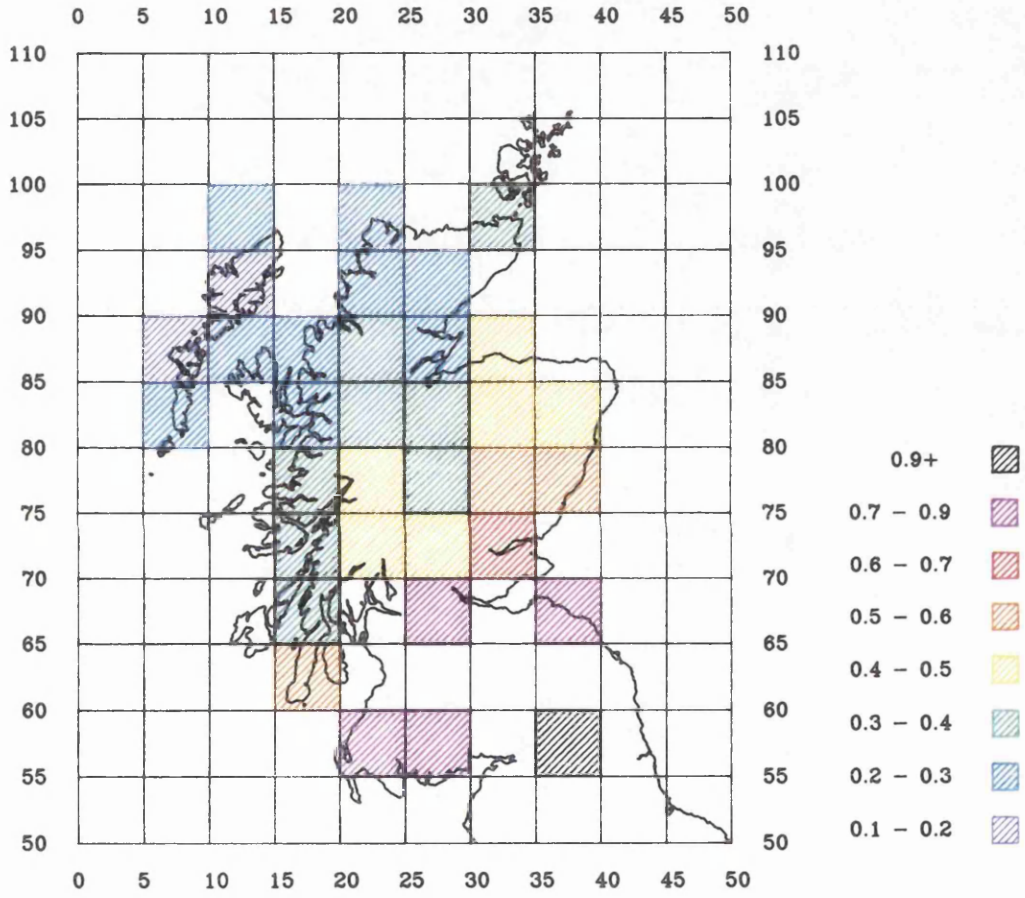

Figure 5.19. Modelled wet sulphur deposition for 89 Scottish and north Pennine sites. (Harwell data). (Values in g S m $^{-2}$ yr $^{-1}$)

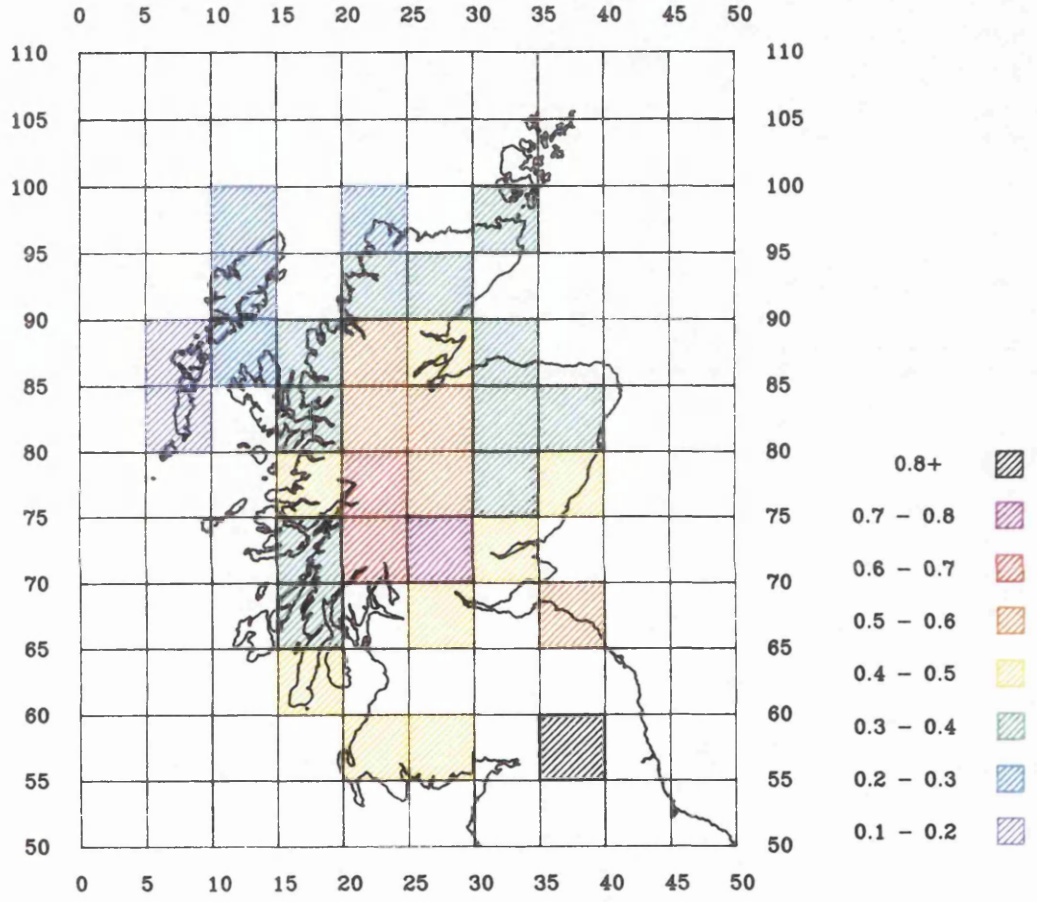

Figure 5.20. Measured total sulphur deposition for Scotland and the north of England. (WSL data). (Values in g S m $^{-2}$ yr $^{-1}$)

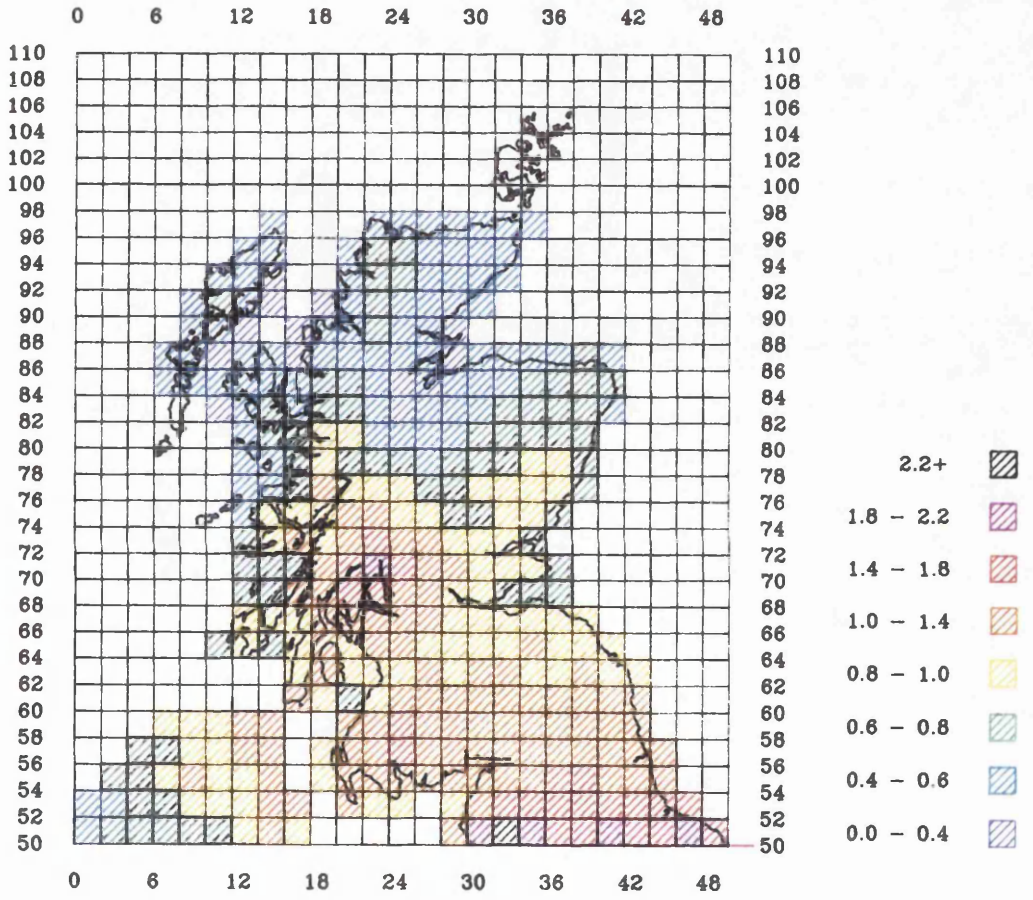

Figure 5.21. Measured dry sulphur deposition for Scotland and the north of England. (WSL data). (Values in g S m^{-2} yr^{-1})

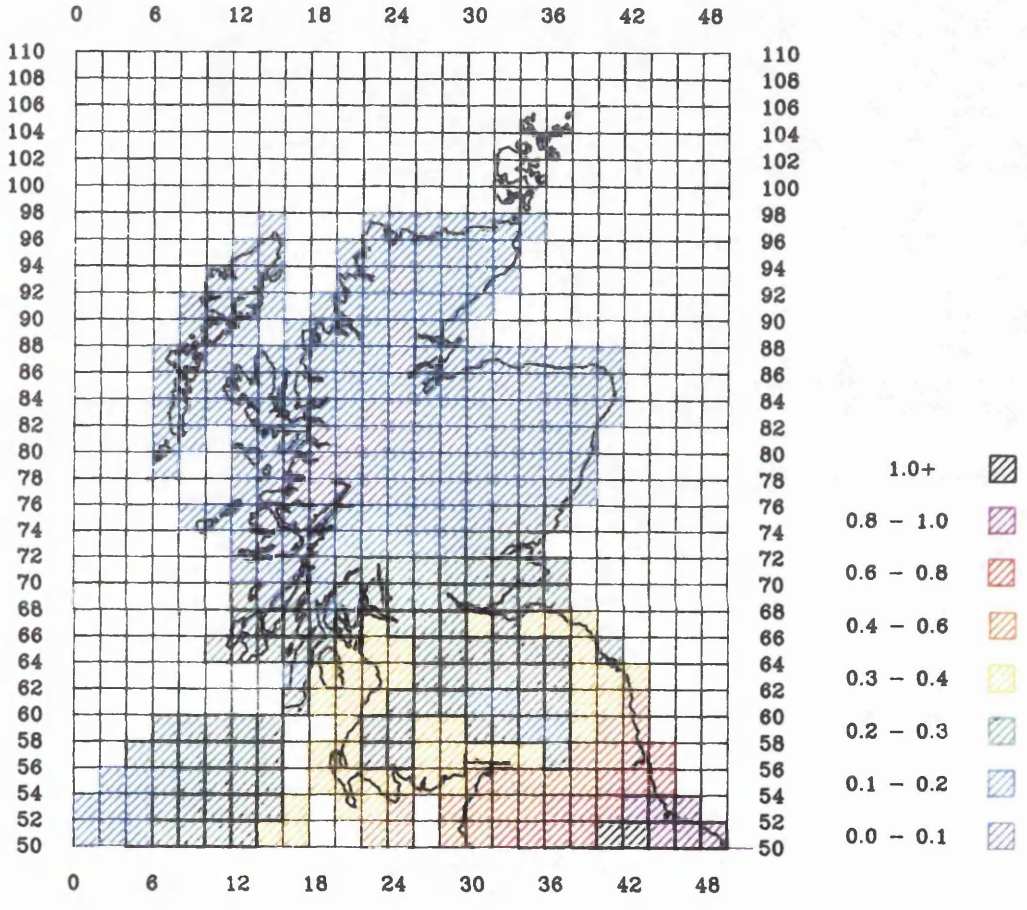

Figure 5.22. Measured wet sulphur deposition for Scotland and the north of England. (WSL data). (Values in g S m $^{-2}$ yr $^{-1}$)

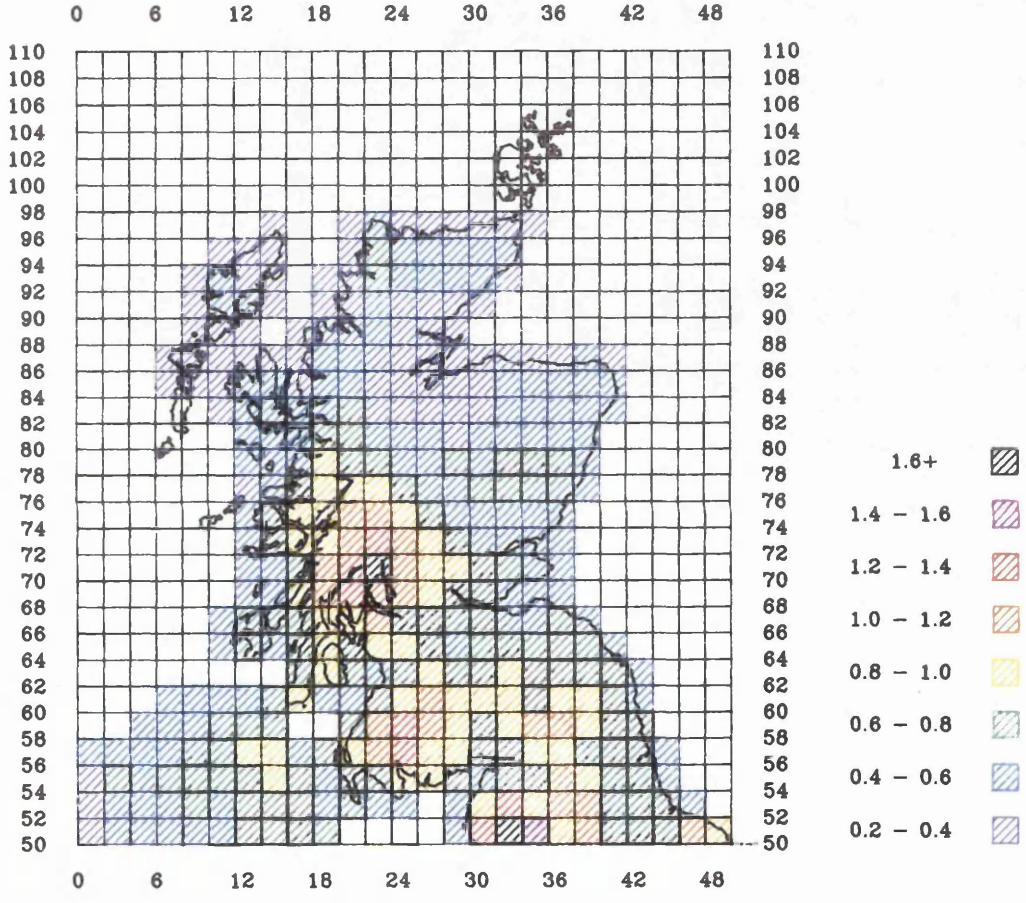

Figure 5.23. Comparison between measured and modelled sulphur deposition data for 89 Scottish and north Pennine sites. (a) total sulphur (r = 0.655, p ≤ 0.001) (b) dry sulphur (r = 0.728, p ≤ 0.001) and (c) wet sulphur (r = 0.519, p ≤ 0.001). (All values in g S m $^{-2}$ yr $^{-1}$)

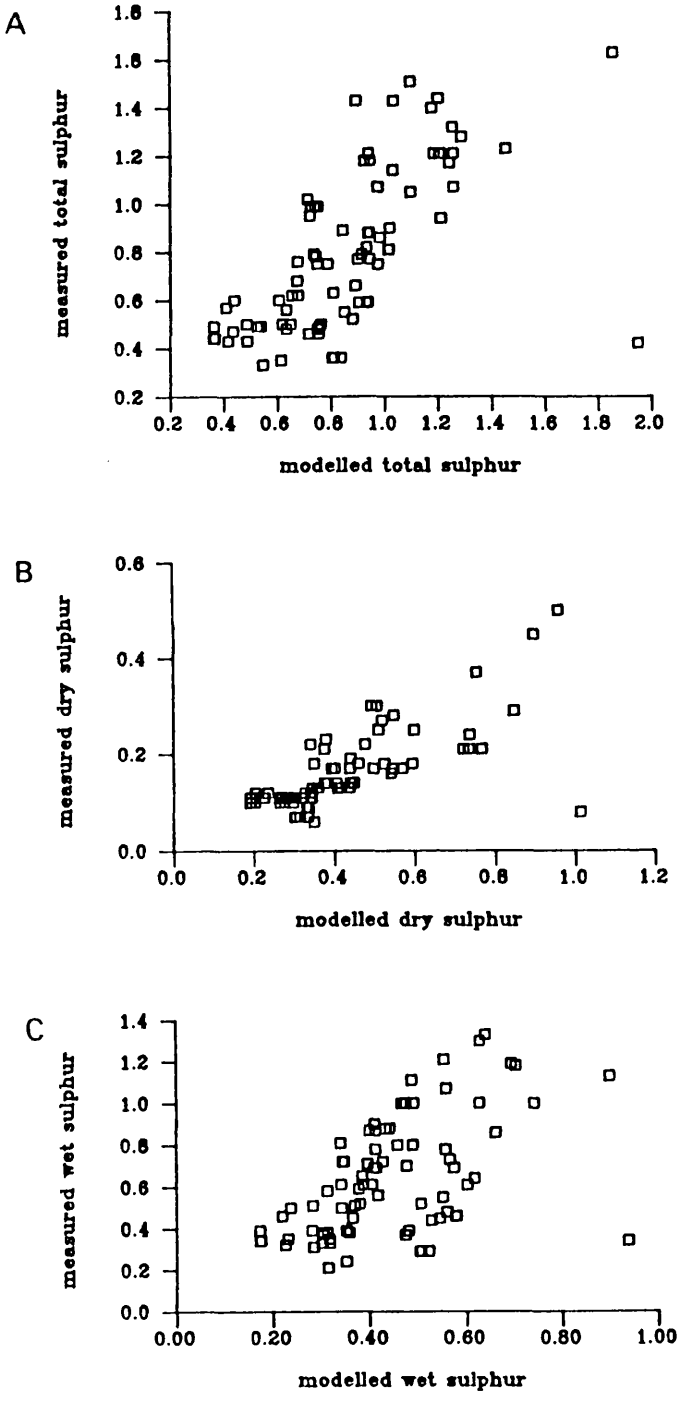

fly-ash concentration on an individual site basis would not be expected. Table 5.2 confirms this by showing the correlations between the particle concentrations and the three sulphur types. In this and subsequent tables, correlations use the standard nomenclature for probability levels.

i.e. ns = p is not significant
* = $0.05 \geq p > 0.01$,
** = $0.01 \geq p > 0.001$
*** = $p \leq 0.001$)

Table 5.2. Correlations between modelled sulphur deposition and fly-ash particle concentrations for individual sites.

	Total S.	Wet S.	Dry S.
C.P.	0.476 (N = 89, ***)	0.224 (N = 89, *)	0.575 (N = 89, ***)
I.A.	0.512 (N = 89, ***)	0.386 (N = 89, ***)	0.504 (N = 89, ***)

Plots of particle concentration against sulphur depositions show that the reason for these low correlations is probably due to the 'within-lake' processes discussed previously. This is shown by the presence of both high sulphur/low particle concentration sites, and low sulphur/high particle concentration sites (Figure 5.24), illustrating that it is the effect on the particle concentration by atypical accumulation rates that moves the points on the plot.

Section 5.2 showed that particle data exhibited better regional trends when averaged on a 50km x 50km and a 100km x 100km grid square basis than when each site was treated individually. As sulphur data also exhibit these regional patterns it might be expected that particle values and sulphur values would show better correlations when treated in the same way. Table 5.3 shows the correlations between the particle concentrations and the modelled sulphur deposition data when averaged on the 50km x 50km grid square basis. As mentioned above, this does not alter the sulphur values a great deal, but does reduce the effect of 'outlier' sites with very high or low accumulation rates on particle concentration values.

Figure 5.24. Scatter plot of carbonaceous particle concentration (gDM $^{-1}$) and modelled total sulphur deposition (g S m $^{-2}$ yr $^{-1}$) for 89 Scottish and north Pennine sites ($r = 0.476$, $p \leq 0.001$).

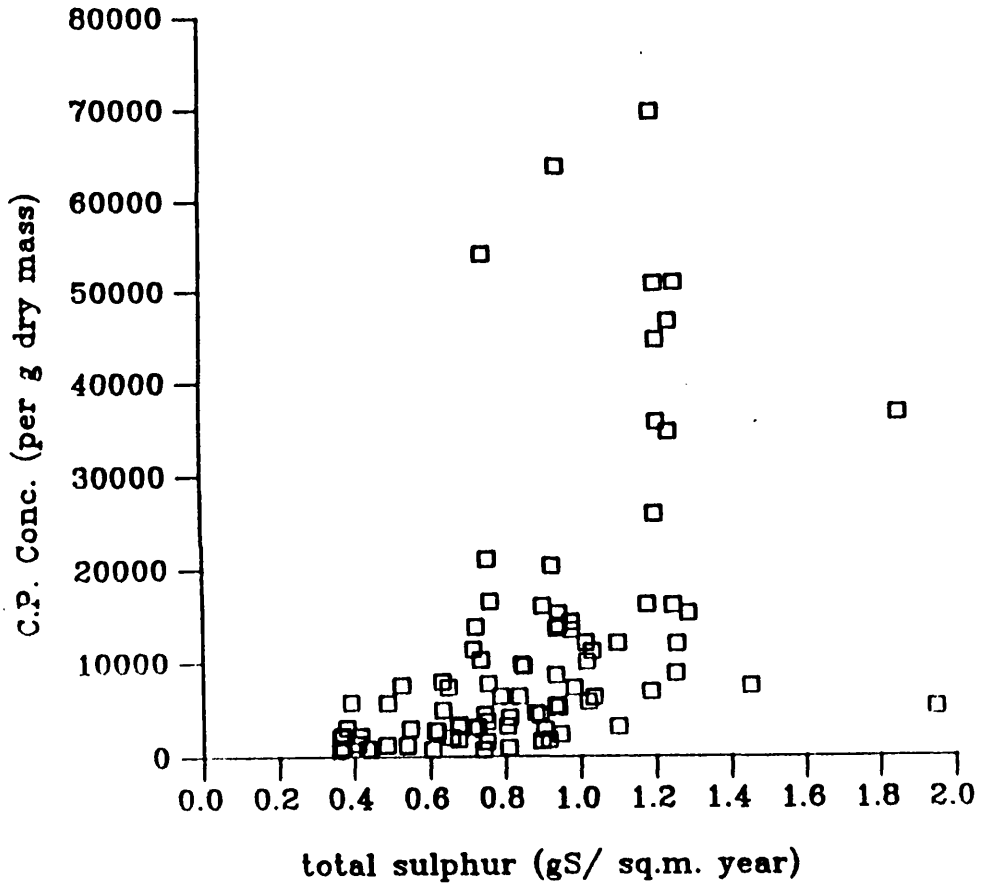

Table 5.3. Correlations between modelled sulphur deposition and fly-ash particle concentrations, averaged on 50km x 50km grid square basis.

	Total S.	Wet S.	Dry S.
C.P.	0.611 (N = 34, ***)	0.332 (N = 34, ns)	0.708 (N = 34, ***)
I.A.	0.496 (N = 34, **)	0.456 (N = 34, **)	0.438 (N = 34, **)

The correlation has improved between carbonaceous particles and each type of sulphur deposition using these averaged data, but the correlation for the inorganic ash spheres only improves for the wet deposited sulphur. These data can then be treated in the two ways described previously, firstly removing the outlier sites and averaging the remainder over the 50km x 50km grid squares, and secondly, averaging all the sites on a 100km x 100km square basis. These results are shown in Tables 5.4 and 5.5 respectively.

Table 5.4. Correlations between modelled sulphur deposition and fly-ash particle concentrations, averaged on a 50km x 50km grid square basis, after 'outlier' removal.

	Total S.	Wet S.	Dry S.
C.P.	0.645 (N = 34, ***)	0.340 (N = 34, *)	0.755 (N = 34, ***)
I.A.	0.605 (N = 34, ***)	0.401 (N = 34, *)	0.648 (N = 34, ***)

Table 5.5. Correlations between modelled sulphur deposition and fly-ash particle concentrations, averaged on a 100km x 100km grid square basis.

	Total S.	Wet S.	Dry S.
C.P.	0.562 (N = 15, *)	0.309 (N = 15, ns)	0.661 (N = 15, **)
I.A.	0.693 (N = 15, **)	0.611 (N = 15, *)	0.657 (N = 15, **)

For the new 50km x 50km values all correlations improve except for that of the

inorganic ash spheres and wet sulphur deposition. For the 100km x 100km values, the carbonaceous particle correlations for all 3 sulphur types are lower than either of the 50km x 50km values, and this is probably due to the few remaining grid squares still containing only one site. If these are removed from the analysis, then the values are mostly improved again (see Table 5.6). The inorganic ash sphere correlations are improved by these manipulations and the larger grid square values give the best results obtained so far, although the significance is reduced due to the low number of values.

Table 5.6. *Correlations between modelled sulphur deposition and fly-ash particle concentrations, averaged on a 100km x 100km grid square basis, after removal of squares containing only 1 site.*

	Total S.	Wet S.	Dry S.
C.P.	0.728 (N = 12, **)	0.580 (N = 12, *)	0.784 (N = 12, **)
I.A.	0.755 (N = 12, **)	0.813 (N = 12, ***)	0.637 (N = 12, *)

5.4.3. Particle concentrations and measured sulphur deposition.

The measured sulphur data can be used in the same way as the modelled data in the previous section and the results are shown in Table 5.7.

These results are very similar to those of the modelled data, and once again show the improvements made to the correlations between particle concentration and the 3 sulphur types, when the data are averaged on a grid square basis. This shows that concentrations for both particle types are quite highly correlated to sulphur deposition on a regional scale, but not on an individual site scale, due to sediment accumulation problems. A scatter plot of total measured sulphur and carbonaceous particle concentration for the 50km x 50km grid squares is shown in Figure 5.25.

There are some differences between the measured and modelled results. The best correlations for the measured data generally come from the total sulphur deposition, and this might be expected as fly-ash particles are deposited by both wet and dry

Figure 5.25. Scatter plot of carbonaceous particle concentration (in gDM^{-1}) and total measured sulphur deposition (in g S m^{-2} yr^{-1}) using mean values for the 50km x 50km grid squares ($r = 0.684$, $p \leq 0.001$).

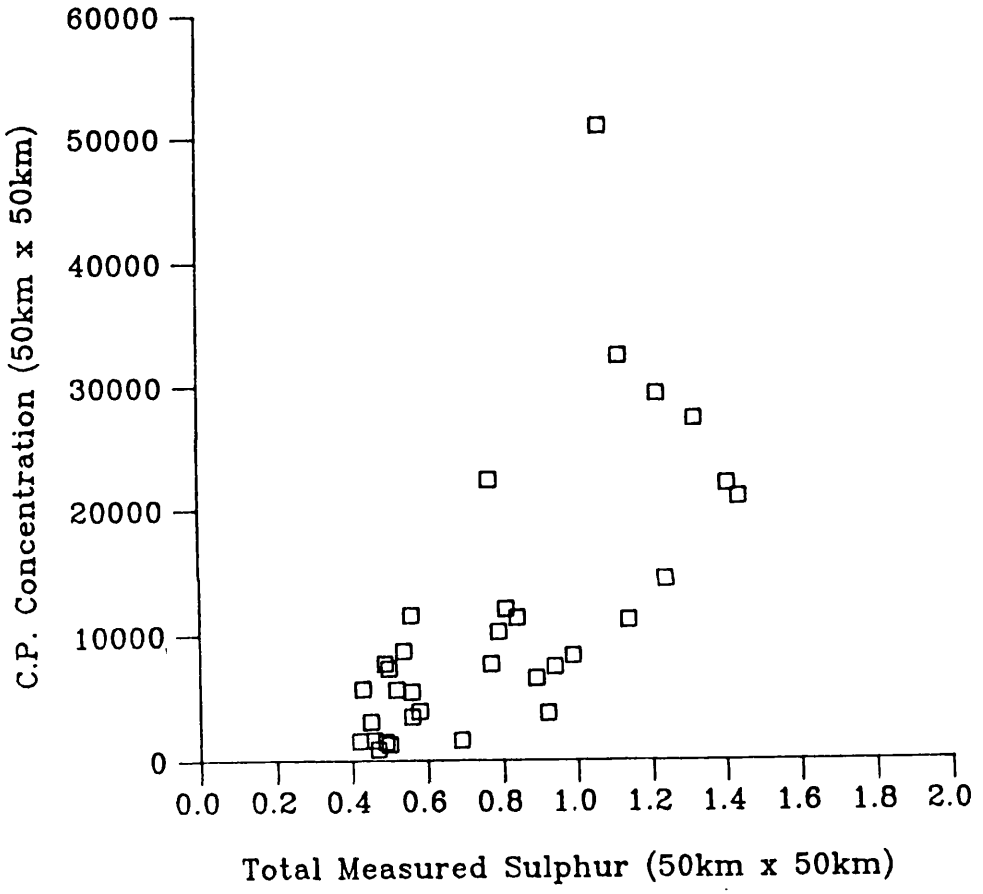

Table 5.7. Correlations between measured sulphur deposition and fly-ash particle concentrations, after the various data manipulations.

	Total S.	Wet S.	Dry S.
Individual Sites			
C.P.	0.440 (N = 89, ***)	0.353 (N = 89, ***)	0.575 (N = 89, ***)
I.A.	0.397 (N = 89, ***)	0.291 (N = 89, **)	0.609 (N = 89, ***)
50km x 50km squares			
C.P.	0.684 (N = 34, ***)	0.618 (N = 34, ***)	0.678 (N = 34, ***)
I.A.	0.625 (N = 34, ***)	0.613 (N = 34, ***)	0.482 (N = 34, **)
50km x 50km squares (outliers removed)			
C.P.	0.636 (N = 34, ***)	0.555 (N = 34, ***)	0.687 (N = 34, ***)
I.A.	0.580 (N = 34, ***)	0.470 (N = 34, **)	0.726 (N = 34, ***)
100km x 100km squares			
C.P.	0.658 (N = 15, **)	0.610 (N = 15, *)	0.642 (N = 15, **)
I.A.	0.721 (N = 15, **)	0.674 (N = 15, **)	0.693 (N = 15, **)
100km x 100km squares (no squares with single sites)			
C.P.	0.840 (N = 12, ***)	0.810 (N = 12, ***)	0.748 (N = 12, **)
I.A.	0.790 (N = 12, **)	0.765 (N = 12, **)	0.694 (N = 12, **)

deposition and are themselves a 'measured' parameter. The modelled data, however, generally give the best correlations with dry sulphur deposition. This may be due to the method of calculation of dry deposition, produced using atmospheric concentrations and deposition velocities of the gas (RGAR, 1987). This is very

similar to the calculations for the determination of particulate fluxes where atmospheric concentration and settling velocities (dependant on particle size) are used (Clark, 1988; Ganor et al., 1988). As both sulphur and particles are assumed to have the same sources and fine aerosols can be treated to a certain extent like gases (Wark & Warner, 1976), then both of these modelled depositions should follow the same trends. The best relationship is however, between measured total sulphur deposition and carbonaceous particle concentrations averaged on a 100km x 100km grid square basis, and this again shows the need for particle flux data if resolution on a finer scale is required.

5.4.4. Logarithmic transformations of the data.

It might be expected that particle deposition decreases exponentially away from the source and if this is the case then a logarithmic transformation of the data may give a better correlation between particle and sulphur deposition. Log transformations and double log transformations (log transformations of both variables) were done for both particle types and both measured and modelled sulphur data for the 89 individual sites (94 Scottish and north Pennine sites without the 5 Shetland Island sites).

For the modelled sulphur data there was little improvement for either type of transformation in cases where wet sulphur deposition or inorganic ash spheres were involved. Improved correlations were seen for both dry and total sulphur depositions with carbonaceous particles upon single log transformation, especially when the particle data was the variable being transformed. However, the best correlations were observed with a double log transformation, where correlations of 0.698 (N = 89, p = ***) and 0.643 (N = 89, p = ***, see Figure 5.26) were obtained for carbonaceous particle data with dry and total sulphur data respectively. This is compared with 0.575 and 0.476 for the non-transformed data (see Table 5.2).

The results for the measured sulphur data were similar to those of the modelled data. There was little improvement for any transformation involving inorganic ash spheres, and for single log transformations the best correlations were achieved when the particles were the transformed variable. These single log transformations gave

Figure 5.26. Scatter plot of log carbonaceous particle concentration and log total modelled sulphur using the individual site data for 89 Scottish and north Pennine sites.

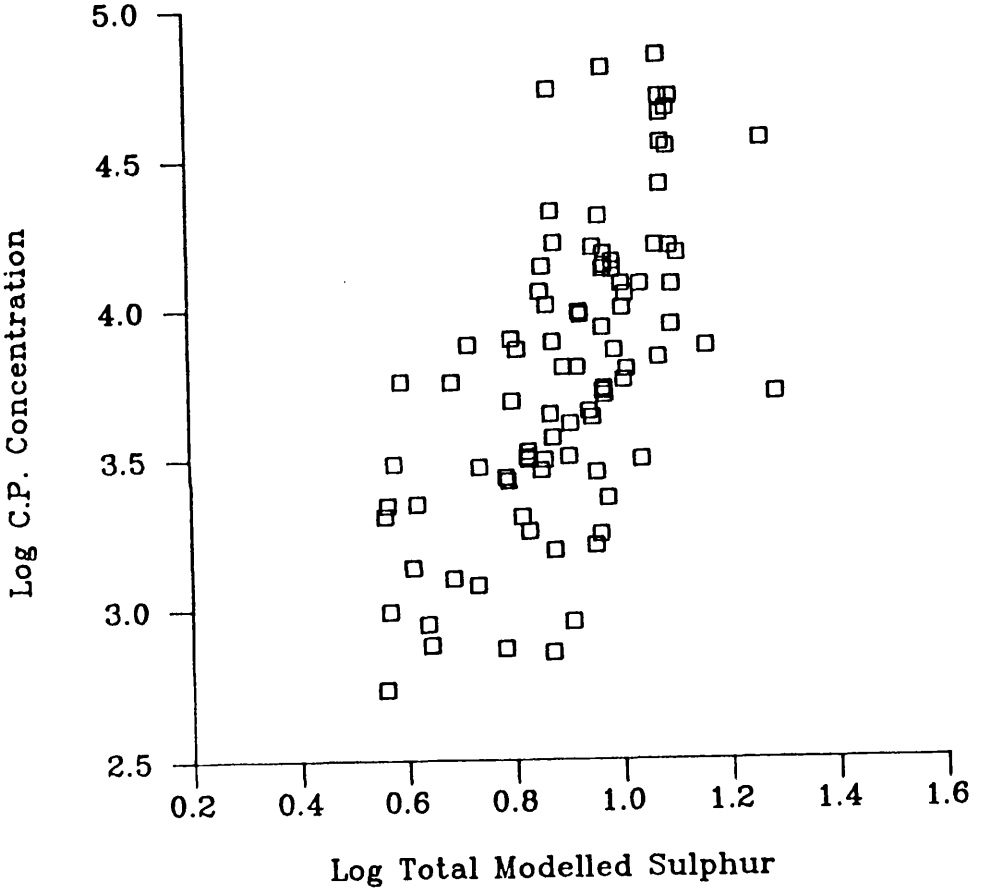

improved correlations over the non-transformed data but again the double log transformations were better still giving correlations of 0.666, 0.418 and 0.494 (all N = 89, p = ***) for carbonaceous particles with dry, wet and total sulphur data respectively. This compares with 0.575, 0.353 and 0.440 for the non-transformed data (see Table 5.7).

Due to the settling velocities of large aerosols like carbonaceous particles, dry particle deposition shows an exponential decrease away from the emission source. However, for wet particle deposition, particles must first become incorporated into the rain-bearing system. When deposition finally occurs, it is likely to decrease in a more linear fashion away from the source. This would explain why dry deposition correlations are improved more than those for wet depositions when the data are log-transformed. The correlation with total sulphur data also improves considerably because of the dry deposition component.

5.4.5. Particle fluxes and sulphur deposition.

Section 4.2. showed some ^{210}Pb-dated sediment cores which were also analysed for carbonaceous particles, and to a lesser extent, inorganic ash spheres. These can be used to study the relationship between surface sediment particle fluxes and sulphur deposition. Six sites in Scotland (Long Loch of Dunnet Head, Loch na Larach, Loch Teanga, Loch Coire nan Arr, Loch Uisge and Loch Doilet) were analysed for both types of particle and had data available for both measured and modelled sulphur. Three sites in Wales (Llyn Glas, Llyn Irddyn and Llyn Conwy) were analysed for carbonaceous particles only and had measured total, wet and dry sulphur data. Four sites in Ireland (Lough Veagh, Lough Muck, Lough Maam and Lough Maumwee), were analysed for carbonaceous particles and had measured total sulphur data only (taken from a Warren Spring Laboratory deposition map). Finally the Men's Bathing Pond on Hampstead Heath was analysed for both types of particle and had measured total, dry and wet sulphur data available. These data are limited in comparison to the concentration data discussed earlier, but give some indication as to the merits of particle fluxes in comparison with sulphur deposition data.

Fluxes for both particle types were calculated and compared with dry, wet and total sulphur deposition values for both measured and modelled data.

The fluxes of the two types of particle show virtually no relationship at all (correlation = 0.029, N = 6, ns) and this appears to be because the inorganic ash fluxes decrease with increasing sulphur. In fact, with the modelled sulphur data, the inorganic ash particles show quite high negative correlations with both dry and total sulphur values (-0.791, N = 6, p = ns; and -0.725, N = 6, p = ns; respectively), but this is most likely due to the very low number of data points present in the analysis.

The carbonaceous particle fluxes show high positive correlation with all three types of sulphur, and again the measured sulphur values correlate better than the modelled. These results and a comparison with the concentration correlations, are shown in Table 5.8.

With the exception of dry sulphur values, particle fluxes show much better correlations with sulphur depositions than particle concentrations on an individual site basis. The correlation between total measured sulphur and carbonaceous particle flux is high and although there are only six points producing this value, it suggests that there may be a direct relationship between the two.

Table 5.8. *Correlations between carbonaceous particle fluxes and measured and modelled sulphur deposition values for individual Scottish sites. (Particle concentration correlations in brackets).*

	Modelled	Measured
Total S.	0.575 (0.476)	0.863, N = 6, * (0.440)
Wet S.	0.558 (0.224)	0.855, N = 6, * (0.353)
Dry S.	0.516 (0.575)	0.442 (0.575)

(For all the above, N = 6 and p = ns, except where shown.)

Scotland with Wales, England and Ireland.

When the Hampstead Heath particle fluxes are included, they produce correlations of 0.999. This is because the particle fluxes from Hampstead Heath are so high that all the other points cluster together and the correlation produced is effectively between two points. Hampstead Heath data have therefore been left out of subsequent considerations. The Welsh sites can be added in with the Scottish ones to extend the comparison of carbonaceous particle fluxes with measured sulphur depositions. With these sites included, the correlations decrease slightly to 0.739 (N = 9, *), 0.568 (N = 9, ns) and 0.780 (N = 9, **) for total, dry and wet sulphur respectively.

When the Irish sites are included, only carbonaceous particle fluxes and measured total sulphur depositions can be compared because of the lack of dry and wet sulphur data. These results continue to show a reasonable correlation (0.715, N = 12, **) and are shown in Figure 5.27. The particle flux for Llyn Glas is very low for the amount of sulphur deposition (this may be due to short water residence times - see section 4.2.2) and this lowers the correlation considerably. Without it, the correlation is 0.894 (N = 11, ***), and supports the idea that there is a direct relationship. If the straight line in Figure 5.27 represents this relationship (and with only 11 points on the diagram, this is quite doubtful) then the following could be said to be true:

$$100 \text{ C.P's cm}^{-2} \text{ yr}^{-1} \approx 0.6\text{g total S m}^{-2} \text{ yr}^{-1}$$

However, it is very difficult estimate errors on this and much more work needs to be done if this relationship is to prove useful. To show the limitations of this relationship, it is interesting to apply the above equation to the Hampstead Heath site. The carbonaceous particle flux at the surface of this core was calculated to be 35,808 cm^{-2} yr^{-1}. Putting this value into the equation shows that this should correspond to a deposition figure of 214g S m^{-2} yr^{-1} approximately 200 times higher than the measured total sulphur value of 1.09g S m^{-2} yr^{-1} (Warren Spring Laboratory data)! The Warren Spring data do not allow for urban areas, however, as the model

Figure 5.27. Scatter plot of carbonaceous particle flux (no. cm $^{-2}$ yr $^{-1}$) and measured total sulphur deposition (g S m $^{-2}$ yr $^{-1}$) for 12 dated sediment cores (r = 0.715, 0.01 ≥ p > 0.001) and best straight line fit for the data excluding the Llyn Glas data-point (see text).

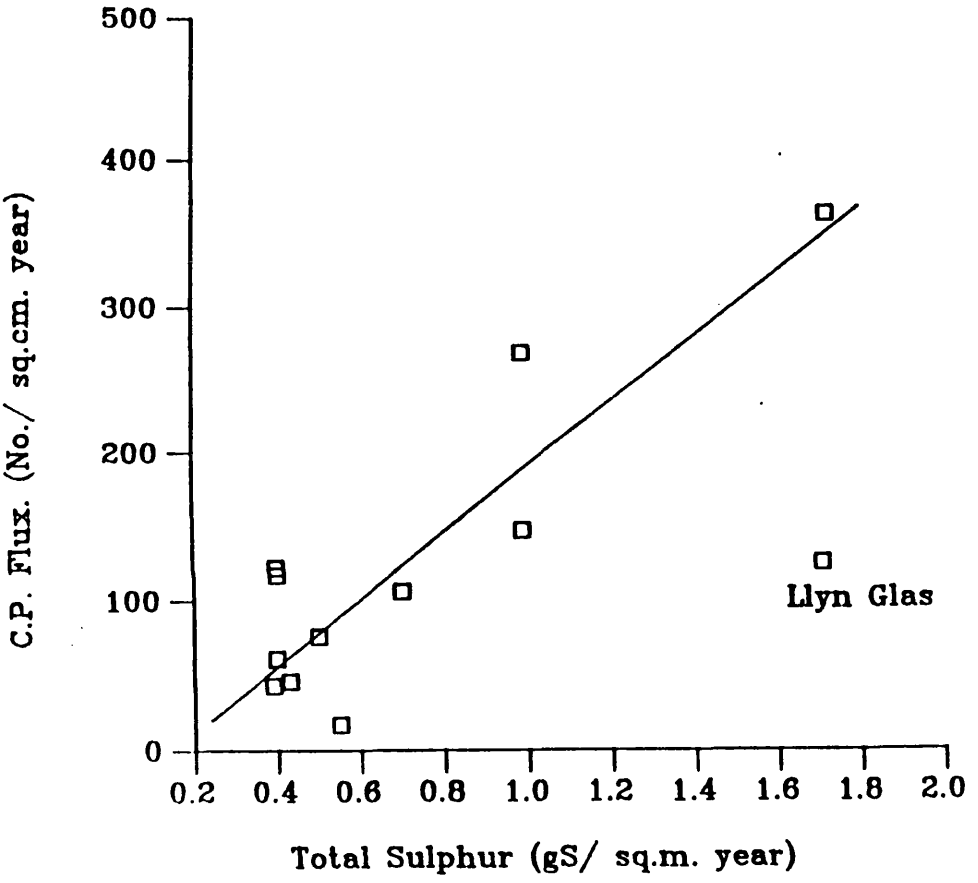

is calculated on a 20km x 20km grid basis and this is not fine enough resolution to reveal such detail (RGAR, 1987). This result may also be due in part to lake residence times. The Men's Bathing Pond on Hampstead Heath is artificial and has no outflow except by seepage, and consequently all the particles falling onto the water surface will be retained in the sediment, unlike the natural lakes used to produce the equation which lose some particles down their outflow streams. This may mean that the particle flux in the Men's Bathing Pond appears artificially high in comparison, resulting in a higher sulphur deposition figure.

5.5. The spatial distribution of carbonaceous particles on a European scale.

It has been shown that on a regional basis, carbonaceous particle concentrations show similar trends to sulphur deposition in Scotland. The RGAR 1987 report shows that concentrations of non-marine sulphate in precipitation are similar in north Scotland, mid - north Norway, western Ireland, and north Spain, i.e. the western 'coast' of Europe. Carbonaceous particle analyses from some of these areas such as the Shetland Isles, the Outer Hebrides, Höylandet in mid-Norway, County Donegal and County Galway in Western Ireland, and the Scilly Isles also show similar levels e.g. 500 - 2,000 gDM^{-1} (see Appendices A & B), showing that these patterns exist on an international scale.

Many of these areas have been used in acid deposition studies as 'clean' areas, and compared to many industrialised parts of Europe, this is indeed the case. However, these sites still contain measurable concentrations of atmospheric pollutants, and even in the far north of Sweden, carbonaceous particles have been found in every contemporary lake sediment sample analysed (Renberg, pers. comm.). It may be that fly-ash particles have now been emitted to the atmosphere for so long that by moving in high altitude air currents they have contaminated all environments in the northern hemisphere including the Arctic, in the same way as other anthropogenic pollutants, such as lead aerosols (Murozumi et al., 1969) and soot (Rosen et al., 1981). Lake sediments from other 'clean' areas (e.g. Greenland, Iceland, Svalbard) need to be studied before it can be ascertained whether there are any 'pristine' sites left in the northern hemisphere, or whether these values observed in northern Norway and Sweden represent a 'hemispherical background' level of

carbonaceous particles, present in all recent lake sediments. It would also be interesting to compare these northern lakes with sites in the southern hemisphere to establish the extent to which there is a global background for these particles.

5.6. Discussion.

5.6.1. Concentrations and fluxes.

The surface levels of lake sediments are subject to many influences. These include 'within-lake' processes such as water currents and 'within sediment' processes such as bioturbation, as well as influences from external sources such as catchment disturbance and atmospheric inputs. Each of these are in turn affected by other factors such as geographical location, altitude, meteorological phenomena, nutrient input and so on, all combining to make each lake system unique. Nevertheless, distribution maps of particle concentration in surface sediments do show a regional pattern even on an individual site basis and this suggests that none of these processes are sufficiently strong to remove the broad spatial patterns of atmospheric deposition.

Both types of fly-ash particle show essentially the same distribution trends, i.e. high areas in the south and south-west of Scotland, decreasing in concentration towards the north-west. This is not unexpected, as the major areas of coal combustion affecting Scotland are in the southern region and still further south in Northern England. However, despite these regional patterns the variability of particle concentrations in the surface sediments of adjacent lakes is such that a single value for a particle concentration is fairly meaningless, unless there are other results (either down the same core as an indication of accumulation rate, or other surface values from the same area), with which to compare it. Consequently, regional trends where particle concentrations are averaged over a large area, produce more interpretable results, but for finer scale studies and comparisons between individual lakes there is no substitute for dating and the use of particle fluxes.

5.6.2. Characterisation

Comparisons between the concentrations of the different particle types (the IA:CP ratio) also give useful information on the influence of different types of fuel combustion on an area. However, this ratio only gives an indication of the relative fuel-type influences and a more quantitative approach such as carbonaceous particle characterisation is needed to confirm the results. The use of the IA:CP ratio is also limited in its usefulness outside Great Britain, as other fossil-fuel types are involved and there will also be variations in the use and efficiency of particle retention techniques (e.g. electrostatic precipitation) between countries. Brown coal and lignite are both members of the coal series and, like peat, produce ash spheres but may not produce spheroidal carbonaceous particles (McCrone & Delly, 1973). Consequently, due to the transboundary nature of fly-ash emissions, the IA:CP ratio in continental Europe will not be merely an indication of the relative use of coal and oil as it is in Britain. Studies on fuel-type influences may then have to rely solely on the chemical characterisation of carbonaceous material. Once other fossil-fuels are included in such a chemical characterisation, all carbonaceous fragments will need to be included in EDS analyses and not just the spheroidal particles indicative of high temperature coal and oil combustion. This will not affect the methods described in Chapters 2 and 3 and, in fact, will make the EDS analysis easier as random fields of view can then be used in the automated data collection procedure, rather than searching the filters for spheroidal particles.

As with the study of the temporal distribution of characterised particles (Chapter 4), the spatial distribution has produced results which are reasonably easy to interpret, and this gives confidence in the characterising technique. Scotland is a country dominated by coal combustion. The results are in agreement with this, and, in addition show two regions of higher oil influence in the south-west and on the east coast. Using this approach as an indication of sources for acid deposition, these results suggest that the acidified Galloway region may be receiving deposition from Northern Ireland as well as from the industrial centres in the north of England. The detection of these low levels from oil-fired sources in Scotland shows that the technique is sensitive, and this is important if the approach is to be used to look at combustion influences on an international scale, where particle sources may be quite

remote from the lake sites studied.

5.6.3. Fly-ash particles and sulphur deposition.

The attempt to ascertain how useful fly-ash particles were at reconstructing sulphur deposition showed again how much better particle fluxes were than concentrations. Particle fluxes showed higher correlation with sulphur deposition at the individual site level than concentrations did when averaged on a 50km x 50km or a 100km x 100km grid square basis, although an improvement in correlation between carbonaceous particle concentration and the sulphur data was observed upon log transformation.

The differences between the measured and the modelled sulphur deposition data were quite significant and both particle concentrations and fluxes showed better correlations with measured sulphur deposition values than modelled ones. Even though the data available were quite limited as far as particle fluxes were concerned, it is interesting to note that the correlation between carbonaceous particle flux and measured total sulphur deposition (0.715, N = 12, p = ** including Llyn Glas, 0.894, N = 11, p = *** without), is higher than the correlation between measured and modelled total sulphur deposition (0.655, N = 89, p = ***). This seems to imply that carbonaceous particle fluxes are better at modelling measured total sulphur deposition than modelled total sulphur data, and it may be that particle flux data can be used to improve sulphur modelling. With such a limited amount of data available, it may seem a little premature to produce an equation directly relating total sulphur and carbonaceous particles. However, the relationship between the two at this early stage does look promising and it is hoped that further work will improve this and, perhaps with the inclusion of 'urban factors' be extended to include sites such as Hampstead Heath where at present the relationship does not hold good.

Excluding the 'urban' sites, the correlation between particle fluxes and sulphur deposition holds despite the drop in particle concentration in surface sediments not necessarily being related to a sulphur decline (i.e. of the two components affecting the drop in particle concentration, the small decrease in fossil-fuel consumption

influences the emission of sulphur but the introduction and development of particle arresting techniques does not). This is because all regions are affected by the particle decline, so preserving the south to north gradient which dominates the relationship. Consequently, a good relationship between sulphur concentration and carbonaceous particle flux exists at any one point in time, but due to changes in fossil-fuel consumption and particle arresting techniques, these relationships may not hold at other times. Further work is needed to ascertain how much this will effect attempts to reconstruct sulphur deposition in sediment cores from the carbonaceous particle record.

CHAPTER 6. CONCLUSIONS.

In this study an attempt has been made to evaluate the use of fly-ash particles for locating potential sources of atmospheric pollutants affecting both individual lakes and geographical regions, indirect dating of lake sediment cores and sulphur modelling using particle concentrations and fluxes. A series of sediment cores from lake sites in the United Kingdom and Ireland were taken and analysed for fly-ash particles to ascertain trends in spatial and temporal distribution. Reference particles were obtained from a range of sources and the surface chemistry measured using EDS techniques. A fuel-type separation was derived using multivariate statistics and this was applied to both surface samples and core samples to show trends in coal and oil use both geographically and historically.

6.1. Particle extraction methods.

The method for the extraction of carbonaceous particles from sediments as developed for this study and described in section 2.4., is an improvement on techniques currently available in the literature. It is more accurate and has a lower detection limit than the Renberg and Wik (1984) method previously used on British lake sediments and is quicker and involves less risk of fragmentation of the particles than the Griffin and Goldberg (1975) method.

The technique described in section 2.5 is the first total extraction method for inorganic ash spheres from lake sediments. Other techniques are either partial (e.g. the magnetic fraction only) or rely on dilute hydrochloric acid to remove $CaCO_3$ in calcareous marine sediments, a technique not generally applicable to lake sediments. As these particles are fused minerals, their chemistry is similar to that of sediment minerals, limiting the range of reagents that can be used. This results in the extraction being less complete than that of the carbonaceous particle method and so the detection limit is higher. However, the extraction is quick and repeatability is high.

6.2. Characterisation of carbonaceous particles.

Using EDS measurements on the surface chemistry of carbonaceous particles it is possible to separate coal and oil fuel-types very effectively. The separation produced in Chapter 3 uses six elements (S, V, Fe, Mg, Ti and Cl) in a linear discriminant function with a post-probability setting of 0.8. This allocates the correct fuel-type to 94% of the reference data-set with over 97% accuracy. The remaining 6% fall into an unclassified group for which the probability of allocation is less than 0.8 and the confidence in correct allocation of the particle is low.

Although not specifically designed to do so, the same linear discriminant function also separates peat particles from coal and especially oil. This demonstrates that a classification involving these three fuel-types could be easily produced.

When principal components analysis is applied to the reference data-set and to particles extracted from lake sediments (or 'fossil' particles) using all 17 EDS measured elements, there appear to be chemical differences between the two particle types (see Figure 4.35). This cannot be due to any chemical treatment, but may be due to adsorption of common mineral elements (e.g. Na, K, Ca and Mg) onto the particle surfaces from the sediment. If the same analysis is done on the same set of particles using only the 6 elements that appear in the final linear discriminant function then the effects of Na, K and Ca are removed and that of Mg becomes low. The chemical differences between the reference data-set and the 'fossil' particles are then not observed (Figure 4.36) and cease to be important. This demonstrates that using only 6 elements in the linear discriminant function instead of all 17 may improve fuel-type allocation of 'fossil' particles.

Although it is possible to allocate particles to the correct fuel-type with a high degree of accuracy, allocation to individual power stations remains impossible to do with any confidence, even using reference data. Oil-fired power stations show good allocation (>70% correct) even with a post-probability set at 0.5 (see Table 3.21b) but at this level, some coal-fired stations have no particles correctly allocated.

However, allocation to fuel-type remains good. Only one ash from each power station was used in this study, and as fuel origin for each station will vary through time, the number of particles correctly allocated here, is likely to be artificially high.

6.3. Temporal distribution of fly-ash particles.

Application of the extraction methods to lake sediment cores reveals characteristic concentration profiles for both types of fly-ash particle.

For carbonaceous particles, post-1985 cores consistently show profiles similar to that shown in Figure 4.41. These can be used for indirect dating of the cores using three features of the profile:

i) the start of the particle record, usually dated in the mid-19th century after the start of the Industrial Revolution in Britain.

ii) the rapid increase in particle concentration which dates from the late-1940's to the 1960's and relates to the post-War boom in the electricity generating industry.

iii) a peak in particle concentration followed by a decline to the sediment surface. This dates from the late-1970's to the early-1980's.

The date for each of these features appears to vary on a regional basis. In general, each feature occurs slightly later in Wales than Scotland, and in Irish sites later still. At present, there are very few data for English sites but those that are available suggest that dates for the features in these cores are the earliest of all the regions.

The peak in particle concentration is particularly useful as a dating level for two reasons. Firstly, it is a recent feature and therefore gives a good indication of modern accumulation rates and secondly, it occurs at a more consistent date, giving a smaller dating error than the other dating features which span several decades. Consequently, it is now possible to use it even for short cores where the base post-

dates the 1940's rapid increase in particle concentration.

Most pre-1985 cores do not show the decrease in particle concentration in the uppermost sediment levels, despite the peak in particle deposition occurring in 1976 (Warren Spring Laboratory data, in Vallack & Chadwick, 1989). This delay in the sediment response to a decrease in atmospheric particle deposition is probably caused by time-averaging due to bioturbation within the sediment, or sample size factors especially in cores with slow accumulation rates.

The features of the carbonaceous particle profiles described above were also found in cores taken in Norway and France. The peak in the Norwegian cores has previously been found and dated at 1969 (Wik & Natkanski, 1990). A ^{210}Pb-dated core from the Vosges region of France showed the start of the particle record and the rapid increase in particle concentration occurred at similar times to those in Britain. However, a ^{210}Pb-date for the sub-surface particle concentration peak in a French core is at present unavailable.

Characterisation of carbonaceous particles extracted from levels of a sediment core show the influence that the combustion of different fuels have had on a lake and its catchment through time. This was applied to a core taken from the Men's Bathing Pond on Hampstead Heath in North London and the results compared well with known combustion histories. In particular, the oil particle concentrations followed trends in oil consumption very closely (Figure 4.42). The start of the oil particle record in the 1920's, the rapid increase in the 1950's due to the influx of cheap fuel-oil and the peak in the mid-1970's followed by a decline due to the oil crisis, can all be seen on the oil particle concentration profile. These trends may not be seen as clearly in profiles from sites further north and in Scotland where the influence of oil combustion has been less, but the results demonstrate well the potential that characterisation of carbonaceous particles has to add more dates to a sediment profile, once regional and local combustion histories are known.

Inorganic ash sphere profiles show similar trends to those of carbonaceous

particles. The obvious difference between the two is the continuous background concentration present in all pre-industrial levels of the inorganic ash sphere profile. When this concentration is removed from all levels the 'industrial' record begins at the same depth/date as the carbonaceous particle record. The background particles must be from a natural source, probably volcanic and possibly also extra-terrestrial (e.g. micro-meteorites). Inorganic ash profiles add little extra information to normal core dating, but may be more useful on a longer time scale. If accumulation rate of the lake sediment remains roughly constant, then any major departure from this background level may represent fallout from major volcanic eruptions in the region. These have been well documented through history and it may be that inorganic ash sphere analysis on long cores can give extra dates in this way, especially in regions of high volcanic activity.

6.4. Spatial distribution of fly-ash particles.

Application of the extraction techniques to the surface sediments of 92 cores from Scotland and 2 from the north Pennines revealed regional trends in particle deposition, even using concentration data. However, there was considerable variability between surface concentrations for adjacent sites, probably due to differences in sediment accumulation rates and water residence times.

The general pattern in particle concentrations is high values in the south and south-west of Scotland decreasing towards the north and north-west. This pattern is seen more clearly when individual site values are averaged over an area (e.g. 50km x 50km grid squares) or interpolated to fill in areas where there are no available data.

Characterisation of carbonaceous particles extracted from some of the Scottish surface sediments show, as expected, that samples are dominated by particles from coal combustion. However, there are two regions where oil particles are present in higher quantities (5-12%) and these are the south-west and the east coast. As there are no oil-fired power stations in Scotland the origins of these particles must be

from outside the region. The most likely source for the oil particles deposited in the south-west are the oil-fired power stations of Ballylumford and Coolkeragh in Northern Ireland, but the origin of those deposited on the east coast is less clear. These are possibly from the burning-off of wastes at oil terminals, from local industry, or may be from industrial and power generating sources in Scandinavia. Further samples are currently being analysed to confirm these findings. The detection of these oil particles in a coal-dominated region shows the characterisation technique to be sensitive and this is important if other fuels are to be introduced into the scheme in future.

The areas which show higher oil particle deposition also show low inorganic ash sphere to carbonaceous particle (IA:CP) ratios. High IA:CP ratios occur in southern Scotland and northern England (i.e. in areas highly influenced by coal combustion) and in the remoter sites, and this is probably due to the smaller ash particles travelling further in air streams than the larger carbonaceous particles. There does not appear to be any direct numerical relationship between the IA:CP ratio and oil or coal particle concentration, but this ratio may be useful as an indication of the relative influences of different fuel combustions at a site where carbonaceous particle characterisation has not been done.

6.5. Fly-ash particles and sulphur deposition.

The regional pattern in particle deposition in Scotland, decreasing from south to north-west is similar to the pattern of sulphur deposition. Although significant at the $p \leq 0.001$ level, the correlations between fly-ash particle concentrations for individual sites and dry, wet and total sulphur depositions are fairly low (between 0.22 and 0.58), these are improved when the particle data are averaged on a regional basis.

The correlations between particle concentration and dry and total sulphur depositions are improved when the data are log transformed. This is probably due to the nature of dry particle deposition which shows an exponential decrease away

from the source. The total sulphur correlations probably increase after log transformation due to the dry deposition component. Wet deposition values are not improved by such transformations, probably because this type of deposition decreases more linearly away from the source.

Although only limited data are available, the correlations between particle fluxes for individual sites and measured total sulphur values are high (0.7 - 0.9, $p \leq 0.001$). A tentative relationship between the two was proposed in section 5.4.5 (i.e. 100 C.P's cm^{-2} yr^{-1} $\approx$ 0.6g total S m^{-2} yr^{-1}), but further work is required to confirm whether or not this relationship holds on a more general basis.

The correlation between carbonaceous particle flux and measured total sulphur deposition is higher than the correlation between measured and modelled total sulphur deposition and it may be that carbonaceous particle fluxes can help improve both contemporary and historical sulphur deposition models (e.g. MAGIC). Further work is needed to ascertain the accuracy of reconstructing sulphur deposition from the carbonaceous particle record and also to try and extend the relationship to urban sites, where at present it does not appear to work.

6.6. Recommendations for further research.

There are two directions that further research based upon this thesis could take. These are (i) applications of the techniques described in the preceding chapters and continuation of the applications outlined in Chapters 4 & 5, and (ii) further development of the techniques. These include:

1) Characterisation of carbonaceous particles from more Scottish surface sediments to examine more closely the distribution of oil-derived particles. This may enable a source for those on the east coast of the country to be identified. This work is currently in progress.

2) Characterisation of carbonaceous particles from Swedish surface sediments to

study the impact of coal-derived particles from outside Sweden. This work is currently in progress.

3) The work of Mejstrik & Svacha (1988) shows that fly-ash produced from power stations burning brown coal and lignite in Czechoslovakia is enriched in Co, Zn, Cr, Ni and Cd. If this is true of all brown coal and lignite ashes then there should be few problems in extending the characterisation to include these fuel-types as well as coal, oil and peat. Spatial and temporal distribution of particles derived from these fuels could then be studied on a Europe-wide scale.

4) Analysis of sediment cores from lakes around power stations to determine the impact that installation of flue-gas desulphurisation equipment has on particle emissions.

5) Analysis of sediment cores from 'pristine' areas in the northern hemisphere (e.g. Greenland, Svalbard) to assess whether particulate contamination is now present in all areas. This could be extended to a global scale with comparisons between northern and southern hemispheres in particular.

6) Further dating of cores to enable the relationship between carbonaceous particle fluxes and sulphur depositions to be studied in more detail.

7) Analysis of a long core for inorganic ash spheres taken from an area with a well-documented volcanic record to ascertain the geochronological potential of the technique.

REFERENCES.

Aitchison, J., 1983. Principal component analysis of compositional data. *Biometrika.* 1: 57-65

Allen, J.R.L., 1987. Microscopic coal-burning residues in the Severn Estuary, Southwestern U.K. *Mar. Pollut. Bull.* 18: 13-18.

Aller, R.C., 1978. Experimental studies of changes produced by deposit feeders on pore water, sediment and overlying water chemistry. *Am. J. Sci.* 278: 1185-1234.

Amdur. M & M.Corn, 1963. Effects of fine aerosol particles on health. *Am. Ind. Hyg. Assoc. J.* 24: 326-328

Anderson, N.J., 1990. Variability of sediment diatom assemblages in an upland, wind-stressed lake (Loch Fleet, Galloway, S.W.Scotland). *J. Paleolim.* 4: 43-59.

Anderson, N.J., R.W.Battarbee, P.G.Appleby, A.C.Stevenson, F.Oldfield, J.Darley & G.Glover, 1986. *Palaeolimnological evidence for the acidification of Loch Fleet.* Palaeoecology Research Unit , Dept. of Geography, University College London. Research Paper No. 17.

Appleby, P.G. & F.Oldfield, 1978. The calculation of ^{210}Pb dates assuming a constant rate of supply of unsupported ^{210}Pb to the sediment. *Catena.* 5: 1-8.

Appleby, P.G., P.Nolan, D.W.Gifford, M.J.Godfrey, F.Oldfield, N.J.Anderson & R.W.Battarbee, 1986. ^{210}Pb dating by low background gamma counting. *Hydrobiologia.* 141: 21-27.

Battarbee, R.W., 1990. The causes of lake acidification, with special reference to the role of acid deposition. *Phil. Trans. R. Soc. Lond.* B 327: 339-347.

Battarbee, R.W. & M.J.Kneen, 1982. The use of electronically counted microspheres in absolute diatom analysis. *Limnol. Oceanogr.* 27: 184-188.

Battarbee, R.W., N.J.Anderson, P.G.Appleby, R.J.Flower, S.C.Fritz, E.Y.Haworth, S.Higgitt, V.J.Jones, A.Kreiser, M.A.R.Munro, J.Natkanski, F.Oldfield, S.T.Patrick, N.G.Richardson, B.Rippey, A.C.Stevenson, 1988. *Lake Acidification in the United Kingdom 1800-1986.* Ensis Publishing. London, 68pp.

Beaudoin, A.B. & R.H.King, 1986. Using discriminant function analysis to identify Holocene tephras based on magnetite composition: a case study from the Sunwapta Pass area, Jasper National Park. *Can. J. Earth Sci.* 23: 804- 812.

Birks, H.J.B., J.M.Line, S.Juggins, A.C.Stevenson & C.J.F. ter Braak, 1990. Diatoms and pH reconstruction. *Phil. Trans. Roy. Soc. Lond.* B327: 263-278.

Block, C. & R.Dams, 1976. A study of fly-ash emission during combustion of coal. *Env. Sci. Tech.* 10: 1011-1017.

Borchardt, G.A., M.E.Harward & R.A.Schmitt, 1971. Correlation of volcanic ash deposits by activation analysis of glass separates. *Quat. Res.* 1: 247-260.

Broman, D., C.Näf, M.Wik & I.Renberg, 1990. The importance of spheroidal carbonaceous particles for the distribution of particulate polycyclic aromatic hydrocarbons in an estuarine-like urban coastal water area. *Chemosphere.* 21: 69-77.

Carpenter, R.L., R.D.Clark & Y-F.Su, 1980. Fly-ash from electrostatic precipitators: Characterisation of large spheres. *J. Air Poll. Cont. Assoc.* 30 679-681

Central Electricity Generating Board, *Annual Reports.*

Chapman, S.L., J.K.Syers & M.L.Jackson, 1969. Quantitative determination of quartz in soils, sediments and rocks by pyrosulfate fusion and hydrofluosilicic acid treatment. *Soil Science* 107: 348-355.

Cheng, R.J., V.A.Mohnen, T.T.Shen, M.Current, J.B.Hudson, 1976. Characterisation of particles from power plants. *J. Air Poll. Cont. Assoc.* 26: 787-783

Chigier, N.A., 1975. Pollution formation and destruction in flames - Introduction. *Prog. Energy Combust. Sci.* 1: 3-15.

Clark, J.S., 1988. Particle motion and the theory of charcoal analysis: Source area, transport, deposition and sampling. *Quat. Res.* 30: 67-80.

Coles, D.G., R.C.Ragaini, J.M.Ondov, G.L.Fisher, D.Silberman & B.A.Prentice, 1979. Chemical studies of stack fly-ash from a coal-fired power plant. *Env. Sci. Tech.* 13: 455-459.

Commission on Energy and the Enviroment, 1981. *Coal and the environment.* 257pp. HMSO. London.

Darley, J., 1985. *Particulate soot in Galloway lake sediments. Its application as an indicator of environmental change and as a technique for dating recent sediments.* Dept. of Geog. University College London. B301 Project.

Davis, J.C., 1986. *Statistics and data analysis in geology.* 2nd. Edition. Pub: John Wiley & Sons. New York. 646pp

Davis, R.B., 1974. Stratigraphic effects of tubificids in profundal lake sediments. *Limnol & Oceanogr.* 19: 466-488

Davison, R.L., D.F.S.Natusch, & J.R.Wallace, 1974. Trace elements in fly-ash. Dependence of concentration on size. *Env. Sci. Tech.* 8: 1107-1113.

Dear, D. & C.Laird, 1984. In pursuit of Acid Rain. *New Scientist.* 22nd Nov: 30-33

Del Monte, M. & O.Vittori, 1985. Air pollution and stone decay: The case of Venice. *Endeavour* 9: 117-122.

Del Monte, M., C.Sabbioni & O.Vittori, 1984. Urban stone sulphation and oil-fired carbonaceous particles. *Sci. Tot. Env.* 36: 369-376.

Deuser, W.G., K.Emeis, V.Ittekkot, E.T.Degens, 1983. Fly-ash particles intercepted in the deep Sargasso Sea. *Nature* 305: 216-218.

Electricity Council, (Annual) *Handbook of electrical supply statistics.*

Falster, H. & L.Jacobsen, 1982. Dust emmision, its quantity and composition, depending on dust collecter; coal quality etc. *Proceedings of the International Conference on coal-fired power plants and the aquatic environment.* Copenhagen, Denmark. 16-18 August 1982.

Fisher, B.E.A., 1986. The effect of tall stacks on the long range transport of air pollutants. *APCA Journal.* 36: 399-401

Fisher, G.L., B.A.Prentice, D.Silberman, J.M.Ondov, A.H.Biermann, R.C.Ragaini & A.R.McFarland, 1978. Physical and morphological studies of size classified coal fly-ash. *Env. Sci. Tech.* 12: 447-451.

Fisher, J.B., W.J.Lick, P.L.McCall & J.A.Robbins, 1980. Vertical mixing of lake sediments by tubificid oligochaetes. *J. Geophys. Res.* 85: 3997-4006.

Flower, R.J., R.W.Battarbee & P.G.Appleby, 1987. The recent palaeolimnology of acid lakes in Galloway, south-west Scotland: Diatom analysis, pH trends, and the role of afforestation. *J. Ecol.* 75: 797-824

Folger, D.W., 1970. Wind transport of land derived mineral, biogenic and industrial matter over the North Atlantic. *Deep Sea Res.* 17: 337-352.

Fredriksson, K. & L.R.Martin, 1963. The origin of black spherules found in Pacific Islands, deep-sea sediments and Antarctic ice. *Geochim. et Cosmochim. Acta.* 27: 245-248.

Fritz, S.C., A.C.Stevenson, S.T.Patrick, P.G.Appleby, F.Oldfield, B.Rippey, J.Darley & R.W.Battarbee, 1986. *Palaeoecological evaluation of the recent acidification of Welsh lakes. I, Llyn Hir, Dyfed.* Palaeoecology Research Unit, University College London. Research Paper No. 16.

Ganor, E., S.Altshuller, H.A.Foner, S.Brenner & J.Gabbay, 1988. Vanadium and nickel in dustfall as indicators of power plant pollution. *Water, Air Soil Poll.* 42: 241-252

Giblin, A.E., G.E.Likens, D.White & R.W.Howarth, 1990. Sulfur storage and alkalinity generation in New England lake sediments. *Limnol. Oceanogr.* 35: 852-869.

Gladney, E.S., J.A.Small, G.E.Gordon, & W.H.Zoller, 1976. Composition and size distribution of in-stack particulate material at a coal-fired power plant. *Atmos. Envir.* 10: 1071-1077.

Goldberg, E.D., 1985. *Black carbon in the environment: Properties and distribution.* Wiley Interscience Publication. 198pp.

Goldberg, E.D., V.F. Hodge, J.J. Griffin, & M. Koide, 1981. Impact of fossil-fuel combustion on the sediments of Lake Michigan. *Env. Sci. Tech.* 15: 466-470.

Goldstein, H.L. & C.W.Siegmund, 1976. Influence of heavy oil composition and boiler combustion conditions on particulate emissions. *Env. Sci. Tech.* 10: 1109-1114.

Golterman, H.L.,(Editor), 1970. *IBP Handbook No. 8. Methods for physical and chemical analysis of fresh waters.* Blackwell Scientific. 213pp.

Griest, W.H. & L.A.Harris, 1985. Microscopic identification of carbonaceous particles in stack ash from pulverised-coal combustion. *Fuel.* 64: 821-826.

Griffin, J.J. & E.D. Goldberg, 1975. The fluxes of elemental carbon in coastal marine sediments. *Limnol. Oceanogr.* 20: 256-263.

Griffin, J.J. & E.D. Goldberg, 1979. Morphologies and origin of elemental carbon in the environment. *Science.* 206: 563-565.

Griffin, J.J. & E.D. Goldberg, 1981. Sphericity as a characteristic of solids from fossil-fuel burning in a Lake Michigan sediment. *Geochim. et Cosmochim. Acta.* 45: 763-769.

Griffin, J.J. & E.D. Goldberg, 1983. Impact of fossil fuel combustion on the sediments of Lake Michigan: A reprise. *Env. Sci. Tech.* 17: 244-245.

Handy, R.L. & D.T.Davidson, 1953. On the curious resemblance between fly-ash and meteoritic dust. *Iowa Acadamy of Sci.* 60: 373-379.

Hintze, J.L., 1988. *SOLO 2.0.* Distributed by: BMDP Statistical Software. Los Angeles. California.

Hodge, P.W. & F.W.Wright, 1964. Studies of particles for extra-terrestrial origin. 2. A comparison of microscopic spherules of meteoritic and volcanic origin. *J.Geophys. Res.* 69: 2449-2454.

Hodge, P.W., F.W.Wright, & C.C.Langway, 1964. Studies of particles for extra-terrestrial origin. 3. Analyses of dust particles from polar ice deposits. *J. Geophys. Res.* 69: 2919-2931

Hodge, P.W., F.W.Wright, & C.C.Langway, 1967. Studies of particles for extra-terrestrial origin. 5. Compositions of the interiors of spherules from Arctic and Antarctic ice deposits. *J. Geophys. Res.* 72: 1404-1406.

Holdren, G.R., T.M.Brunelle, G.Matisoff & M.Wahlen, 1984. Timing the increase in atmospheric sulphur deposition in the Adirondack Mountains. *Nature.* 311: 245-248.

Hulett, L.D. & A.J.Weinberger, 1980. Some etching studies of the microstructure and composition of large aluminosilicate particles in fly-ash from coal burning power plants. *Env. Sci. Tech.* 14: 965-970.

Hulett, L.D., A.J.Weinberger, K.J.Northcutt & M.Ferguson, 1980. Chemical species in fly-ash from coal-burning power plants. *Science.* 1356-1358.

Jones, V.J., A.C.Stevenson & R.W.Battarbee, 1989. Acidification of lakes in south west Scotland: A diatom and pollen study of the post-glacial history of the Round Loch of Glenhead. *J. Ecol.* 77: 1-23.

Kaakinen, J.W., R.M.Jorden, M.M.Lawasani, & R.E.West, 1975. Trace element behaviour in a coal fired power plant. *Env. Sci. Tech.* 9: 862-869.

Kajak, Z., 1966. Field experiment in studies on benthos density of some Mazurian lakes. *Gewässer und Abwässer* 41/42: 150-158.

Kiely, P.V. & M.L.Jackson, 1965. Quartz, feldspar and mica determination for soils by sodium pyrosulfate fusion. *Soil Sci. Soc. Am. Proc.* 29: 159-163.

King, R.H., M.S.Kingston & R.L.Barnett, 1982. A numerical approach toward the classification of magnetites from tephra in southern Alberta. *Can. J. Earth Sci.* 19: 2012-2019

Klein, D.H., A.W.Andren, J.A.Carter, J.F.Emery, C.Feldman, W.Fulkerson, W.S.Lyon, J.C.Ogle, Y.Talmi, R.I.Van Hook, N.Bolton, 1975. Pathways of 37 trace elements through a coal-fired power plant. *Env. Sci. Tech.* 9: 973-979.

Kothari, B.K. & M.Wahlen, 1984. Concentration and surface morphology of charcoal particles in sediments of Green Lake, New York. Implications regarding the use of energy in the past. *Northeastern Env. Sci.* 3: 24-29.

Krausse, G.L., C.L.Schelske, & C.O.Davis, 1983. Comparison of three wet alkaline methods of digestion of biogenic silica in water. *Freshwat. Biol.* 13: 73-81.

LeFevre, R., A.Gaudichet & M.A.Billon-Galland, 1986. Silicate microspherules intercepted in the plume of the Etna volcano. *Nature.* 322: 817-820.

Le Maitre, R.W, 1968. Chemical variation within and between volcanic rock series - A statistical approach. *J. Pet.* 9: 220-252.

Lightman, P. & P.J.Street, 1968. Microscopical examination of heat treated pulverised coal particles. *Fuel.* 47: 7-28.

Lightman, P. & P.J.Street, 1983. Single drop behaviour of heavy fuel oils and fuel oil fractions. *J. Inst. Energy.* 56: 3-11.

Livingstone, D.A. 1955. A lightweight piston sampler for lake deposits. *Ecology,* 36, 137-139.

Mackereth, F.J.H. 1969. A short core sampler for subaqueous deposits. *Limnol. Oceanogr.* 14: 145-151.

Mamane, Y. & R.F.Pueschel, 1979. Oxidation of SO_2 on the surface of fly-ash particles under low relative humidity conditions. *Geophys. Res. Lett.* 6: 109-112.

Mamane, Y., J.L.Miller, & T.G.Dzubay, 1986. Characterisation of individual fly ash particles from coal and oil-fired power plants. *Atmos. Env.* 20: 2125-2135.

Marvin, U.B. & M.T.Einaudi, 1967. Black, magnetic spherules from Pleistocene and recent beach sands. *Geochim. et Cosmochim. Acta.* 31: 1871-1884.

McCammon, R.B., 1966. Principal component analysis and its application in large scale correlation studies. *J. Geol.* 74: 721-733.

McCrone, W.C. & J.G.Delly, 1973. *The Particle Atlas. An encyclopedia of techniques for small particle identification.* 2nd Edition. Ann Arbor Science Publishers. Michigan. USA.

McElroy, M.W., R.C.Carr, D.S.Ensor & G.R.Markowski, 1982. Size distribution of fine particles from coal combustion. *Science.* 215: 13-18.

Mejstrik, V. & J.Svacha, 1988. The fallout of particles in the vicinity of coal-fired power plants in Czechoslovakia. *Sci. Tot. Env.* 72: 43-55

Miesch, A.T., E.C.T.Chao & F.Cuttitta, 1966. Multivariate analysis of geochemical data on tektites. *J. Geol.* 74: 673-691.

Munro, M.A.R. & S.Papamarinopoulos, 1978. The investigation of an unusual magnetic anomaly by combined magnetometer and soil susceptibility surveys. *Archaeo Physiko.* 10: 675-680.

Murozumi, M., T.J.Chow & C.Patterson, 1969. Chemical concentrations of pollutant lead aerosols, terrestrial dusts and sea salts in Greenland and Antarctic snow strata. *Geochim. et Cosmochim. Acta.* 33: 1247-1294.

National Society for Clean Air, 1971. *History of air pollution in Great Britain. Clean Air Yearbook.*

Natusch, D.F.S. & J.R.Wallace, 1974. Toxic trace elements: Preferential concentration in respirable particles. *Science.* 183: 202-204.

Nriagu, J.O. & C.J.Bowser, 1969. The magnetic spherules in sediments of Lake Mendota, Wisconsin. *Water Res.* 3: 833-842.

Nriagu, J.O. & R.D.Coker, 1983. Sulphur in sediments chronicles past changes in lake acidification. *Nature.* 203: 692-694.

Oldfield, F., R.Thompson & K.E.Barber, 1978. Changing atmospheric fallout of magnetic particles recorded in recent ombotrophic peat sections. *Science.* 199: 679-680.

Oldfield, F., K.Tolonen & R.Thompson, 1981. History of particulate atmospheric pollution from magnetic measurements in dated Finnish peat profiles. *Ambio.* 10: 185-188.

Parker, A. (Ed.), 1978. *Industrial air pollution handbook.* McGraw-Hill.

Parkin, D.W., D.R.Phillips, R.A.L.Sullivan, & L.Johnson, 1970. Airborne dust collections over the North Atlantic. *J. Geophys. Res.* 75: 1782-1793.

Paulson, C.A.J. & A.R.Ramsden, 1970. Some microscopic features of fly-ash particles and their significance in relation to electrostatic precipitation. *Atmos. Env.* 4: 175-185.

Puffer, J.H., E.W.B.Russell, & M.R.Rampino, 1980. Distribution and origin of magnetite spherules in air, waters, and sediments of the Greater New York City area and the North Atlantic Ocean. *J. Sed. Pet.* 50: 247-256.

Raask, E., 1968. Cenospheres in pulverised fuel ash. *J. Inst. Fuel.* 41: 339-344

Raask, E., 1984. Creation, capture and coalescence of mineral species in coal flames. *J. Inst. Energy* 57: 231-239.

Raask, E. & P.J.Street, 1978. Appearance and pozzolanic activity of pulverised fuel ash. *Proc. Conf. on Ash Tech. and Marketing.*

Raeymaekers, B., M.Demuynck, W.Dorrine & F.Adams, 1988. Characterisation of oil fly-ash particles by electron probe microanalysis. *Intern. J. Env. Anal. Chem.* 32: 291-312.

Ramsden, A.R. & M.Shibaoka, 1982. Characterisation and analysis of individual fly-ash particles from coal-fired power stations by a combination of optical microscopy, electron microscopy and quantitative electron microprobe analysis. *Atmos. Env.* 16: 2191-2206.

Renberg, I & M. Wik, 1984. Dating of recent lake sediments by soot particle counting. *Verh. internat. Ver. Limnol.* 22: 712-718.

Renberg, I. & M. Wik, 1985a. Soot particle counting in recent lake sediments. An indirect counting method. *Ecol. Bull.* 37: 53-57.

Renberg, I. & M. Wik, 1985b. Carbonaceous particles in lake sediments - Pollutants from fossil fuel combustion. *Ambio.* 14: 161-163.

Review Group on Acid Rain, 1987. *Acid Deposition in the United Kingdom 1981-1985.* Pub: Warren Springs Laboratory. Dept. Trade and Industry.

Review Group on Acid Rain, 1990. *Acid Deposition in the United Kingdom 1986-1988.* Pub: Warren Springs Laboratory. Dept. Trade and Industry.

Rippey, B., 1990. Sediment chemistry and atmospheric contamination. *Phil. Trans. Roy. Soc. Lond.* B327: 311-317.

Rose, N.L., 1990a. A method for the extraction of carbonaceous particles from lake sediment. *J. Paleolim.* 3: 45-53.

Rose, N.L., 1990b. A method for the selective removal of inorganic ash particles from lake sediments. *J. Paleolim.* 4: 61-68.

Rosen, H., T.Novakov & B.A.Bodhaine, 1981. Soot in the Arctic. *Atmos. Env.* 15: 1371-1374.

Shen, T.T., R.J.Cheng, V.A.Mohnen, M.Current & J.B.Hudson, 1976. Characterisation of differences between oil-fired and coal-fired power plant emissions. *Proceedings of the 4th International Clean Air Congress*: 386-391.

Stokes, S. & D.J.Lowe, 1988. Discriminant function analysis of late Quaternary tephras from five volcanoes in New Zealand using glass shard major element chemistry. *Quat. Res.* 30: 270-283.

Srivastava, M.S. & E.M.Carter, 1983. *An introduction to applied multivariate statistics.* Pub: North-Holland. New York.

Street, P.J., R.P.Weight & P.Lightman, 1969. Further investigations of structural changes occuring in pulverised coal particles during rapid heating. *Fuel.* 48: 343-365.

U.S. Dept. of Health, Education and Welfare, 1969. *National Air Pollution Control Board: Air quality criteria for particulate matter.* Pub. No, AP-49.

Vallack, H.W. & M.J.Chadwick, 1989. *Airborne dust sampling around Drax Power Station. 1987-1988.* Report of Beijer Institute for Resource Assesment and Management, York.

Vallack, H.W. & M.J.Chadwick, 1990. *A two year survey of airborne dust in the Selby District, North Yorkshire.* Report of Stockholm Environment Institute at York.

Wadge, A. & M.Hutton, 1987. The leachability and chemical speciation of selected trace elements in fly-ash from coal combustion and refuse incineration. *Env. Poll.* 48: 85-99

Wark, K. & C.F.Warner, 1976. *Air Pollution : It's Origin and Control.* I.E.P., New York. 519pp.

Watt, J., 1990. Automated feature analysis in the scanning electron microscope. *Microscopy & Analysis.* Issue 15.

Watt, J.D. & D.J.Thorne, 1965. Composition and pozzolanic properties of pulverised fuel ashes. I. Composition of fly ashes from some British power stations and properties of their componant particles. *J. App. Chem.* 585-594

Webb, W.M. & L.I.Briggs, 1966. The use of principal components analysis to screen mineralogical data. *J. Geol.* 74: 716-720.

Wilkins, E.T., 1954. Air pollution and the London fog of December 1952. *J. Roy. Sanitary. Inst.* 74: 17-24.

Wik, M & J.Natkanski, 1990. British and Scandinavian lake sediment records of carbonaceous particles from fossil-fuel combustion. *Phil. Trans. R. Soc. Lond.* B327: 319-323.

Wik, M. & I.Renberg, 1987. Distribution in forest soils of carbonaceous particles from fossil-fuel combustion. *Water, Air Soil Poll.* 33: 127-129.

Wik, M., I.Renberg & J. Darley, 1986. Sedimentary records of carbonaceous particles from fossil-fuel combustion. *Hydrobiologia.* 143: 387-394.

Wohletz, K.H. & R.G.McQueen, 1984. Volcanic and stratospheric dustlike particles produced by experimental water-melt interactions. *Geol.* 12: 591-594.

APPENDIX A

CARBONACEOUS PARTICLE AND INORGANIC ASH SPHERE CONCENTRATIONS FOR SURFACE SEDIMENTS.

(All values in gDM^{-1})

		C.P.	I.A.
1.	LOCH SAUGH	5 771	6 733
2.	UNNAMED H	7 281	5 601
3.	BRAERODDACH LOCH	2 328	5 866
4.	UNNAMED G	9 722	11 676
5.	LILY LOCH	54 225	12 991
6.	LOWER LAKE	3 203	4 714
7.	LOCH OIRE	7 718	3 978
8.	LOCH DALLAS	21 054	5 176
9.	LOCH MHIC LEOID	11 350	9 080
10.	LOCH ETTERIDGE	4 332	5 042
11.	UATH LOCHAN	13 561	14 873
12.	LOCH BEAG	5 301	6 820
13.	LOCH A'CHLACHAIN	6 357	12 932
14.	LOCH BRAN	9 521	11 596
15.	LOCH TARFF	4 533	6 920
16.	LOCH LAIDE	3 202	3 626
17.	LOCH NA BA RUAIDHE	4 122	7 611
18.	LOCH ACHILTY	16 483	18 448
19.	LOCH SGAMHAIN	901	3 604
20.	LOCH BHARRANCH	2 024	3 707
21.	UNNAMED U	4 911	7 104
22.	LOCH IAIN OIG	3 129	7 564
23.	LOCH COIRE NAN CNAMH	713	1 155
24.	LOCH BAD AN LOSGUINN	1 765	2 010
25.	LOCH DOIRE NAN SGIATH	8 631	5 492
26.	LOCH CURRAN	15 977	24 781
27.	STORMONT LOCH	12 077	8 220
28.	LOCH NA CRAIG	12 031	22 113
29.	LOCH KINARDOCHY	10 041	18 601
30.	LOCHAN LAIRIG CHEILE	16 167	20 209
31.	LOCH RESTIL	3 127	3 648
32.	AUCHA LOCHY	13 425	4 682
33.	LOCH ARIAL	13 798	15 747
34.	LOCH LEATHAN	2 883	3 386
35.	LOCH NAN DRUIMNEAN	10 258	27 771
36.	LOCHAN NA GEALAICH	5 130	6 473
37.	LOCH WALTON	51 139	46 390
38.	LOCH RUSKY	15 227	10 057
39.	LOCH IDRIGILL	1 256	3 096
40.	LOCH A LHIGHE BHIG	2 238	5 595
41.	LOCH A BHUNA	755	2 213

42.	LOCH DIBADALE	888	1 110
43.	LOCH DUBH OIRTHEANAN	1 369	1 169
44.	DALLICAN WATER	974	5 875
45.	UNNAMED 7	1 836	12 110
46.	LOCH OF ROONIES	979	4 274
47.	LOCH OF THE WARD	378	1 372
48.	GOSSA WATER	2 781	5 691
49.	LOCH GAUSCAVAIG	735	1 495
50.	LOCH LANG	5 727	19 724
51.	LOCH AN RUBHA DHUIBH	976	1 637
52.	HORSETAIL	2 035	3 731
53.	LOCH AN FAOILEAG	2 210	3 788
54.	CAMALOCHAN	540	2 217
55.	LOCH NA LARACH	3 077	6 255
56.	LONG LOCH	3 063	14 701
57.	LOCH TEANGA	3 040	21 363
58.	LOCH COIRE NAN ARR	1 806	1 047
59.	COIRE AN LOCHAN	14 318	10 873
60.	LOCH UISGE	4 762	3 712
61.	LOCH DOILET	683	2 593
62.	LOCHAN DUBH	4 431	6 938
63.	LOCH NA H'ACHLAISE	6 282	4 756
64.	LOCH LAIDON	11 178	5 167
65.	LOCH CHON	25 913	40 394
66.	LOCH TINKER	70 073	363 504
67.	LOCHAN UAINE	6 359	7 631
68.	LOCH NAN EUN	13 937	8 325
69.	DUBH LOCH	15 202	12 508
70.	LOCHNAGAR	5 411	11 635
71.	COIRE FHIONN LOCHAN	20 321	14 178
72.	LOCH TANNA	63 990	30 957
73.	ROUND LOCH OF GLENHEAD	50 999	20 443
74.	LOCH DOON	8 790	4 375
75.	LOCH GRANNOCH	46 838	12 068
76.	LOCH FLEET	34 750	15 823
77.	LOCH SKAE	11 977	11 204
78.	LOCH KIRRIMORE	6 841	2 921
79.	LOCH ENOCH	44 801	16 359
80.	LOCH DEE	35 834	13 064
81.	COLDINGHAM LOCH	7 462	16 338
82.	WHITFIELD LOUGH	36 841	61 266
83.	TINDALE TARN	5 195	17 493
84.	LOCH MUIGHBHLARAIDH	1 558	2 266
85.	LOCH DUBH CADHAFUARAICH	7 921	8 685
86.	LOCH NA GAINEIMH	3 335	5 854
87.	LOCH COIRE NA SAIDHE DUIBHE	1 195	1 680
88.	LOCH BEALICH NA H-UIDHE	7 576	2 977
89.	LOCHAN NIGHEADH	2 956	7 642
90.	LOCH NA BEISTE	2 732	3 802
91.	LOCHAN NAM BREAC	2 657	3 841
92.	LOCH NA H-AIRBHE	2 836	4 261

93.	LOCH NA H-OIDHCHE	1 619	2 159
94.	LOCH HOWIE	16 063	9 798

SCILLY ISLES

ABBEY POOL	843
GREAT POOL	2 488
PORTH HELLICK	892
BIG POOL, BRYHER	620
BIG POOL, ST AGNES	2 752

IRELAND

LOUGH INCHIQUIN	1 749
ANNAGH LOUGH	2 569
LOUGH SHEEVER	2 001

APPENDIX B.

CARBONACEOUS PARTICLE CONCENTRATIONS FOR SEDIMENT CORES DESCRIBED IN THE TEXT

LOCH ARIAL (ARIA 1) - 9/9/89

Sed. Depth (cm)	Particle No. (gDM^{-1})
0.0 - 0.5	13 798
0.5 - 1.0	14 411
1.0 - 1.5	24 209
1.5 - 2.0	22 421
2.0 - 2.5	28 490
3.0 - 3.5	26 473
4.0 - 4.5	25 781
6.0 - 7.0	10 197
8.0 - 9.0	3 828

LOCH COIRE NAN ARR (ARR 2) - 15/6/86

Sed. Depth (cm)	Particle No. (gDM^{-1})
0.0 - 0.5	1806
1.0 - 1.5	1354
2.0 - 2.5	794
3.0 - 3.5	1007
4.0 - 4.5	739
5.0 - 5.5	1191
6.0 - 6.5	592
7.0 - 7.5	296
8.0 - 8.5	265
9.0 - 9.5	198
10.0 - 10.5	332
12.0 - 12.5	418
14.0 - 14.5	65
16.0 - 17.0	75

LOCH BRAN (BRAN 1) - 16/8/89

Sed. Depth (cm)	Particle No. (gDM^{-1})
0.0 - 0.5	9 521
0.5 - 1.0	10 296
1.0 - 1.5	7 385
1.5 - 2.0	2 828
2.0 - 2.5	1 918
3.0 - 3.5	1 530
4.0 - 4.5	977
6.0 - 7.0	123
8.0 - 9.0	298

LOCH DUBH CADHAFUARAICH (CADH 1) - 23/10/89

Sed. Depth (cm)	Particle No. (gDM^{-1})
0.0 - 0.5	7 921
0.5 - 1.0	8 010
1.0 - 1.5	7 043
1.5 - 2.0	6 687
2.0 - 2.5	2 417
3.0 - 3.5	743
4.0 - 4.5	412
6.0 - 7.0	719
8.0 - 9.0	334

LLYN CONWY (CON 4) - 25/5/87

Sed. Depth (cm)	Particle No. (gDM^{-1})
0.0 - 0.5	12 044
2.0 - 2.5	23 766
4.0 - 4.5	28 896
6.0 - 6.5	5 524
8.0 - 8.5	4 102
10.0 - 10.5	6 282
12.0 - 12.5	6 762
14.0 - 14.5	3 188
16.0 - 16.5	447
18.0 - 18.5	2 882
20.0 - 21.0	1 650
22.0 - 23.0	712
24.0 - 25.0	394
26.0 - 27.0	1 006
28.0 - 29.0	1 403
30.0 - 31.0	803

LAC DES CORBEAUX (CORB 1) - 7/7/89

Sed. Depth (cm)	Particle No. (gDM^{-1})
0.0 - 1.0	9 142
1.0 - 2.0	7 028
2.0 - 3.0	5 063
3.0 - 4.0	2 942
4.0 - 5.0	2 221
5.0 - 6.0	1 615
6.0 - 7.0	902
7.0 - 8.0	1 439
8.0 - 9.0	443
9.0 - 10.0	221
11.0 - 12.0	102
13.0 - 14.0	37
15.0 - 16.0	56
17.0 - 18.0	30

LOCH DALLAS (DALL 1) - 14/8/89

Sed. Depth (cm)			Particle No. (gDM^{-1})
0.0	-	0.5	21 054
0.5	-	1.0	27 273
1.0	-	1.5	27 939
2.0	-	2.5	21 702
3.0	-	3.5	20 284
4.0	-	4.5	11 320
6.0	-	7.0	4 457
8.0	-	9.0	1 569

LOCH DOILET (DOI 2) - 8/6/86

Sed. Depth (cm)			Particle No. (gDM^{-1})
0.0	-	0.5	683
2.0	-	2.5	360
4.0	-	4.5	1073
6.0	-	6.5	531
8.0	-	8.5	690
10.0	-	10.5	152
12.0	-	12.5	653
14.0	-	14.5	131
16.0	-	16.5	264
18.0	-	18.5	892
20.0	-	21.0	92
22.0	-	23.0	0
24.0	-	25.0	0
26.0	-	27.0	22
28.0	-	29.0	0
30.0	-	31.0	0

LOCH FLEET (K1090) - 10/90

Sed. Depth (cm)	Particle No. (gDM^{-1})
0.0 - 0.5	34 567
0.5 - 1.0	42 120
1.0 - 1.5	54 465
1.5 - 2.0	62 611
2.0 - 2.5	69 870
2.5 - 3.0	60 707
3.0 - 3.5	69 603
3.5 - 4.0	71 556
4.0 - 4.5	44 437
4.5 - 5.0	54 150
5.0 - 6.0	24 701
7.0 - 8.0	16 551
9.0 - 10.0	5 960
14.0 - 15.0	1 753

LAC DE GERARDMER (GERA 1) - 7/89

Sed. Depth (cm)	Particle No. (gDM^{-1})
0.0 - 0.5	144 125
1.0 - 1.5	176 679
2.0 - 2.5	137 373
3.0 - 3.5	83 910
4.0 - 4.5	47 599
6.0 - 6.5	16 500
8.0 - 8.5	7 871
10.0 - 10.5	5 926
12.5 - 13.0	5 147
15.0 - 15.5	1 765
17.5 - 18.0	3 131
20.0 - 21.0	2 641
25.0 - 26.0	620
30.0 - 31.0	181
35.0 - 36.0	74
40.0 - 41.0	0

LLYN GLAS (GLAS 1) - 1987

Sed. Depth (cm)	Particle No. (gDM^{-1})
0.0 - 0.5	4 017
1.0 - 1.5	5 334
2.0 - 2.5	3 077
3.0 - 3.5	2 119
4.0 - 4.5	609
5.0 - 5.5	620
6.0 - 6.5	150
7.0 - 7.5	107
8.0 - 8.5	97
9.0 - 9.5	112
10.0 - 10.5	0
12.0 - 12.5	96
14.0 - 14.5	0

" **GRANITE 'A'** " (GRNA 1) - 7/88

Sed. Depth (cm)	Particle No. (gDM^{-1})
0.0 - 0.5	1 251
0.5 - 1.0	771
1.0 - 1.5	938
1.5 - 2.0	748
2.0 - 2.5	337
2.5 - 3.0	86
3.0 - 3.5	102
3.5 - 4.0	104
4.0 - 4.5	24
4.5 - 5.0	20

LLYN HIR (HIR88) - 1988

Sed. Depth (cm)	Particle No. (gDM^{-1})
0.0 - 0.5	21 198
0.5 - 1.0	25 886
1.0 - 1.5	27 474
1.5 - 2.0	22 255
2.0 - 2.5	21 047
2.5 - 3.0	18 851
3.0 - 3.5	16 073
3.5 - 4.0	13 922
4.0 - 4.5	12 783
4.5 - 5.0	11 211

LLYN IRDDYN (IRD 2) - 5/87

Sed. Depth (cm)	Particle No. (gDM^{-1})
0.0 - 0.5	26 408
1.0 - 1.5	34 417
2.0 - 2.5	20 855
4.0 - 4.5	3 796
6.0 - 6.5	1 195
8.0 - 8.5	1 174
10.0 - 10.5	624
12.0 - 12.5	396
14.0 - 14.5	394
16.0 - 16.5	82
18.0 - 18.5	46
20.0 - 21.0	129
22.0 - 23.0	0
24.0 - 25.0	32
26.0 - 27.0	40
28.0 - 29.0	0

LANGTJÖRNA (LAG 1) - 7/88

Sed. Depth (cm)			Particle No. (gDM^{-1})
0.0	-	0.5	1 034
0.5	-	1.0	637
1.0	-	1.5	412
1.5	-	2.0	187
2.0	-	2.5	50
2.5	-	3.0	34
3.0	-	3.5	100
3.5	-	4.0	48
4.0	-	4.5	29
4.5	-	5.0	17

LOCH NA LARACH (LAR 8) - 16/6/86

Sed. Depth (cm)			Particle No. (gDM^{-1})
0.0	-	0.5	3 077
0.5	-	1.0	2 890
1.0	-	1.5	3 091
1.5	-	2.0	3 336
2.0	-	2.5	2 950
2.5	-	3.0	3 128
3.0	-	3.5	1 594
4.0	-	4.5	1 513
5.0	-	5.5	1 660
6.0	-	6.5	1 593
8.0	-	8.5	497
10.0	-	10.5	728
12.5	-	13.0	954
15.0	-	16.0	349
17.0	-	18.0	0
19.0	-	20.0	0

LONG LOCH OF DUNNET HEAD (LON 2) - 18/6/86

Sed. Depth (cm)			Particle No. (gDM^{-1})
0.0	-	0.5	3 063
1.0	-	1.5	2 935
2.0	-	2.5	3 768
3.0	-	3.5	3 839
4.0	-	4.5	1 526
6.0	-	6.5	1 535
8.0	-	8.5	1 808
10.5	-	11.0	942
12.0	-	12.5	698
14.0	-	14.5	1 477
16.0	-	17.0	2 387
18.0	-	19.0	717
22.0	-	23.0	234
26.0	-	27.0	121
30.0	-	31.0	74
34.0	-	35.0	0

LILY LOCH (LILY 1) - 13/8/89

Sed. Depth (cm)			Particle No. (gDM^{-1})
0.0	-	0.5	54 225
0.5	-	1.0	37 150
1.0	-	1.5	11 606
1.5	-	2.0	12 040
2.0	-	2.5	3 321
3.0	-	3.5	826
4.0	-	4.5	0
6.0	-	7.0	0

LOUGH MAAM (MAAM 3) - 5/88

Sed. Depth (cm)	Particle No. (gDM^{-1})
0.0 - 0.5	8 056
0.5 - 1.0	7 197
1.0 - 1.5	8 840
1.5 - 2.0	7 944
2.0 - 2.5	4 751
2.5 - 3.0	3 474
3.0 - 3.5	3 936
3.5 - 4.0	2 567
4.0 - 4.5	3 476
4.5 - 5.0	1 814
5.5 - 6.0	1 970
6.5 - 7.0	1 324
7.5 - 8.0	927
8.5 - 9.0	340
9.5 - 10.0	112

MALHAM TARN (MALH 1) - 10/88

Sed. Depth (cm)	Particle No. (gDM^{-1})
0.0 - 1.0	9 547
1.0 - 2.0	16 068
2.0 - 3.0	14 116
3.0 - 4.0	13 736
4.0 - 5.0	16 811
5.0 - 6.0	10 757
6.0 - 7.0	10 283
7.0 - 8.0	9 924
8.0 - 9.0	5 419
9.0 - 10.0	5 116
11.0 - 12.0	1 916
13.0 - 14.0	436
15.0 - 16.0	487
17.0 - 18.0	0
19.0 - 20.0	0

MEN'S BATHING POND, HAMPSTEAD HEATH (MEN 2) - 10/87

Sed. Depth (cm)	Particle No.(gDM^{-1})
0.0 - 1.0	77 507
1.0 - 2.0	76 563
2.0 - 3.0	91 359
3.0 - 4.0	89 352
4.0 - 5.0	98 765
5.0 - 6.0	86 177
6.0 - 7.0	66 185
7.0 - 8.0	94 068
8.0 - 9.0	91 202
9.0 - 10.0	73 478
14.0 - 15.0	64 456
19.0 - 20.0	101 035
24.0 - 25.0	91 080
29.0 - 30.0	77 301
34.0 - 35.0	109 352
39.0 - 40.0	120 666
44.0 - 45.0	123 642
49.0 - 50.0	93 663
54.0 - 55.0	76 673
59.0 - 60.0	69 657
69.0 - 70.0	34 274
79.0 - 80.0	26 084
89.0 - 90.0	20 257
99.0 - 100	10 011
109 - 110	12 762
119 - 120	8 584

LOUGH MAUMWEE (MAUW 1) - 5/88

Sed. Depth (cm)	Particle No. (gDM^{-1})
0.0 - 0.5	4 612
1.0 - 1.5	4 821
2.0 - 2.5	3 184
3.0 - 3.5	1 497
4.0 - 4.5	888
6.0 - 6.5	936
8.0 - 8.5	838
10.0 - 10.5	1 096
12.5 - 13.0	694
15.0 - 15.5	721
17.5 - 18.0	497
20.0 - 21.0	104
23.0 - 24.0	0
26.0 - 27.0	0

LOUGH MUCK (MUCK 2) - 5/88

Sed. Depth (cm)	Particle No. (gDM^{-1})
0.0 - 0.5	5 844
0.5 - 1.0	5 609
1.5 - 2.0	9 174
2.0 - 2.5	3 962
2.5 - 3.0	5 740
3.0 - 3.5	4 642
4.0 - 4.5	4 335
6.0 - 6.5	6 093
8.0 - 8.5	3 321
10.0 - 10.5	631
12.0 - 12.5	1 974
14.0 - 14.5	452
16.0 - 16.5	1 026
20.0 - 21.0	1 335

LOUGH NAMMINA (NAMM 1) - 5/88

Sed. Depth (cm)			Particle No. (gDM^{-1})
0.0	-	1.0	5 363
1.0	-	2.0	6 043
2.0	-	3.0	5 460
3.0	-	4.0	4 859
4.0	-	5.0	3 183
5.0	-	6.0	3 883
6.0	-	7.0	1 956
7.0	-	8.0	861
8.0	-	9.0	539
9.0	-	10.0	336

ROUND LOCH OF GLENHEAD (RLGH 88) - 10/88

Sed. Depth (cm)			Particle No. (gDM^{-1})
0.0	-	0.5	50 999
0.5	-	1.0	98 391
1.0	-	1.5	115 020
1.5	-	2.0	112 359
2.0	-	2.5	75 103
2.5	-	3.0	64 989
3.0	-	3.5	49 392
3.5	-	4.0	37 026
4.0	-	4.5	34 657
4.5	-	5.0	24 030
5.0	-	6.0	16 604
6.0	-	7.0	11 653

RÖYRTJÖRNA (ROY 1) - 7/88

Sed. Depth (cm)			Particle No. (gDM^{-1})
0.0	-	0.5	1 463
0.5	-	1.0	1 649
1.0	-	1.5	1 543
1.5	-	2.0	694
2.0	-	2.5	768
2.5	-	3.0	674
3.0	-	3.5	691
3.5	-	4.0	316
4.0	-	4.5	158
4.5	-	5.0	27
24.0	-	25.0	0

LOCH SAUGH (SAUG 1) - 12/8/89

Sed. Depth (cm)			Particle No. (gDM^{-1})
0.0	-	0.5	5 771
0.5	-	1.0	5 938
1.0	-	1.5	6 675
1.5	-	2.0	6 682
2.0	-	2.5	5 151
3.0	-	3.5	6 028
4.0	-	4.5	3 422
6.0	-	7.0	3 910
8.0	-	9.0	3 865

LOCH TEANGA (TEAN 5) - 9/87

Sed. Depth (cm)			Particle No. (gDM^{-1})
0.0	-	0.5	3 040
0.5	-	1.0	2 835
1.0	-	1.5	2 960
1.5	-	2.0	2 140
2.0	-	2.5	1 828
2.5	-	3.0	2 071
3.0	-	3.5	1 997
3.5	-	4.0	1 403
4.0	-	4.5	1 102
4.5	-	5.0	976
5.5	-	6.0	787
6.5	-	7.0	571
7.5	-	8.0	395
8.5	-	9.0	793
9.5	-	10.0	168
10.5	-	11.0	153
11.5	-	12.0	326
12.5	-	13.0	74
13.5	-	14.0	0

LOCH TINKER (TIN 1) - 20/6/85

Sed. Depth (cm)			Particle No. (gDM^{-1})
0.0	-	0.5	70 073
0.5	-	1.0	60 634
1.0	-	1.5	40 287
1.5	-	2.0	32 017
2.5	-	3.0	31 471
3.5	-	4.0	29 002
4.5	-	5.0	45 947
5.5	-	6.0	12 722
6.5	-	7.0	9 660
7.5	-	8.0	9 652
8.5	-	9.0	9 859

LOCH TINKER (cont.)

9.5	-	10.0	5 250
10.5	-	11.0	4 304
11.5	-	12.0	8 303
12.5	-	13.0	3 649
13.5	-	14.0	1 280
14.5	-	15.0	1 314
15.5	-	16.0	633
16.5	-	17.0	1 101
17.5	-	18.0	1 740
18.5	-	19.0	293
19.5	-	20.0	174
20.0	-	21.0	400
21.0	-	22.0	133
22.0	-	23.0	68
23.0	-	24.0	29
24.0	-	25.0	0

TUNNEL END RESERVOIR (TUNN 2) - 1989

Sed. Depth (cm)			Particle No. (gDM^{-1})
0.0	-	0.5	9 973
1.0	-	1.5	12 742
2.0	-	2.5	18 552
3.0	-	3.5	15 863
4.0	-	4.5	15 400
6.0	-	6.5	12 779
8.0	-	8.5	17 404
10.0	-	10.5	12 915
12.5	-	13.0	8 483
15.0	-	15.5	17 175
17.5	-	18.0	10 055
20.0	-	21.0	22 524
23.0	-	24.0	21 040
26.0	-	27.0	25 211
29.0	-	30.0	7 771
31.0	-	32.0	7 736

LOCH UISGE (UIS 1) - 9/6/86

Sed. Depth (cm)	Particle No. (gDM^{-1})
0.0 - 0.5	4 762
1.0 - 1.5	5 674
2.0 - 2.5	6 002
3.0 - 3.5	4 935
4.0 - 4.5	3 775
6.0 - 6.5	1 653
8.0 - 8.5	1 943
10.0 - 11.0	1 994
12.0 - 13.0	618
14.0 - 15.0	502
16.0 - 17.0	641
18.0 - 19.0	485
20.0 - 21.0	254
22.0 - 23.0	456
24.0 - 25.0	124
26.0 - 27.0	37

LOUGH VEAGH (VEAGH 2) - 5/88

Sed. Depth (cm)	Particle No. (gDM^{-1})
0.0 - 0.5	4 279
0.5 - 1.0	11 840
1.0 - 1.5	10 878
1.5 - 2.0	9 367
2.0 - 2.5	6 887
2.5 - 3.0	6 907
3.0 - 3.5	5 378
5.0 - 5.5	1 671
7.0 - 7.5	1 211
8.0 - 8.5	1 005
9.0 - 9.5	564
10.0 - 10.5	1 319
12.0 - 12.5	138
14.0 - 14.5	55

LOCH WALTON (WALT 1) - 11/9/89

Sed. Depth (cm)	Particle No. (gDM^{-1})
0.0 - 0.5	51 139
0.5 - 1.0	51 638
1.0 - 1.5	52 275
1.5 - 2.0	40 041
2.0 - 2.5	35 954
3.0 - 3.5	22 321
4.0 - 4.5	10 964
6.0 - 7.0	6 478
8.0 - 9.0	3 163

WHITFIELD LOUGH (WHIF 1) - 6/89

Sed. Depth (cm)	Particle No. (gDM^{-1})
0.0 - 0.5	36 841
0.5 - 1.0	37 300
1.0 - 1.5	26 622
1.5 - 2.0	20 311
2.0 - 2.5	23 018
3.0 - 3.5	13 600
4.0 - 4.5	4 747
6.0 - 7.0	2 461
8.0 - 9.0	2 002

APPENDIX C.

INORGANIC ASH SPHERE CONCENTRATIONS FOR SEDIMENT CORES DESCRIBED IN THE TEXT

MEN'S BATHING POND, HAMPSTEAD HEATH (MEN 2) - 10/87

Sed. Depth (cm)	Particle No. (gDM^{-1})
0.0 - 1.0	112 527
1.0 - 2.0	75 172
2.0 - 3.0	106 582
3.0 - 4.0	62 488
4.0 - 5.0	64 624
5.0 - 6.0	70 434
6.0 - 7.0	64 629
7.0 - 8.0	70 545
8.0 - 9.0	59 293
9.0 - 10.0	52 183
14.0 - 15.0	53 447
19.0 - 20.0	89 454
24.0 - 25.0	121 324
29.0 - 30.0	68 374
34.0 - 35.0	33 875
39.0 - 40.0	41 771
44.0 - 45.0	70 728
49.0 - 50.0	37 525
54.0 - 55.0	37 328
59.0 - 60.0	46 620
69.0 - 70.0	39 008
79.0 - 80.0	21 008
89.0 - 90.0	19 715
99.0 - 100	13 962
109 - 110	6 114
119 - 120	13 060

LOCH TEANGA (TEAN 5) - 10/87

Sed. Depth (cm)	Particle No. (gDM^{-1})
0.0 - 0.5	23 801
0.5 - 1.0	18 400
1.0 - 1.5	25 215
1.5 - 2.0	21 329
2.0 - 2.5	16 903
2.5 - 3.0	20 216
3.0 - 3.5	16 533
3.5 - 4.0	11 875
4.0 - 4.5	11 185
4.5 - 5.0	8 055
5.5 - 6.0	5 869
6.5 - 7.0	5 598
7.5 - 8.0	3 179
8.5 - 9.0	2 919
9.5 - 10.0	2 025
10.5 - 11.0	2 612
11.5 - 12.0	1 471
12.5 - 13.0	1 612
13.5 - 14.0	1 481
14.5 - 15.0	1 329
20.0 - 21.0	1 243
25.0 - 26.0	1 216
30.0 - 31.0	1 259
39.0 - 40.0	1 256

LOCH TINKER (TIN 1) - 20/6/85

Sed. Depth (cm)	Particle No. (gDM^{-1})
0.0 - 0.5	344 300
1.0 - 1.5	285 300
2.0 - 2.5	250 500
3.0 - 3.5	243 500
4.5 - 5.0	257 300
5.0 - 5.5	65 530
6.0 - 6.5	86 560
7.0 - 7.5	70 880
8.0 - 8.5	72 790
9.5 - 10.0	65 310
10.5 - 11.0	57 170
11.0 - 11.5	56 700
12.0 - 12.5	35 230
13.0 - 13.5	38 150
14.0 - 14.5	22 790
15.0 - 15.5	30 490
16.0 - 16.5	24 390
17.0 - 17.5	22 850
18.0 - 18.5	14 170
19.0 - 19.5	26 180
20.0 - 21.0	13 950
21.0 - 22.0	6 508
22.0 - 23.0	12 530
24.0 - 25.0	7 650
30.0 - 31.0	2 822
40.0 - 41.0	2 637
50.0 - 51.0	3 271
60.0 - 61.0	7 250
80.0 - 81.0	2 323
100 - 101	3 759

Journal of Paleolimnology 3: 45–53, 1990.

A method for the extraction of carbonaceous particles from lake sediment

N.L. Rose
Palaeoecology Research Unit, Department of Geography, University College London, 26 Bedford Way, London WC1H OAP, England

Received 3 July 1989; accepted 9 September 1989

Key words: carbonaceous particles, extraction methods, lake sediment, Loch Tinker

Abstract

The methods found in the literature for the extraction of carbonaceous particles from lake sediment are discussed. The technique used by Griffin & Goldberg (1975) on Lake Michigan sediments was improved by modifying the procedure to halve the extraction time and reduce the risk of fragmentation. This method was then applied to a sediment core taken from Loch Tinker in Western Scotland, which had previously been analysed using the Renberg & Wik method. Although the basic trends for both methods are the same, the new method is found to be more sensitive to low particle numbers and more accurate, due to a more efficient extraction and a higher magnification for microscope counting.

Introduction

Lake sediments provide a record of atmospheric contamination and so have been important in recent studies on surface water acidification. Carbonaceous particles derived from fossil-fuel combustion are found in considerable numbers in the recent sediment of cores taken from areas with high acid deposition (Griffin & Goldberg, 1981; Renberg & Wik, 1984). Sites in the United Kingdom show close correlation between the onset of atmospheric contamination as indicated by carbonaceous particles, heavy metals etc., and the acidification of lakes as indicated by diatom analysis (Battarbee *et al.*, 1988).

The particulate emissions from high temperature fossil fuel combustion can be divided into two groups: carbonaceous particles, which are composed mainly of elemental carbon (Goldberg, 1985); and mineral ash spheres, which are formed by the fusing of inorganic minerals within the fuel (Raask, 1984). Of the three fossil fuels commonly used in the UK, only coal and oil produce spherical carbonaceous particles. Those produced from peat combustion have an amorphous appearance, many still retaining some cellular structure.

In order to make an accurate count of these particles, and to characterise them into fuel type by using energy dispersive X-ray analysis (EDAX), it is first necessary to concentrate the particles to a much higher extent than that in which they occur in lake sediments. Elemental carbon is resistant to chemical attack and so unwanted fractions of the sediment can be removed by selective digestion. This paper describes previous extraction methods and proposes modifications which enable particle concentrations to be calculated with a high degree of sensitivity and precision.

Background and previous methods

Smith *et al.* (1975) first produced a method for the extraction of elemental carbon from marine sediments. An acid treatment with hydrofluoric and hydrochloric acids was used to remove some mineral species and a basic peroxide treatment was used if organic material was present. The remaining carbon material was ground up and Infra-Red spectroscopy was used to determine quantitatively the elemental carbon levels. This method was adapted by Griffin & Goldberg (1975) for coastal marine sediments, where there was a higher organic content, and again I-R spectroscopy was used to determine elemental carbon fluxes. This carbonaceous material was thought to be principally from forest fires, as concentrations increased on a latitudinal basis; particles being transported by the major wind systems. However, it was also suggested that the more spherical and perforated particles might have been formed by high temperature fossil fuel combustion.

Griffin & Goldberg (1979), then turned to the freshwater sediments of Lake Michigan. The elemental carbon particles were extracted and compared against oil, coal and wood fly-ash. It was concluded that forest and grass burning could contribute a significant amount of carbonaceous material to the atmosphere, but the concentration of the 'spherical' carbon particles reflected the history of fossil fuel combustion in the area. Similar results were obtained at Green Lake, New York (Kothari & Wahlen, 1984), where a similar digestion technique to that of Griffin & Goldberg, was employed except that nitric acid was used to remove the organic fraction instead of basic peroxide.

Goldberg *et al.* (1981), showed that the concentration of certain trace elements, such as tin, chromium, nickel, lead, copper, cobalt, cadmium, zinc and iron, showed a similar profile in the sediment to carbonaceous particles. Magnetic mineral ash spherules, which were formed by the oxidation of iron minerals in the furnace to haematite (Fe_2O_3) and magnetite (Fe_3O_4), were also correlated.

Griffin & Goldberg (1983) later used sphericity and surface morphology to separate anthropogenic particles into coal, oil and wood/coal. Nine classifications were used depending on shape and surface texture of the particles. Sub-micron spherical carbon particles, which had aggregated into chains (i.e. soot), were extracted from Lake Michigan sediment using a similar chemical technique. These particles showed a constant concentration over the previous 40 years and were attributed to material transported over a long distance before deposition.

In Sweden, an alternative method of carbonaceous particle concentration determination was developed, using hydrogen peroxide (H_2O_2) to remove organic material, followed by direct counting of a small fraction of the residue to obtain the number of particles per gram dry weight of sediment (Renberg & Wik, 1985a). This was used as an indirect dating method by matching concentration levels with that of a core previously dated by varve counting. As for Lake Michigan (Griffin & Goldberg, 1975, 1979, 1983; Goldberg *et al.*, 1981) and Green Lake (Kothari & Wahlen, 1984), the elemental carbon concentrations were found to reflect the increase of industrial activity and the fossil fuel combustion history of the twentieth century (Wik *et al.*, 1986). Apart from this temporal distribution of carbonaceous particles, there was also seen to be a spatial distribution which reflected the industrial regions of Sweden. This was seen in both lake sediments (Renberg & Wik, 1985b) and forest soils (Wik & Renberg, 1987).

The work so far on carbonaceous particles in lake sediments in Britain has been done using the Renberg and Wik method. The lakes involved have been principally in Scotland (Wik *et al.*, 1986; Darley, 1985; Battarbee *et al.*, in press) and Wales (unpub. data). Here also, the carbonaceous particle record follows the history of fossil-fuel burning. The record begins in the mid-nineteenth century at the time of the onset of the Industrial Revolution in Britain, and a sharp increase in concentration occurs after World War II which reflects the expansion of the power generation industry (Darley, 1985).

The method

The aim of this work was to develop a sensitive technique, based on particle concentrations, suitable for use even at low carbonaceous particle numbers, by removing unwanted sediment material by selective chemical attack. Neither of the two methods in the literature were perfectly suitable.

The Renberg and Wik method, due to the amount of residue left at the end of the digestion, is insensitive at low particle concentrations and counting at $\times 50$ will miss particles in the $< 10\ \mu m$ fraction.

The method used by Griffin & Goldberg (1975) deals with all charcoal, not just spherical particles produced from high temperature combustion, and so the results are expressed in per cent carbon by weight, rather than particle concentration. Also, only the $> 38\ \mu m$ fraction is considered, which excludes many smaller particles and preferentially those which are oil derived.

However, this method reduces 10 g of dried Lake Michigan sediment to 10–30 mg of some of the more persistent minerals, primarily pyrite (FeS_2), anatase and rutile (TiO_2) and zircon ($Zr(SiO_4)$), but most importantly elemental carbon. It involves a more complete digestion than that of Renberg and Wik and therefore is used as the basis of the method proposed here.

Laboratory procedure

1) Place 0.2 g of dried sediment in a covered 250 ml beaker.
   Add 30 ml 6 M KOH and 4 ml 30% H_2O_2.
   Leave overnight and then centrifuge at 2000 rpm (RCF = 650 g) for 5 minutes at room temperature. Rinse the walls of the beaker and wash the residue twice with distilled water.
   Return the residue to the beaker.

This stage breaks up the sediment for further reaction and removes some of the organic and humic fractions. The use of 10 g of dried sediment (Smith *et al.*, 1975) and involving large quantities of reagents is unnecessary. As replicate digestions were to be done, an arbitrary value of 0.2 g of dried sediment was decided upon and the reagent quantities reduced to match. 250 ml beakers were used as in some samples violent effervescence causes some of the material to be lost in smaller containers. Griffin & Goldberg used ultrasonic dispersion to break up the sediment in the early stages of their digestion. However, carbonaceous particles are quite fragile physically and this can cause fragmentation. As they ground up the eventual residue for infrared analysis, this was not important, but for this study, the particles are required whole and so ultrasonic dispersion was not used. It was found that the first basic peroxide step broke up the sediment satisfactorily.

2) Add 30 ml 6 M HCl to the residue.
   Heat on a hotplate at 80 °C for 2 hours.
   When cool, centrifuge and wash as before.

This removes the HCl soluble salts, such as carbonates and bicarbonates, and removes the soluble materials that may form insoluble fluorides in the next step.

3) Transfer the residue to PTFE (teflon) beakers (with PTFE lids).
   Add 20 ml 40% HF and heat on a hotplate at 150 °C for 3 hours. Wash as before.

This breaks down the siliceous minerals and removes the silicon as SiF_4. The time was reduced (compared to the Griffin & Goldberg method) by changing the hydrofluoric acid step from 6 days at room temperature to 3 hours at 150 °C. Using SEM, this change showed no effect on the particles and almost halves the length of the digestion, which can now be completed in 6–7 days.

4) Return the residue to the 250 ml beakers.
   Add 30 ml 6 M HCl and heat on a hotplate at 80 °C for 2 hours.
   Wash the residue as before.

This step removes any fluorides formed in the last step.

5) Add 20 ml 6 M KOH and 25 ml 30% H_2O_2 in 5 ml aliquots, to the residue.
Leave overnight in an oven at 55 °C. Cool and wash the residue as before.

6) Transfer the residue to a 25 ml beaker and add 4 ml 6 M KOH and 1 ml 30% H_2O_2.
Leave overnight in an oven at 55 °C. When the reaction is complete, cool and wash again.

Steps 5 & 6 remove the remaining organic and humic matter.

7) Add 10 ml 6 M HCl and heat on a hotplate for 2 hours at 80 °C.
Wash again. Transfer the residue to storage vessel.

(N.B. All containers should be kept covered to stop possible atmospheric contamination. The presence of carbonaceous particles in dust shows the need for a dust free preparation room.)

Density separations

Further extraction of the material by density separation was considered. However, due to the high variability of 'apparent' density of the carbonaceous particles, this idea was discarded. Carbonaceous particles with internal gas pockets and with no opening to the exterior would give the particle a density of approximately 1 g cm^{-3}. Fragmented particles and those having open structures would have the density of elemental carbon i.e. 2–3 g cm^{-3} and others with varying pore sizes would have a density between these two extremes.

Also, although the minerals remaining at the end of the digestion have a higher density than that of elemental carbon, there is a sufficiently small amount of them that it does not seem worth the extra time and potential loss of recovery to include density separation in the standard digestion technique. However, for sediments with an exceptionally high concentration of these minerals, a density separation could be used.

Filtration

After digestion there is a great deal of fine, amorphous, black material present in some layers and this can cause problems in the counting stage by obscuring the shapes of the particles. This material does not always follow the same trends as the carbonaceous particle record as there is sometimes little in the surface layers. Therefore, it seems that it is not of the same origin as the particles and it has been thought it may be a precipitation product of the digestion technique itself (Renberg, pers. commun.). As it is fine material, the obvious way to remove it is by filtration. This will enable a higher fraction of the residue to be counted, increasing repeatability, as well as making counting easier. However, filtration also removes the smaller carbonaceous particles, 10 μm and 5 μm filters reducing the recovery rate to 40% and 65% respectively. As carbonaceous particles from oil combustion are usually smaller than those from coal, this approach may selectively remove oil particles from the residue, making filtration of limited use.

Effects of the method on the carbonaceous particles

In order to see the effect of the method on the carbonaceous particles, a sediment sample was spiked with material from a coal fired power station. In this way, the particle characteristics could be compared before and after digestion. Scanning electron microscopy and EDAX analysis on the carbonaceous particles showed that the extraction technique has no apparent effect on particle morphology or chemistry. Figures 1a and 1b show photographs and EDAX spectra of two coal fired power station particles before and after digestion respectively.

Counting

A known fraction (determined by the weight difference before and after sub-sampling) of the remaining residues were evaporated onto cover-

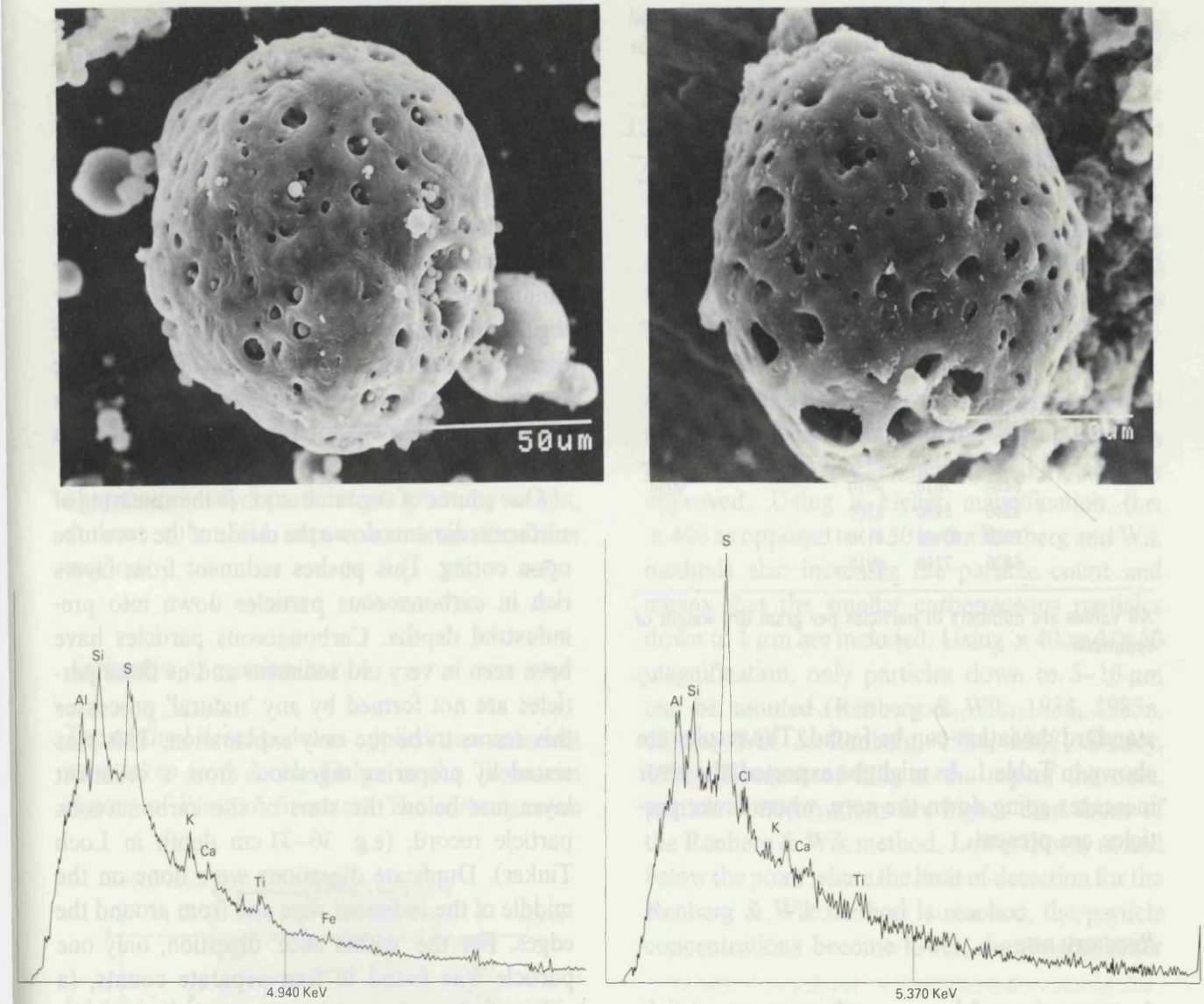

Fig. 1. SEM photographs and EDAX spectra of carbonaceous particles from a coal fired power station, before (a), and after (b), application of the digestion technique.

slips. These were then mounted using 'Naphrax' diatom mountant, and the whole of each coverslip counted at ×400 using a light microscope. Random views were not used, as at the bottom of the particle record, where there was either one or zero particles to be counted on the whole coverslip, this raised the limit of detection. Also, this negated any effect aggregation might have on random view counting. The method of adding a known amount of polystyrene microspheres and calculating the number of carbonaceous particles from the ratio (Battarbee & Kneen, 1982) was found to have higher errors, especially at low concentrations. Only spherical particles, or particle fragments greater than half a sphere were counted. This was to avoid multiple counts for one particle should large particles break up during the digestion process.

Repeatability

To find if separate digestions of a sediment sample would give the same particle concentrations, 5 replicate digestions from 3 different sediment levels were done. This was followed by triplicate counts from each digestion. This then gives 15 concentrations for each level from which the

Table 1. Replicate counts, means, standard deviations and 95% confidence limits on the statistical counting error for three different sediment levels in Loch Tinker.

Level	Counts			Mean	S.D.	95% C.L.
0–0.5 cm	61280	73390	69000	70070	6400	68040–
	68130	75690	74800			71660
	66070	70140	74500			
	55270	66380	66120			
	75270	76430	78660			
4.5–5 cm	41980	52240	40970	45950	4930	43980–
	33620	45710	46430			47760
	45420	49760	48300			
	52030	42960	47820			
	44100	46000	51870			
11.5–12 cm	8940	8350	8470	8300	1020	7460–
	6480	7610	9610			9030
	8240	8890	8500			
	7430	10440	8130			
	6820	7740	8910			

All values are numbers of particles per gram dry weight of sediment.

standard deviation can be found. The results are shown in Table 1. As might be expected, the error increases going down the core, where fewer particles are present.

Recovery rate

A suspension of known carbonaceous particle concentration was made up by adding a small amount of oil-fired residue from a power station to water and homogenising the solution. A known fraction was then removed and counted at $\times 400$ under a light microscope. The concentration of the solution could then be calculated. A known number of particles from this solution were added to a sediment sample before digestion. The sediment sample was from sufficiently low down the core that it could be assumed that no carbonaceous particles were present within it. After the digestion, the number of particles was counted as before and the numbers were compared to give a recovery rate. The digestions were done in triplicate and the recovery range was from 93.9%–100.1%, showing that very few particles are lost during the digestion. This is confirmed by taking the supernatant fraction from each stage (usually discarded) and centrifuging at 2000 rpm until a residue is deposited. Using SEM, the residue showed no particles on any size to be present in the supernatant fractions of any stage of the digestion.

Blank digestions were also done (i.e. no sediment involved), to check on atmospheric contamination and cross contamination from other digestions. These showed that as long as the digestion vessels are kept covered and reasonable precautions taken in manipulating the digestion material, no atmospheric or cross contamination occurs.

One source of contamination is the smearing of surface sediments down the inside of the core tube upon coring. This pushes sediment from layers rich in carbonaceous particles down into pre-industrial depths. Carbonaceous particles have been seen in very old sediment and as these particles are not formed by any 'natural' processes this seems to be the only explanation. This was tested by preparing digestions from a sediment layer just below the start of the carbonaceous particle record, (e.g. 30–31 cm depth in Loch Tinker). Duplicate digestions were done on the middle of the sediment slice and from around the edges. For the 'within slice' digestion, only one particle was found in four separate counts, (a value of about 8 particles per gram dry weight), but particles resulting in a value of about 200 particles per gram dry weight (gDW^{-1}) were counted on the 'slice edge' samples. This shows smearing does take place, and at lower levels within the carbonaceous particle record could have a significant effect on particle number calculations, demonstrating the need for 'trimming' core slices, i.e. using sediment from the interior of the core only.

Detection limit

The Renberg & Wik method, removing as it does, only the organic fraction from the sediment, leaves a large amount of material at the end of a digestion. Therefore, unless a very long time is

spent counting each sample, only a small fraction of the residual material will be counted and hence the limit of detection is quite high i.e. if only 1 particle is counted in the residual sample fraction, the result is a value of 80–100 particles per gram dry weight.

Using the method described above, the material remaining after digestion is predominantly carbonaceous. Therefore, at the bottom of the core, very little material remains and if so desired, 100% of this material could be counted in a fairly short space of time. As approximately 0.2 g of dried sediment is used for the digestion if only 1 particle is counted, this will give a detection limit of approximately 5 particles per gram dry weight, at least a ten-fold improvement on the other method.

Application to a sediment core

The method described was applied to a sediment core taken from Loch Tinker in the Trossachs regions of Western Scotland. The carbonaceous particle record has previously been counted using the Renberg and Wik method so a comparison between the two methods can be drawn. The core was also dated using ^{210}Pb and the results are shown in Fig. 2. There are several points to note:

i) The basic trends are the same for both methods. i.e. the carbonaceous particle record begins in the early nineteenth century and there is a large rise in concentration after the 1940's.

ii) As a higher percentage of the digested material is available to be counted all the way up the core, particle counts are higher and the accuracy improved. Using a higher magnification (i.e. × 400 as opposed to × 50 in the Renberg and Wik method) also increases the particle count and means that the smaller carbonaceous particles down to 1 μm are included. Using × 40 and × 50 magnification, only particles down to 5–10 μm can be counted (Renberg & Wik, 1984, 1985a, 1985b; Wik & Renberg, 1984, 1987; Darley, 1985). Because of this, at the top of the core, particle concentrations are higher than those of the Renberg & Wik method. Lower down, at and below the point where the limit of detection for the Renberg & Wik method is reached, the particle concentrations become lower, due to the better

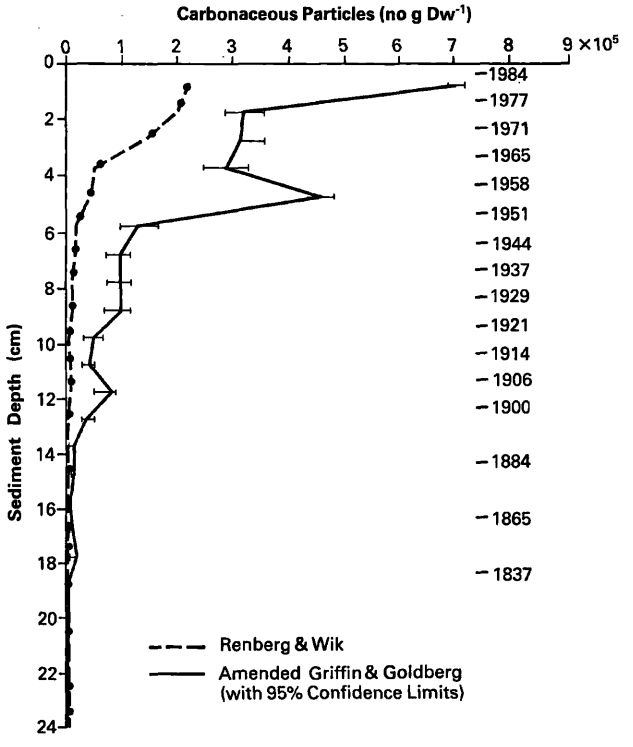

Fig. 2. Comparison of the two methods using Loch Tinker sediments.

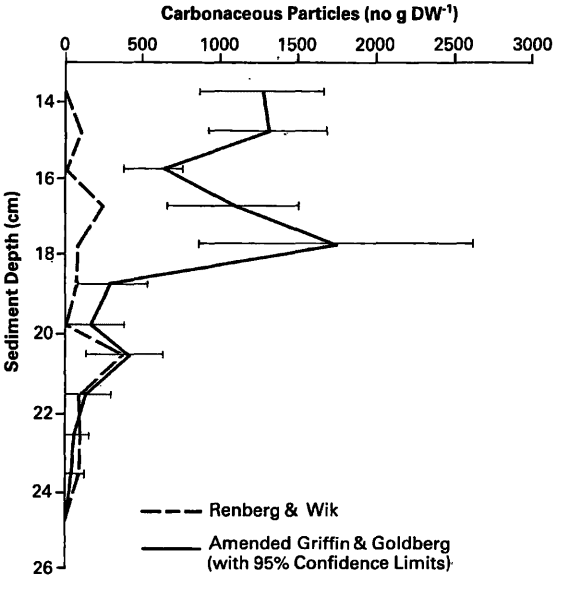

Fig. 3. Expanded bottom section of the Loch Tinker profile to compare the detection limits of the two methods.

sensitivity of the method described here. This is best illustrated in an expanded bottom section of the graph, (See Fig. 3). Consequently, there is no single factor by which it is possible to convert the numbers obtained in one method to that of the other, without redigesting and recounting the material.

Conclusions

The method described above, has a number of advantages over previous methods used to extract carbonaceous particles from sediments. It is more accurate and has a lower detection limit than the Renberg and Wik method previously used on British lakes, and it is quicker and involves less risk of fragmentation of the particles than the Griffin and Goldberg method upon which it is based.

Although the majority of the residue at the end of the digestion is carbonaceous material, the extraction is not perfect and some minerals survive albeit in low concentrations. This includes some silicates, and even one or two siliceous spheres may appear in the residue, due to particles being washed in from the beaker walls after the HF digestion step. This is not particularly important as the remaining non-carbonaceous material is sufficiently different both chemically and morphologically, that the counting and EDAX procedures will not be confused by their presence.

Acknowledgements

Dr. R.W. Battarbee contributed ideas and provided valuable criticism on the manuscript. I am also grateful to J. Natkanski for allowing me to use her data and to P. Appleby who dated the sediment core. The EDAX spectra were obtained with the help of J. Watt at Imperial College. Technical help in the laboratory was given by S. Phethean and D. Monteith, and the diagrams were drawn by L. McClue and T. Aspden. This work forms part of a study funded by the CEGB.

References

Battarbee, R. W. & M. J. Kneen, 1982. The use of electronically counted microspheres in absolute diatom analysis. Limnol. Oceanogr. 27 (1): 184–188.

Battarbee, R. W., N. J. Anderson, P. G. Appleby, R. J. Flower, S. C. Fritz, E. Y. Haworth, S. Higgitt, V. J. Jones, A. Kreiser, M. A. R. Munro, J. Natkanski, F. Oldfield, S. T. Patrick, N. G. Richardson, B. Rippey, A. C. Stevenson, 1988. Lake Acidification in the United Kingdom 1800–1986. Ensis Publishing. London, 68 pp.

Battarbee, R. W., C. Fletcher, R. J. Flower, J. Natkanski, B. Rippey, A. C. Stevenson, M. Wik, (in press). Causes of lake acidification in Galloway, south-west Scotland: a palaeoecological evaluation of the relative roles of atmospheric contamination and catchment change for two acidified sites with non-afforested catchments. J. Ecol.

Darley, J., 1985. Particulate soot in Galloway lake sediments. Its application as an indicator of environmental change and as a technique for dating recent sediments. Dept. of Geog. University College London. B301 Project.

Goldberg, E. D., 1985. Black carbon in the environment: Properties and Distribution. Wiley Interscience Publication. N.Y., 198 pp.

Goldberg, E. D., V. H. Hodge, J. J. Griffin & M. Koide, 1981. Impact of fossil fuel combustion on the sediments of Lake Michigan. Envir. Sci. Technol. 15 (4): 466–470.

Griffin, J. J. & E. D. Goldberg, 1975. The fluxes of elemental carbon in coastal marine sediments. Limnol. Oceanogr. 20: 256–263.

Griffin, J. J. & E. D. Goldberg, 1979. Morphologies and origin of elemental carbon in the environment. Science 206: 563–565.

Griffin, J. J. & E. D. Goldberg, 1981. Sphericity as a characteristic of solids from fossil fuel burning in a Lake Michigan sediment. Geochim. et Cosmochim. Acta. 45: 763–769.

Griffin, J. J. & E. D. Goldberg, 1983. Impact of fossil fuel combustion on the sediments of Lake Michigan: A reprise. Envir. Sci. Technol. 17 (4): 244–245.

Kothari, B. K. & M. Wahlen, 1984. Concentration and surface morphology of charcoal particles in sediments of Green Lake, New York. Implications regarding the use of energy in the past. Northeastern Envir. Sci. 3 (1): 24–29.

Raask, E., 1984. Creation, capture and coalescence of mineral species in coal flames. J. Inst. Energy. 57: 231–239.

Renberg, I. & M. Wik, 1984. Dating of recent lake sediments by soot particle counting. Verh. int. Ver. Limnol. 22: 712–718.

Renberg, I. & M. Wik, 1985a. Soot particle counting in recent Lake Sediments. An indirect dating method. Ecol. Bull. 37: 53–57.

Renberg, I. & M. Wik, 1985b. Carbonaceous particles in lake sediments – Pollutants from fossil fuel combustion. Ambio. 14 (3): 161–163.

Smith, D. M., J. J. Griffin & E. D. Goldberg, 1975. Spectrophotometric method for the quantitative determination of elemental carbon. Analyt. Chem. 47 (2): 233–238.

Wik, M. & I. Renberg, 1987. Distribution in forest soils of carbonaceous particles from fossil fuel combustion. Wat. Air Soil Pollut. 33: 127–129.

Wik, M., I. Renberg & J. Darley, 1986. Sedimentary records of carbonaceous particles from fossil fuel combustion. Hydrobiologia. 143: 387–394.

A method for the selective removal of inorganic ash particles from lake sediments

N. L. Rose
Palaeoecology Research Unit, Department of Geography, University College London, 26 Bedford Way, London WC1H OAP

Received 6 October 1989; in revised form 11 January 1990; accepted 25 March 1990

Key words: inorganic ash particles, extraction methods, lake sediments, Loch Tinker

Abstract

Inorganic ash particles are formed by the fusing of inorganic material present during the high temperature combustion of fossil fuels. As they accumulate in lake sediments, they record the history of atmospheric contamination produced from such sources. A technique has been developed for concentrating these particles from lake sediments involving the stepwise removal of unwanted components of the sediment, including organic material and biogenic silica.

When applied to a sediment core taken from Loch Tinker, central Scotland, a particle concentration profile, very similar to that of the carbonaceous particle profile (the other component of fossil-fuel combustion ash) is produced. The concentration of the inorganic ash spheres in the sediment is approximately an order of magnitude higher than the carbonaceous particles and there appears to be a continuous pre-industrial background value. This seems to imply a similar source (i.e. coal combustion rather than oil) for both inorganic ash and carbonaceous particles. This method has also been used with success on peat cores.

Introduction

Lake sediments provide a record of atmospheric contamination and have been important in recent studies of lake acidification. Carbonaceous particles derived from fossil-fuel combustion are found in considerable numbers in upper levels of lake sediment cores taken from areas with high acid deposition. At sites in the United Kingdom, there is close correlation between the onset of atmospheric contamination as indicated by fossil fuel derived particles, heavy metals and magnetic particle deposition, and the acidification of lakes as indicated by diatom analysis (Battarbee *et al.*, 1988; Jones *et al.*, 1990).

Inorganic ash spheres, like carbonaceous particles, are produced from the high temperature combustion of coal, oil and peat. They comprise over 80% of the particulates formed from coal combustion (Watt & Thorne, 1965), but much less in peat and only 0.1% in oil (Henry & Knapp, 1980).

To facilitate particle enumeration and determine an origin for these particles by using diagnostic chemical techniques such as energy dispersive X-ray analysis (EDAX), it is first necessary to concentrate the particles by removing unwanted fractions of the sediment.

This paper describes a concentrating technique and uses it to determine particle concentrations in

a sediment core taken from Loch Tinker, central Scotland.

Inorganic ash spheres in the environment

Ash spheres, generated in coal fired power stations, nearly all fall within the size range 0.05 μm–10 μm (McElroy *et al.*, 1982) and so will travel long distances in air streams. Industrially derived ash spheres have been found in virtually every environment. Their presence has been recorded in mid-ocean air samples (Folger, 1970; Parkin *et al.*, 1970), marine sediments in both coastal (Puffer *et al.*, 1980) and deep-sea areas (Fredriksson & Martin, 1963), ombotrophic peat bogs (Oldfield *et al.*, 1978, 1981), high latitude ice deposits, in both Greenland (Hodge *et al.*, 1964b) and the Antarctic (Hodge *et al.*, 1967, Fredriksson & Martin, 1963), as well as estuarine (Allen, 1987) and lake sediments (Puffer *et al.*, 1980, Nriagu & Bowser, 1969).

Natural sources of spherical inorganic particles in this size range include volcanic emissions (Lefèvre *et al.*, 1986) and micrometeorites (Hodge & Wright, 1964a), and so in a sediment profile it might be expected that a record of these particles exists at depths corresponding to pre-industrial times.

Development of the technique

Inorganic ash particles formed from coal combustion will be mostly aluminosilicate in composition with different amounts of iron depending on the inorganic inclusions present in the fuel. Thus, they have a similar chemistry to many of the minerals in the sediment and this restricts the range of reagents that can be used in the removal of unwanted fractions.

Concentration steps

Organic material can be removed by oxidation using 30% hydrogen peroxide (H_2O_2), at about 50–60 °C. Basic peroxide (a mixture of 6M KOH and 30% H_2O_2) and nitric acid (HNO_3) are more effective oxidants than H_2O_2 alone, but these etch the ash particle surfaces.

Biogenic silica, predominantly diatom frustules and chrysophyte cysts, can be removed from other forms of silica, such as mineral silica and non-crystalline or amorphous silica e.g. inorganic ash, by preferential digestion. Wet alkaline extractions are best for this purpose (Krausse *et al.*, 1983), other methods such as fusion and mineral acid attacks are not selective for different forms of silica.

Trials performed on lake sediment, spiked with some coal-fired power station ash (to ascertain the extent of etching on the spheres), compared the effect of different concentrations of sodium carbonate (Na_2CO_3) and sodium hydroxide (NaOH) at 100 °C for various lengths of time. Analyses for dissolved silica (Goltermann, 1970) were performed on sub-samples removed at intervals from the digestion supernate. When the dissolved silicate concentration stops increasing, biogenic silica dissolution has ceased. In most cases, silica dissolved from mineral sources is insignificant compared to the quantity of biogenic silica (Krausse *et al.*, 1983). If this were not the case, the silica concentration in the supernatant liquid would keep increasing with time rather than levelling off as occurs after about 2 hours. No etching of the ash particles occurred until after 6 hours and so 2 to 3 hours was the time selected for the technique.

Various techniques were tried to selectively remove silicate minerals and not the inorganic ash. Hydrofluoric acid (HF) has been used in other extractions to remove silicates as SiF_4, but is also very effective at dissolving the silicate ash and even at low concentrations such as a 1% solution, will etch the surface of the particles to reveal the underlying structure, of quartz (SiO_2) and mullite ($3Al_2O_3\,2SiO_2$) (Hullett & Weinberger, 1980). Fluorosilicic acid (H_2SiF_6) preferentially removes feldspars from quartz, but this also severely etched the ash spheres.

Pyrosulphate ($Na_2S_2O_7$) fusions (Chapman *et al.*, 1969; Kiely & Jackson, 1965), digested the

ash spheres as well as the minerals leaving only quartz grains, but a 2M solution had no effect on either ash spheres or silicate minerals. The same result occurred for pyrophosphate ($Na_4P_2O_7$) digestion attempts.

No satisfactory separation was achieved for mineral silicate and the inorganic ash spheres.

The strongest acid that dissolves carbonate and bicarbonate minerals, but leaves the ash spheres unaffected, was found to be 3M HCl at 80 °C for 2 hours.

Studies of the density of ash from power stations (Watt & Thorne, 1965) show that virtually no particles have a density greater than 2.9 g cm^{-3}. Thus, more dense minerals can be separated by using heavy liquids such as 1,1,2,2-tetrabromoethane (TBE) [$(CHBr_2)_2$] or sodium polytungstate [$3Na_2WO_4\ 9WO_3H_2O$]. The greater than 2.9 g cm^{-3} fraction removed from lake sediment, when viewed under SEM, reveals large angular mineral grains. No spheres were noted in the heavy fraction.

Sodium polytungstate has the advantages over TBE of being non-toxic and non-corrosive. Its density is adjustable up to 3.1 g cm^{-3}, it is neutral in aqueous solution and is stable in the pH range 2 to 14. It is very easy to handle, but quite viscous at these higher densities and so a centrifuge is required for effective separation. It is obtainable in powder form from: SOMETU, Falkenried 4, D-1000 Berlin 33, West Germany.

Magnetic separation can be attempted either by repeatedly swirling a covered magnet in a solution of the sediment, until no more magnetic particles are removed (Nriagu & Bowser, 1969), or by using a more sophisticated technique, such as an automated self-circulating magnetic separator (Munro & Papamarinopoulos, 1978). Both methods, however, only give a partial extraction, as some minerals and not all ash particles are magnetic.

Laboratory procedure

The technique described below removes at least 85% of unwanted material from dried lake sediment in four steps:

1) Place 0.2 g of dried sediment in a 250 ml beaker and add 50 ml 30% H_2O_2. Once the initial reaction has died down, place in an oven at 55 °C and leave overnight. If, after this, there is still effervescence, add another 10 ml of H_2O_2 and return to the oven. When there is no more effervescence, cool, centrifuge at 2000 r.p.m. (R.C.F. = 650 × g) for 5 minutes to settle the residue, and wash twice in distilled water.

2) Return the residue to the beaker, washing the centrifuge tube with a small amount of distilled water, and add 50 ml 0.3 M NaOH. Heat at 100 °C for 2.5 hours (including heating up time). Cool, centrifuge, and wash as before.

3) Density separation

a) with TBE. (density = 2.96 g cm^{-3})

i) Wash the residue twice with acetone to remove the water, as water and TBE are immiscible. Pipette off as much of the supernate as possible.

ii) Add 2 ml of TBE to a glass centrifuge tube and then carefully add the sediment residue, using a pipette.

iii) Gently centrifuge at 500 r.p.m. for 2 minutes.

iv) Pipette off the <2.96 fraction into another tube and then discard the >2.96 fraction.

v) Wash the <2.96 fraction in acetone to remove the TBE and then in water to remove the acetone.

b) with sodium polytungstate (density adjusted to 2.95 g cm^{-3})

i) Pipette off as much supernatant water from the residue as possible.

ii) Add 2 ml of polytungstate to a centrifuge tube and carefully add the residue using a pipette. The density of the polytungstate is not changed sufficiently so as to affect the separation process by this addition.

iii) Centrifuge at 500 r.p.m. for 2 minutes.

iv) Discard the >2.95 fraction.

v) Wash the lighter fraction in distilled water.

N.B. Both TBE and polytungstate are recoverable from these methods.

4) Pipette the residue into a 100 ml beaker, add 30 ml 3 M HCl and heat for 2 hours at 80 °C.

Wash twice with distilled water and centrifuge as before.

Counting

A known fraction of the final residue is evaporated on a coverslip, mounted with Naphrax (a diatom mountant, available from: Northern Biological Supplies, Martlesham Heath, Ipswich, U.K.) and the particles on the whole coverslip counted at × 400 using a light microscope. Polystyrene microspheres, used for calculating diatom concentrations (Battarbee & Kneen, 1982), were not used due to their similar appearance to the ash spheres. A known concentration of exotic spores could be added to count in this way, but large counting errors would be introduced when ash sphere concentrations are low.

At each stage of the development of the method, samples were checked under the SEM (Fig. 1) to see the effect of the treatment upon the particles. There is no visible effect on the particles, and using EDAX there appears to be no chemical effect either.

Five replicate digestions from three sediment levels were done, followed by triplicate counts from each digestion. This gave 15 particle concentrations for each level from which 95% confidence limits on the statistical counting error were calculated (Table 1).

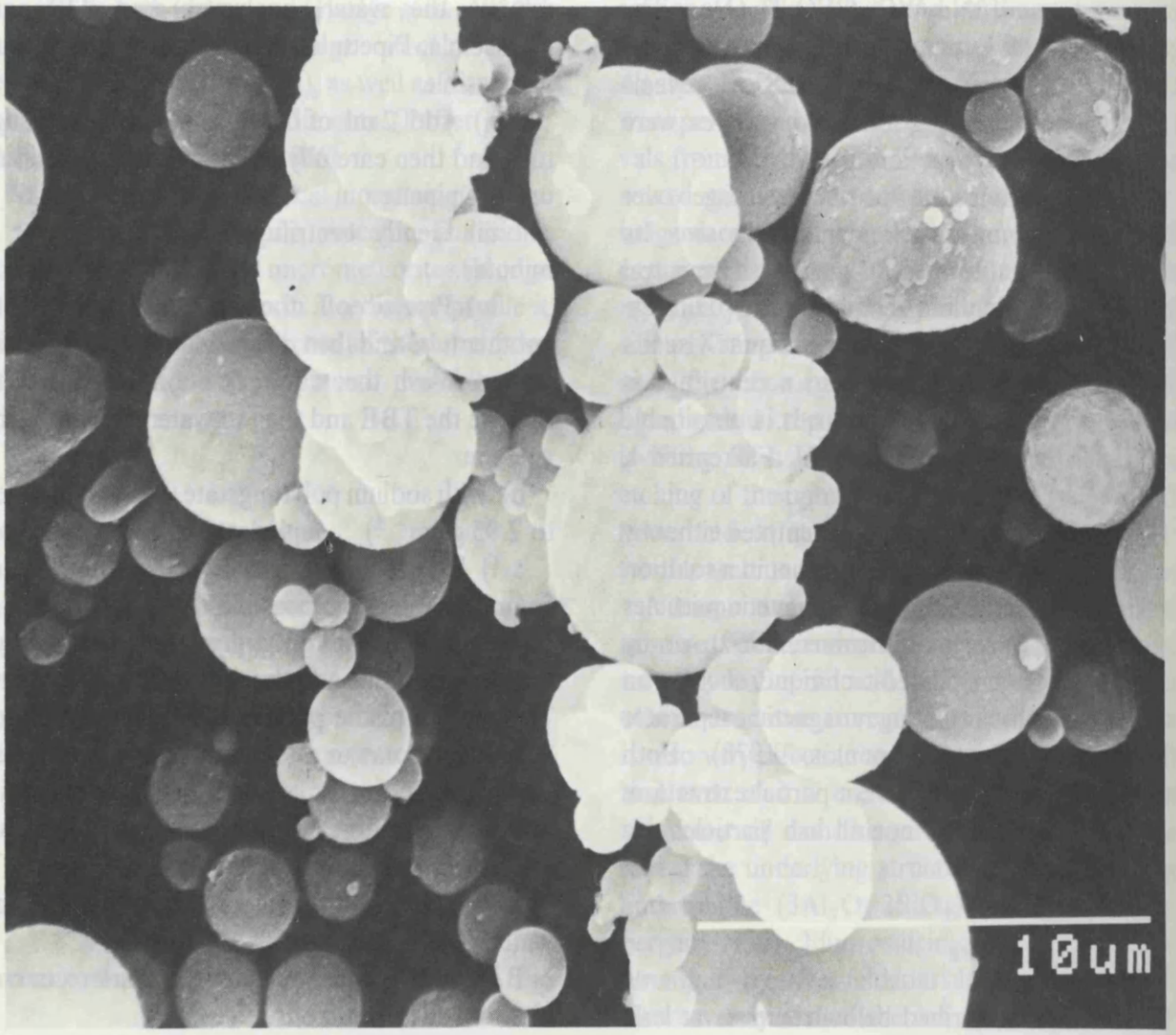

Fig. 1. Scanning electron microscope photograph of inorganic ash spheres formed during high temperature fossil fuel combustion.

Table 1. Means, standard deviations and 95% confidence limits on the statistical counting error for inorganic ash sphere counts from three different sediment levels in Loch Tinker. All values as concentrations per gram dry weight of lake sediment.

Level	Mean	S.D.	95% Confidence
4.5– 5.0 cm	257300	21500	250500–262360
11.0–11.5 cm	56700	2760	53460– 59350
22.0–23.0 cm	12530	1250	11320– 13780

Detection limit

The limit of detection for this method is about 180–200 particles per gram dry weight; particle numbers in the examined sediment were all greater than this value. The size detection limit for inorganic ash spheres, counting at a magnification of $\times 400$, is 1 to 2 μm diameter.

Recovery rate

A suspension of inorganic ash spheres was made up by adding a small amount of coal-fired residue from a power station to water. After homogenisation a known fraction was then removed and counted at $\times 400$ under a light microscope, to calculate the concentration of the suspension. A known volume of the homogenised suspension was then added to an undigested sediment sample from 100–101 cm depth of Loch Tinker, a level which had only a 'background' value of inorganic spheres. After the digestion, the particle concentrations were counted as before and the value compared with the number of particles added to give a percentage recovery. These digestions were done in triplicate and the recovery range was 82%–102%.

Blank digestions show that no cross contamination from other digestions need occur as long as reasonable precautions are taken. Inorganic spheres were found to be present in petri-dishes left open in the laboratory (with closed windows) for the duration of a digestion, but this source of contamination is negated by keeping the beakers covered. One source of contamination could be core smearing, caused by the coring process or core extrusion. The presence of low numbers of carbonaceous spheres (not found in volcanic or meteoritic dusts) in sediment levels corresponding to pre-industrial times, shows smearing does occur, but this can be avoided by core 'trimming', i.e. using sediment from the interior of the core only.

Application of the method to a sediment core

The technique was applied to a Pb-210 dated sediment core from Loch Tinker. The results appear in Fig. 2. The basic trend of the profile is

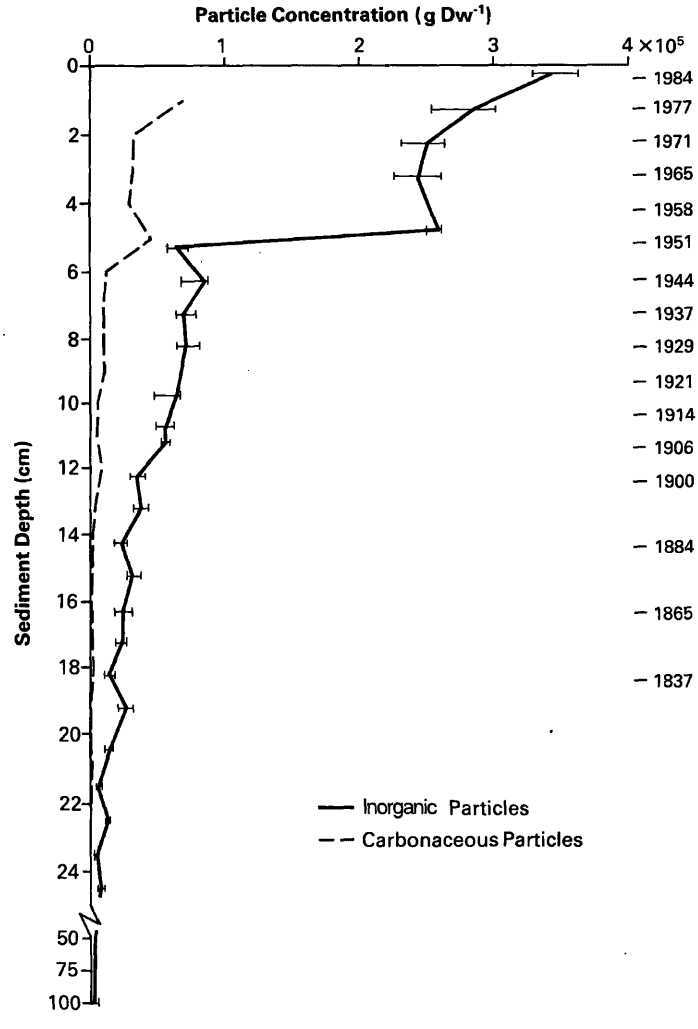

Fig. 2. Inorganic ash sphere and carbonaceous particle concentration profiles for Loch, Tinker with 95% confidence limits.

similar to that of the carbonaceous particle profile produced for Loch Tinker (Rose, 1990) especially in the top 5 cm (Fig. 2). The main difference between these profiles is the continuous background value of the inorganic ash, whereas the carbonaceous particle record falls to zero at about 24 to 25 cm depth. Below this, the inorganic ash record is fairly uniform and low, between 2000 and 3500 particles per gram dry weight. If this record is attributable to a constant background flux from non-industrial sources through time, the start of the 'industrial' inorganic ash record can be identified and occurs here at approximately the same depth/date as the carbonaceous particle record.

Marked changes in the pre-industrial background concentration of particles may be related to significant changes in sediment accumulation, or to changes in atmospheric flux e.g. following a volcanic eruption. The identification of such events using this technique may be of additional palaeoecological or chronological value.

Conclusions

Although the method described does not remove all extraneous material it concentrates the particles suffciently to make particle counting quick and accurate. The remaining mineral residue is similar to inorganic ash both chemically and in some physical aspects and it is difficult to carry out further extractions and, at the same time, retain all the inorganic ash spheres.

The close similarity in shapes between inorganic ash and carbonaceous particle profiles shows that their origins may well be linked, and as the inorganic ash in modern sediment is derived mainly from coal-fired power stations, it seems reasonable to think that in Loch Tinker, the majority of the carbonaceous particles are too.

Acknowledgements

Dr. R. W. Battarbee contributed ideas and provided valuable criticism of the manuscript. Technical help in the laboratory was given by S. Phethean and D. Monteith, and the diagrams were drawn by L. McClue and T. Aspden. This work forms part of a study funded by the Central Electricity Generating Board.

References

Allen, J. R. L., 1987. Microscopic coal-burning residues in the Severn Estuary, Southwestern U.K. Mar. Pollut. Bull. 18: 13–18.

Battarbee, R. W. & M. J. Kneen, 1982. The use of electronically counted microspheres in absolute diatom analysis. Limnol. Oceanogr. 27: 184–188.

Battarbee, R. W., N. J. Anderson, P. G. Appleby, R. J. Flower, S. C. Fritz, E. Y. Haworth, S. Higgitt, V. J. Jones, A. Kreiser, M. A. R. Munro, J. Natkanski, F. Oldfield, S. T. Patrick, N. G. Richardson, B. Rippey & A. C. Stevenson, 1988. Lake Acidification in the United Kingdom 1800–1986. Evidence from analysis of lake sediments. ENSIS Publishing. London.

Chapman, S. L., J. K. Syers & M. L. Jackson, 1969. Quantitative determination of quartz in soils, sediments and rocks by pyrosulfate fusion and hydrofluosilicic acid treatment. Soil Sci. 107: 348–355.

Folger, D. W., 1970. Wind transport of land derived mineral, biogenic and industrial matter over the North Atlantic. Deep Sea Res. 17: 337–352.

Fredriksson, K. & L. R. Martin, 1963. The origin of black spherules found in Pacific Islands, deep-sea sediments and Antarctic ice. Geochim. Cosmochim. Acta 27: 245–248.

Golterman, H. L., (Editor), 1969. IBP Handbook No. 8. Methods for physical and chemical analysis of fresh waters. Blackwell Scientific Publications. Oxford. 213 pp.

Henry, W. M. & K. T. Knapp, 1980. Compound forms of fossil fuel fly-ash emissions. Envir. Sci. Technol. 14: 450–456.

Hodge, P. W. & F. W. Wright, 1964a. Studies of particles for extraterrestrial origin. 2. A comparison of microscopic spherules of meteoritic and volcanic origin. J. Geophys. Res. 69: 2449–2454.

Hodge, P. W., F. W. Wright & C. C. Langway, 1964b. Studies of particles for extraterrestrial origin. 3. Analyses of dust particles from polar ice deposits. J. Geophys. Res. 69: 2919–2931.

Hodge, P. W., F. W. Wright & C. C. Langway, 1967. Studies of particles for extraterrestrial origin. 5. Compositions of the interiors of spherules from Arctic and Antarctic ice deposits. J. Geophys. Res. 72: 1404–1406.

Hullett, L. D. & A. J. Weinberger, 1980. Some etching studies of the microstructure and composition of large aluminosilicate particles in fly-ash from coal burning power plants. Envir. Sci. Technol. 14: 965–970.

Jones, V. J., A. M. Kreiser, P. G. Appleby, Y.-W. Brodin, J.

Dayton, J. Natkanski, N. Richardson, B. Rippey, S. Sandoy & R. W. Battarbee, 1990, in press. The recent palaeolimnology of two sites with contrasting acid deposition histories. Phil. Trans. Roy. Soc. Lond.

Kiely, P. V. & M. L. Jackson, 1965. Quartz, feldspar and mica determination for soils by sodium pyrosulfate fusion. Soil Sci. Soc. Am. Proc. 29: 159–163.

Krausse, G. L., C. L. Schelske & C. O. Davis, 1983. Comparison of three wet alkaline methods of digestion of biogenic silica in water. Freshwat. Biol. 13: 73–81.

Lefèvre, R., A. Gaudichet & M. A. Billon-Galland, 1986. Silicate microspherules intercepted in the plume of Etna volcano. Nature 322: 817–820.

McElroy, M. W., R. C. Carr, D. S. Ensor & G. P. Markowski, 1982. Size distribution of fine particles from coal combustion. Science 215 (4528): 13–18.

Munro, M. A. R. & S. Papamarinopoulos, 1978. The investigation of an unusual magnetic anomaly by combined magnetometer and soil susceptibility surveys. Proceedings of the 18th International Symposium on Archaeometry and Archaeological Prospection. Archaeo physiko 10: 675–680.

Nriagu, J. O. & C. J. Bowser, 1969. The magnetic spherules in sediments of Lake Mendota, Wisconsin. Wat. Res. 3: 833–842.

Oldfield, F., R. Thompson & K. E. Barber, 1978. Changing atmospheric fallout of magnetic particles recorded in recent ombotrophic peat sections. Science 199: 679–680.

Oldfield, F., K. Tolonen & R. Thompson, 1981. History of particulate atmospheric pollution from magnetic measurements in dated finnish peat profiles. Ambio 10: 185–188.

Parkin, D. W., D. R. Phillips, R. A. L. Sullivan & L. Johnson, 1970. Airborne dust collections over the North Atlantic. J. Geophys. Res. 75: 1782–1793.

Puffer, J. H., E. W. B. Russell & M. R. Rampino, 1980. Distribution and origin of magnetite spherules in air, waters, and sediments of the Greater New York City area and the North Atlantic Ocean. J. Sed. Pet. 50: 247–256.

Rose, N. L., 1990. A method for the extraction of carbonaceous particles from lake sediment. J. Paleolimnology 3: 45–53.

Watt, J. D. & D. J. Thorne, 1965. Composition and pozzolanic properties of pulverised fuel ashes. I. Composition of fly ashes from some British power stations and properties of their component particles. J. App. Chem. 585–594.